UNIVERSITAT POLITÈCNICA DE VALÈNCIA

INSTITUTO DE INGENIRÍERIA ENERGÉTICA

DEPARTAMENTO DE INGENÍERIA MECÁNICA Y MATERIALES

Doctoral program "Ingeniería y producción industrial"

ANALYSIS OF THE CONDENSATION PROCESS AND AIR MALDISTRIBUTION EFFECT IN FINNED TUBE AND MINICHANNEL CONDENSERS

PhD candidate: Alessandro Pisano

Supervisors: Dr. José Miguel Corberán Salvador

Dr. Santiago Martínez Ballester

Valencia, 14 de Julio de 2017

ACKNOWLEDGMENTS

Summarizing in few words my experience in Spain would be the hardest task ever. More than four years in Valencia changed me a lot, maybe too much. Every experience and every moment enriched enormously my cultural baggage, opened my mind and made me a better person.

My doctoral work has been developed in the context of the subprogram of research staff training (FPI - Formación personal de investigación) founded by the Spanish Ministry of Economy and Competitiveness. The Project, entitled “Estudio de evaporadores y condensadores de minicanales para su aplicácion en equipos de aire condicionado, refrigeracion y bomba de calor estacionarios”, has been mainly focused on the development of the round tube-plate fins (RTPFs) and minichannel (MCHX) heat exchangers applicable in refrigeration and air conditioning systems. To this end, the Polytechnic University of Valencia (UPV) and the Polytechnic University of Cartagena (UPCt) have been collaborating in order to carry out respectively numerical and experimental studies.

I have been spending in the IIE (Institute for Energy Engineering) of the Polytechnic University of Valencia many days and many hours. During this time, I have not only met new colleagues, but a real second family. My biggest “thank you” is directed to all the people working there.

I’ll be forever in debit with the Prof. J.M. Corberán Salvador and the Dr. S. Martínez Ballester. For both of them, just say "thank you" would not be enough. On one hand, they offered me the possibility to spend some wonderful years in Spain at the IIE, on the other, they provided all their best support for the development of my thesis. Thanks a lot.

Beside them, my acknowledgments are also for the Prof. J. Gonzálvez Maciá. He gave me the possibility to be part of the IMST-ART/MPower development team. If today I’m working at MODINE, it is also due to his efforts.

A special thanks is for Rafa. Without his help, maybe I would be still struggling with most of the issues related to the FORTRAN/C++ programming. Again thanks to Javier and Barbara. They have been the best Spanish teachers ever, as well as my special psychological support. Thanks to Abdel. We have been supporting each other like brothers.

As already mentioned, my work has also been partially developed in the laboratories of the Polytechnic University of Cartagena. For the support that they provided to me, a big thanks is directed to the Professors Fernando Illán Gómez and J. Ramon García Cascales. For his patience, I’m also very grateful to the Ing. Fernando Hidalgo Monpeán.

I have to be really grateful to some people working for MODINE Manufacturing Company. Thanks to Dr. Victor Nino for hosting me in Racine. Since I arrived in US, He treated me like a member of

the VTG (Virtual Technology Group). I want sincerely to acknowledge also Sid, Pavan, Loordha and John. They made my stay in USA unforgettable.

I miei ultimi ringraziamenti vorrei farli in Italiano.

Raffaè, ma dimmi tu come avrei potuto ringraziarti in inglese? Negli anni di Valencia, non sei stato solo un amico. Abbiamo condiviso notti e giorni, gioie e dolori, risate (tante) e lacrime (solo qualcuna). Mi sei stato vicino in ogni momento duro e in ogni momento felice come nessun altro avrebbe potuto fare. Dirti solamente grazie sarebbe davvero veramente troppo troppo poco e non avrebbe alcun senso.

Non ultimo è il ringraziamento per mia madre, i miei zii e la mia famiglia in generale. Siamo parte di generazioni che hanno vissuto società molto differenti. Spesso penso che le mie problematiche "moderne" siano troppo distanti dal vostro modo di pensare. Nonostante questo, ho sempre sentito forte il vostro supporto. Il solo sapervi orgogliosi di me, ripaga ogni sforzo e sofferenza. Grazie.

The thesis has been supported by the following research grants:

This PhD work has been financed by the Ministry of Economy and Competitiveness of Spain in the context of the Subprogram of Research Staff Training (FPI - Formación personal de investigación) and has been performed in the framework of the project entitled "Estudio de evaporadores y condensadores de minicanales para su aplicación en equipos de aire acondicionado, refrigeración y bomba de calor estacionarios" (Reference Number: DPI2011-26771-C02-01).

Additionally, the author received a grant for supporting a research stay at MODINE Manufacturing Company, Racine, Wisconsin (USA) from April to August 2015. The financial support was granted again by the Ministry of Economy and Competitiveness of Spain as part of the FPI program.

SUMMARY

This PhD work has been dedicated to the improvement of the modelling of air condensers of both round tube and fins (RTPFs) and Minichannel technologies. The calculation platform employed is IMST-ART. This is a dedicated software for the design of refrigeration, air-conditioning and heat pump equipment following the vapor compression cycle. The model implemented in IMST-ART for condensers and evaporators is the combination of a segment-by-segment approach with the numerical method SEWTLE (Semi Explicit method for Wall Temperature Linked Equations) for the solution of the resulting system of equations.

The target of the first part of this thesis was the comparative analysis of the empirical correlations aimed at the evaluation of the heat transfer coefficients and pressure drop in both the air and refrigerant sides of a condenser. The Literature review pointed out the presence of many studies concerning the condensation modelling. Therefore, after selecting the most interesting to compare, the first objective of this first part of the PhD became the identification of a suitable methodology for defining the best combination of correlations for the estimation of the thermo-hydraulic performance of the condensers. After an in-depth analysis of different possibilities, a well-defined methodology was identified as the best for the purpose. In the thesis, it was successfully applied to the identification of the best set of correlations for the heat transfer coefficients and friction factors for both the round-tube and minichannel condensers.

The second part of the PhD was targeted to the improvement of the condensation modelling. In particular, the attention was focused on the analysis of the phenomena taking place at the beginning of the condensation process, when the superheated vapor finds the wall of the condenser being at a temperature lower than the refrigerant saturation temperature, i.e. convective condensation superheated vapor zone (CSH zone). It is well known that, in this zone, the condensation starts with some kind of droplet/thin film condensation on the walls. Afterwards, the bulk of the refrigerant flow reaches the saturation temperature and the condensation occurs at saturated conditions. Hence, the PhD thesis has been dedicated to the implementation in the general model for condensers (in IMST-ART software) of this CSH zone, which it was found to have an important effect on the prediction of the wall temperatures distribution in the tested air condensers. Two different numerical solutions were implemented and compared, i.e. Temperature and Enthalpy approaches, and validated against experimental results. Prediction results are very similar, thus the Enthalpy approach was selected because it required lower computational time.

The final part of thesis was oriented towards the study of the effect of airflow maldistribution on the performance of air condensers. An innovative experimental methodology for generating and measuring any uneven air velocity profile at the inlet of a heat exchanger was first developed in a dedicated wind tunnel and then applied for the analysis of the performance degradation of one sample

of condenser of each RTPFs and Minichannel technologies. Three different velocity profiles were produced and tested along a wide set of operating conditions, including different refrigerant charges and hence subcoolings. The experimental results showed that, although differences in wall temperature distribution were significant, the effect of air maldistribution on the performance of the two tested condensers was small. The improved model was validated against the experimental results and also showed little effect on condenser performance. Finally, the agreement between the results of the simulation and the experimental results was very satisfactory.

RESUMEN

Este trabajo de doctorado se ha dedicado a la mejora del modelado de condensadores de aire, con tecnología de tubos y aletas o minicanales. La plataforma de software empleada es IMST-ART, que es un software dedicado a asistir el diseño de equipos de refrigeración, aire acondicionado y bomba de calor, basados en el ciclo de compresión de vapor. El modelo de IMST-ART para condensadores y evaporadores se basa en una aproximación segmento a segmento combinada con el método numérico SEWTLE (Semi Explicit method for Wall Temperature Linked Equations) para la solución del sistema de ecuaciones resultante.

El objetivo de la primera parte de esta tesis fue el análisis comparativo de las correlaciones empíricas destinadas a evaluar los coeficientes de transferencia de calor y la caída de presión para condensadores de aire, tanto para el lado del aire como para el del refrigerante. La revisión de la Literatura mostró la existencia de numerosos estudios sobre el modelado de la condensación en este tipo de intercambiadores. Por lo tanto, después de la selección de las correlaciones más interesantes a comparar, el primer objetivo de esta primera parte de la tesis resultó el encontrar la metodología más adecuada para la identificación de cuáles eran las correlaciones que mejor estimaban el comportamiento termo-hidráulico de los condensadores. Después de un análisis en profundidad de diferentes posibilidades, se encontró la metodología claramente más adecuada y se pasó a aplicarla a la identificación del mejor conjunto de correlaciones para los coeficientes de transferencia de calor y factores de fricción para condensadores de aire.

La segunda parte del doctorado se dirigió a la mejora del modelado del comienzo del proceso de condensación cuando el vapor sobrecalentado encuentra la pared del condensador a una temperatura que está por debajo de la temperatura de saturación del refrigerante en lo que se puede denominar como condensación convectiva en la zona de vapor sobrecalentado (zona CSH). Es bien sabido que la condensación comienza en esta zona con algún tipo de condensación de gotas/película delgada sobre las paredes antes de que el núcleo del flujo de refrigerante alcance la temperatura de saturación y la condensación se produzca en condiciones saturadas. La segunda parte del doctorado se ha dedicado a la implementación en el modelo general de condensadores (en el software IMST-ART) de esta zona CSH, que se encontró que tenía un efecto importante en la predicción de la distribución de las temperaturas de la pared en los condensadores de aire ensayados. Se implementaron y compararon dos soluciones numéricas diferentes, denominados aproximación de temperatura y aproximación de entalpía respectivamente, y se validaron por comparación con resultados experimentales. La predicción resultó ser muy similar con ambas aproximaciones por lo que finalmente se seleccionó la aproximación de entalpía por ser considerablemente más rápida.

La parte final de la tesis se orientó hacia el estudio del efecto de la mala distribución del flujo de aire en el rendimiento de los condensadores de aire. Para este fin se desarrolló una metodología

experimental innovadora capaz de generar y medir cualquier perfil de velocidad de aire no uniforme a la entrada de un intercambiador de calor. El desarrollo se llevó a cabo primero en un túnel de viento específicamente dedicado a este propósito y luego se aplicó para el análisis de la degradación de las prestaciones de dos muestras de condensador de cada una de las tecnologías estudiades: RTPFs y Minicanal. Mediante la metodología desarrollado se generaron tres perfiles de velocidad diferentes que se ensayaron a lo largo de un amplio conjunto de condiciones de funcionamiento, incluyendo diferentes cargas de refrigerante y, por tanto, grados de subenfriamiento en el refrigerante. Los resultados experimentales mostraron que el efecto de la mala distribución del aire en las prestaciones de los dos condensadores probados fue pequeño, aunque las diferencias en la distribución de la temperatura de la pared fueron significativas. El modelo mejorado fue validado mediante los resultados experimentales y también mostró que sólo se producía una pequeña degradación en las prestaciones debido a la mala distribución del aire. La concordancia entre los resultados del modelo y los resultados experimentales fue plenamente satisfactoria.

RESUM

Aquest treball de doctorat s'ha dedicat a la millora de la modelització de condensadors d'aire, amb tecnologia de tubs i aletes o minicanals. La plataforma de software emprada és IMST-ART, que és un software dedicat a assistir el disseny d'equips de refrigeració, aire condicionat i bomba de calor, basats en el cicle de compressió de vapor. El model de IMST-ART per condensadors i evaporadors es basa en una aproximació segment a segment combinada amb el mètode numèric SEWTLE (Semi Explicit method for Wall Temperature Linked Equations) per a la solució del sistema d'equacions resultant.

L'objectiu de la primera part d'aquesta tesi va ser l'anàlisi comparativa de les correlacions empíriques destinades a avaluar els coeficients de transferència de calor i la caiguda de pressió per condensadors d'aire, tant per al costat de l'aire com per al del refrigerant. La revisió de la Literatura va mostrar l'existència de nombrosos estudis sobre la modelització de la condensació en aquest tipus d'intercanviadors. Per tant, després de la selecció de les correlacions més interessants a comparar, el primer objectiu d'aquesta primera part de la tesi va resultar el trobar la metodologia més adequada per a la identificació de quines eren les correlacions que millor estimaven el comportament termo-hidràulic dels condensadors. Després d'una anàlisi en profunditat de diferents possibilitats, es va trobar la metodologia clarament més adequada i es va passar a aplicar-la a la identificació del millor conjunt de correlacions per als coeficients de transferència de calor i factors de fricció per condensadors d'aire.

La segona part del doctorat es va dirigir a la millora de la modelització del començament del procés de condensació quan el vapor sobreescalfat troba la paret del condensador a una temperatura que està per sota de la temperatura de saturació del refrigerant, en el que es pot denominar com condensació convectiva a la zona de vapor sobreescalfat (zona CSH). És ben sabut que la condensació comença en aquesta zona amb algun tipus de condensació de gotes/pel·lícula sobre les parets abans que el nucli del flux de refrigerant arribi a la temperatura de saturació i la condensació es produeixi en condicions saturades. La segona part del doctorat s'ha dedicat a la implementació en el model general de condensadors (en el programari IMST-ART) d'aquesta zona CSH, que es va trobar que tenia un efecte important en la predicció de la distribució de les temperatures de la paret en els condensadors d'aire assajats. Es van implementar i van comparar dues solucions numèriques diferents, denominades aproximació de temperatura i aproximació d'entalpia respectivament, i es van validar per comparació amb resultats experimentals. La predicció va resultar ser molt semblant amb les dues aproximacions pel que finalment es va seleccionar l'aproximació d'entalpia per ser considerablement més ràpida.

La part final de la tesi es va orientar cap a l'estudi de l'efecte de la mala distribució del flux d'aire en el rendiment dels condensadors d'aire. Amb aquesta finalitat es va desenvolupar una metodologia

experimental innovadora capaç de generar i mesurar qualsevol perfil de velocitat d'aire no uniforme a l'entrada d'un intercanviador de calor. El desenvolupament es va dur a terme primer en un túnel de vent específicament dedicat a aquest propòsit i després es va aplicar per a l'anàlisi de la degradació de les prestacions de dues mostres de condensador de cadascuna de les tecnologies estudiades: RTPFs i Minicanal. Mitjançant la metodologia desenvolupada es van generar tres perfils de velocitat diferents que es van assajar al llarg d'un ampli conjunt de condicions de funcionament, incloent càrregues diferents de refrigerant i, per tant, graus de subrefredament en el refrigerant. Els resultats experimentals van mostrar que l'efecte de la mala distribució de l'aire en les prestacions dels dos condensadors provats va ser petit, tot i que les diferències en la distribució de la temperatura de la paret van ser significatives. El model millorat va ser validat mitjançant els resultats experimentals i també va mostrar que només es produïa una petita degradació en les prestacions causa de la mala distribució de l'aire. La concordança entre els resultats del model i els resultats experimentals va ser plenament satisfactòria.

List of publications

JOURNALS

Title: A discussion about the methodology for validating a model of a finned-tube condenser considering different correlations for the heat transfer coefficients and pressure drop

Authors: A. Pisano, S. Martínez-Ballester, J. Miguel Corberán, Fernando Hidalgo Monpeán, Fernando Illán Gómez, J-Ramon García Cascales

Journal: Science and Technology for the Built Environment

Volume: 21; Pages: 585-594*; Date:* June 2015

ISSN: 2374-4731 print / 2374-474X online

doi: 10.1080/23744731.2015.1040341

CONGRESSES

Title: Metodología para la Validación de Correlaciones de los Coeficientes de Intercambio de Calor en Condensadores de Tubos aleteados.

Authors: A. Pisano, S. Martínez-Ballester, J. Miguel Corberán, Fernando Hidalgo Monpeán, Fernando Illán Gómez, J-Ramon García Cascales

Congress: CYTEF - VII Congreso Ibérico, y V Iberoamericano de Ciencias y Técnicas del Frío

Date: 18-20th June 2014

Title: A Discussion about the Methodology to Validate the Correlations of Heat Transfer Coefficients and Pressure Drop during the Condensation in a Finned-tube Heat Exchanger.

Authors: A. Pisano, S. Martínez-Ballester, J. Miguel Corberán, Fernando Hidalgo Monpeán, Fernando Illán Gómez, J-Ramon García Cascales

Congress: 2014 Purdue Refrigeration and Air Conditioning Conference

Date: 14-17th July 2014

Title: Development of an Experimental Method to Generate a Non-uniform Air Flow Distribution at the Inlet of a Heat Exchanger

Authors: A. Pisano, S. Martinez-Ballester, J.M. Corberán

Congress: 9ª Edición del Congreso Nacional de Ingeniería Termodinámica

Date: 3-5th June 2015

Title: Experimental Study on the Influence of the Air Maldistribution on the Performance of a Finned Tube Condenser

Authors: A. Pisano, S. Martínez-Ballester, J. Miguel Corberán, Fernando Hidalgo Monpeán,

Fernando Illán Gómez, J-Ramon García Cascales

Congress: 24th Edition of the International Congress of Refrigeration

Date: 16-22th August 2015

Title: Experimental Investigation on the Performance Degradation of a Microchannel Condenser due to the Air-Side Flow Maldistribution

Authors: A. Pisano, S. Martínez-Ballester, J. Miguel Corberán

Congress: VIII Congresso Ibérico | VI Congresso Ibero-Americano das Ciências e Técnicas do Frio

Date: 3-6th May 2016

Title: Influence of Different Correlations to Estimate the Heat Transfer Coefficients on the Prediction of the Performance of a Microchannel Condenser

Authors: A. Pisano, S. Martínez-Ballester, J. Miguel Corberán, Fernando Hidalgo Monpeán, Fernando Illán Gómez, J-Ramon García Cascales

Congress: VIII Congresso Ibérico | VI Congresso Ibero-Americano das Ciências e Técnicas do Frio

Date: 3-6th May 2016

Table of contents

List of figures

List of tables

Nomenclature

a, b	constants [-]
A	cross section area [m^2]
b_w	slope of h vs. T curve
C_p	specific heat [J/kg K]
D_h	hydraulic diameter [m]
e	wall thickness [m]
f	friction factor [-]
g	gravity [m/s^2]
G	mass velocity [kg/s m^2]
h	enthalpy [J/kg]
H	relative humidity [%]
L	length [m]
k	conductivity [W/mK]
m	mass flow rate [kg/s]
P	perimeter [m]
p	pressure [Pa]
Δp	pressure drop [Pa]
q	heat flux [W/m^2]
Q	heat [W]
ΔQ_{cond}	cond. latent heat [W]
S	slip ratio [-]
SC	subcooling [K]
T	temperature [$°C$]
ΔT	temperature difference [$°C$]
u	velocity [m/s]
W	humidity [kg vap. / kg dry air]
x	vapor quality [-]
z, y	Spatial co-ordinates [m]

Abbreviations

HX	Heat exchanger
MCHX	Microchannel heat exchangers
RTPFs	Round tube plate fins HX

Greek Symbol

α	heat transfer coefficient [W/m^2K]
θ	angle with horizontal [rad]
Φ^2	2-phase fric. multiplier
γ	void fraction [-]
ρ	density [kg/m^3]
∇^2	laplacian operator
Δ	Gradient

Subscript

a	air
cell	cell
CSH	condensing superheated vapor
eq	equivalent
f	saturated liquid
g	saturated vapor
i	cell index [-]
in	inlet
l	liquid
out	outlet
r, ref	refrigerant
s, sat	saturation
v, vapor	vapor
w, wall	wall

CHAPTER 1

1. Introduction

In order to understand the importance of the design and optimization of heat exchangers, it is enough thinking about all the industrial processes in which the necessity to transfer thermal energy between different fluids exists. Refrigeration, air conditioning, process and power engineering are just some of the sectors where heat exchangers are currently widely used. There are several types of heat exchangers depending on the working fluids (refrigerants, oil, water-glycol mixtures, air, etc., etc.), applications and operating conditions.

In general, the working fluids are named depending on their temperature. Of course, the "hot" fluid is characterized by the highest temperatures, while the "cold" fluid by the lowest. When our objective is the temperature reduction of the hot fluid, the heat exchangers are classified as liquid-cooled or air-cooled, depending on the fluid used in the cold side. The liquid-cooled heat exchangers usually employ water (or water-glycol mixtures) as cold fluid and are widely adopted in the automotive sector as charge-air coolers, oil coolers or even EGR (Exhaust Gas Recirculation) when high thermal capacities are required. On the other hand, the air-cooled heat exchanger is also widely used especially for their simplicity. Indeed, only using ambient air, high temperature reduction in the hot side can be obtained. Such type of heat exchanger are mainly used as radiators, oil-coolers, charge-air coolers or even as condensers.

Focusing the attention on the latter category of devices, the further classification of the heat exchangers is based on their geometrical characteristics. In particular, the first classification is based on the channel characteristics. Round tube exchangers, plane tube heat exchangers, bar plate heat exchangers and, more recently, the microchannel heat exchangers (MCHXs) are the most common denominations. Some examples of these types of heat exchangers are shown in Figure 1.1.

Nowadays, the research in the refrigeration and A/C is significantly focused on the identification of the best technological solutions able to reduce both energy consumption and Green House Gas emissions. Therefore, many research projects are currently being aimed at finding new design solutions for the efficient use of alternative refrigerants (e.g. natural refrigerants). Until very recently, the development of new equipment was entirely based on experimental testing. In recent years, accurate mathematical models have been developed which are able to accurately predict the performance of almost any kind of heat exchanger, providing a tool to assist their design and moreover to assists their optimization. Of course, testing is still essential for final validation and

tuning up of the prototypes. However, thanks to these new mathematical models, the long and costly development campaigns have been considerably reduced with great savings in time and costs. Moreover, final design are much closer to the optimum than years before, when the development had to be limited to a reduced number of prototypes and trials. Still, there is a lot of work to do with the mathematical models. On one hand, faster calculation provided by the continuous speed growth of computers allows to include more details and more second order phenomena. On the other hand, there is still a lot to be known and to be correctly characterized in the model of heat exchangers. Phase change, mass transfer and more complex physical phenomena are some examples.

Figure 1.1: Some example of Air-to-refrigerant heat exchangers

In this context, the present work aims at providing a contribution to the improvement of the modelling of actual condensers, both microchannel and tube-and-fin types, with the analysis of the existing empirical correlations for the evaluation of the heat transfer and pressure drop on both sides (refrigerant and air), with the improvement on the modelling of the condensation of superheated vapour inside the refrigerant channel, and finally, with the experimental characterization and analysis of the effect of air maldistribution on condensers.

1.1 Air-to-refrigerant Heat Exchangers in the HVAC&R systems

In principle, the heat exchange between air and refrigerant has been traditionally performed by means of the utilization of the round tube heat exchangers. Historically, the fin-and-tube heat exchangers were initially used in the transportation sectors as radiators - automotive, aircraft, submarine and spacecraft – where they have been used almost until the end of the 20th century. However, nowadays, their main application is in Heating, Ventilation, Air conditioning and Refrigeration (HVAC&R) systems as evaporators and condensers (Figure 1.2).

Differently by the liquid-to-liquid heat exchanger, where the heat transfer coefficients are generally higher, the air-to-refrigerant heat exchangers are equipped with a finned surface on the air side. The

presence of the fins is mainly due to the need of reducing the thermal resistance of the air side which is typically much higher than the one corresponding to the refrigerant side. The fins, on one side, provide a way to considerably increase the heat transfer area, and on the other, they increase the heat transfer coefficient due to a decrease on the hydraulic diameter and to the generation of local unsteadiness on the laminar flow or even turbulence. As the tubes, also the fins are characterized by their geometry. In principle, the best thermal performance is usually obtained using louvered fins. Nevertheless, the plane, wavy or slit fins are also widely used.

Figure 1.2: Condenser configurations in the HVAC&R systems

The most common round-tube heat exchangers (HEs) are made up of copper tubes (Dh ≥ 3mm) and thin aluminum fins. From a manufacturing point of view, once decided the pitch (distance between two consecutive fins), tubes and fins are assembled to form the complete heat exchanger. Afterwards, the tubes are connected each other by means of the returns bends (or headers), defining the number and the configuration of the circuits. Once installed, the condensers are classified as co-current or counter-current depending on the flows arrangement. Recently, in the air conditioning applications, the traditional heat exchangers are usually replaced by more complex configurations. Some examples are the A-shape and the U-Shape condensation units, the application of which is very common especially in the biggest HVAC&R systems.

The microchannel heat exchangers (MCHX) are becoming widely used in the automotive sector as condensers, but it seems that this technology is also spreading in the market of the air conditioning and refrigeration systems (Figure 1.3). MCHXs are replacing gradually the traditional Round-tube heat exchangers especially because their application leads a substantial refrigerant charge reduction.

Although widely adopted in literature, the term “microchannel” includes a big family of HEs. (Kandlikar and Grande, 2002) proposed a new method of classification of the HEs based on the value of the hydraulic diameter. They classified the round tubes with hydraulic diameter higher than 3 mm as “conventional” channels. Minichannel, microchannel, transitional channels and molecular nanochannels are the name assigned to the tubes with hydraulic diameter from 3 mm up to 0.1 μm.

In the HVAC&R systems, the condensers and evaporators are generally made up of extruded aluminum tubes characterized by a variable number of channels (between 8-12 channels per tube depending of the application). Rectangular, round or triangular channels with hydraulic diameter between 200 μm and 3 mm are commonly adopted. Effectively, this design parameter represents the strength of the MCHX. Indeed, the lower is the hydraulic diameter, the higher is the heat transfer coefficient. It means that, compared with the conventional HEs, the MCHX makes possible to have a very high compactness ratio (high ratio between UA and volume). In other words, to equal heat transfer areas, high compactness means reduced size and volume and reduced internal volumes. The result is a lighter heat exchanger combined with the advantage to use very low refrigerant charge.

Figure 1.3: Microchannel Heat Exchangers

Many authors studied the behavior of the MCHX in different areas of work. Jordan and Jacobi (2005); Zhong *et al.* (2005); Xia *et al.* (2006); Lia *et al.* (2011); Qu *et al.* (2009); Zilio *et al.* (2011); Ayad *et al.* (2012); Zheng *et al.* (2014); Datta *et al.* (2014) analyzed some of the aspects linked to the utilization of MCHX in the automotive sector. The application of MCHX in the HVAC&R industry was analyzed by Fernando *et al.* (2008); Kew and Reay (2001) and Meng *et al.* (2015). Park and Hrnjak (2007) and Shao *et al.* (2010) analyzed the performance of the air conditioning system replacing the round-tube condenser with a microchannel heat exchanger. Numerous other studies were focused on the application of microchannel heat exchanger in highly specialized fields, such as bioengineering, electronics and high temperature solar receivers.

After banishing the utilization of the CFC (chlorofluorocarbon) refrigerants in 2009, the European Union issued a new regulation (the 1005/09), which marked also the progressive and final disposal of the HCFC (hydro-chloro-fluoro-carbon). Therefore, the refrigeration industry has been forced to evaluate the possibility to use new or alternative refrigerants. Since then, the utilization of natural refrigerants has been the focus of considerable research. Although the systems equipped with propane (R290), isobutene (R600a) and butane (R600) can achieve similar or, sometimes, better performance compared with the traditional refrigeration systems, the problem to work with these

refrigerants in large amount is mainly connected to their high flammability. As highlighted by many authors (Fernando *et al.*, 2004; Palm, 2007; Hrnjak, 2010; Corberan and Montagud, 2014; Tammaro *et al.*, 2015), the necessity to reduce the refrigerant charge is well fulfilled by the utilization of the microchannel heat exchangers.

However, the utilization the MCHX also present some disadvantages, e.g., difficulties in draining the condensate water in evaporators, refrigerant mal-distribution, high cost of manufacturing, fast fouling. Therefore, due to this secondary issues, the utilization of the Tube-and-fin heat exchangers is still ensured for a long while.

1.2 Literature review and background

1.2.1 Heat transfer coefficients and pressure drop

In the past, the design of a heat exchanger was carried out by means of long and expensive experimental campaigns. However, in order to reduce the economic efforts and time consumption, in both industrial and scientific sectors, specific simulation tools are now being widely used. In this context, different models have been developed for the simulation of the Round-tube and MCHX condensers over the years. A detailed literature review led to identify the models proposed by Lee and Domanski (1997); Corberàn *et al.* (2001); Jiang *et al.* (2006); Oliet *et al.* (2007); Singh *et al.* (2008); CoilDesigner (2010); EVAPCOND (2010); IMST-ART (2010); Oliet *et al.* (2010) as the most suitable for the simulation of round-tube heat exchangers. On the other hand, the most cited works for the simulation of MCHXs can be listed as follows: Kim and Bullard (2001); Yin *et al.* (2001); Asinari (2004); Jiang *et al.* (2006); Oliet *et al.* (2007a); Shao *et al.* (2009); García-Cascales *et al.* (2010); MPower (2010); Fronk and Garimella (2011); (Padilla, 2012); (Martínez-Ballester *et al.* (2013) and Mao *et al.* (2013). Even though these models and software are based on different approaches, such as the application of the energy conservation equations to every control volume or the utilization of the traditional ε-NTU method, they can be globally classified as semi-empirical models. This denomination can be attributed to the fact that the mathematical problem is the solution of the simplified governing equations system combined with some parameters, as the heat transfer coefficient or the friction factor. In general, the estimation of such parameters leads to the use of some empirical correlation. Focusing the attention on the main phenomena occurring during condensation inside a tube, Cavallini and Zecchin (1974) and Briggs and Rose (1994) early identified the heat transfer coefficient (HTC) and the frictional pressure drop (PD), on both the refrigerant and air sides, as the most relevant parameters to be determined experimentally in order to improve the accuracy of the results of simulation software. About the experimental and numerical evaluation of such parameters, many publications, books and manuscripts have been written during last years.

However, since some of these works will be object of a detailed analysis in the next chapters, only a general overview of the most relevant works and publications will be presented in this Section.

As just mentioned, several authors have contributed to the development of more reliable and flexible correlations for the evaluation of the HTC and PD inside both the conventional channels and microchannels (Kandlikar and Grande, 2002). Nevertheless, the detail used to describe the phenomena of the condensation represents one of the possible criterion to classify the studies performed. In principle, for the evaluation of the HTC during the condensation in the conventional tubes, we have simple correlations or more complex models. The simple models apply only a global approach to dealing with the condensation process (Akers *et al.*, 1959; Soliman *et al.*, 1968; Travis *et al.*, 1971; Cavallini and Zecchin, 1974; Shah, 1979; Haraguchi *et al.*, 1994; Tondon *et al.*, 1995; Dobson and Chato, 1998; Boissieux *et al.*, 1999). In contrast, the more complex and detailed correlations, first need to determine the flow pattern (Cavallini *et al.*, 2001; Cavallini *et al.*, 2002; Thome, 2003), then it is possible to find the most adequate correlation. Actually, these latter correlations can be considered as condensation models, which analyze in detail the complex phenomena occurring inside the tube depending on the flow regime. As will be mentioned later, such correlations allow obtaining a very good agreement between the predicted results and the experimental data, usually at the cost of a small increase of the calculation time.

Regarding the evaluation of the two-phase flow pressure drop in the conventional tubes, the correlations proposed by Lockhart and Martinelli (1949), Gronnerud (1972), Chisholm (1973), Friedel (1979), Muller-Steinhegen and Heck (1986), Oliver and Liebenberg (2004) and Quiben and Thome (2007) are the most cited in the Literature. Unfortunately, these correlations have been developed from the observation and analysis of experimental data, therefore their applicability can be considered limited to the studied cases and working conditions.

The same can be said about the correlations for the estimation of the HTC and friction factor on the air side. In fact, most of the published studies employ statistical approaches based on the analysis of wide set of experimental data for the generation of their correlations. For the high number of analyzed experimental data, and for their capacity to simulate with good accuracy a broad number of condensers, in the author's opinion, the most interesting correlations are those presented by McQuiston (1978), Gray and Webb (1986), Wang *et al.* (2000) and Granryd *et al.* (2003). Some of them will be employed in the third chapter of the thesis, therefore they will be discussed in detail below.

Due to the different flow patterns and heat transfer mechanisms, some of the correlations working out for tube-and-fins heat exchangers, do not work so accurately for MCHX (Kandlikar and Grande, 2002; Thome, 2004; Garimella *et al.*, 2005; Revellin and Thome, 2007; Bertsch *et al.*, 2008; Cavalini *et al.*, 2009; Revellin *et al.*, 2009; Agarwal *et al.*, 2010; Park *et al.*, 2011). For this reason, in the last

two decades, a number of authors have been developing new correlations and models for the two-phase HTC and friction factor specific for the microchannel condensers. As will be commented later, in the author's opinion, the most interesting correlations for the two-phase flow HTC have been developed by Webb (1998), Wang and Chi (2000), Koyama *et al.* (2003), Cavallini et al. (2005), Bahndauer *et al.* (2006), Lopez-Belchi *et al.* (2015). In spite of the fact that Webb's *et al.* (1998) work was mainly focused on studying the heat transfer in the macroscale channels, the correlation that they developed has been considered particularly suitable also for simulating the behavior of minichannel condensers. More details regarding the capability of each correlation to estimate the local value of the HTC will be given and discussed in the next chapters.

If on the one hand the pressure drop in a conventional condenser is calculated with reasonable approximation thanks to the application of some of the correlations cited above, on the other hand, the numerical evaluation of the total pressure drop through MCHXs is currently characterized with very low accuracy. The main reason for this are the difficulties related with the estimation of the refrigerant pressure drop and distribution along the headers (distributors and collectors). Indeed, if in the traditional condensers the global pressure drop is well estimated only considering the friction in the tubes, in the MCHX, the pressure drop can be evaluated correctly only if it includes the phenomena taking place in the headers. Nowadays, the estimation of the pressure drop in the headers is object of much experimental work. However, the results published until now are strongly connected to specific geometries and testing conditions. In addition to these issues, the pressure drop and heat transfer in the MCHX is also strongly connected to the flow regime of the refrigerant inside the microchannel tubes as it has been demonstrated by Wambsganss and Jendrzejczyk (1992), De Souza and Pimenta (1995), Yang and Webb (1996), Triplett *et al.* (1999), Chen *et al.* (2001), Zhang and Webb (2001), Garimella *et al.* (2001), Cavallini *et al.* (2005), Hwang and Kim (2006), Revellin and Thome (2007), Zhao *et al.* (2011), Choi *et al.* (2011) and Kim and Mudawar (2012). Unfortunately, considering the huge variety of geometries characterizing tubes (hydraulic diameter and port shape) and headers (rectangular, round square, etc.), it is possible to affirm that every heat exchanger has its specific refrigerant distribution, hence its specific flow regime inside the tubes. Of course, starting from this assumption, it is rather easy to understand why the estimation of a simple model for the estimation of the global pressure drop in the MCHX represents still todays a big challenge for a lot of researchers and, therefore, it will not be dealt with in this thesis.

As discussed until now, the geometry and characteristics of the MCHX are very different to those of the conventional tube and fin HXs. Also, at the air side the correlations developed for the round tube HX cannot be employed for simulating the MCHX with good accuracy. On the other hand, although the internal geometry is specific for every heat exchanger, it is rather evident that the external geometry of the MCHXs is rather simple. Indeed, in the totally of the cases, tube and fins are welded one over the others forming the core of the heat exchanger. This characteristic makes easier the

development of the HTC and pressure drop correlations, which are able to provide results very close to experimental data. Actually, in order to increase the air side heat transfer coefficient, most of the MCHX in the market are equipped with louvered fins. The correlations available in literature can be more or less complex depending on the number of geometrical parameters and the flow regimes considered for their development. As discussed in the third chapter of the thesis, among all the correlations available in literature, the following have been selected: Chang and Wang (1996); Chang *et al.* (2006); Kim and Bullard (2002) and Park and Jacobi (2009) for comparison. They will be analyzed and compared, attempting to identify the most accurate and useful correlation.

1.2.2 The convective condensation of the superheated vapor

Thanks to the important effort carried out in the last years on the evaluation of heat transfer coefficients and frictional factors, the behavior of the tube-and-fins and MCHX condensers under different operating conditions is in general simulated with good accuracy. Nevertheless, although the results of a modern simulation software become more and more reliable, there is still ample room for improvement. It is enough to consider that most of the models currently used for the simulation of condensers only take into account the presence of three different zones during the entire heat rejection process, e.g. the refrigerant coming from the compressor is first cooled down in the superheated vapor zone (I), then, it goes through the condensation process (II) and finally, its temperature keeps on decreasing in the subcooled liquid region (III). However, since the second half of the last century, researchers highlighted the presence of a fourth zone in which a different heat transfer took place: when the tube wall temperature goes down below the condensation temperature, dropwise or thin layer condensation occurs at the wall while the bulk of the flow is still superheated vapor and is cooling down progressively. Since the beginning, such a heat transfer mechanism was named as the convective condensation of superheated vapor. Initially, this phenomenon was only observed experimentally by Belakjian and Katz (1958) and Altman *et al.* (1960). Later, Stern and Votta (1968), Bell (1972), Miropolky *et al.* (1974), Fuji *et al.* (1978) performed new experimental studies, confirming that, in the zone closer to the condensation, the phenomenon of convective condensation of the superheated vapor altered considerably the local value of the heat transfer coefficient. Only some years later, Lee *et al.* (1991) and Webb (1998) carried out new research focused on the generation of suitable correlations for the estimation of the HTC during the condensation of the superheated vapor. Webb (1998) simplified the correlation proposed by Lee *et al.* (1991) according which the heat transfer in the condensing superheated vapor zone is due to the combination of a sensible component and a latent one. The latter model, which will be discussed later in detail, was validated by means of the experimental data obtained by the observation of the condensation of R22 inside a horizontal tube. Recently, other experimental studies have been published. Using their own experimental apparatus, Kondou and Hrnjak (2012) and Meyer and Hrnjack (2014) have studied respectively the trend of the HTC and the pressure drop in the condensing superheated vapor zone

for different refrigerants working under several operating conditions. Koundou and Hrnjak (2012) determined the HTC for the condensation from the superheated vapor of CO_2 and R410a, while Meyer and Hrnjack (2014) have been testing R32, R134a and R1234ze(E). The most significant result of their analysis shows that the HTC and the pressure drop in the condensing superheated vapor zone are significantly higher than those calculated with the correlations provided respectively by Gnielinski (1976) and Colburn (1933) that only thake into account the sensible heat transferred from the superheated vapor. Starting from this conclusion, Agarwal and Hrnjak (2014) proposed a new method for the calculation of the HTC in the condensing superheated zone. Validating the model with their own experimental data (Argawal and Hrnjak; 2013), they concluded that, for three different fluids (R1234ze, R134a and R32) and several operating conditions, the model was able to calculate the local HTC of all data points with an absolute mean deviation of 16%.

Recently, Padilla (2012) described a new condenser model for microchannel heat exchangers, which included the variation of the HTC due to the convective condensation of the superheated vapor. The model was based on the segmentation of the heat exchanger in control volumes employing the ε-NTU method combined with a suitable correlation for the heat transfer coefficient. The model was validated in terms of thermal capacity, providing very good agreement with the experimental data. To the knowledge of the author, this is the only example of condenser model considering the convective condensation of the superheated vapor. Indeed, some of the most used commercial software for the simulation of round-tube HEs and MCHX, such as CoilDesigner (2010); EVAPCOND (2010); IMST-ART (2010); MPower (2010), don't take into account the presence of this additional mechanism of heat transfer.

1.2.3 Airflow maldistribution: experimental and numerical studies

In the author's opinion, the simulation of the thermo-hydraulic performance of an air-to-refrigerant HE can be improved if the influence of the airflow maldistribution is also taken into account. However, whatever is connected to the airflow distribution requires a big effort, since it is very difficult to reproduce experimentally in an adequate way.

It is enough to think that the characteristics of the air maldistribution are strictly dependent on some factors such as the position of the heat exchanger within the airflow, the geometry of the ducts, the geometry and operation of the fans, and the presence of obstructions or fouling at the surface. Therefore, each refrigeration equipment has its own air velocity distribution at the inlet of the condenser or evaporator. According to these considerations, the characterization of the velocity profiles can be mainly performed applying two strategies: the experimental approach or the utilization of CFD (Computational Fluid Dynamics) software.

Duo to the difficulties related to the air velocity measurement (Mc Williams, 2002), the velocity profile at the inlet of a heat exchanger has been only experimentally characterized in a very few cases. Yashar and Cho (2007) and Yashar *et al.* (2008) measured the air velocity profile at the inlet of an evaporator using the PIV (Particle Image Velocimetry) technology. Thanks to this technology, the air velocity field was characterized in detail for different positions of the tube-and-fins HX inside a wind tunnel. In addition to the experimental work, after analyzing the collected images, the authors employed a commercial CFD software to evaluate the air velocities, showing a very good agreement between the experimental and the calculated air velocity profiles.

Some years before, simpler techniques were used by Timoney and Foley, (1993); Choi *et al.* (2003), who measured the air velocity profile inside a wind tunnel by means the utilization of a hot-wire anemometer. In these studies, the air maldistribution was generated artificially by means of the application of a perforate plate inside the wind tunnel. Their work also included the evaluation of the influence of the created maldistribution on the refrigeration unit performance.

In particular, Timoney and Foley (1993) studied the effects of the air maldistribution on the performance of a single circuit round-tube evaporator. They found out that, in comparison with the uniform profile and depending on the operating conditions, the uneven velocity profile allowed obtaining an unusual improvement in thermal capacity up to 4%.

Also Choi *et al.* (2003) analyzed experimentally the effects of the airflow maldistribution on a plate and fin evaporator obtaining the opposite result. Actually, during the tests campaign, they considered two different scenarios: some of the tests were performed maintaining constant the airflow rate, the others, considering the airflow reduction due to the presence of the perforated plate. Although the maximum performance degradation was about 9%, they were able to reduce the negative effect of the air maldistribution actuating on the distribution of the refrigerant along the evaporator circuits. With this optimization strategy, they were able to obtain a maximum heat recovery of about 4%.

Recently, differently from the previous works, Datta *el al.* (2014) studied the performance of an automotive air-conditioned system with restricted airflow through the condenser. In their work, they block the frontal area of a microchannel condenser, obtaining a reduction of the airflow rate of about 30, 40 and 50% depending on the type of blockage used: peripheral, side and middle, respectively. In this work, Datta *et al.* (2014) analyzed different thermal-hydraulic parameters on both air and refrigerant side, concluding that the performance degradation of the automotive air conditioning system is strongly connected not only to the air flow reduction through the condenser, but it also depends on the characteristics of the air maldistribution generated by the different types of blockage.

In general, the experimental work dealing with air maldistribution is always expensive and very time consuming; therefore, the most employed methodology for the characterization of the air maldistribution at the inlet of a HX is the utilization of CFD software. Recently, Yaïci *et al.* (2014)

presented a study regarding the effect of air maldistribution at the inlet of a round tube plate fins HEs. They employed a commercial CFD, which first was validated with success using both experimental data (Wang *et al.*, 1996) and another CFD model (Bhuiyan *et al.*, 2013). The application of the validated CFD model led to affirm that the air maldistribution affected considerably the values of some parameters, such as the Colburn factor (or heat transfer coefficient), friction factor and hence, on the air temperature distribution and pressure drop throughout the heat exchanger. Similar results were showed also by (Rossetti *et al.*; 2015). As Yaïci *et al.* (2014), also Rossetti *et al.* (2015) used a CFD model for characterizing the heat transfer and pressure drop through a round-tube heat exchanger. Moreover, apart from the characterization of the air maldistribution, they also applied their model for the optimization of the round-tube HE used as evaporator in an open display cabinet.

In many studies, the results CFD calculations have been used in combination with simpler thermodynamic models. In these cases, the air velocity distribution was evaluated by means of a commercial CFD software, while the performance variation was calculated with simpler thermodynamic model. This strategy allows reducing the evaluation effort maintaining at the same time very good agreement with the experimental data. The combination of CFD and1D model was used with success for the optimization of different types of heat exchangers. Singh *et al.* (2011) simulated with high accuracy (error < 4%) the performance of a round tube condenser characterized by maldistribution in the air side. Similarly, Lee *et al.* (2010) and Kumar *et al.* (2016) worked on the optimization of big A-Shape condensation units. These two studies targeted the optimization of the relative position of the heat exchangers in specific A-Shape condenser used in large air conditioning systems.

Although the combination of CFD and 1D software allowed reducing significantly the calculation efforts, most of the studies published in the last years about the effect of the air maldistribution were performed supposing theoretical air velocity profiles at the inlet of the heat exchangers or using experimental data already available in literature.

One of the first studies based on this approch was presented in 1997 by Lee and Domanski (1997). Actually, they developed a new software (EVAP5M) able to take into account at the same time both the refrigerant and the air maldistribution. In their work, Lee and Domansky (1997) considered the possibility to simulate three different tube-and-fin evaporators under different refrigerant and air maldistribution types. The results showed that, although in a different way, both types of maldistribution affect negatively the thermal capacity of the heat exchangers. In the worst case, the cooling capacity was about 40% less than the baseline test (characterized by uniform flow distribution).

Similar results were obtained by Aganda *et al.* (2000), which studied numerically the performance of an evaporator built-in a package air conditioning. They used the heat transfer model (ACOL5) for

simulating independently each circuit of the evaporator, then, the global thermal capacity degradation was evaluated as sum of each addend. The results of this study highlighted that the air maldistribution and refrigerant distribution were strongly connected each other; in the worst case the loss of heat capacity of the heat exchanger turned out to be around 38%.

Some years later, the experimental work performed by Yashar *et al.* (2008) was used by Domanski *et al.* (2010). Their intention was to develop a new model able to optimize automatically the design of the HX circuits, depending on the typology of air maldistribution. They obtained very good results combining the EVAP-COND (2010) software and ISHED (Intelligent System for Heat Exchanger Design). Essentially the results of work led to redesign the heat exchanger, which with a reduced number of tubes and a new disposition of the circuits was able to obtain a thermal capacity improvement up to 5.2% compared with the original configuration.

Encouraged by the good results presented by Domansky *et al*. in 2010 some other researchers also tried to analyze the effects of the air and refrigerant maldistribution on the performance of heat exchangers of air conditioning systems. For instance, Kaern et al. (2011) analyzed separately the effects of different flow maldistribution on the performance of a residential air-conditioning system equipped with a round tube evaporator using their own heat transfer model. In this study, no experimental data were used and the model validation was performed comparing the results of the model with those provided by the commercial software Coildesigner (2010). The simulations carried out in this work included numerous studies oriented to analyze the effect of the air maldistribution on the performance of an A-Shape evaporation unit. As obtained by Lee and Domansky (1997) and Aganda et al. (2000), when a strong air maldistribution characterize the evaporator inlet, also Kaern *et al.* (2011) found a strong performance reduction of about 50%.

In 2012, the segment-to-segment approach was implemented in the evaporator model built-in the software ACHP (Bell, 2012) for analyzing the behavior of an 8-circuit evaporator. Considering four different theoretical air velocity profiles (linear, pyramidal and half-linear), the authors conclude that the negative effects of the air maldistribution can entail a substantial performance reduction of about 80%. This so negative result pushed the author to identify a new strategy for limiting such high performance reduction, named hybrid evaporator, which allowed recovering up to the 94% of the heat degradation in comparison with the original configuration. In 2014, Bach *et al.* (2014) presented a new numerical study aimed at the mitigation of the effects of the air maldistribution on the performance of a round-tube evaporator.

In regard to the effect of air maldistribution on condenser performance, Mao *et al.* (2013) published a new mathematical model for the estimation of the performance of a multi louver plate tube condenser. The model was based on the integration of the energy balance equations by mean of the FVM (Finite Volume Method) and it was validated adopting a wide range of experimental data. The

results of this publication showed that, when no air maldistribution is considered, very good agreement with the overall set of experimental data could be obtained. In the work, the model is used for calculating the effects of the air maldistribution on the global performance of the condenser. Simulating four different theoretical airflow patterns (uniform, parabolic, saddle and linear), Mao *et al.* (2013) found out a maximum thermal capacity reduction was only of about 5%. Furthermore, they also noticed a strict relationship between the value of the refrigerant mass flow rate and the performance degradation due to the air maldistribution. Essentially, under the same uneven air velocity profile, the higher is the refrigerant mass flow rate, the more important is the performance degradation.

1.3 Motivation and research objectives

Given the important role of HEs on the performance of all thermal systems, over the last few years, heat exchangers modelling became an important focus for Research. As discussed in the previous sections, different new solutions have been rolled out. The application of new calculation methods combined with sophisticated numerical solution strategies ensures that all modern simulation HE software packages are able to reproduce the behavior of the heat exchangers in different operating conditions with high accuracy. If on the one hand, such success is the result of the ability to set-up properly the mathematical problem, on the other hand, it is due the numerous efforts made for understanding and adequately model the complex physical phenomena occurring at the heat exchanger. The study of the heat transfer mechanisms, combined with the analysis of the pressure drop, being the key point for obtaining the most accurate predictions. In this context, given the huge variety of correlations available in literature, the first question for the software developers is how to decide which ones are the most accurate and the most suitable for their needs. Starting from this observation, one of the objective of this thesis is to provide a general procedure through which, depending on the application, it is possible to identify the best set of correlations for both HTCs and friction factors. The author will attempt to provide a methodology as general as possible for this complex task, with the additional objective of being independent on:

- The employed mathematical model.
- The number of considered correlations.
- The extension and amount of the available experimental data.

Even though the HT and pressure drop correlations play a fundamental role in the simulation of heat exchangers, also the modelling of other secondary phenomena that take place inside the tubes during the heat transfer processes is of help to improve even more the accuracy of the current condenser models. Starting from this consideration, the second objective of this work is the definition of a simple method for taking into account the convective condensation of the superheated vapor. As

already mentioned, this phenomenon takes place in the condensers when the internal surface of the tubes reaches the local saturation temperature of the vapor. The presence of condensation at the wall affects the local heat transfer mechanism and greatly influences the heat transfer coefficient. The performed work shows that the inclusion of this mechanism in a traditional condenser model significantly improves the accuracy of the predicted wall temperature distribution.

Finally, one of the aspects which came out from the performed literature review is that, there is a lack of experimental information about what is the effect of the air maldistribution on the condenser performance. This is the reason why, the third main objective of the thesis is represented by the attempt to provide a simple methodology for the experimental analysis of the effects of air maldistribution on the performance of the conventional and microchannel condensers. This part of the study will consist of the following items:

- It will be qualitatively analyzed the flow regimes characterizing the air side of a condenser.
- Several technologies for measuring the air velocity at the inlet of a heat exchanger will be compared.
- A simple methodology for generating artificially any air velocity profile at the inlet of a heat exchanger will be presented.
- The experimental results obtained measuring the performance of a condenser under a "real" air maldistribution will be measured and discussed.

1.4 Thesis organization

The entire thesis has been divided in 6 main chapters. In the first chapter, the introduction, the literature review and the objectives of the thesis have been just presented.

In the three central chapters (3, 4 and 5) three "macro" topics will be dealt with in detail. As will be pointed out later, for each of them, the work has been developed in parallel dealing for a round tube plate fins (RTPFs) and for the microchannel condenser (MCHX) at the same time. If on one hand, this parallelism lead to be sometimes repetitive, on the other, it presents the enormous advantage to compare "step by step" the results obtained from testing and simulating two different technologies of heat exchangers.

All simulations have been carried out by means of IMST-ART software (IMST-ART, 2010). In this calculation platform, the round-tube and MCHX share the same segment-by-segment calculation methodology. A general overview of the main model, the governing equations and the numerical solution strategy are presented in the Chapter 2.

Part of this PhD thesis has been developed in collaboration with the Universidad Politecnica de Cartagena where most of the experimental work was carried out. In Chapter 3, after the description

of the experimental installation, the results of an extended experimental campaign used for a discussion about the methodology for validating a condenser model considering different correlations for the HTC and pressure drop will be deeply analyzed. As it will be shown later, the results of the validation process lead to identify the set of correlations according which the best agreement between experimental data and the simulation results is obtained.

However, according with the experimental observation of the temperature profiles along the entire heat rejection process, the incorrect evaluation of the heat rejection was located just before the condensation process. This evaluation error was attributed to the incorrect evaluation of the heat transfer coefficient in the area of the heat exchanger usually called "condensing superheated vapor zone". Therefore, in Chapter 4, two different strategies for including in the current condenser model the condensation of the superheated vapor will be firstly described and then compared.

Chapter 5 is totally dedicated to the study of the effect of the air maldistribution on the performance of the condensers. The chapter is opened up with a detailed description of the necessary steps for generating the desired air velocity profile at the inlet of any air-to-refrigerant heat exchanger. Afterwards, the experimental results will be deeply discussed, and finally employed for the validation of the final model.

The thesis finishes with Chapter 6, where the global conclusions and the future work related to the present thesis will be listed and commented.

Chapter 2

2. Condenser model description

Traditionally, the Logarithmic Mean Temperature Difference (LMTD) method and/or the ε-NTU method have been widely used for the simulation of the performance of all the types of heat exchangers. Nevertheless, being based on some simplification hypothesis, such as steady flow, single-phase flows, constant fluids proprieties and negligible longitudinal heat conduction, both these methods turn out to be too inaccurate when phenomena like two-phase flow process, air dehumidification and flows maldistribution are taking place.

According to what mentioned above, the ε-NTU method (or the Logarithmic Mean Temperature Difference method) is particularly suitable for the simulation of the one-phase flow heat exchangers. For this type of devices, the estimation of the temperature profiles of the working fluids along the heat exchanger is not a priority. Indeed, the good prediction of the performance can be also obtained only considering at the average temperature between the heat exchanger inlet and outlet. On the other hand, for the condensers or evaporators, the correct estimation of the global performance is strictly connected to the detailed evaluation of the thermo-hydraulic proprieties of the refrigerant and air along the entire heat exchanger. With this purpose, over the years, two different approaches have been widely used. At the beginning, with the moving boundary 3 phases approach, the two-phase heat exchangers were only divided in three big control volumes identified by the areas occupied by superheated vapor, two phase flow (condensation or evaporation) and subcooled liquid. For some kinds of applications such simple modelling approach would be sufficient. Indeed, especially in the past, the moving boundary 3 phases approach was widely used because the objective to have very low calculation efforts was much more important than the necessity to have very detailed results. Nowadays, the utilization of more and more powerful computer allows using also very complex model for the simulation of the heat exchangers. In this context, the most widely used modelling approach is based on the segment-by-segment method. In general, this method requires the discretization of the heat exchanger in a certain number of cells (or control volumes), the definition of the numerical scheme (or mathematical problem) resulting by the integration of the governing equations, and then, the application of mathematical method for its solution.

In the present chapter, a description of the condenser model built-in the simulation software IMST-ART (IMST-ART, 2010) will be carried out. The model is based on the segment-by-segment approach, hence the governing equations, their integration and the global solution strategy will be

described in detail for the round tube heat exchanger. Afterwards, since the governing equations on the refrigerant side and the global resolution strategy are the same, only a general overview of the microchannel heat exchanger model proposed by Martinez-Ballester *et al.* (2013) will be also provided.

2.1 Fin-and-tube condenser

2.1.1 Geometric discretization

As will be discussed later, in order to discretize the governing equations and solve numerically the resulting system of algebraic equations, the heat exchanger must be necessarily discretized. It means that the volumes occupied by the working fluids and the separating walls must be divided in a certain number of cells (or control volumes). The discretization process has to be performed only respecting one main condition: the volume occupied by the fluids and the wall have to be completely covered without any overlapping. In addition to this restriction, in order to keep the calculation time as low as possible, the assumption that characteristics of the fluid only change along one dimension has to be also considered. In other words, the discretization of the volumes must be done in such a way that the real flows are represented as accurately as possible with a series of one dimensional paths. With the segment-to segment approach no restrictions on the cell size are necessary, given that any separating wall cell between two fluid cells must be coincident with the shared side of the fluid cells. In order to clarify what has been just described, in Figure 2.1 is depicted the general cell discretization of a cross flow heat exchanger.

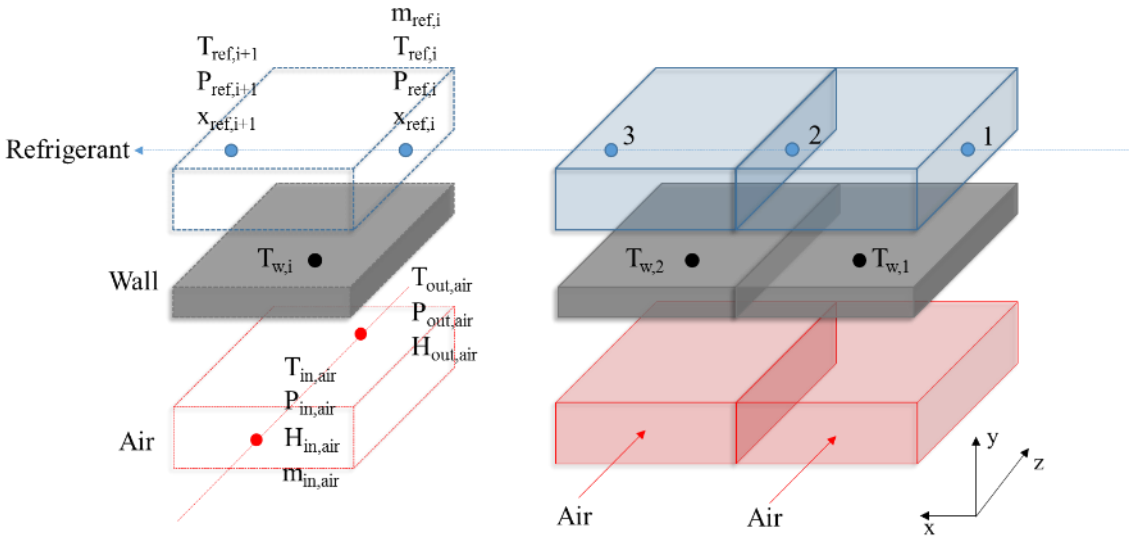

Figure 2.1: Cell discretization

As will be discussed in this chapter, the integration of the governing equations requires the definition of a certain number of "nodes" where the thermodynamic properties have to be calculated. In Figure 2.1 is also depicted the position of the nodes used in the condenser model built-in the IMST-ART (2010). Synthetically, two nodes (one inlet and one outlet) characterize the fluid cell, while the wall cells just present one centered node. As discussed by Corberán *et al.* (2001), such configuration allows combining reasonable calculation times with the highest accuracy of the results.

Finally, in the same figure, the axes according with the governing equation will be referred are also represented. Actually, the refrigerant is considered going through the heat exchanger in the x direction, while the air is crossing the device along the z direction.

2.1.2 Governing equations

2.1.2.1 Refrigerant side

According with the Cartesian reference in Figure 2.1, the governing equations for a single phase 1D steady flow along a channel of a round tube plate fins (RTPFs) heat exchanger are:

$$G = \rho u = const. \tag{2.1}$$

$$\frac{dp}{dx} = -\frac{d\left(\rho u^2\right)}{dx} - f\,\frac{1}{2}\rho\frac{u^2}{D_h} - \frac{d\left(zg\rho\right)}{dx} \tag{2.2}$$

$$A\cdot G\frac{d\left(h+\frac{u^2}{2}\right)}{dx} = P\alpha\left(T_{w,i}-T\right) \tag{2.3}$$

All the equations are written considering that the fluid interacts only with the tube wall. Hence, Eq. 2.1 represents the conservation equation in one of the sides of the HX; the static and dynamic pressure variation is calculated with the momentum conservation equation (Eq. 2.2), while the temperature in each node is evaluated using the general energy balance for open systems (Eq. 2.3).

In the case of an evaporator or a condenser, the 2-phase flow with phase change occurs. In this case, considering the *separated flow model*, the governing equations can be written as follows:

$$G = \rho u = const. \tag{2.4}$$

$$-\frac{dp}{dx} = \frac{2f\cdot G^2\left(1-x\right)^2}{D_h\rho_f}\Phi_f^2 + G^2\frac{d}{dx}\left(\frac{x^2}{\rho_g\gamma} + \frac{\left(1-x\right)^2}{\rho_f\left(1-\gamma\right)}\right) + \left(\gamma\rho_g + \left(1-\gamma\right)\rho_f\right)g\sin\theta \tag{2.5}$$

$$AG\frac{\partial}{\partial x}\left[x\cdot\left(h_g+\frac{G^2x^2}{2\rho_g^2\gamma^2}\right)+(1-x)\left(h_f+\frac{G^2(1-x)^2}{2\rho_f^2(1-\gamma)^2}\right)\right] + AG\frac{\partial}{\partial x}(zg\sin\theta)=P\alpha(T_w-T) \tag{2.6}$$

Eq.2.4 states the conservation of the mass flow rate and the mass velocity all along a fluid path. The mass flow rate is considered one of the inlet conditions, so that G is always considered as a known variable.

Like the one phase flow equations, in the momentum equation is considered the sum of three different components. With reference to the Eq. 2.5, the first component is represented by the frictional pressure drop. As mentioned, considering the *separate fluid model*, the 2-phase multiplier (Φ^2) is used. The second component of the equation allows the evaluation the pressure drop due to the acceleration of the fluid, while with the last one, the geodetic pressure drop is evaluated. The energy balance (Eq. 2.6) is also written under the hypothesis of the *separated flow model*. Unlike the one phase flow, in addition to the to the enthalpy and kinetic energy variations, also the potential energy variation is considered. Of course, this component depends on the inclination of the tubes respect to the horizontal axes, therefore, the angle θ plays a fundamental role.

In the equations 2.4, 2.5 and 2.6, the unknown variables are eight: quality (x), void fraction (γ), saturated conditions (ρ_l, ρ_v, h_l, h_v), pressure (p) and temperature (T). Evidently, the number of equations is clearly lower than the number of unknown variables, hence some further relationships must be stated. First, the assumption of thermodynamic equilibrium is adopted, so that the following set of state equations can be added to the system:

$$\begin{aligned} &T=T_{sat}(p) && \rho_v=\rho_g(p)\\ &h_v=h_{v\_sat}(p_{sat}=p)=h_g(p) && \rho_l=\rho_f(p)\\ &h_l=h_{l\_sat}(p_{sat}=p)=h_f(p) \end{aligned} \tag{2.7}$$

At this point, in order to close the system, only one equation is missing. Such equation has to describe the relationship between the void fraction and the rest of the variables. With this aim, also the following equation has to be added to the final system:

$$\gamma=\frac{1}{1+S\frac{1-x}{x}\frac{\rho_g}{\rho_f}} \tag{2.8}$$

However, Eq. 2.8 introduces a new variable, the slip ratio, which has to be evaluated with a further correlation. The only way to close definitively the problem is to consider some empirical relationship

between the variables in Eq. 2.8. Numerous correlations can be found in the literature, however, in this work, the (Chisolm , 1972) correlation has been considered as the most suitable to be used:

$$S = \left[1 - x\left(1 - \frac{\rho_l}{\rho_g} \right) \right]^{\frac{1}{2}} \tag{2.9}$$

Considering the Eq. 2.9, the mathematical system is now definitively closed (nine equations are combined with nine unknown variables). Thus, to be integrated and solved, only a proper set of suitable boundary conditions has to be defined. In the next chapter, such topic will deeply discussed.

2.1.2.2 Air side

Unlike to the evaporators, due to the heat rejection, in the condenser models the air dehumidification process does not have to be take into account. Nevertheless, in IMST-ART (2010), the governing equations for this kind of heat exchangers can be considered as the simplification of the equation used for the evaporators. For this reason, in the present section, the complete governing equation will be briefly described. Like in the refrigerant side, also for the air, the governing equations are those stated for the mass, energy and momentum conservation. In the case of the differential surface shown in Figure 2.1, the following approximated equations are stated:

$$-\dot{m}_a\, dh = dQ - \dot{m}_a \cdot dW \cdot h_{s,wat} \tag{2.10}$$

$$dQ = \left[\alpha_c (T - T_{wat}) + \alpha_d (W - W_{s,wat})(h_{g,T} - h_{f,wat})\right] P dz \tag{2.11}$$

$$\frac{dp}{dz} = -\frac{d\left(\rho u^2\right)}{dx} - f\,\frac{1}{2D_h}\rho u^2 \tag{2.12}$$

Where $h_{s,wat}$ is the enthalpy of the saturated air at the water surface temperature.

The approach followed to treat the dehumidification process is the one proposed by (Threlkeld, 1974). Figure 2.2 shows an air cell in the more general case in which dehumidification of humid air takes place when the humid air is in contact with a cold surface. A water film is formed over the surface.

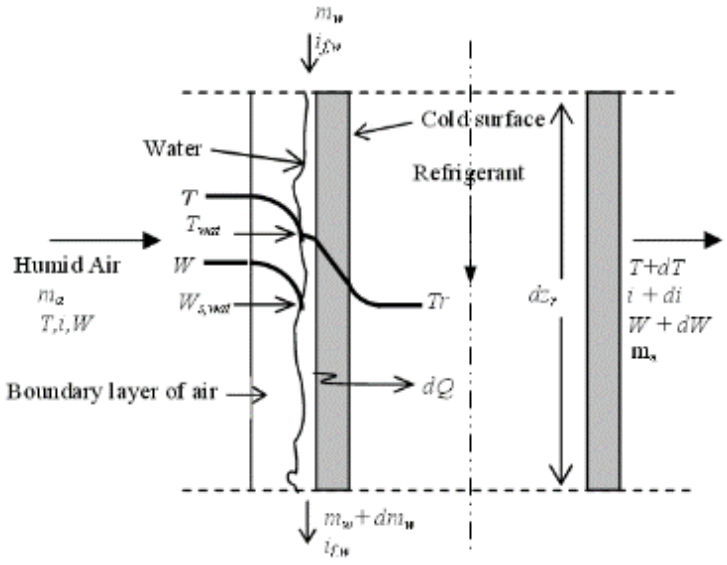

Figure 2.2: Schematic cooling and dehumidification of the humid air (Manual, IMST-ART 2010)

There is a limited boundary layer of air next to the water surface. The hypothesis that the air in contact with the water film is saturated at the temperature of the water surface, T_{wat}, is assumed.

Using the relationship, $L_e=\alpha_c/\alpha_d * C_{p,a}$, Eq.2.11 can be written as:

$$dQ = \frac{\alpha_c P dz}{C_{p,a}}\left[(h - h_{s,wat}) + \frac{(W - W_{s,wat})(h_{g,T} - h_{f,wat} - 1061 L_e)}{L_e}\right] \tag{2.13}$$

The second term in Eq.2.13 is negligible compared with the first one, so that the heat transferred can be approximately calculated as follows:

$$dQ = \frac{\alpha_c}{C_{p,a}}(h - h_{s,wat}) P dz \tag{2.14}$$

Eq.2.14 allows an analysis much easier than Eq.2.13. An additional equation is also normally used to simplify the description of the process, i.e. the assumption that the enthalpy of the saturated air is a linear function of the temperature: $h_{sat} = a+b*T_{sat}$, where a and b are some coefficients, which must be calculated from suitable plots proposed by Threlkeld (1974). Finally, in order to take into account the conduction across the water film, Eq.2.14 is now modified, leading to:

$$dQ = \frac{\alpha_w}{b_w}(h - h_{s,w}) P dz \tag{2.15}$$

Where $h_{s,w}$ is the enthalpy of the saturated air at the wall temperature, and:

$$\alpha_w = \frac{1}{\frac{C_{p,a}}{(b_w \alpha_C)} + \frac{e_w}{k_w}} \tag{2.16}$$

Where k_w is the water thermal conductivity, b_w is the slope of the curve h-T and e_w is the thickness of the water film. Eq.2.15 shows that the heat transfer process is governed by the difference between the enthalpy of the humid air and the enthalpy of the saturated air at wall temperature as a driving potential.

However, for the numerical scheme in the wall temperature calculation, it is more convenient to use a temperature difference as the driving potential. Starting from this assumptions the energy balance can be written as in Eq. 2.17. As already discussed earlier, the total heat transferred consists of a sensible part and the latent part.

$$dQ = [\alpha_c (T - T_w) + \alpha_D h_{f,g} (W - W_{s,w})] P dz \tag{2.17}$$

The above expression can be casted as a function of the temperature difference in the following way:

$$dQ = \alpha_C \left[1 + \frac{h_{f,g}}{C_{p,a}} \frac{W - W_{s,w}}{T - T_w} \right] (T - T_w) P dx = \alpha_{eq} (T - T_w) P dz \tag{2.18}$$

Where $\alpha_{eq} > \alpha_C$ and the term into brackets represents the enhancement factor of α_C due to the condensate. As discussed at the beginning of this section, in a condenser, the dehumidification process does not take place. Therefore, for this kind of heat exchangers, the term in the brackets is always equal to 1, hence α_{eq} is always equal to α_C. The value of the heat transfer coefficient comes from semi empirical correlations. In the next chapter, will be discusses in detail how to choose the best correlations among those available in literature.

2.1.2.3 Walls

For the walls, the equation to be written is the balance of the heat exchanged with the surrounding fluids and the heat transferred by longitudinal conduction along the wall, i.e.:

$$\begin{aligned} & ke \nabla^2 T_w + \textstyle\sum_{i=1,2} q_i = 0 \\ & q_i = \frac{Q_i}{\Delta x_i \Delta z} \\ & Q_i = \int_0^{\Delta z_i} P_i \alpha_i (T_w - T_i) d x_i \end{aligned} \tag{2.19}$$

Where the heat flux is the heat over the total heat transfer area. According with this sentence, in the equations 2.19 is index *"i*", which can assume the value 1 or 2, is used for indicating the heat transfer in the refrigerant or the air side.

Normally, the effect of the longitudinal conduction is negligible so that the wall energy equation becomes the balance equation for the heat exchanged between fluids:

$$\sum_{i=1,2} Q_i = 0 \tag{2.20}$$

The boundary conditions are given by the conditions of the fluids at the entrance of the heat exchanger. They will be commented in the next chapter.

2.1.3 Numerical scheme and global solution strategy

As already mentioned, the traditional calculation methods, such as the Logarithmic Mean Temperature Difference (LMTD) and the ε-NTU methods are based on some simplification hypothesis, which do not allow using them when some complex phenomena take place in the heat exchangers. For considering the presence of the two-phase flow, air dehumidification and flows maldistribution (refrigerant and air), the segment-by-segment approach is now widely used. Based on such modelling approach, Corberán *et al*. (2001) proposed a new method called SEWTLE (for Semi Explicit method for Wall Temperature Linked Equations) for integrating and solving the mathematical system composed by the governing equations (see previous section). The method is characterized by high flexibility, it can be applied to any flow arrangement and geometrical configuration and, furthermore, it offers excellent computational speed. In addition, as in the present work of thesis, it can be used for combining single and 2-phase flow.

According to the SEWTLE method, the numerical scheme is the result of the strategy used for "sectioning" the heat exchanger. According to the discretization and the arrangement of the nodes represented in Figure 2.1, in case of single phase heat exchangers, the energy and momentum equations are considered completely uncoupled. Hence, integrating together the Eq. 2.3 and the equations of state (Eq. 2.1), the temperature solution at the outlet of the fluid cells can be easily calculated. Independently by the temperature evaluation, the integration of momentum Eq. 2.2 allows estimating the pressure and density variation along the fluids paths.

In case of two phase HX, the energy (Eq. 2.6) and momentum (Eq. 2.5) equations are coupled each other by the pressure. In other words, since all the variables mainly depend on the pressure, the momentum equation may be integrated first. Afterwards, only when the pressure at the outlet of the fluid cell is known, the energy equation can be integrated too, leading to the evaluation of the enthalpy, the vapor quality and the rest of variables at the outlet of the cell. Actually, in this chapter the complete numerical scheme is not reported. However, the result of the integration of all the governing equations is described in detail by Corberán *et al*. (2001).

When all the equation have been integrated, once assigned the correct set of boundary conditions, the SEWTLE method further includes an iterative procedure for solving the resulting mathematical problem (algebraic, non-linear system of equations). The numerical procedure is aimed to identify the temperature in every wall cell, such as the energy balance in the internal and external side of the

HX becomes equal (Convergence criteria). To do that, first a guess is made about the wall temperature distribution. Afterwards, the governing equations for the fluid flows are solved in an explicit manner. All the outlet conditions are calculated in any fluid cell starting from the inlet conditions. Hence, excluding the first cell, the outlet conditions of the cell *i* always represent the inlet conditions for the cell *i*+1. Once the solution of the fluid properties is obtained for all the nodes, the new wall temperature distribution is estimated applying the energy balance (Eq. 2.20). The numerical scheme developed for the calculation of the temperature at every wall cell is also explicit, so finally, the global resolution strategy can be considered as an iterative series of explicit calculation steps. The procedure is repeated for certain number of iterations, as far as the convergence criteria is respected in all the cells of the HX.

2.2 Microchannel heat exchangers

The model used in this work of thesis for calculating the performance of a microchannel condenser is the 1Dx3 proposed by Martínez-Ballester *et al.* (2013). As for the conventional heat exchangers, also the 1Dx3 model is based on the application of the segment-by-segment approach combined with the application of the SEWTLE method (Corberán *et al.*, 2001). Nevertheless, although the global solution strategy adopted by Martínez-Ballester *et al.* (2013) is very similar to that presented in the previous subsection, the microchannel condenser model presents some particularities due to the different interpretation of the phenomena occurring in the air side.

Effectively, (Martinez-Ballester, et al., 2011) studied the heat transfer mechanism in the air side of a microchannel condenser by means of the application of their own Fin2D model. The model provided very detailed results (especially in terms of temperature distribution in the air side and along the fins) but, it was characterized by very high calculation time. Aimed to reduce the computational costs and maintaining a reasonable level of accuracy, Martinez-Ballester *et al.* (2013) proposed a modified version of the of the Fin2D, the 1x3D model. The latter model was designed considering the following aspects:

- The longitudinal conduction in the fin along the air flow direction can be considered negligible.
- The air temperature profile can be considered quite flat along the direction between the tubes, except for the air close to the wall.
- Due to this characteristic of the air temperature profile, instead of discretizing the fins, the hypothesis behind the *fin theory* can be considered verified.

According to this background, Martinez-Ballester *et al.* (2013) proposed a new discretization of the airside volume (Figure 2.3).

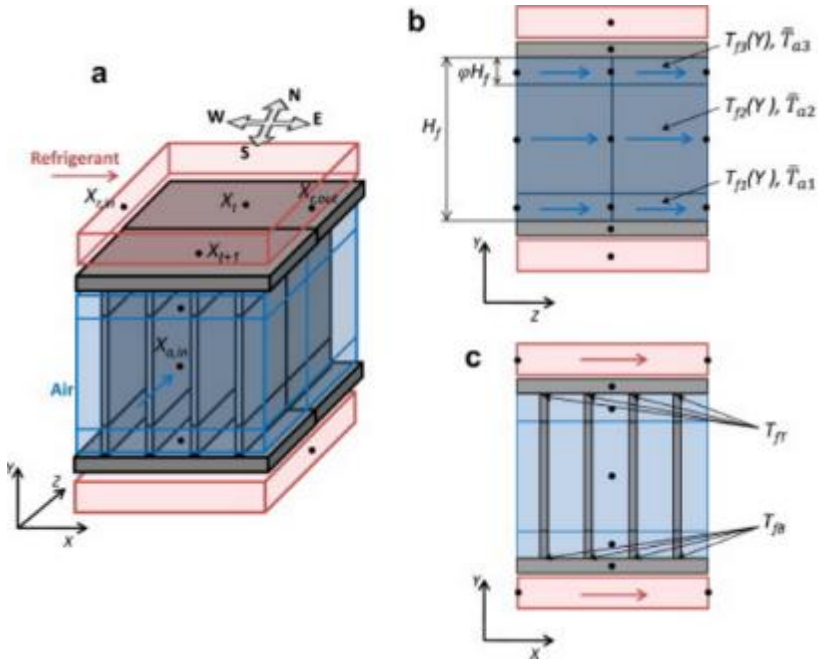

Figure 2.3: Different views of a discretized portion of the heat exchanger (Martinez-Ballester et al., 2013)

As depicted in in the figure, the entire air side volume was mainly divided in two columns (z direction), then, each column was furtherly divided considering three cells along the y-direction: two cells close to the tube walls for caching the temperature variation; the third is between them. Otherwise, with respect to the round-tube condenser model, Martinez-Ballester *et al.* (2013) maintained unchanged the discretization of the refrigerant volume and tube wall. Starting from this "new" air side discretization, as for the round-tube condenser model, the numerical scheme was obtained by the integration of the governing equation by means of the SEWTLE method. Finally, the solution to the mathematical problem was obtained using the same methodology described for the round-tube condenser (Paragraph 2.1.3).

Chapter 3

3. Analysis of heat transfer and pressure drop correlations

Excluding the effects on the heat transfer of the air dehumidification, what differentiates a condenser model from an evaporator model are fundamentally the different correlations (or models) used for the estimation of the heat transfer coefficients and friction factor in both refrigerant and air side. As pointed out in the introduction, numerous authors have proposed their studies related to these topics, therefore the number of correlations available in literature (or model) has been growing rapidly over the years. In principle, the choice of the best correlations is firstly driven by important parameters such as accuracy, robustness and ability to extrapolation, but also other aspects have to be taken into account. If on one hand, a good correlation may fall into an error band of 20%-30%, when the calculated HTC and PD are compared with the relative experimental data, on the other, once used in a condenser model, it has to allow the correct evaluation of the thermal capacity, condenser temperature or even the COP when the model predicts the global performance of a refrigerator system.

In most of the studies described in the introduction, the authors usually choose a specific set of correlations and thus report the results of the simulations only in terms of thermal capacity regardless the objective of using the model. From this point of view, the importance of the validation process could be considered sometimes even neglected. However, the validation methodology represents a crucial process and becomes one of the fundamental steps in the overall simulation process (Corberán and Melòn, 1998), if it is used for the identification of the best set of correlations for calculating both HTC and friction factors.

In this chapter, a discussion about the different methodologies to validate a model will be dealt with. Two different options to define the boundary conditions in the refrigerant side will be compared and a discussion about a correct interpretation of parameters such as mean error, mean square error and standard deviation will be presented. The results obtained by using the traditional boundary conditions (inlet temperature, mass flow rate and inlet pressure), widely used in several previous studies, will be commented on and compared with those obtained by using subcooling, mass flow rate and inlet temperature. The discussion is supported by an experimental study that includes a specific test campaign designed to cover a wide range of operating points and perform a suitable sensitivity analysis.

The RTPFs and the MCHX models described in the previous section are already implemented in the simulation software IMST-ART (2010), which, therefore, will be used over all the next chapters of the thesis.

3.1 Experimental set-up

As mention in the introduction, the main project related to this work of thesis has been developed in collaboration with the Universidad Politécnica de Cartagena, where most of the experimental work was carried out. In particular, being the first goal of thesis the definition of a strategy for the identification of the best set of correlations for the evaluation of the HTC and PD, a wide experimental campaign was performed. During almost two years, a sophisticated experimental air-to-refrigerant heat pump was initially set-up and, then, accurately tested in order to provide the most suitable experimental dataset.

The installation was built in order to measure with the highest accuracy possible the thermo-hydraulic characteristics of both the refrigerant and air. Therefore, the refrigerant loop and the air loop where equipped with a significant number of sensors as depicted in the figures (Figure 3.1) and (Figure 3.2).

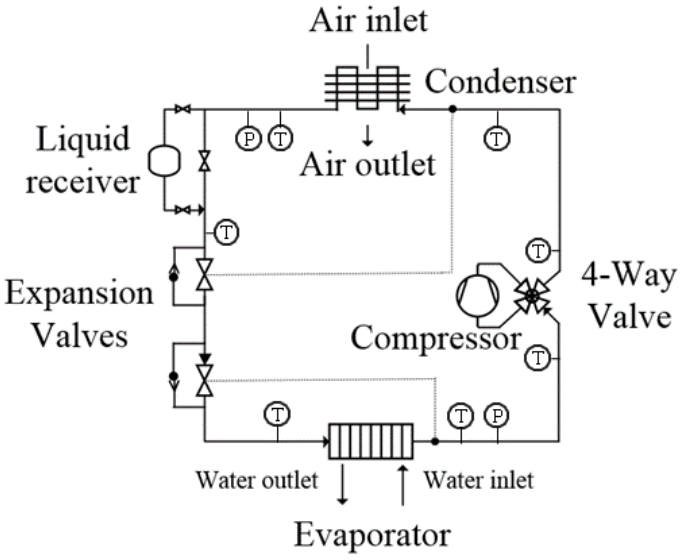

Figure 3.1: Refrigerant loop

In the refrigerant side, the reversible heat pump worked with R134a and it was equipped with a multi-speed hermetic reciprocating compressor with a displacement of 34.38 cm^3; a brazed plate evaporator (water-to-refrigerant) and an electronic valve as the expansion device. At the condenser outlet, a liquid receiver imposes the saturated conditions, while a 4-way valve is able to invert the cycle modifying the heat exchanger operation mode. Tests with a certain subcooling have been performed bypassing the liquid receiver and suitably adjusting the refrigerant charge.

The temperatures were measured along the refrigerant circuit positioning thermocouples and thermoresistences as depicted in Figure 3.1. Differential transducers evaluated the pressure drop across the heat exchangers in both the refrigerant and secondary fluid (condenser and evaporator), while the refrigerant mass flow rate is measured by means of a Coriolis mass flow meter (positioned in the liquid line).

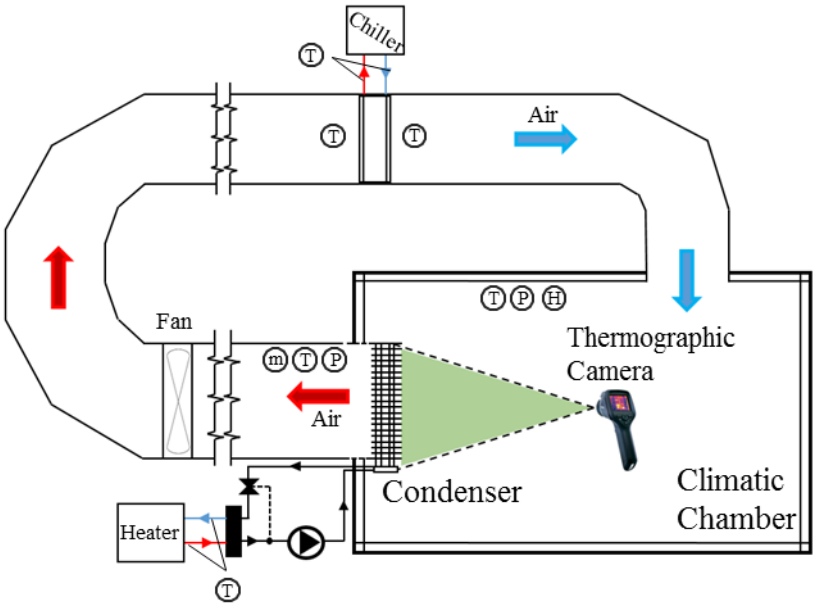

Figure 3.2: Scheme of the experimental installation

In the airside, during the tests, the air flow rate at the condenser outlet was measured inside the duct, just upstream of the variable rotation speed fan. Temperature, pressure and humidity were controlled in the climatic chamber and measured in some points along the air loop.

3.1.1 Heat exchangers: characteristics

The experimental campaign has been carried out in two consecutive steps: during the first part, a round tube plate fins heat exchanger (RTPF) has been tested. Later, the tests have been performed using a microchannel heat exchanger (MCHX).

The RTPF condenser consisted of two asymmetrical circuits (26 and 28 tubes). The refrigerant coming from the compressor got into the upper distributor, it went through the heat exchanger and, finally, it was mixed in the lower collector. The main dimensions of the sample are reported in Figure 3.3, while the other technical data are described in Table 3.1.

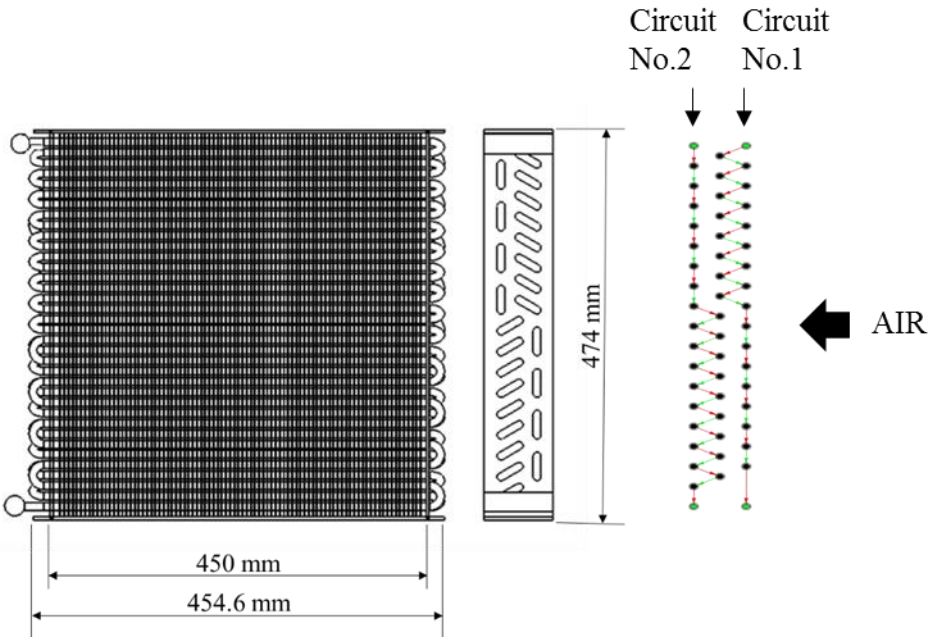

Figure 3.3: Round Tube Plate Fins (RTPFs) heat exchanger

Table 3.1: RTPFs technical data

General Dimensions	Number of rows	3
	Number of Tube per row	19
	Exchanger Width [m]	0.45
	Long. Spacing [mm]	21.9
	Trans. Spacing [mm]	25.35
	Number of Circuits	2
Tube Data	Tube material	Copper
	Outer Diameter [mm]	9.52
	Thickness [mm]	0.813
	Inner surface	Smooth
Fin Data	Thickness [mm]	0.1
	Fin Pitch [mm]	2.6
	Type	Plain
	Material	Aluminium

The second heat exchanger tested was a 33 multiport aluminum plate tubes MCHX: 340 mm width, 483 mm wide (Finned length) and 21.1 mm deep (Figure 3.4). In this case, the vapor got into the heat exchanger from the upper side, went through four passes (12 –7 – 6 – 8 tubes) and got out saturated or subcooled liquid depending on the system operating conditions. Louvered fins with a density equal to 14 FPI (Fin per inch) improved the heat transfer coefficient. Regarding the refrigerant side, the tube is characterized by eight triangular ports, having the hydraulic diameter equal to 0.78 mm.

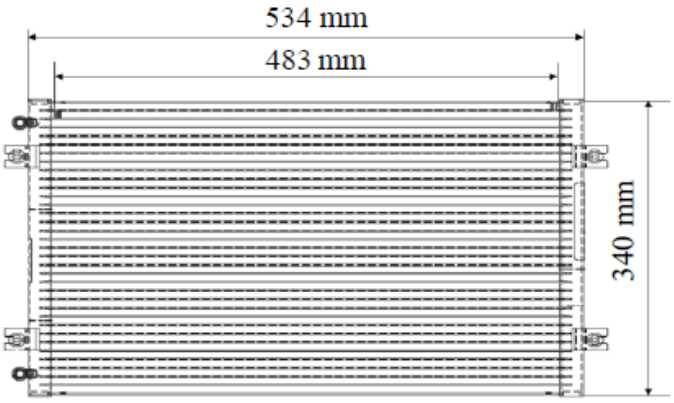

Figure 3.4: Microchannel heat exchanger

3.2 Experimental campaign

3.2.1 Tube-and-fins heat exchanger

The experimental campaign was planned in order to study independently the effect of several variables on the capability of the model to predict correctly the experimental data. To this end, the parameters modified during in the tests were divided in two main groups:

- Internal variables
  - **m_{ref}**: refrigerant mass flow rate
  - **SC**: condenser subcooling
  - **SH**: Evaporator superheat
- External variables
  - **T_{air}**: air temperature at the condenser inlet
  - **V_{air}**: volumetric air flow rate. Depending on its value, different air velocities (v_{air}) can be measured at the condenser inlet.
  - **$T_{water, inlet}$**: water temperature at the evaporator inlet.
  - **m_{water}**: water mass flow rate at the evaporator inlet

Effectively, the operating conditions can be changed mainly actuating on the thermo-hydraulic characteristics of the working fluid in both the heat exchanger sides. Hence, as previously listed, the experimental campaign was designed based on the modification of two sets of variables: internal and external. The first set of parameters can be changed regulating directly the components of the refrigerant loop (compressor and valves) or using a different refrigerant charge. On the other hand, the external variables can be changed actuating on the components out of the refrigerant loop, such as the climatic chamber, the fan or the heater (Figure. 3.2). In particular the parameters considered more interesting to analyze were the Air inlet temperature at the condenser inlet, the Air inlet velocity

and the Refrigerant mass flow rate. The latter parameter was modified playing with the subcooling at the condenser outlet (using different refrigerant charges), the compressor speed and finally modifying the evaporator temperature (regulating the inlet temperature of the water going through the brazed plate evaporator). In Table 3.2, the seventeen different tests performed are summarized.

Once defined a reference test (No.1), the further tests were carried out modifying just one (or two) of the operating parameters, keeping the rest of them constant and equal to their related reference value.

Table 3.2: Tube and fins heat exchanger - experimental data

Test	Variable parameter	Variable values
1	Reference test	T_{air}=35°C; T_{evap}=1.75°C; v_{air}=2.5 m/s; SC=0 K
2-3-4-14-15	Air inlet temperature	20-27-30-40-46°C
7-8-9	Air inlet velocity	1.5-3.2-4 m/s
12-13	Subcooling	5-10 K
10-11	Compressor speed	40-45 Hz
5-6-16-17	Evaporator temp. Air inlet temperature	-2.85-6.97-11.95-13.72°C 35-20-27-26.7°C

In Table 3.3, the experimental uncertainty is reported for all the main experimental parameters. In the upper part of the table, the uncertainty due to the direct measurement of some experimental parameters, such as temperature, pressure, mass flow rate and compressor performance, is shown.

Table 3.3: Experimental uncertainties

Uncertainty	Parameter	Instrument	Value
Instrument	Temperature	RTD 4 Wire	±0.055 K
		Thermocouple	±0.5 K
	Absolute Pressure	Pressure	±0.15 %
	Differential Pressure	Transducer	±0.15 %
	Mass Flow Rate	Coriolis Flow Meter	±0.10 %
	Compressor Power	Wattmeter	±0.5 %
	Compressor Speed	Frequency converter	±0.1 Hz
Propagated	Capacity	-	±0.018 kW
	Air-Ref. Capacities	-	> 0.98 %
	Condensation Temperature	-	±0.058 K

The uncertainty was calculated for the thermal capacity (measured in the refrigerant side) and the condensation temperature according to the Propagation of uncertainty. The numbers reported in the table are the average uncertainty calculated considering the entire set of experimental data. Uncertainties of about ±0.058°C in condensation temperature and less than 2% in capacity can be considered.

Moreover, also the global energy balance at the condenser expresses the reliability of the data. Expressed as the ratio between the thermal capacities measured in the refrigerant and that measured in the air side, the energy balance is reported in the table in the form of percentage. Once more, values always as close as possible to the 100% point out the accuracy adopted for the estimation of all the thermos-hydraulic parameters characterizing the regular operation of the experimental heat pump.

3.2.2 Microchannel heat exchanger

For the validation of MCHX model two different set of data have been used. Indeed, as well as using the data obtained in our experimental installation, the validation of the MCHX model has been extended including the data provided by an external company. Regarding the first group of data, as for the RTPFs condenser, starting from a reference test (air velocity = 2.5m/s; air temp.=35 ºC; Sucooling = 0 K), the others have been obtained modifying one by one the air inlet temperature (20-30-40ºC), the air inlet velocity (1.5-3.2-4 m/s), the subcooling (5-10-15-17-20-27 K) and the compressor speed (40-45 Hz).

Table 3.4: MCHX experimental data

Test	Variable parameter	Variable values
1	Reference test	T_{air}=35°C; T_{evap}=1.75°C; v_{air}=2.5 m/s; SC=0 K
2-3-4	Air inlet temperature	20-30-40°C
5-6-7	Air inlet velocity	1.5-3.2-4 m/s
8-9-10-11-12	Subcooling	5-10-15-17-20-27 K
13-14	Compressor speed	40-45 Hz

Some minor changes can be notice comparing Table 3.4 with data reported in Table 3.2. Indeed, for this heat exchanger, instead of studying the effect of changing the evaporation temperature on its performance, more and more attention was paid for analyzing the effects of the subcoling. Unlike the RTPFs, for the MCHX the subcoolig has been widely extended arriving up to almost 27 K. As will be shown later on, for such high value, the heat exchanger was almost totally filled up by liquid R134a with an evident performance reduction.

The second group of data includes the experimental results obtained testing five new samples in an external lab. Their main geometric characteristics are summarized in Table 3.5. The experiments were conducted in a big calorimeter, where, changing the air volumetric flow rate at the inlet of the heat exchanger, the condensation temperature, refrigerant inlet conditions and subcooling were maintained constant.

Table 3.5: Main geometric characteristics of five new samples

Case [-]	No. of tubes [-]	Tube depth [mm]	Finned length [mm]	Port design [-]	Fine type [-]	FPI [-]
1	40	27	794.5	Rectangular	Louvered	20
2	40	18.8	794.5	Rectangular	Louvered	20
3	40	27	794.5	Rectangular	Louvered	14
4	50	18.8	586.6	Triangular	Louvered	18
5	33	18.8	813.5	Triangular	Louvered	14

3.3 Validation methodology

As already highlighted previously, being based on the models described in the previous chapter, the commercial software IMST-ART (2010) has been used to predict the performance of both the tested condensers. The validation methodology discussed in this paragraph has a general value and can be applied to different types of heat exchangers, regardless by the correlations and the experimental data.

Once performed the experimental campaign, the second step of this work is to validate a condenser model, isolating the effect on the results of the different correlations to calculate the heat transfer coefficients and pressure drop in both air and refrigerant sides. To this end, when a certain correlation is studied, the rest of heat transfer and the pressure drop coefficients were kept constant. For instance, if the two phase-flow heat transfer coefficient is studied, the air side heat transfer coefficient and the pressure drop in both refrigerant and air sides remained constants. In this way the accuracy and robustness of a correlation is not affected, negatively or positively, by other correlations. The only exception is for the correlations developed for single-phase flow (either vapor or liquid), which are calculated with the correlations of Gnielinski (1976) and (Churchill, 1977), for heat transfer and pressure drop respectively. This decision was taken because it was assumed that they are accurate and robust enough for internal one-phase convection.

The values for the constant heat transfer coefficients and friction factors (Table 3.6) were the results of a pre-adjusting process of the model. It consisted on identifying enhancement factors such as the model is able to provide the minimum mean error in terms of total heat transfer and pressure drop. In other words, first the complete set of experimental data was simulated by means of IMST-ART considering the default setting (default correlations). Afterwards, the simulation were repeated applying different enhancement factors to the two-phase HTC, to the Air side HTC and to the friction coefficient in both the refrigerant and air sides, until the results of the model fitted with very good accuracy the experimental data. The constant heat transfer coefficients and friction factor were identified for each type of condenser (Tube-and-Fin and Microchannel) and for each of the experiments described in Tables 3.2 and 3.4.

Table 3.6: Values of the coefficients held constants

Correlation subject of analysis	**$HTC_{2\text{-phase flow}}$** [$W/m^2K$]	**$HTC_{air\ side}$** [W/m^2K]	**$\Delta P_{2\text{-phase flow}}$** [Pa/m]	**$\Delta P_{air\ side}$** [Pa/m]
$HTC_{ref.\ side}$ [W/m^2K]	Correlation analyzed	Fitted Value	Fitted Value	Fitted value
$HTC_{air\ side}$ [W/m^2K]	Fitted Value	Correlation analyzed	Fitted. Value	Fitted value
$PD_{2\text{-phase flow}}$ [Pa/m]	Fitted Value	Fitted Value	Correlation Analyzed	Fitted value
PD_{air} [Pa/m]	Fitted Value	Fitted Value	Fitted value	Correlation analyzed

Generally, to define the calculation of a condenser, two sets of boundary conditions are used. Table 3.7 lists the input parameters and output parameters for both the options. The main difference is the use of the subcooling (B) instead of using of the refrigerant inlet pressure (A). Based on this choice, there are some important consequences for the results. In Figure 3.5, the process (with the superscript ‘) in a pressure-enthalpy chart for both options A and B compared with the experimental one (without any superscript) is depicted. Figure 3.5 shows the scenario for a model that underestimates the heat transfer and one can notice how different the results for the options A and B will be. As one can observe in Figure3.5, for option A, the validation parameter would be the subcooling or alternatively the capacity, which will depend on the accuracy of the model. When the model underestimates the heat transfer defined with option A, which is widely used, it will result in a two-phase outlet: the lower prediction of HTC, the higher outlet vapor quality.

Table 3.7: Model input and output parameters

Methodology	**Input Parameters**		**Output Parameters**
	Common	**Specific**	
A	• Geometry • Refrigerant and secondary mass flow rates • Refrigerant and secondary inlet temperature	• Refrigerant inlet pressure	• Capacity • Subcooling
B		• Condenser subcooling	• Capacity • Inlet pressure

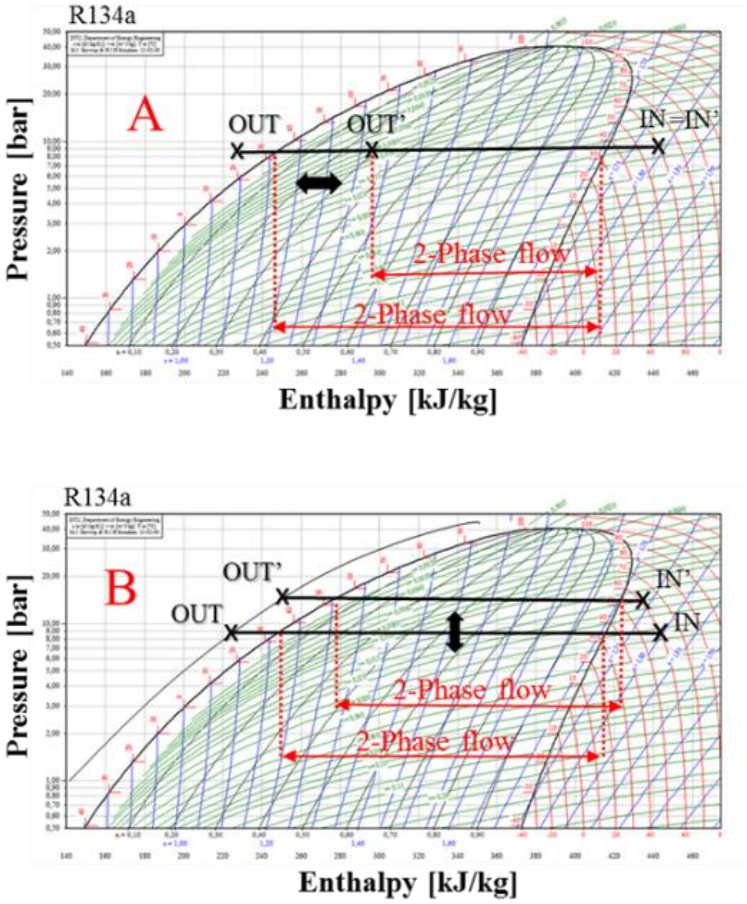

Figure 3.5: Illustration of the two discussed options (A and B) for defining the boundary conditions

This fact is contrary to the objective of validating the whole condensation process. Actually, the objective of a HTC correlation for simulating condensers is to correctly predict their global performance rather than accurately predicting the local values of the HTC. Indeed, an efficient correlation may overestimate the HTC in the range of high vapor quality and compensate this deviation, underestimating the same parameter in the last part of the condensation. Thus, by using option A, the comparison of the correlation could be carried out incorrectly since, if the saturated conditions at the condenser outlet are not reached, this compensation effect could be hidden. However, option B is different since now the subcooling is fixed and the validation parameter would be the condensing temperature: the lower prediction of the HTC, the higher condensing temperature (while for the capacity it is always opposite). Now, regardless of the accuracy of the model or the HTC correlation, the condensation will be completed. Since in the practical applications there is no condenser working with two-phase conditions at the outlet, the authors propose using the set of boundary conditions including the condenser inlet temperature; the refrigerant mass flow rate; and the subcooling (Table3.7). In this way all the correlations are tested in the whole and the same range of vapor quality regardless of its accuracy in the condensation path.

3.4 Analysis of heat transfer and pressure drop correlations

3.4.1 Tube-and-fins heat exchanger

3.4.1.1 Correlation for refrigerant heat transfer coefficients

According to the complexity of the heat exchanger models adopted and the suitability of the tested conditions, the correlations for calculating the HTC on the refrigerant side, which are considered the most interesting to compare and discuss in the present section, are: Shah (1976) , Dobson and Chato (1998), Cavallini *et al.* (2002) and Thome *et al.* (2003).

In Figure 3.6, these correlations are compared considering R134a as refrigerant and four different scenarios. Changing the vapor quality in the range 0.05-0.95, the behavior of the heat transfer coefficient has been simulated for four combinations of hydraulic diameter (D_h) and mass flux (G). This preliminary analysis has an important objective: detecting possible discontinuities, interruptions or anomalies in the heat transfer coefficient. Such issues can be so critical for numerical resolution strategy used for solving the condenser model. Indeed, due to the discontinuity of the heat transfer coefficient, the convergence could not be reached and the results provided by the model could be completely wrong.

Although the correlations show different local values of the HTC, a general trend can be detected. The two-phase HTC increases with the vapor quality. Furthermore, the analysis of Figure 3.6 leads to say that the no correlation presents discontinuities. The models proposed by Cavallini *et al*. (2002) and Thome *et al.* (2003) show a different slope that changes just in correspondence of the vapor quality where the flow regime changes. This behavior can be observer especially for the lowest vapor quality, where the flow regime changes from annular to stratified, wavy or mist flow, depending on the operating conditions. The older correlations proposed by Shah (1979) and Dobson and Chato (1998) behave differently. Their trends are uniform over the entire range of qualities because, during their development, no different regimes were considered. What is important to notice is that, for a specific value of the vapor quality and input parameters (for instance, D_h = 7 mm; G = 200 kg/m^{2}s), each correlation provides a different HTC in comparison with the others. For this reason, as will be commented later, the model provides different results depending on the correlation tested.

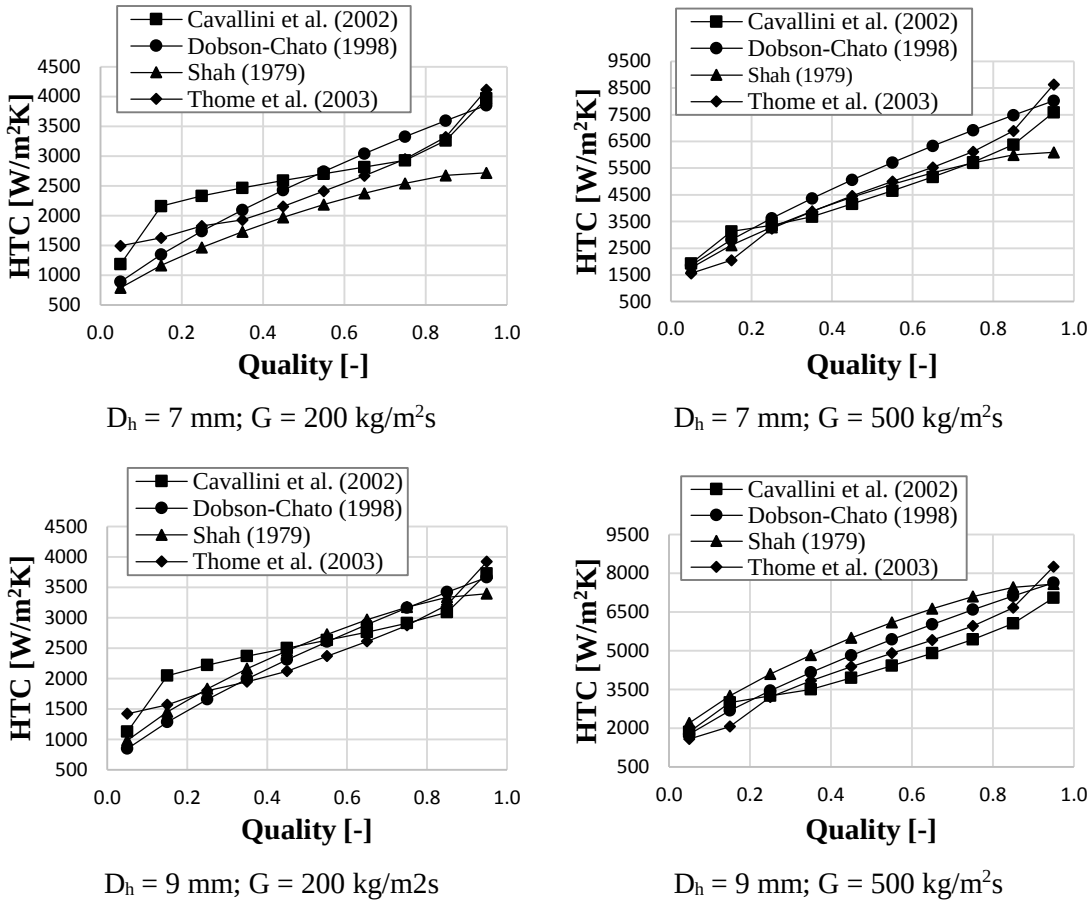

Figure 3.6: Preliminary analysis of the HTC correlations

The effect of each correlation on the global results has been analyzed in detail adopting the validation methodology presented in the previous subsection. The error, defined as the difference between the predicted value and the experimental one, is depicted in Figure 3.7 and Figure 3.8. The results confirm what was described above: if a correlation overestimates the HTC, the model will estimate lower condensation temperature, as well as higher capacity.

In the same figures, the results are presented highlighting the influence on the model prediction of each experimental variable shown in Table 3.2. The air temperature variation at the condenser inlet does not affect the performance of the model negatively. In fact, the error, although assuming a different magnitude depending on the correlation studied, can be considered rather constant. Subcooling and compressor speed variations mainly affect the refrigerant mass flow rate, but it does not clearly affect the magnitude of the error. However, the model shows high sensitivity to the air velocity and evaporation temperature variations.

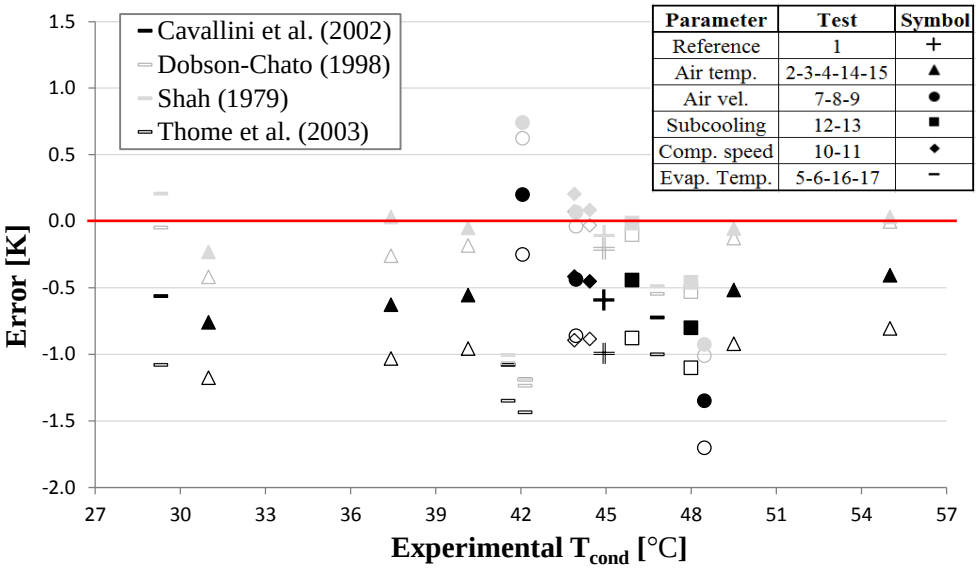

Figure 3.7: Comparison model plotted versus experimental saturation temperature

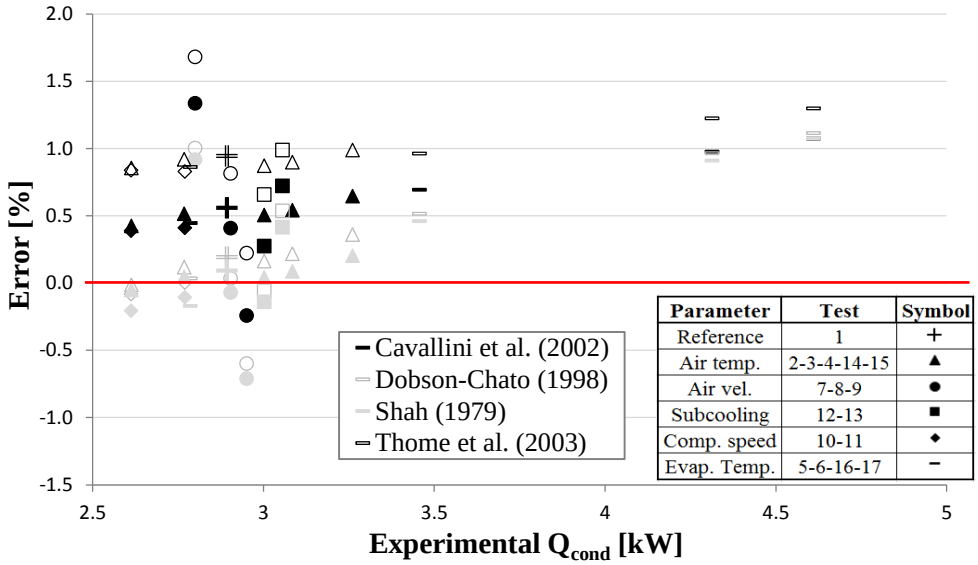

Figure 3.8: Comparison model versus condenser heating capacity

Figure 3.9 and Figure 3.10 show the thermal resistance ratio versus the air velocity and the evaporator temperature respectively. Figure 3.9 shows that, by increasing the air velocity, the air side resistance gets less weight in the global thermal resistance. However, as Figure 3.10 depicts, for the highest evaporator temperature, when the refrigerant mass flow rate assumes the highest values, the air side resistance is the most important.

Furthermore, in the same figures it can be observed that the air side resistance, being heavily dependent on the extended fin surface area, is about one order of magnitude larger than for the refrigerant side. Thus, the air side will be the dominant one in the validation process.

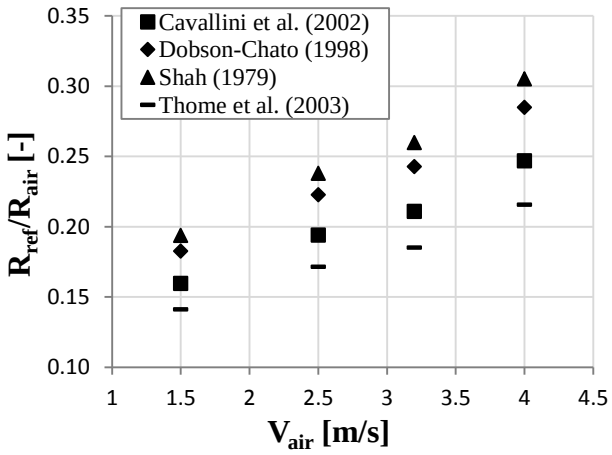

Figure 3.9: Thermal resistance ratio versus the air velocity

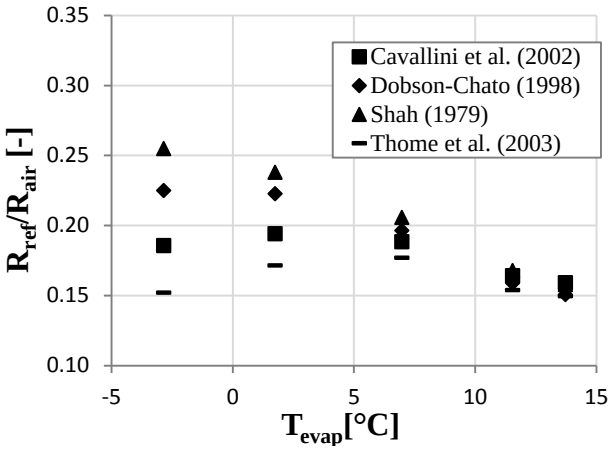

Figure 3.10: Thermal resistance ratio versus the evaporation temperature

Overall, from Figure 3.7 and Figure 3.8, Shah (1979~~)~~ could be identified as the correlation with lowest error. However, an opposite conclusion is suggested in the air velocity variation curve of these figures. When the air velocity reaches the highest value (the lowest value for the condensing temperature) the air thermal resistance has the lowest value so that the refrigerant side becomes more important in the heat transfer prediction. So, in the situation when the refrigerant correlation is more relevant, the worst prediction is given by Shah, while the best one corresponds to Thome *et al.* (2003).

In order to quantify the suitability of a correlation some metrics have to be defined. To this end, as shown in Table 3.8, the analysis of the results has been carried out also in terms of mean error (ME), standard deviation (SD) and mean square error (MSE).

Table 3.8 shows that for the refrigerant side the correlation with the lowest ME and MSE is Shah's correlation, while the correlation of Thome *et al.* (2003) has the largest values. However, the conclusion is the opposite if we analyze the SD.

Table 3.8: Analysis of the results varying the two-phase HTC correlations

	Cavallini et al. (2001)		Dobson and Chato (1998)		Shah (1978)		Thome et al. (2003)	
	T_{cond} [°C]	Q_{cond} [%]	T_{cond} [°C]	Q_{cond} [%]	T_{cond} [°C]	Q_{cond} [%]	T_{cond} [°C]	Q_{cond} [%]
ME	-0.63	0.57	-0.30	0.26	-0.19	0.16	-1.02	0.93
SD	0.354	0.347	0.466	0.445	0.489	0.463	0.308	0.297
MSE	0.51	0.0005	0.29	0.0004	0.26	0.0003	1.13	0.0010

The mean error is strongly influenced by the constant value used for the air side HTC, and both the ME and MSE are easily adjustable by using suitable factors. However, the dependence of the prediction with the variation of the conditions is much more complicated to obtain. The SD provides the information on the ability of each correlation to follow the trend of the experimental data. So in the authors' opinions the SD should support the validation methodology with more importance than MSE.

3.4.1.2 Correlation for air side heat transfer coefficients

On the airside, the studied correlations were the model presented by Granryd *et al.* (2003), Wang *et al.* (2000) and a customized version of Wang *et al.* (2000), available in IMST-ART (2010).

The same analysis has been carried out taking into account the refrigerant side HTC and the pressure drop constant during the simulations (Table 3.6). The results are shown in Figure 3.11 and Figure 3.12, similarly to what was previously undertaken for the refrigerant side HTC.

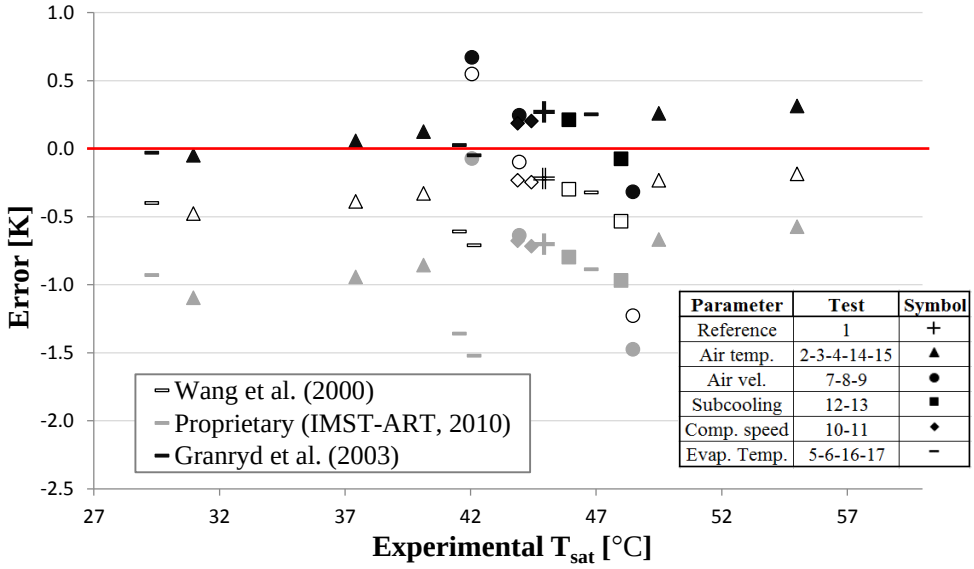

Figure 3.11: Comparison model plotted versus experimental saturation temperature

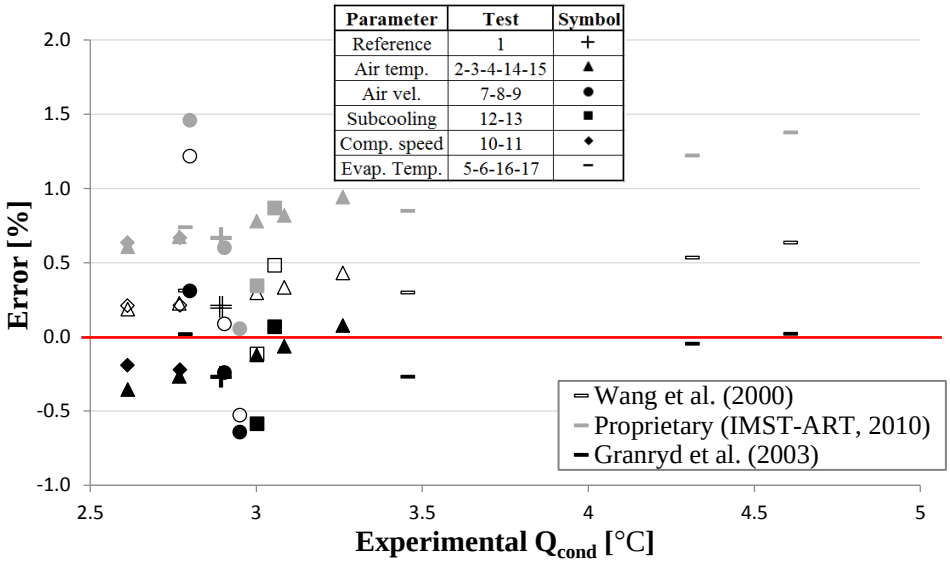

Figure 3.12: Comparison model versus condenser heating capacity

As observed for the refrigerant HTC, Figure 3.11 and Figure 3.12 show the error provided in capacity and condensation temperature when the air temperature, compressor speed, subcooling and air velocity change. It is quite sensitive to variations of the air velocity while it can be considered quite constant with the other parameters' variation. Analyzing the trend when the air velocity is changing, the error reaches the largest values when the condenser temperature rises (or when the air velocity decreases). This behavior is quite similar adopting all the correlations, but the model provides an acceptable level of accuracy only when the correlation proposed by Granryd *et al.* (2003) is used. Table 3.9 provides the values for all the metrics (ME, SME and SD), confirming numerically what has been observed from the analysis of Figure 3.11 and Figure 3.12.

Table 3.9: Analysis of the results varying the air-side HTC correlations

	Wang et al. (2000)		**Proprietary (IMST-ART, 2010)**		**Granryd et al. (2003)**	
	T_{cond} [°C]	**Q_{cond} [%]**	**T_{cond} [°C]**	**Q_{cond} [%]**	**T_{cond} [°C]**	**Q_{cond} [%]**
ME	-0.351	0.295	-0.875	0.783	0.135	-0.163
SD	0.351	0.354	0.355	0.344	0.217	0.239
MSE	0.239	0.0002	0.885	0.001	0.062	0.0001

3.4.1.3 Correlations for refrigerant pressure drop

In any finned tube heat exchanger, the total pressure drop is strongly depending on its geometry and characteristics (For example: the presence of the distributor, different geometry of the circuits, number of tube per circuits, etc. etc.). Hence, the correct evaluation of the pressure drop through the entire heat exchanger cannot be only connected to the accuracy of the correlations for calculating the friction factor in the tubes. Nevertheless, compared with the geodetic pressure drop (equal to zero for horizontal tubes), the pressure drop due to the acceleration of the fluid (Thome 2004) and the

local phenomena taking place in the distributors or in the return bends (Chisholm, 1983), the pressure drop due to the friction represents the most important component of the total one.

According to what just said, the analysis presented in this section is aimed to compare the correlations proposed by Chisholm (1973) and Friedel (1979) for the evaluation the frictional pressure drop in the two-phase flow. With this aim, the entire set experimental working conditions has been further simulated.

The results are depicted in Figure 3.13, where the results of the simulations are compared against the experimental ones in terms of in terms of $\Delta T_{sat.}$. Indeed, defined as the difference between the saturated vapor and saturated liquid temperatures, such parameter represents exactly the pressure drop during the condensation process.

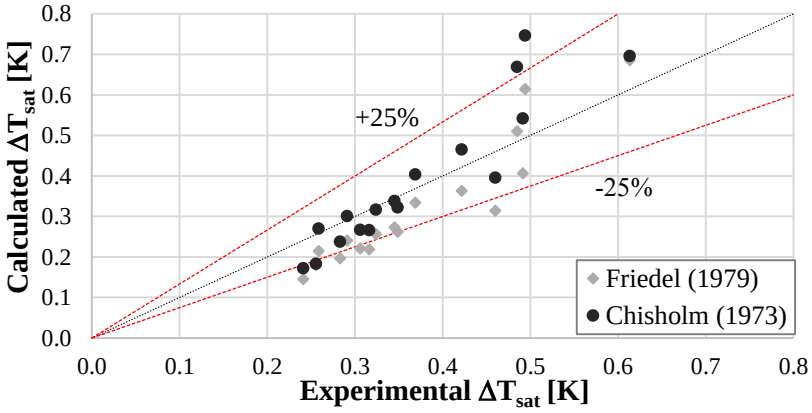

Figure 3.13: Experimental ΔT_{sat} versus calculated ΔT_{sat}

As for the HTCs, also in this case, the results have also been analyzed in terms of simple statistic metrics. Affectively, Friedel's correlation underestimates the pressure drop (ME and SD equal to -17.9% and ±16.9%), while Chisolm's correlation, even though the mean error assumes 0.8%, presents a higher dispersion of the results (SD equal to ±21%). Nevertheless, although the mean error results to be lower applying the Chisolm's correlation, the lower standard deviation obtained testing the Fridel's model indicates that such model is able to follow the trend of the entire set with experimental data with higher accuracy. Therefore, it will be used during the global validation process presented in the following section.

3.4.1.4 Correlation for air side pressure drop

Figure 3.14 shows the comparison between air pressure drop measurements and the model prediction for the entire data set.

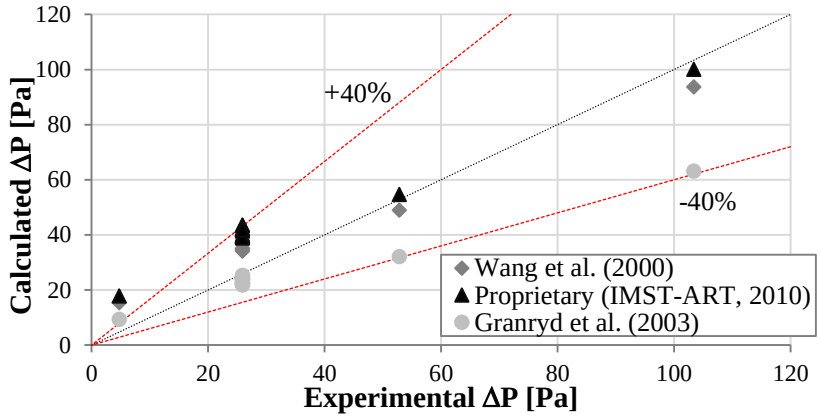

Figure 3.14: Experimental pressure drop versus calculated pressure drop

The model provides different results when applying the different correlations. When the air velocity is 1.5 m/s the model commits the highest prediction error. The correlations of Wang *et al*. (2000) and the proprietary correlation (IMST-ART 2010) overestimate the pressure drop with a relative error higher than the 50%. When the air velocity is higher (3.2-4 m/s), the same correlations allow the evaluation of the pressure drop with an acceptable degree of accuracy. Indeed, the model provides a relative error of less than 10%. By applying the correlation proposed by Granryd *et al*. (2003), although the pressure drop is overestimated for the lowest air velocity, the pressure drop is widely underestimated when the air velocity is 3.2 m/s and 4 m/s (a relative error of about 40%).

3.4.1.5 Global Validation

Condensation temperature and performance are strongly depending on the correct evaluation of HTCs (air and refrigerant side) and the friction factor in the refrigerant side. Therefore, once the best correlations have been identified independently, the last step of the validation involves the repetition of all the simulations. According to the previous analysis, the correlation used in the global validation without the application of any enhancement factor can be listed as follows:

- Granryd *et al.* model (2003) for evaluating the air side HTC.
- Thome *et al*. correlation (2003) for the refrigerant side HTC.
- Friedel correlation (1979) for the two-phase friction factor.

The results are shown in Figure 3.15-3.24 in which the results are compared with the experimental data. The comparison is carried out distinguishing the effects on the performance of air temperature (Figure 3.15, 3.16), condenser subcooling (Figure 3.17, 3.18), compressor speed (Figure 3.19, 3.20), air velocity (Figure 3.21, 3.22) and the evaporation temperature (Figure 3.23, 3.24). Considering the tests 5-17 (Table 3.2), changing both the air inlet temperature at the condenser inlet and the evaporation temperature at the same time, in Figure 3.23 and Figure 3.24 the difference air temperature-condensation temperature is depicted against the evaporation temperature. The

advantage of this representation is to allow an analysis of the performance of the condenser by varying the evaporation temperature, regardless of the value which the air temperature has in each experimental test. Finally, in the same figures are also reported the results obtained considering all the other correlations aimed to calculate the two-phase HTC.

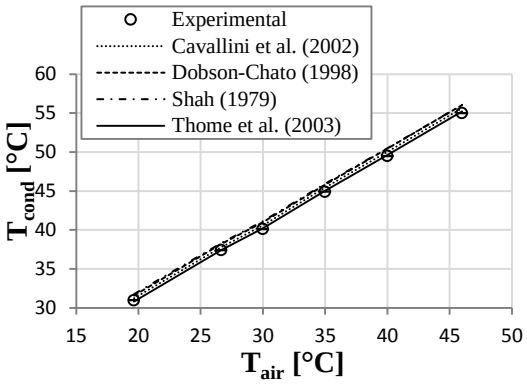

Figure 3.15: Condensation temperature versus Inlet air temperature - RTPFs

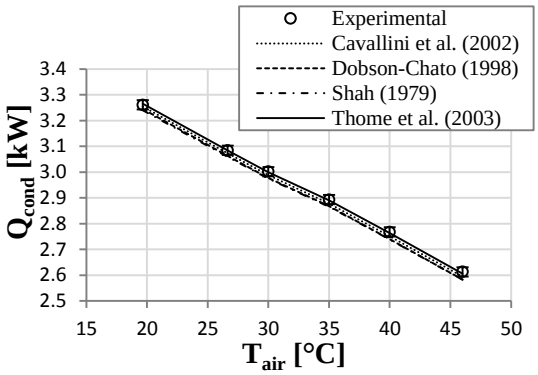

Figure 3.16: Capacity versus the Inlet air temperature - RTPFs

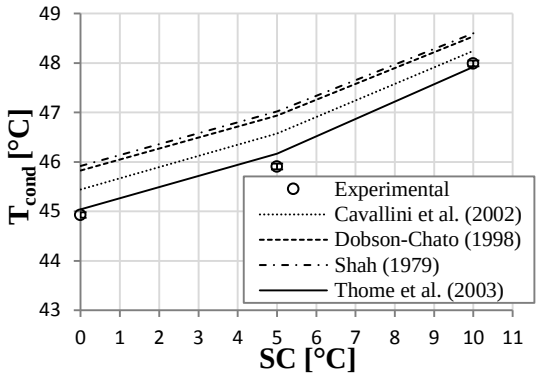

Figure 3.17: Condensation temperature versus subcooling - RTPFs

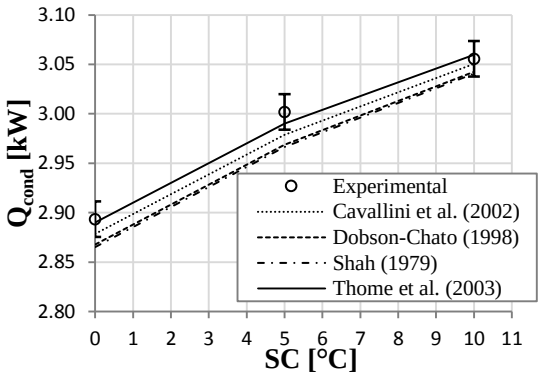

Figure 3.18: Capacity versus subcooling – RTPFs

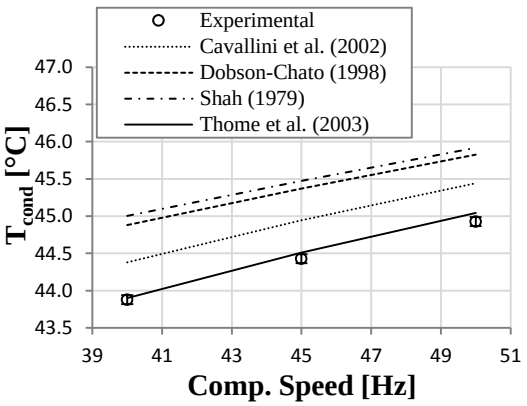

Figure 3.19: Condensation temperature versus compressor speed - RTPFs

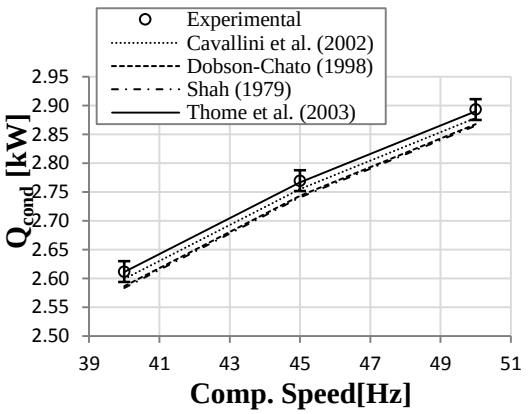

Figure 3.20: Capacity versus compressor speed – RTPFs

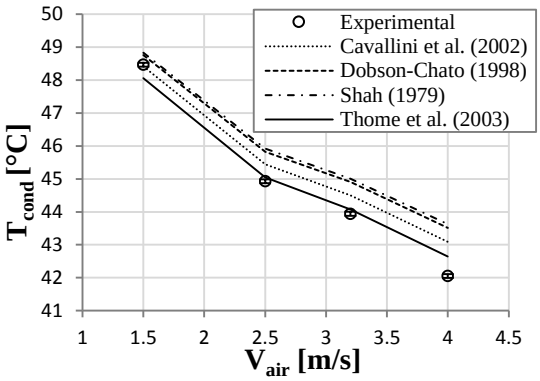

Figure 3.21: Condensation temperature versus air velocity - RTPFs

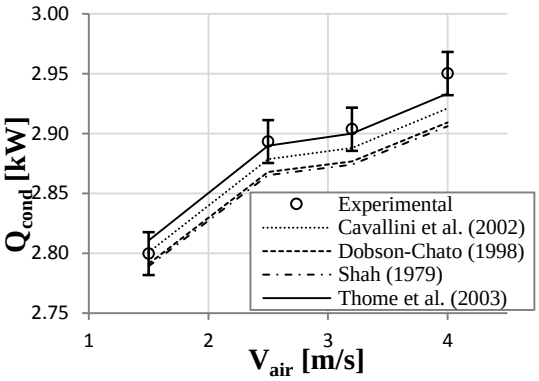

Figure 3.22: Capacity versus air velocity – RTPFs

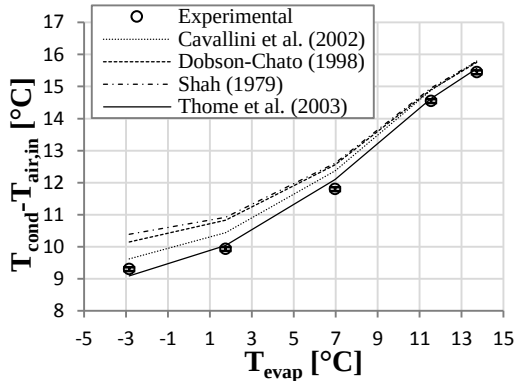

Figure 3.23: Condenser temperature difference versus evaporation temperature - RTPFs

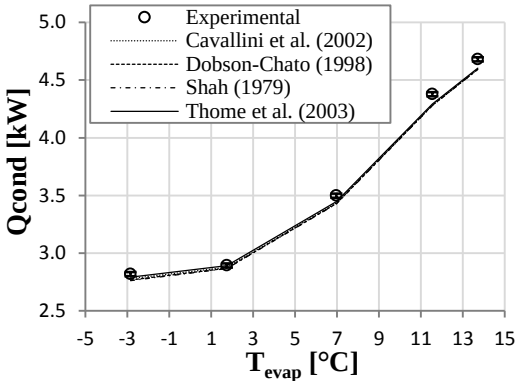

Figure 3.24: Capacity versus evaporation temperature – RTPFs

Although in most of the operating points the calculation error is lower than the uncertainty of the measurements (Table 3.3), the ME and the SD are respectively 0.08°C and ±0.2°C in terms of condensation temperature and 0.11% and ±0.25% in capacity.

Regarding the total pressure drop on both the heat exchanger sides, the results of the global validation can be considered overlapped to those showed in the Figure 3.13 and 3.14. Therefore, for any additional detail the paragraph 3.4.1.3 and 3.4.1.4 can be consulted.

3.4.2 Microchannel heat exchanger

3.4.2.1 Correlation for refrigerant heat transfer coefficients

Following the same procedure used for the round tube heat exchanger, in the present paragraph will be presented the analysis of the main correlations for the calculation of the two-phase flow heat transfer coefficient in the microchannel heat exchangers. The process started with the revision of the state of art, which led to identify four correlations as the most interesting to compare: (Webb *et al*., 1998), (Wang *et al.*, 2002), Koyama *et al.* (2003), Cavallini *et al.* (2005), Bahndauer *et al.* (2006) and (Lopez-Belchì, 2014). Afterwards, as for the RTPFs heat exchanger, all the correlations were preliminary compared considering R134a as refrigerant and four different combinations of hydraulic

diameter-mass velocity (Figure 3.25). In the Figures 3.25A and 3.25B the trends of the two-phase HTCs as function of the vapor quality (0.05-0.85) are compared taking into account the hydraulic diameter equal to 1 mm and two different refrigerant mass velocity (200 kg/sm2 and 500 kg/sm2 respectively). For the same mass velocities, in Figure 3.25C and 3.25D the hydraulic equal to 3 mm are considered.

As for the traditional tubes, although the general trend is mainly the same, depending on the correlation, the local value of the HTC can be rather different. As shown in Figure 3.25A, the correlations proposed by Cavallini *et al*. (2005), Webb *et al.* (1998), Bahndauer *et al.* (2006) can be considered practically overlapped in the range of vapor quality between 0.15 and 0.65. Otherwise, at the beginning of the condensation process (vapor quality > 0.65), the HTC calculated by Bahndauer *et al.* (2006) assumes the highest values. On the other hands, close to the subcooling liquid region (<0.15), the lowest HTC is calculated with the Cavallini *et al.* (2005) correlation. Analyzing the same figure, it is possible to notice that the highest average value of the HTC is provided by the correlation proposed by Lopez *et al*. (2014), while the lowest is calculated with the Koyama *et al.* (2003) model. The values of the HTC calculated by Wang *et al.* (2002) is in general always between those calculated by Koyama *et al.* (2003) and the other correlations. Figure 3.25B, 3.25C and 3.25D leads to different conclusions, therefore, a general "ranking" of correlations cannot be defined.

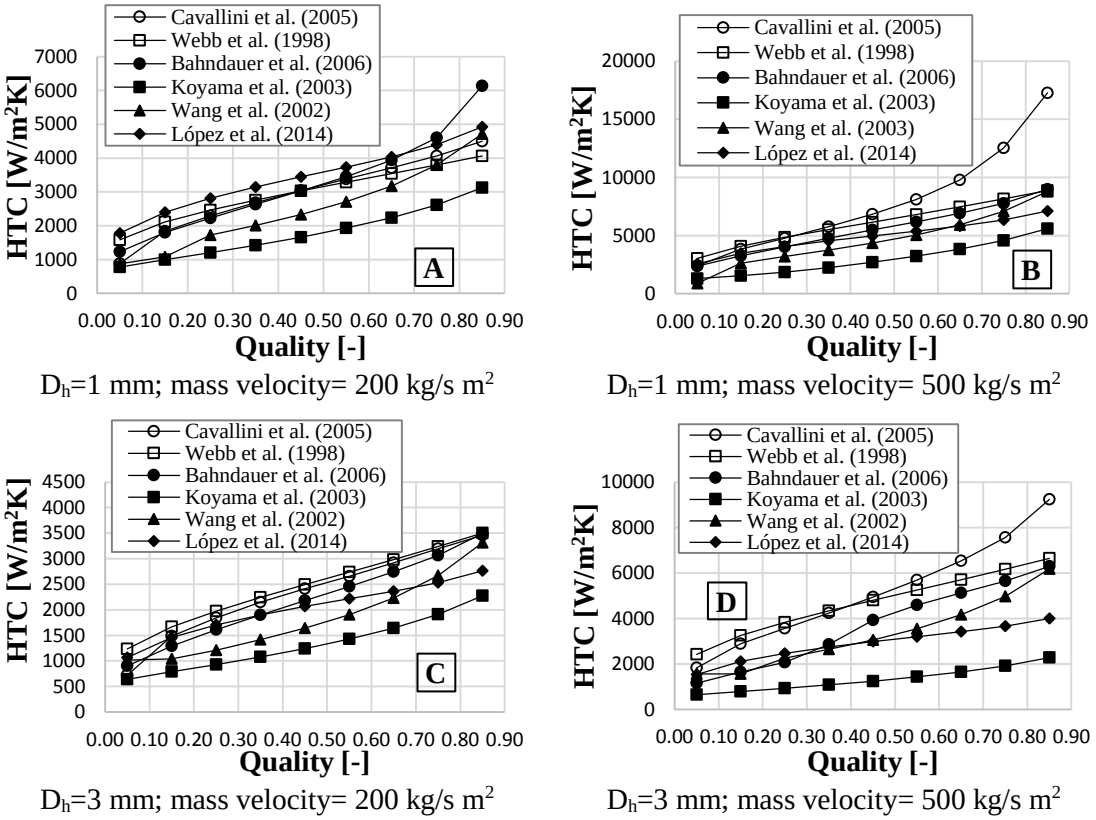

D_h=1 mm; mass velocity= 200 kg/s m^2 D_h=1 mm; mass velocity= 500 kg/s m^2

D_h=3 mm; mass velocity= 200 kg/s m^2 D_h=3 mm; mass velocity= 500 kg/s m^2

Figure 3.25: two-phase HTC as function of quality, mass flow rate and hydraulic diameter

No correlation presents discontinuities, but it is worth to notice that the Wang *et al.* (2002) model generates some convergence problems when the iterative solving procedure is applied for solving the condenser model (Chapter 2). As some of the others, also this model calculates the HTC in a different way depending on the flow regime. For low values of the vapor quality, when the gravitational force dominates the process of heat transfer, the stratified, wavy or slugged flow regime is taking place. In these conditions, Wang *et al.* (2002) affirms that the HTC depends strongly by the difference between saturation temperature and the tube wall temperature. As already commented, this dependence is the cause of many convergence issues when the numerical solution strategy is applied.

As shown in the Figure 3.26 and Figure 3.27, this issue is directly affecting the results of the simulations. In this figures, the error in the evaluation of the condensation temperature and thermal capacity is represented against the respective experimental parameter, distinguishing the effect on the condenser performance of different experimental parameters such as air temperature, air velocity, subcooling and compressor speed (Table 3.2). The charts have been obtained following the validation procedure described in the paragraph 3.1. Synthetically, when a certain correlation is studied, the rest of heat transfer and the pressure drop coefficients have been kept constant.

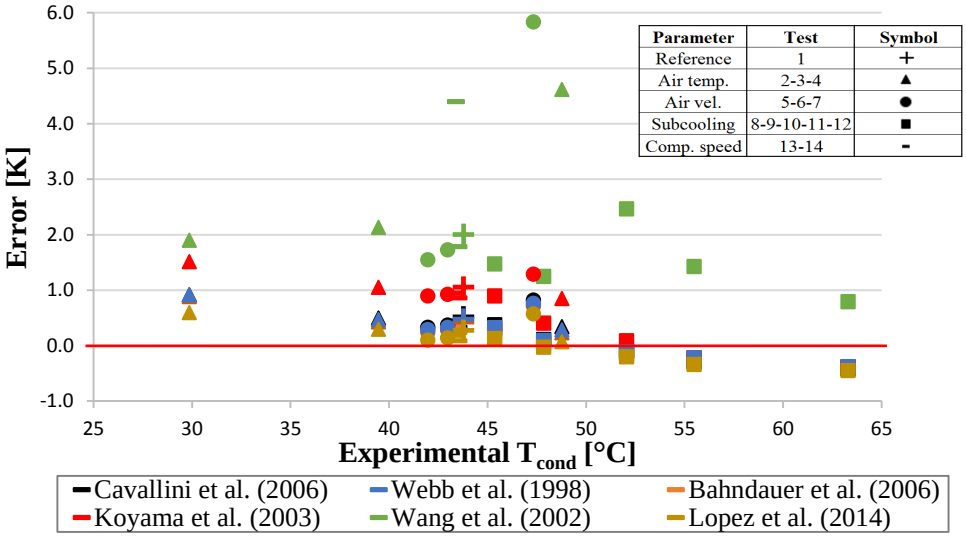

Figure 3.26: MCHX model versus experimental condensation temperature – Two-Phase HTC

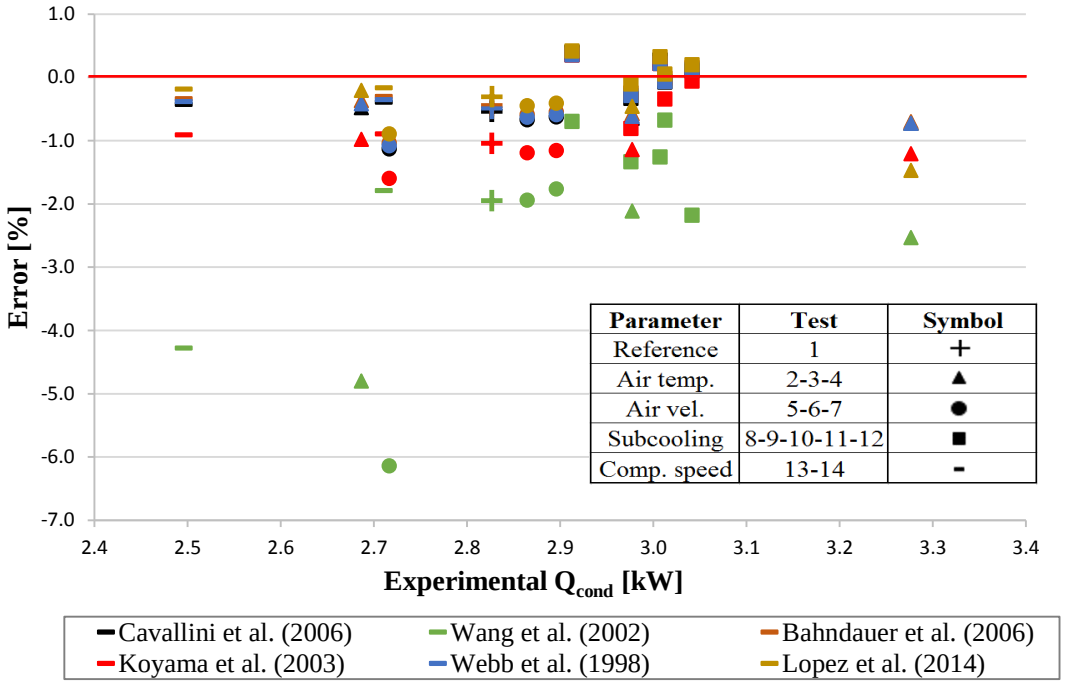

Figure 3.27: MCHX model versus experimental thermal capacity – Two-Phase HTC

For some operating points, the Wang *et al.* (2002) correlation provides very high errors (up to 6°C in condensation temperate and 6% in capacity). Otherwise, for the other correlations, their errors can be considered very similar between them.

As commented during the analysis of the results obtained for the RTPF heat exchanger, according to the validation methodology proposed in this chapter, for the identification of the best correlations for calculating the HTC the values assumed by the Mean Error (ME) is not so representative. Otherwise, the Standard Deviation plays the fundamental rule. Indeed, if on one hand the ME depends on the constant HTC used in the airside, on the other, the lower is the standard deviation, the better is the ability of the correlation to follow the experimental trend of the HTC.

Table 3.10: Analysis of the results in term of statistical parameters

	Cavallini *et al.* (2006)		**Webb *et al.* (1998)**		**Bahndauer *et al.* (2006)**	
	T_{cond} [°C]	**Q_{cond} [%]**	**T_{cond} [°C]**	**Q_{cond} [%]**	**T_{cond} [°C]**	**Q_{cond} [%]**
ME	0.303	-0.376	0.280	-0.352	0.240	-0.316
St. Dev.	0.375	0.420	0.352	0.397	0.341	0.386
MSE	0.471	0.552	0.440	0520	0.407	0.488
	Koyama *et al.* (2003)		**Wang *et al.* (2002)**		**Lopez *et al.* (2014)**	
	T_{cond} [°C]	**Q_{cond} [%]**	**T_{cond} [°C]**	**Q_{cond} [%]**	**T_{cond} [°C]**	**Q_{cond} [%]**
ME	0.726	-0.767	2.382	-2.389	0.102	-0.261
St. Dev.	0.552	0.584	1.479	1.592	0.297	0.490
MSE	0.900	0.951	2.776	2.839	0.304	0.539

In Table 3.10 is reported the analysis of the results in terms of mean error (ME), mean square error (MSE) and standard deviation (SD). According to what has been previously commented, the Lopez *et al.* (2014) correlation provides the best results, showing the lowest standard deviation in both condensation temperature and capacity. In accordance with this result, as will be dealt later, this correlation is going to be combined with the best airside correlation for the global process of model validation.

3.4.2.2 Correlation for the air side heat transfer coefficient

As for the RTPFs condensers, also for the MCHX the global performance is strongly affected by the air side thermal resistance. This is mainly due to the value of the air side heat transfer coefficients, which is significantly lower in comparison with the two-phase flow. Over the years, different authors have been working on the evaluation of the heat transfer coefficients proposing their own correlations. In this paragraph, the three following correlations have been preliminarily compared in terms of Colburn factor (Figure 3.28).

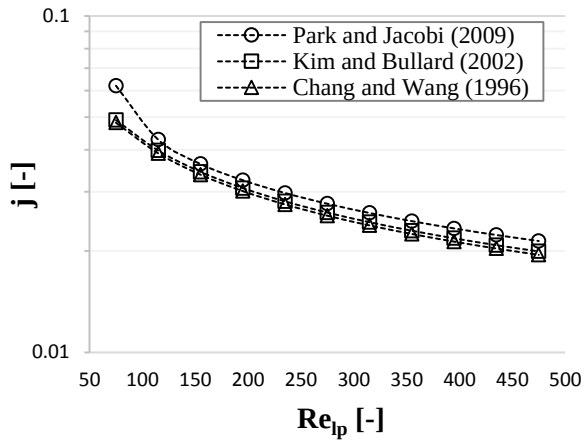

Figure 3.28: Comparison for the correlations for j-factor on airside

Actually, for each correlation, the Colburn factor (j) has been calculated as function of the Reynold number based on the louver pitch (Kim and Bullard, 2002), considering one the fin geometries used by Kim and Bullard in their work (Kim and Bullard, 2002). The results show that the correlations proposed by Kim and Bullard (2002) and Chang and Wang (1996) are practically overlapped on the entire Re_{lp} range, while the third correlation (Park and Jacobi, 2009) provides slightly higher j-factors. Although the three trends can be considered very similar, being the Colburn factor strictly connected to the airside heat transfer coefficient, hence to the airside thermal residence, even very small variations can affect significantly the prediction of the global performance of the heat exchanger. This affirmation is supported by the results shown in Figure 3.29 and Figure 3.30, where the simulated condensation temperature and global performance are compared with the experimental ones.

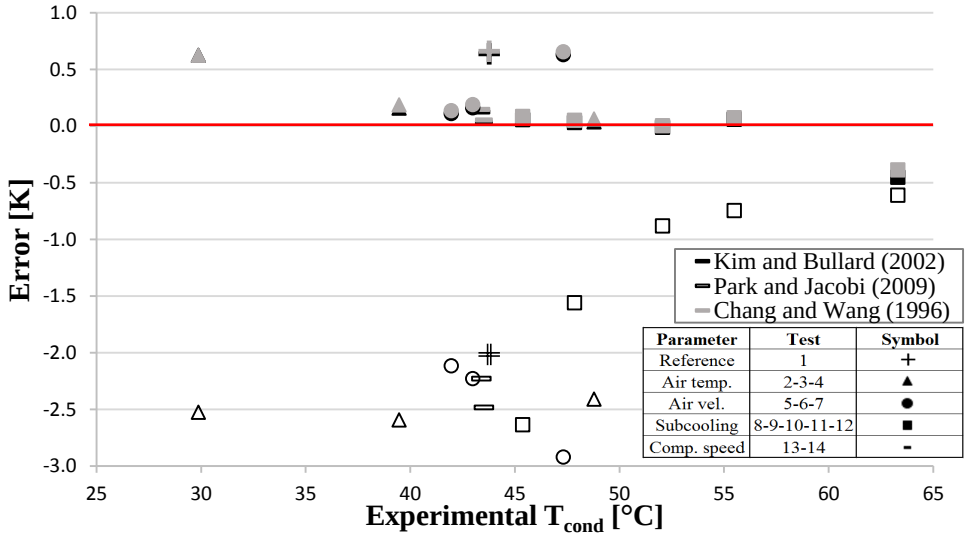

Figure 3.29: MCHX model versus experimental condensation temperature – airside HTC

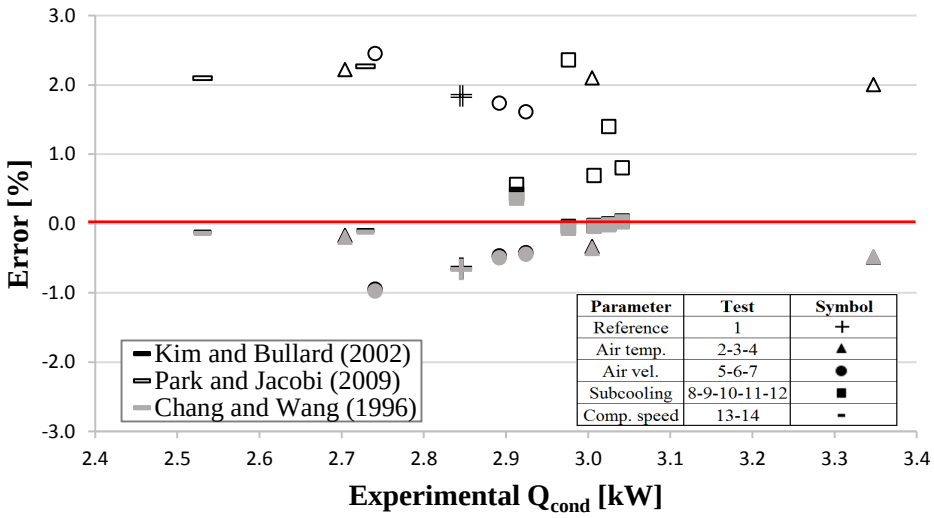

Figure 3.30: MCHX model versus experimental thermal capacity – airside HTC

According with the results depicted in Figure 3.28, the application of the Kim and Bullard (2002) and Chang and Wang (1996) correlations allow obtaining overlapped results. Whereas, the utilization of Park and Jacobi (2009) correlation entails the calculation of the highest mean error and standard deviation. For all the correlations tested, such statistics are summarized in Table 3.11.

By the analysis of the ME (Mean error) and standard deviation, although the differences can be considered very small, it is possible to affirm that the Park and Jacobi (2009) model is over predicting the airside HTC. Otherwise, as highlighted by the very low mean error in condensation temperature (< 0.5°C) and global performance (<0.3%), for the tested MCHX, the other two correlations allow evaluating with high accuracy the airside heat transfer coefficient.

Table 3.11: Analysis of the results varying the air-side HTC correlations

	Park and Jacobi (2009)		Kim and Bullard (2002)		Chang and Wang (1996)	
	T_{cond} [ºC]	Q_{cond} [%]	T_{cond} [ºC]	Q_{cond} [%]	T_{cond} [ºC]	Q_{cond} [%]
ME	-1.995	1.724	0.158	-0.238	0.182	-0.261
St. Deviation	0.752	0.634	0.297	0.341	0.288	0.366
MSE	7.466	6.450	0.589	0.892	0.682	0.977

As will be pointed out later on, according these results, the global validation process will be carried out considering the correlation proposed by Kim and Bullard in 2002.

3.4.2.3 Correlations for refrigerant pressure drop

I the refrigerant side, the total pressure can be split in two main components. Indeed, although most of the pressure drop is due to the core (tubes), for a good estimation of the total pressure drop, the phenomena taking place in the in the headers cannot neglected. However nowadays, most of the studies related to the analysis of the fuidodynamics inside the headers are carried out by means of CFD and no correlations are still available in literature for the evaluation of the friction factor. For this reason, in the current MCHX model, the total pressure drop is only considered due to the friction inside the tubes. Furthermore, no specific correlations for calculating the two-phase flow friction factor in the microchannel tubes have been implemented in the model; therefore, based on the results obtained for the round tube condenser, the model proposed by Friedel (1979) was used.

The absence of the pressure drop in the headers and the utilization of an unsuitable correlation for the estimation of the friction factors led to have a very low accuracy in the evaluation of the total refrigerant pressure drop. This topic has not been dealt in detail during the development of the current work of thesis, but due to the interests in the scientific community, it will be dealt with in future studies.

3.4.2.4 Correlation for air side pressure drop

In addition to the analysis of the heat transfer coefficient, in this section, the study of the correlations for the evaluation of the air side friction factor is presented. Considering the same geometry used for the analysis of the air side HTCs (Kim and Bullard, 2002), the friction factor (*f*) has been calculated using four different correlations: Park and Jacobi (2009), Kim and Bullard (2002), Chang *et al.* (2000) and its modified version published by the same authors in 2006 (Chang *et al.*, 2006). Indeed, after the first publication, the correlation proposed by Chang *et al.* in 2000 showed a discontinuity for $Re_{lp} = 150$ (Figure 3.31).

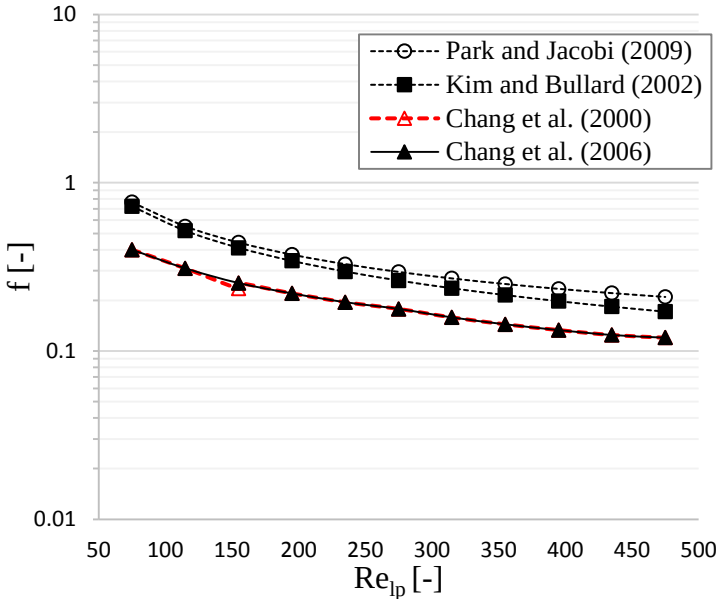

Figure 3.31: Friction factor as function of the Reynold number

This problem was solved some years later (Chang *et al.*, 2006), when the same authors provided a modified version of the original correlation. In Figure 3.31, the friction factor evaluated with both the correlations proposed by Chang *et al.* (2000, 2006) is compared with that evaluated with the Park and Jacobi (2009) and Kim and Bullard (2002) correlations.

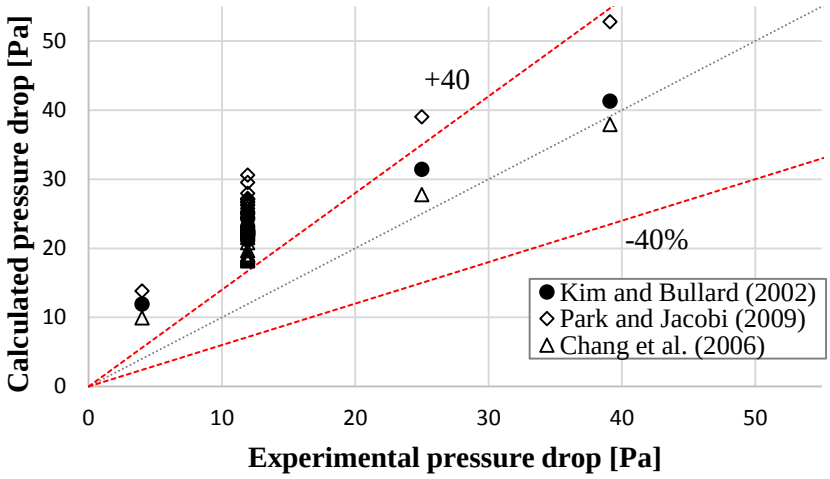

Figure 3.32: pressure drop evaluation whit different correlation - comparison with the experimental values

If the last two correlations can be considered practically overlapped for the lowest values of the Re_{lp}, the Chang *et al.* (2006) correlation is providing the lowest friction factor over the entire rage of the Reynold numbers. This different behavior is also observable if the calculated pressure drop is depicted against the experimental values (Figure 3.32) obtained in our experimental installation.

The analysis of the Figure 3.32 leads to affirm that, for the geometry of the heat exchanger tested in this work, all the correlations are over predicting (error up to +60%) the pressure drop for the lowest

air flow rate (lower Reynolds numbers). On the other hand, for the highest air velocities (3.2 and 4 m/s), the Chang *et al.* (2006) correlation is the only one that archives reasonable deviations (<12%) followed by Kim and Bullard (2002). Indeed, for the same air velocities, the other correlations provide very bad agreement with the experimental data with errors of about +40-45%.

In conclusion, for very low airflow rate (velocity < 2.5 m/s), all the correlations are not able to calculate correctly the total pressure drop, while, for the highest velocities (> 2.5 m/s), reasonable results are only given by the Chang *et al.* (2006) model and Kim and Bullard (2002).

3.4.2.5 Global validation

As for the RTPF condenser, the last step of the model validation involves the repetition of all the simulations considering the best set of correlations for the evaluation of the HTCs and pressure drop in the refrigerant side.

As depicted in the Figures 3.33-3.40, the combination of the correlations provides by Kim and Bullard (2002) (air side HTC), Lopez *et al* (2014) (refrigerant side HTC) and Friedel (1979) (two-phase friction factor) allows obtaining the most accurate simulation of the behavior of the microchannel condenser. The result is confirmed by the values assumed by the statistic metrics for both condensation temperature and capacity: the mean error and standard deviation are respectively equal to -0.046 ºC and ±0.307 ºC in terms of condensation temperature and -0.121% and ±0.333% in thermal capacity.

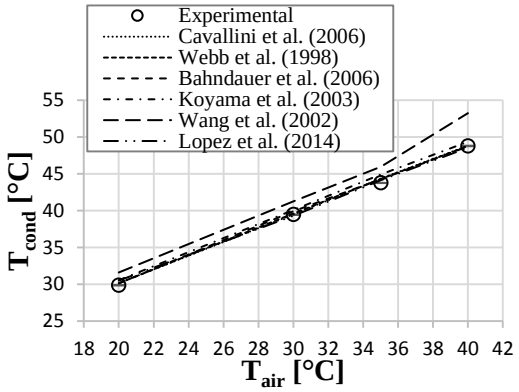

Figure 3.33: Condensation temperature versus Inlet air temperature - MCHX

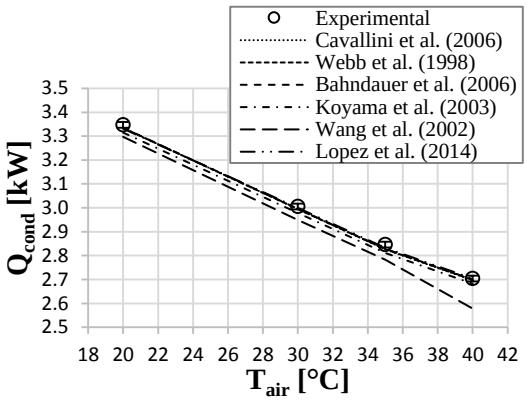

Figure 3.34: Thermal resistance ratio versus the evaporation temperature – MCHX

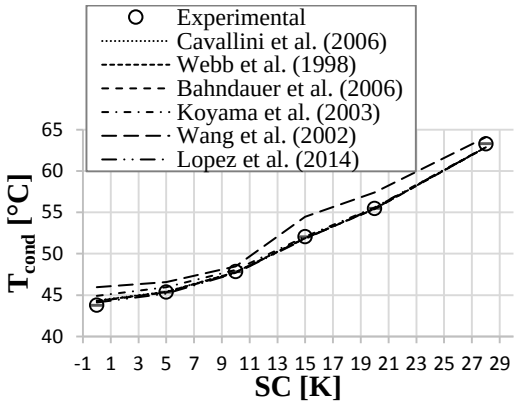

Figure 3.35: Condensation temperature versus subcooling - MCHX

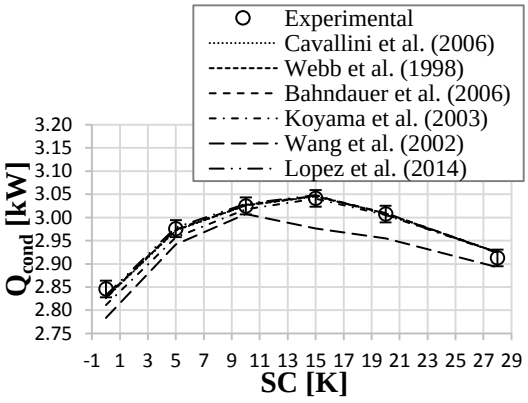

Figure 3.36:Figure 3.33: Capacity versus subcooling – MCHX

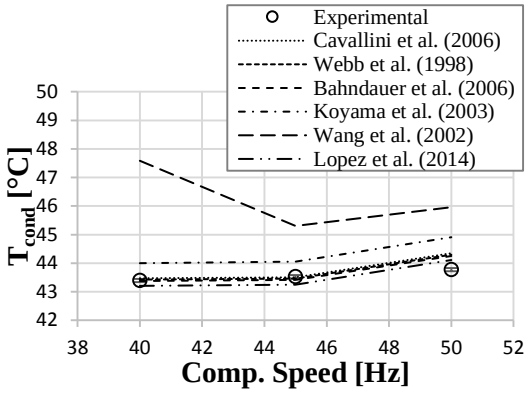

Figure 3.37: Condensation temperature versus compressor speed - MCHX

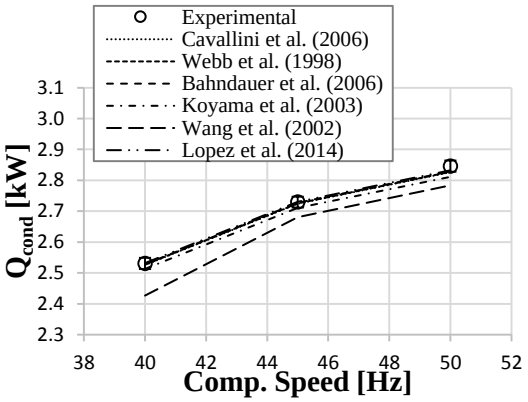

Figure 3.38: Capacity versus compressor speed – MCHX

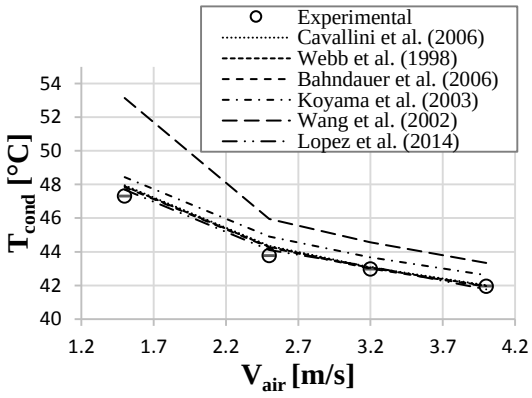

Figure 3.39: Condensation temperature versus air velocity - MCHX

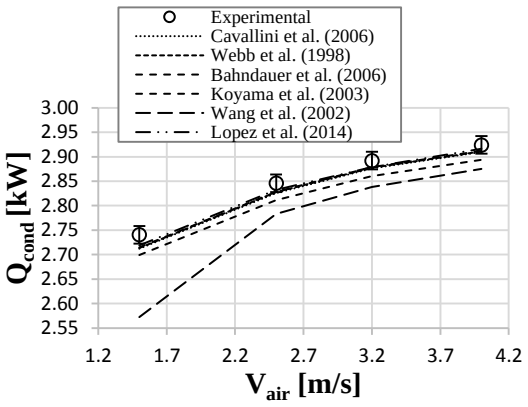

Figure 3.40: Capacity versus air velocity – MCHX

3.4.2.6 Further validation

The model validation has been extended by considering new experimental data sets obtained testing five different heat exchangers (Table 3.5) in an external laboratory. The results of the further simulations are depicted in Figure 3.41 and Figure 3.42, where the calculated condensation temperature and thermal capacity are compared with the experimental data.

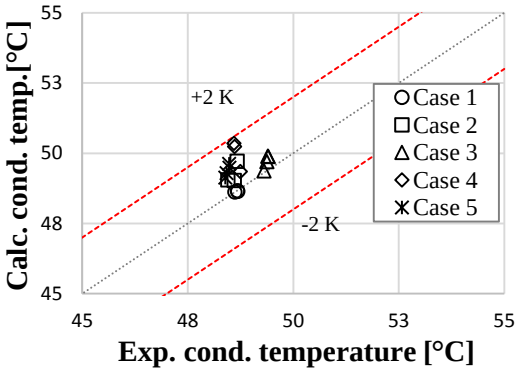

Figure 3.41: Exp. Tcond Vs. Calculated Tcond

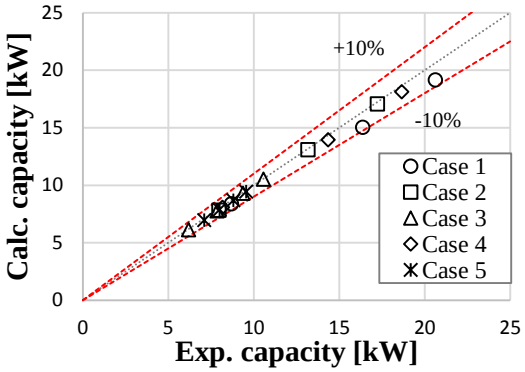

Figure 3.42: Exp. capacity Vs. Calculated capacity

The results confirm that, once identified the best set of correlations, independently on the geometry characteristics and the operating conditions, the model provides very accurate results without using any enhancement factor. Indeed, for the seventeen new tests, the model predicts the condensation temperature inside a very narrow error band (mean error equal to 0.66ºC). The correct evaluation of the condensation temperature entails consequently a good prediction of the thermal capacity. As depicted in Figure 3.42, the results fall down in a narrow error band of ± 10% with a mean error equal to -2.66%.

3.5 Conclusions

In this chapter, a methodology for the validation of a condenser model has been discussed. Initially, a specific experimental campaign was carried out in order to obtain a suitable and reliable set of experimental data including a wide range of operating conditions. The tests were performed by measuring the performance of an air-to-water heat pump equipped with two different condensers: a round-tube plate fins heat exchanger and a microchannel heat exchanger.

Depending on the characteristics of the heat exchanger, different correlations for evaluating the heat transfer coefficients and the pressure drop have been implemented in the model and then compared. The first part of the discussion has been focused on the use of different set of boundary conditions. The use of the condenser subcooling as a boundary condition instead of the inlet pressure is suggested when the best set of correlations for the evaluation of the HTCs want to be identified. Afterwards, a new validation procedure of the condenser model has been proposed. It is mainly aimed to isolate the effect on the results of the different correlations to calculate the heat transfer coefficients and pressure drop in both air and refrigerant sides. To this end, when a certain correlation was studied, the rest of heat transfer and the pressure drop coefficients were kept constant.

The conclusions of the studies for the identifications of the most suitable correlations for evaluating the HTC in the external and internal side of the condenser can be summarized as follows:

- The results of the validation can be analyzed in terms of metrics such as Mean Error, Mean Square Error and Standard Deviation However, according to the proposed validation methodology, the most important statistic parameter is the standard deviation (SD) instead of the mean deviation (ME). Indeed, when one correlation is analyzed, the ME strongly depends on the constant values used for the rest of the HTC and pressure drop coefficients. Otherwise, being independent by the constant parameters used, the SD gives the most important information regarding the capability of the correlations to follow the trend of the experimental data.
- For the RTPFs condenser, the lowest standard deviation was obtained by using the models proposed by Thome et al. (2003) for evaluating the HTC in the refrigerant side and Granryd et al.'s (2003) correlation for evaluating the same coefficient on the air side.
- For the microchannel condenser, the Kim and Bullard (2002) correlation has been selected as the best correlation for evaluation of the air side HTC; the model proposed by Lopez *et al.* (2014) was considered the most suitable for the estimation of the HTC in the refrigerant side.

In the condensers, the correct estimation of the condensation temperature and global performance also depends on the correct evaluation of the two-phase pressure drop. The analysis of the main correlations for the estimation of the two-phase friction factors in the RTPF condenser led to the following results:

- While the Fridel's correlation (1979) underestimates the total pressure drop (ME equal to -17.9%) with a SD equal to ±16.9%, Chisholm's correlation (1973) allows us to get a lower Mean Error (0.8%), but a higher standard deviation (±21%). Due to the lower SD the correlation proposed by Friedel was considered the most suitable to be used during the final model validation.

For the MCHX heat exchanger, no specific correlations were implemented in the model, so the two-phase flow friction factor was calculated with the Friedel's correlation.

Without applying any adjusting factor, the combination of the best correlations for the HTCs and two-phase friction factor allowed obtaining very good matching between the experimental data and the results of the models. It is confirmed by the results of the final global validation expressed in terms of mean error and standard deviation for condensation temperature and performance:

- For the RTPFs, the error inside an error band of ±0.4°C for the condensation temperature and in a band of ±0.6% in terms of thermal capacity.
- The MCHX model allows simulating the behavior of the condenser even with higher accuracy: the final values of mean error and standard deviation are respectively equal to -

0.046 ºC and ±0.307 ºC in terms of condensation temperature and -0.121% and ±0.333% in thermal capacity. The further validation process presented in the subsection 3.4.2.5 allows to affirm that, once optimized, the model is able to provide very good results independently of the heat exchanger geometry and operating conditions.

Condensation temperature and performance are independent on the correlation used for the estimation air side pressure drop. However, especially for the selection of the fans, the good estimation of this parameter plays a fundamental role during the design phase of an air conditioning system. Unfortunately, for both the RTPF and the MCHX the correlations tested do not provide reasonable results. Indeed, for the range of air velocity considered in this study, no correlation allows a good agreement with the experimental data.

- About the RTPFs model, the correlations proposed by Wang *et al.* (2003) and the proprietary (IMST-ART 2010) provide very low accuracy for the lowest air velocities, but fit quite well the experimental data when the velocity is higher. The correlation proposed by Granryd *et al.* (2003) provides good agreement only when the air velocity is equal to 2.5 m/s.
- Among the correlations considered more interesting to compare, the airside pressure drop in the microchannel heat exchanger is calculated with reasonable approximation only using the Chang at al. (2006) or Kim and Bullard (2002). However, such good agreement can be detected only for air velocities higher than 2.5 m/s. Indeed, below such value, all the correlations under analysis over predict the friction factor with error in the evaluation of the pressure drop up to more than +50%

Chapter 4

4. Improvement of the models: convective condensation of the superheated vapor

As shown in the previous chapter, once identified the best set of correlations for the evaluation of the heat transfer coefficients, the models are able to simulate the performance of both the RTPFs and MCHX condensers with high accuracy. Nevertheless, in the author's opinion, the agreement between the results of the simulations and the experimental data can be even improved, modelling with more accuracy the heat transfer phenomena that take place inside the tubes during the entire process of heat rejection. In this context, as already pointed out in the introduction, one of the phenomena generally neglected during the development of the condenser models is the convective condensation of the superheated vapor on the tube wall. Therefore, in this chapter, beside the analysis of the results of a specific experimental campaign, with the purpose to estimate with more and more accuracy the global performance of a condenser, the methods for including such phenomena in the current condenser models will be discussed. In particular, the attention will be focused on the pros and cons of the application of two different methods based respectively on what will be defined as the Temperature Approach and the Enthalpy Approach. Synthetically, as will be highlighted along the chapter, the Temperature Approach method allows obtaining very good agreement with the experiments, but its application leads to increase the computational efforts. On the contrary, being based on some simplification hypothesis, the application of the Enthalpy Approach method still provides accurate results, but without compromising excessively the calculating time in comparison with the original model.

4.1 Analysis of the refrigerant temperature along the condenser

4.1.1 Tube-and-fins condenser: experimental evaluation of the temperature profiles

In principle, due to the nature of the convective condensation of the superheated vapor, the analysis of its influence on the performance of a condenser has to be based on the estimation of the temperature profiles along the heat exchanger. In this thesis, such profiles have been measured in the traditional RTPFs condenser depicted Figure 3.3. With this objective, the experimental campaign summarized in Table 3.2 was extended with some additional tests, during which the temperatures along the refrigerant path were measured respectively by means of the utilization of two different

technologies. The refrigerant temperature was estimated by means of the utilization of T-type thermocouples. At the same time, the tube wall temperature was obtained by means of infrared thermography. During the tests, the thermocouples were placed on the return bends of the heat exchanger according to the scheme depicted in (Figure 4.1). Ten T-type thermocouples were placed on the left side of the heat exchanger, while twenty on the other. In order to avoid any heat transfer from the wall to the ambient, all the thermocouples were accurately insulated with polyurethane foam. Thanks to this precaution, the refrigerant temperature profiles along the circuits 1 and 2 were measured with a good accuracy of about ±0.5°C.

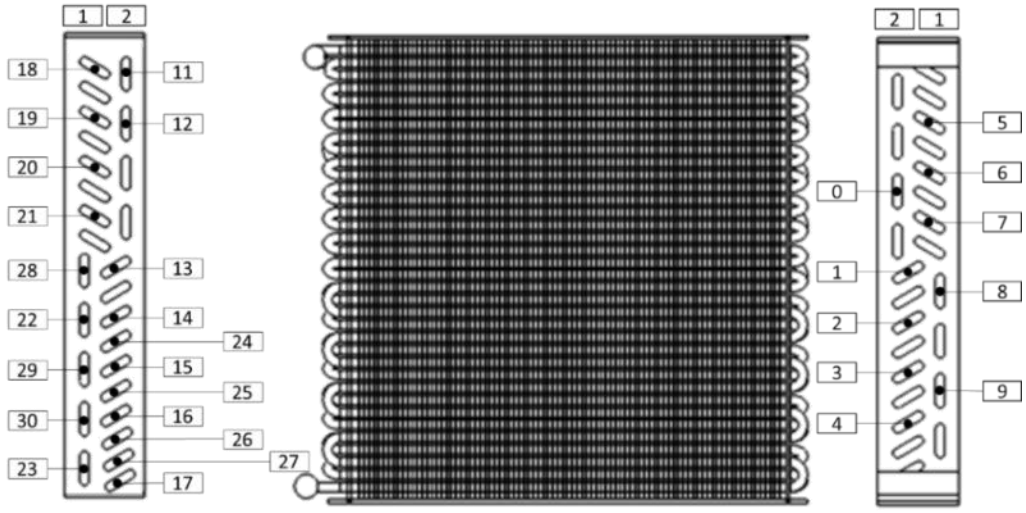

Figure 4.1: Position of the thermocouple along the refrigerant circuits

Placing the infrared camera inside the climatic chamber in front of the heat exchanger as depicted in Figure 3.2, only the wall temperature profile of the frontal circuit (No. 1) was estimated. In general, the results provided by the thermography are influenced by many factors and, in particular, they strongly depend on the emissivity of the measured surface. In this work, such parameter was evaluated and adjusted, performing what was called "calibration test". The test consisted of taking a picture of the frontal surface of the heat exchanger when no refrigerant is circulating within. In this conditions, if the temperature of the climatic chamber is maintained constant, after a transition period, the external surface of the heat exchanger assumes the same temperature of the air. Hence, the value of the emissivity can be easily adjusted overlapping the temperature measured by infrared camera to the experimental temperature of the air going through the heat exchanger. During the test, the external surface of the condenser was covered by unreflecting black paint and the temperature of the climatic chamber was maintained constant and equal to 30°C. In such conditions, the emissivity of the surface was evaluated as 0.96, value that was assumed constant during the entire experimental campaign.

Once the "calibration test" was performed, as already mentioned, the original experimental campaign described in the Chapter 3 was further extended with some additional tests. In practice, starting from

a reference test (SC=0 K; $T_{air,inlet}$=35°C; $v_{air,inlet}$=2.5 m/s; m_{ref}=0.014 kg/s), the temperature profiles along the condenser were measured in four new operating conditions. For each of them, all the experimental conditions were maintained unchanged to the reference test and only the refrigerant charge circulating in the refrigerant loop was adjusted manually. As a consequence, four different condenser subcoolings were achieved (10, 14, 17 and 20 K). As depicted in Figure. 4.2, the volume occupied by the liquid increases significantly from "almost" zero (SC= 0 K) up to a value of about 60% when the subcooling was set on 20 K. More details regarding the values of the local temperatures will be discussed in the next paragraph.

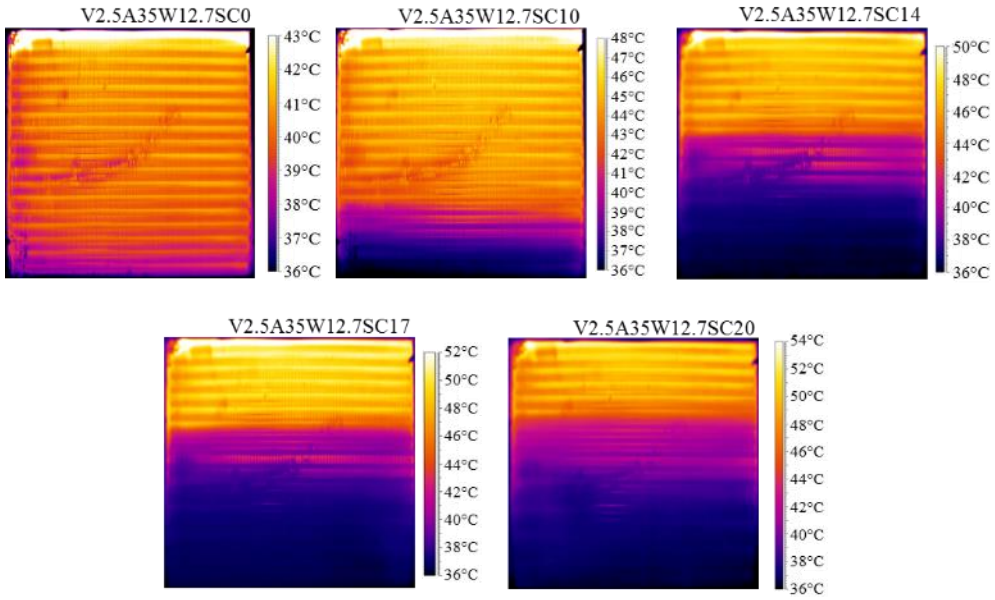

Figure 4.2: Thermography for different subcooling

4.1.2 Comparison between the results of the standard model and the experiments

In general, the analysis of the temperature profiles along the refrigerant path turns out to be rather difficult due to the high number of parameters to take into account. Indeed, the temperature of the refrigerant, as well as the temperature of the tube wall, are extremely sensible to the refrigerant and airflow distribution, the air inlet temperature, the air volumetric flow rate, the refrigerant flow rate and the total subcooling. The analysis can be even more complex, if a certain geometric asymmetry characterizes the heat exchanger. In this case, beside the combination of all the parameters listed above, also the different length of the circuits can strongly affect the heat transfer, hence the temperature profiles along the heat exchanger.

With reference to the RTPFs heat exchanger used for the development of the present thesis, in the first instance, the analysis of the experimental temperature profiles along the condenser was approached considering one by one the factors that may affect the heat transfer. Afterwards, all these

effects were mixed together with the objective to interpret the experimental results as correctly as possible.

Initially, the discussion was simplified taking into account some simplifying assumptions. Imagining the two circuits of the heat exchanger as completely independent, assuming the total absence of refrigerant maldistribution and considering exactly the same air and temperature distribution at the air side inlet, the heat transferred in the circuit No. 2 of the RTPFs should have been the highest. Indeed, only because longer than the circuit No.1, the presence of an additional heat transfer area should be enough for explaining such higher heating capacity. However, being based on some very restrictive hypothesis, this affirmation cannot be considered fully reliable and the discussion about the temperature distributions along the two circuits has to be necessarily conducted taking into account also other more complex aspects. In principle, as previously mentioned, a general analysis of the phenomena taking place inside and outside of each circuit can help to identify their effect (or the effects) on the temperature distribution in the two circuits.

Based on this, the first considerations were related to the temperature variation in the air side. First of all, the average air temperature at the inlet of the circuit No. 2 has to be assumed rather higher than the temperature at the inlet of the frontal one (No. 1).

In addition to this aspect, it is also necessary to consider that the air temperature distribution at the inlet of the circuit 2 is much more irregular in comparison with the air temperature profile at the inlet of the frontal one. This effect is due to the position of the refrigerant inlet (Fig. 3.3) with respect to the air flow. Indeed, in our heat exchanger, the air going through the top of the condenser (refrigerant inlet) is wormed up more than air going through the lower part of the heat exchanger. It means that the refrigerant in the subcooled liquid region of the rear circuit (No.2) is cooled down more quickly than the refrigerant in the superheated vapor region.

Only this consideration would be enough to point out the difficulties related to the interpretation of the experimental results. Nevertheless, it is also necessary to remember that all the multi-circuit heat exchangers are generally affected by refrigerant maldistribution. Indeed, even excluding a detailed analysis of the fluid dynamics inside the distributor (Figure 3.3), it is reasonable to imagine that the refrigerant mass flow rate going through each circuit is not same.

As widely supported by the entire scientific community, the refrigerant distribution plays a fundamental role in the heat transfer. However, being connected to the specific geometry of every heat exchanger, it is still very difficult identifying a proper way for its theoretical estimation. On the other way around, as will be pointed out later on, the temperature profiles represents the only simple method for estimating the refrigerant distribution inside a heat exchanger.

The phenomena which affect the characteristics of the heat rejection process in each circuit can be summarized as follows:

- The heat transfer and the temperature profile are strongly connected to the refrigerant mass flow rate going through each circuit. Consequentially, total heat rejection can be very different in each of them.
- With reference to our heat exchanger, considering that the circuits do not have the same length (different heat transfer areas) and the air is irregularly warmed up going through the circuit No.1, the circuit No.2 should be characterized by:
    - A more extended subcooling region in comparison with the circuit No.1.
    - Significantly less extended superheated vapor region in comparison with the circuit No. 1.

Effectively, these assumptions are confirmed by observing the experimental temperature profiles depicted in Figure 4.3 and Figure 4.4.

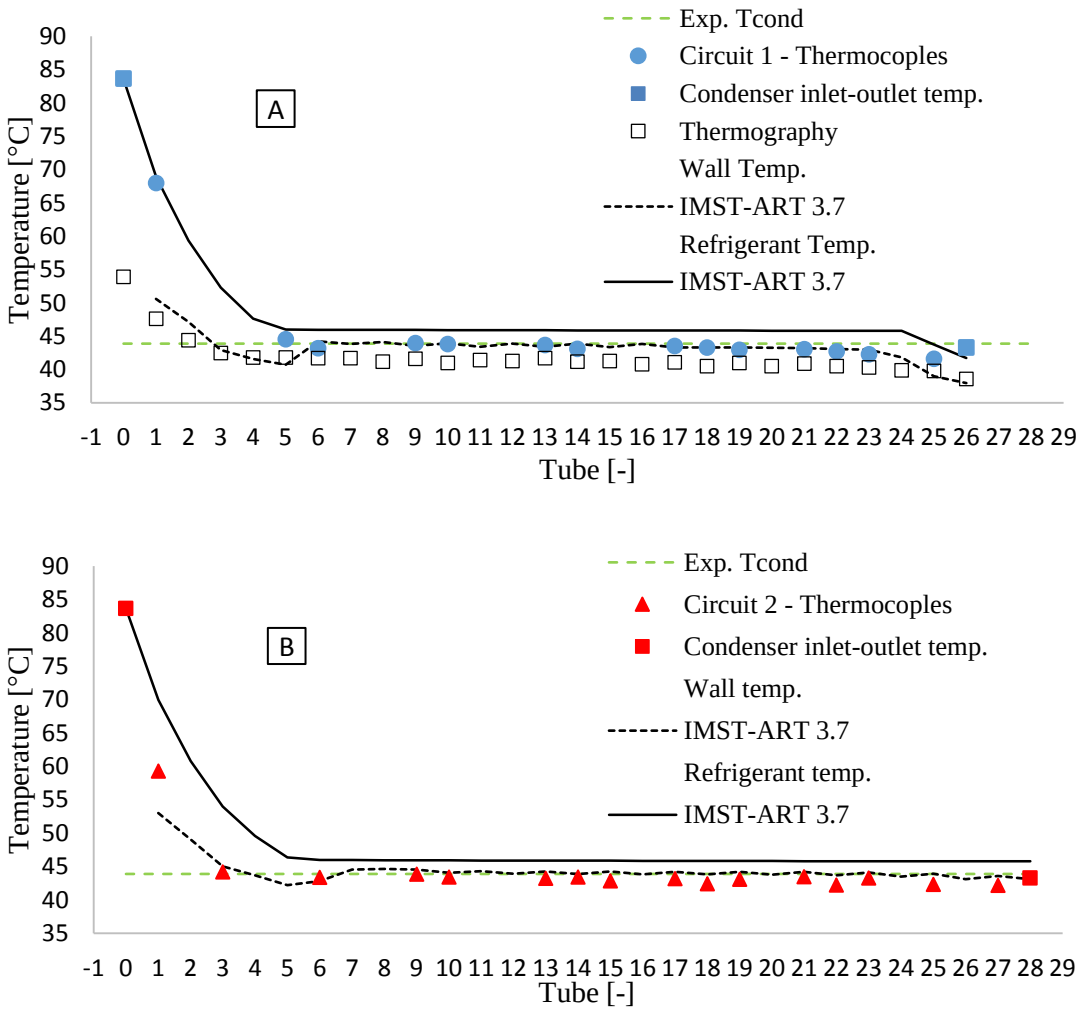

Figure 4.3: Analysis of the experimental temperature profile and comparison with IMST-ART 3.7 – Reference test

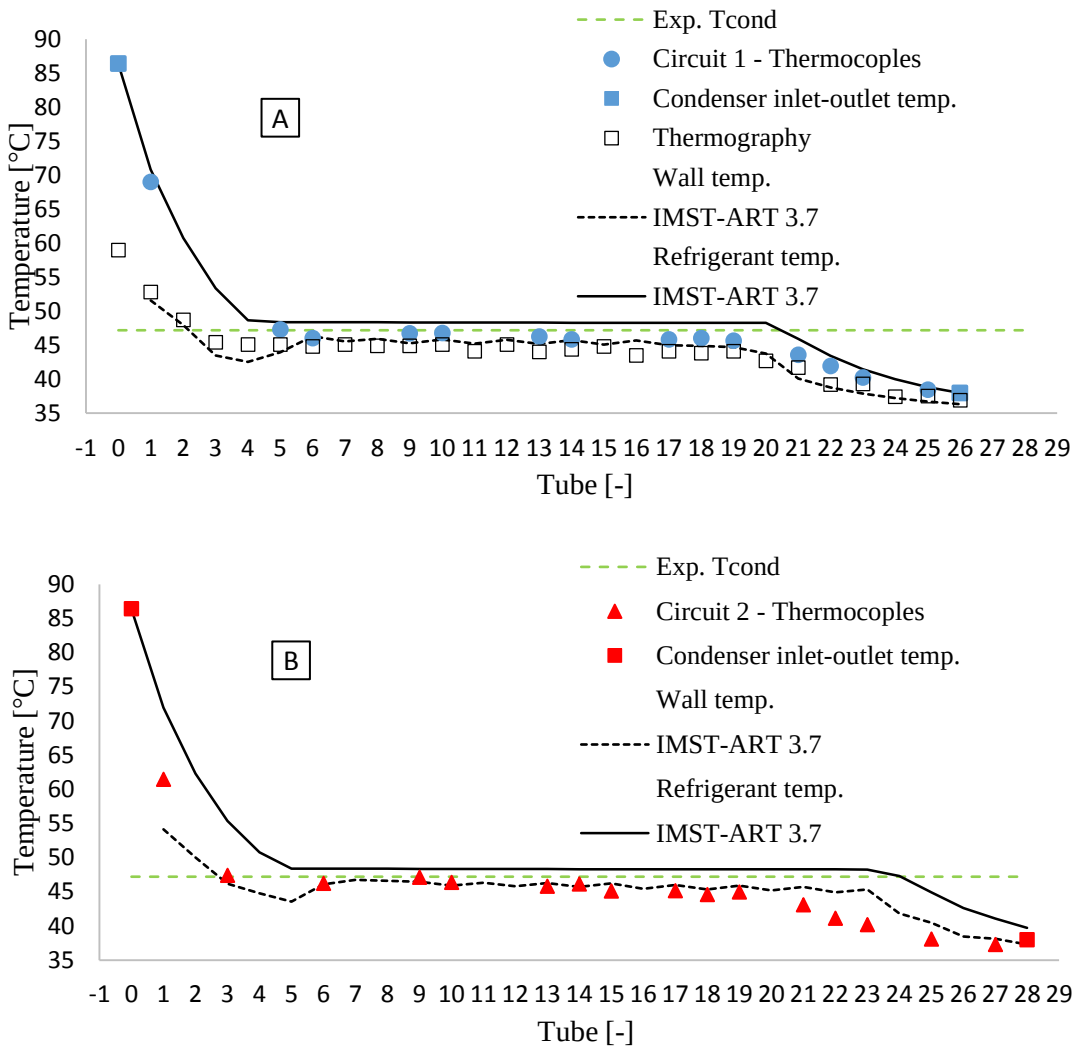

Figure 4.4: Analysis of the experimental temperature profile and comparison with IMST-ART 3.7 – test with SC=10°C

In particular, Figure 4.3 shows the experimental temperature profiles characterizing the reference test. For this operating point, being the nominal subcooling equal to zero, it is important to pay attention on the extension the superheated vapor region in each circuit. Confirming what was previously commented regarding the heat transfer and the refrigerant distribution, in the rear circuit, the superheated zone appears evidently less extended in comparison with the frontal one. Effectively, in the circuit No.2, the condensation seems to start in the second or third tube, while in the No. 1 it starts a bit later (between tube 4 and 5). Without knowing the vapor quality, it is very difficult to assume the outlet conditions for each circuit. Meanwhile, from the analysis of the charts, at the outlet of both the circuits the temperature seems to be completely constant, conditions that confirm the complete absence of subcooled liquid.

Similar conclusions can be drawn by analyzing the profiles in Figure 4.4. In this case, being the subcoling set up on 10 K, first it is possible to highlight that the refrigerant outlet temperature can be considered the same for both the circuits. Afterwards, it is possible to observe the different extension

of one-phase zones. Actually, in the second circuit, the subcooled liquid and the superheated vapor zones are respectively bigger and smaller than the corresponding zones in first circuit. At the same time, the extension of the condensation is practically the same.

This behavior is common to all the tests under analysis. It is confirmed by the data reported in Table 4.1, where for all the operating points, the percentage of volume occupied by liquid, two-phase flow (2-phase) and vapor is reported for each circuit (1 and 2).

Table 4.1: percentage of volume occupied by vapor, two-phase flow and liquid

Volume	SC=0°C		SC=10°C		SC=14°C		SC=17°C		SC=20°C	
	1	2	1	2	1	2	1	2	1	2
% vapor	15.4	11.5	14.3	10.5	13.1	9.2	12.2	8.8	11.3	7.1
% 2-phase	84.6	88.5	58.8	60.9	40.7	40.8	26.3	26.9	25.2	28.7
% liquid	0	0	26.9	28.6	46.2	50	61.5	64.3	63.5	64.3

In Figure 4.3 and Figure 4.4, the temperature profiles calculate by means of IMST-ART 3.7 are depicted as well. Although the condensation temperature is calculated with reasonable accuracy (the error is lower than +1°C), the model is not able to reproduce accurately the entire temperature profiles. In the author's opinion, this result depends on three factors: i) the heat transfer coefficient is underestimated at the end of the condensation process; ii) in the model the convective condensation of the superheated vapor is neglected iii) the refrigerant distribution in the circuits is assumed the same.

For both the cases under analysis (SC=0°C and SC=10°C), the results show that the simulated condensation process is taking place in a different portion of the heat exchanger in comparison with the experimental results. In other words, it means that the local value of the HTC along the entire refrigerant path is not perfectly calculated. As already mentioned, the causes of such result can depend on numerous factors. For example:

- The correlations are underestimating/overestimating both the two-phase and one-phase heat transfer coefficients.
- In the model is not taken into account the presence of the condensing superheated vapor region and the condensing subcooled liquid region. Indeed, as studied by Agarwal and Harnjak (2014), as the condensation of vapor starts just before achieving the saturation condition, the process of condensation actually expands also in the subcooled liquid region (condensing subcooled liquid region). In other word, the HTC at the beginning of the subcooled liquid zone and at the end of the superheated vapor zone are higher that the respective value calculated with the Gnielinski (1976) correlation.
- The uniform refrigerant distribution in the circuits affects negatively the results provided by the model.

These aspects are also strongly connected the presence of a strongly inconsistent trend of the wall temperature in the superheated vapor zone just in correspondence of the beginning of the condensation process. This aspect is further pointed out by the presence of a "dip" in the wall temperature profile, just where the convective condensation of the superheated vapor starts. In this work, the possibility to consider the refrigerant maldistribution or the presence of the condensing subcooled region have not been considered. On the contrary, most of the efforts have been focused on the implementation in IMST-ART of a reliable methodology for considering the heat transfer coefficient variation due to the presence of the condensing superheated vapor zone.

4.2 Improved condenser model

4.2.1 Heat transfer of superheated vapor with droplets condensation

The simulation of the phenomena characterizing the convective condensation of the superheated vapor entails a substantial modification of the traditional condenser model described in the second chapter of this thesis. Actually, although the general governing equations and the main numerical resolution method have been maintained unvaried, the approach for modelling the transition from the one-phase zone to the two-phase zone has been substantially modified due the introduction of the condensing superheated vapor zone.

In order to simplify the discussion, instead of a complete heat exchanger, the heat rejection process will be described considering only a "one-tube" condenser. As described in the Chapter 2 of the present thesis, the modelling strategy is based on the segment-to-segment approach. Therefore, as depicted in Figure 4.5, the one-tube HX has to be discretized in a certain number of control volumes. For simplicity, the one-tube condenser has been divided in 4 cells. This discretization of the total internal volume entails that in some of them more than one heat transfer mechanism can take place.

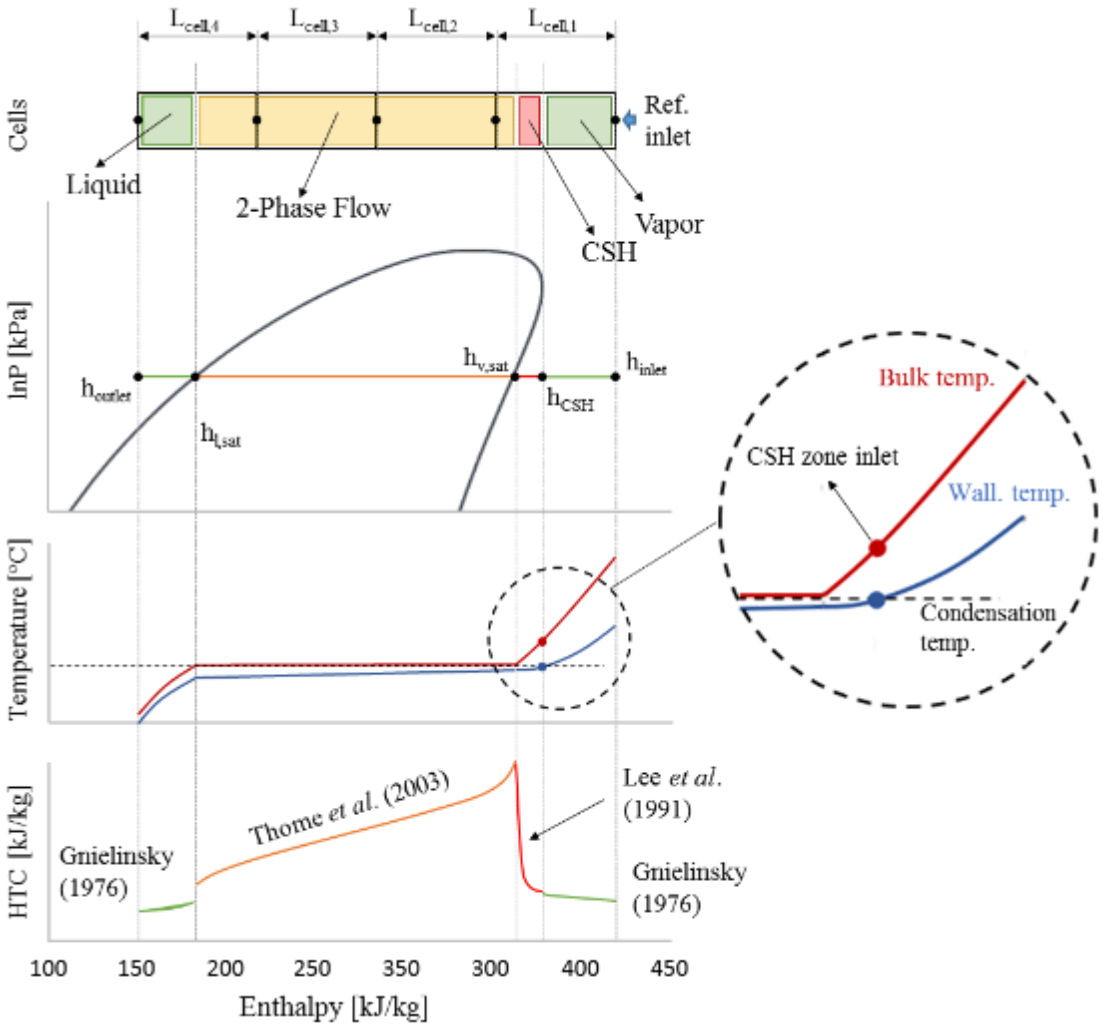

Figure 4.5: The CSH zone; P-h diagram; Temperature profiles; HTC profiles.

The most interesting control volume to analyze is represented by the inlet cell (cell No. 1). Here, one-phase flow, convective condensation of the superheated vapor and two-phase flow coexist. The cell is divided in three portions and the total heat transfer and the pressure drop have to be evaluated as the sum of the contribution of each part. From the modeling point of view, the central cells (No. 2 and No. 3) are the easiest to deal with. Indeed, the complete volume is only occupied by the condensation and no additional partitions are necessary. Finally, focusing the attention on the outlet control volume (cell No.4), it is possible to notice that just one partition is present. Actually, unlike the cell No. 1, the cell presents only one transition section. Therefore, without considering any intermediate zone, the refrigerant moves directly from the condensation zone to the subcooled liquid region.

In general, during the iterations, the model is designed for identifying the sections where a certain cell have to be divided (Corberán *et al.*, 2000), then heat transfer and the pressure drop in each portion are calculated starting from the related boundary conditions.

Effectively, the correct evaluation of the global performance of the complete condenser is strongly dependent on the extension of each portion, hence, on the correct identification of the position of the transition sections. From this point of view, the necessity to include the condensing superheated vapor zone (CSH) in the traditional model adds a further difficulty. Indeed, as well as the identification of the section where the condensation begins and finishes, also the section of the condenser where the convective condensation of the superheated vapor begins has to be additionally located. A priori, the problem seems to be easy to solve. Indeed, as observed experimentally, the condensing superheated vapor zone begins where the wall temperature becomes equal to the saturation temperature ($T_{wall} = T_{sat}$) and finishes when the refrigerant reaches the saturation conditions ($T_{bulk}=T_{sat}$).

However, in a model where the solution of the mathematical problem is evaluated numerically, hence where the wall temperature and the refrigerant temperature are continuously changing iteration by iteration until satisfying the convergence criteria in all the cells, locating the section where the CSH zone starts becomes a very tedious task. In fact, being part of the numerical procedure, the identification of the beginning of the CSH becomes one of the main causes of convergence problems. In this work, such convergence problems have been initially solved adopting what was called Temperature Approach Method.

As will be pointed out later, this method implies higher calculation efforts, which means higher calculation times in comparison with the traditional approach. Consequently, aimed to solve this kind of issue, also the Enthalpy Approach Method was developed.

Synthetically, with the method based on the temperature approach, the traditional numerical resolution procedure (See Chapter 2) has been enriched with the equations for the identification of the enthalpy h_{CSH} (Figure 4.5) based on the relationship between the vapor temperature, the wall tube temperature and the saturation temperature of the refrigerant. On the contrary, the application of the second method involves only a partial modification of the traditional resolution procedure for the identification of the enthalpy h_{CSH}. Actually, with the Enthalpy approach method, no new equation has been used, because the identification of the beginning of the condensing superheated vapor zone has been entirely included in the traditional iterative resolution procedure. As discussed in the next paragraphs, the latter method allows maintaining very low the calculation efforts, providing at the same time a good agreement with the experimental results.

4.2.2 Heat transfer coefficients and friction factors

As discussed in the previous chapter, for an accurate calculation of the performance of a condenser (RTPFs of MCHX), the selection of the suitable set of correlations for the evaluation of the heat transfer coefficients and friction factors plays a fundamental role. Nevertheless, in order to include

in the traditional model the condensation of the superheated vapor, also an additional correlation has to be used. Effectively, beside the correlations proposed by Thome *et al.* (2003) and Gnielinsky (1976) for estimating respectively two-phase flow HTC and One-Phase flow HTC, the correlation presented in 1991 by Lee *et al.* (1991) was considered as the most adequate for calculating the HTC in the condensing superheated vapor region. As it will be discussed afterwards, the combination of the strategy for identifying the beginning of the CSH with the utilization of this correlation leads to eliminate the discontinuity that, otherwise, there would be between the one-phase flow HTC and the two-phase HTC in correspondence of the beginning of the condensation.

Lee *et al*. (1991) studied experimentally the phenomena that take place in a single tube during the process of heat rejection. Considering R22 as refrigerant, they observed that in the one-phase flow region, due to the sensible heat rejection, the temperature of the refrigerant decreased rapidly until reaching the saturation temperature. At the same time, they also measured the wall temperature. Such parameter also underwent a rapid reduction, however, the temperature became almost constant rather earlier than the refrigerant (Figure 4.5). Lee *et al*. (1991) explained such behavior calculating the local value of the HTC along the entire heat rejection process. They noticed that, in the superheated vapor zone, after that the wall temperature became equal to the saturation temperature, the local value of refrigerant heat transfer coefficient underwent a substantial increase. They attributed such behavior to what was called "*convective condensation of the superheated vapor*". In other words, they found out that the condensation occupied part of the superheated vapor zone. It means that a slight film of liquid already appeared on the inner surface of the tube as soon as the wall temperature became equal to the condensation temperature. Due to the simultaneous process of condensing on the wall surface and desuperheating in the bulk flow, Lee *et al*. (1991) estimated that, in the condensing superheated vapor zone, the total heat flux was the sum of two components:

$$q_{CSH} = q_{latent} + q_{sensible} \tag{4.1}$$

The value of the latent component was due to the condensation of the vapor; it is dependent on the heat transfer coefficient for the saturated vapor ($\alpha_{2-phase}$) and the driving temperature difference (T_{sat}-T_{wall}). Otherwise, the sensible component was evaluated as the product of the heat transfer coefficient for forced convection to the gas ($\alpha_{1-phase}$) and the temperature difference (T_{ref}-T_{sat}). Starting from the Eq. 4.1, Lee *et al*. (1991) estimated the q_{CSH} as:

$$q_{CSH} = \alpha_{CSH}\left(T_{ref} - T_{wall}\right) \tag{4.2}$$

Hence, the HTC in every point of condensing superheated zone (α_{CSH}) could be determined using the following equation:

$$\alpha_{CSH} = \alpha_{1-phase}\frac{\left(T_{ref} - T_{sat}\right)}{\left(T_{ref} - T_{wall}\right)} + \alpha_{2-phase}\frac{\left(T_{sat} - T_{wall}\right)}{\left(T_{ref} - T_{wall}\right)} \tag{4.3}$$

According to Eq. 4.3, when the wall temperature gets equal to the refrigerant saturation temperature, the convective condensation of the superheated vapor begins. In this conditions the α_{CSH} is still equal to $\alpha_{1-phase}$. On the other hand, when the vapor reaches the saturation condition ($T_{ref} = T_{sat}$) the α_{CSH} becomes equal to $\alpha_{2-phase}$. Therefore, as already commented, the discontinuity between the one-phase HTC and the two-phase HTC was definitively eliminated. As will be discussed in the next paragraph, such equation will be used for the estimation of the HTC in the condensing superheat vapor zone only when the Temperature Approach Method is used.

4.2.3 Temperature approach method

As already mentioned, the process aimed to the identification of the section of the condenser where the convective condensation of the superheated vapor starts becomes part of the numerical method for the resolution of the algebraic equations system obtained by the integration of the governing equations (Chapter 2). Actually, with the application of the Temperature approach method, the main calculation process is not completely revolutionized, on the contrary, it is enriched of a new "appendix" aimed to the identification of the correlation between all the parameters that affect the convective condensation of the superheated vapor. Effectively, the perfect integration of this appendix in the traditional iterative calculation procedure represented the actual challenge, because it represented the biggest cause of most of the convergence problems.

As described in the section 4.2.1, the heat transfer in every cell *i* depends on the number and position of the partitions along the refrigerant path. In the traditional model, the transition from the one-phase zone to the two-phase zone was defined exclusively by the value of the condensation temperature; otherwise, the inclusion of the convective condensation of the superheated vapor zone adds the further necessity to identify the cell and the position along the refrigerant path where T_{wall} reaches the condensation temperature. With this aim, initially, the Temperature Approach Method was ideated for the identification of the cell in which this condition is respected. Afterwards, it was further modified with the objective to identify with high precision the section of the condenser in which the convective condensation of the superheated vapor effectively begins. The name "Temperature approach method" is due to the parameters that have to be considered during the calculation. Indeed, as will be discussed later, the identification of the beginning of the convective condensation of the superheated vapor is strongly connected to the values of three temperatures: the refrigerant bulk temperature, the wall temperature and condensation temperature.

From a practical point of view, applying the Temperature approach method, at the beginning of the procedure for the evaluation of the heat transfer in every refrigerant cell *i* (Figure 4.6) the parameter $\Delta T_{CSH,i}$ has to be calculated. It is simply defined as the difference between the saturation temperature (T_{sat}) and the tube wall temperature ($T_{wall,i}$):

$$\Delta T_{CSH,i} = T_{wall,i} - T_{sat} \tag{4.4}$$

Once this parameter is calculated, depending on the relationship between the refrigerant temperature at the inlet node ($T_{ref,i}$), the saturation temperature (T_{sat}) and temperature at the wall node ($T_{wall,i}$), the heat transfer in the cell can be completely characterized. To do that, in addition to the $\Delta T_{CSH,i}$, also its maximum value has to be arbitrary fixed ($\Delta T_{CSH,max}$). Consequently, depending on the ratio $\Delta T_{CSH,i}/\Delta T_{CSH,max}$, for every cell *i*, it is possible the identification of all the thermodynamic parameters in correspondence of each node, the correlations to use for the estimation of the heat transfer coefficients, hence the position of the section where the refrigerant gets in the CSH zone. In Table 4.2, all the possible scenarios are summarized.

Table 4.2: Definition of the regions in the Round-Tube condenser model

Case	Initial Cond.	$\Delta T_{CSH,i}$	Cell regions	Correlations (inlet node / outlet node)
A	$T_{ref,i}$; $T_{wall,i} > T_{sat}$	$\Delta T_{CSH,i} > \Delta T_{CSH,max}$	Superheated vap.	Gnielinski (1976) / Gnielinski (1976)
		$\Delta T_{CSH,i} \leq \Delta T_{CSH,max}$	Superheated vap. CSH vapor	Gnielinski (1976) / Gnielinski (1976) Lee *et al.* (1991) / Thome *et al.* (2003)
		$\Delta T_{CSH,i} = 0$	Superheated vap. CSH vapor	Gnielinski (1976) / Gnielinski (1976) Lee *et al.* (1991) / Lee *et al.* (1991)
B	$T_{ref,i} > T_{sat}$; $T_{wall,i} < T_{sat}$	$\Delta T_{CSH,i} < 0$	CSH vapor	Lee *et al.* (1991) / Thome *et al.* (2003)
C	$T_{ref,i} = T_{sat}$; $T_{wall,i} < T_{sat}$	-	2-Phase region	Thome *et al.* (2003) / Thome *et al.* (2003)
D	$T_{ref,i} < T_{sat}$; $T_{wall,i} < T_{sat}$	-	Subcooled liquid	Gnielinski (1976) / Gnielinski (1976)

Focusing the attention on the cases A and B (Table 4.2), depending on the value of the ratio $\Delta T_{CSH}/\Delta T_{CSH,max}$, is possible to evaluate if the refrigerant is still in the superheated vapor zone, if the cell have to be divided in two parts or if the cell is completely inside the CSH zone. All the possible calculating conditions are depicted in Figure 4.6.

When the refrigerant temperature at the cell inlet is higher than the saturation temperature ($T_{ref,i} > T_{sat}$), if the ΔT_{CSH} is higher (case A-1) or equal (case A-2) to $\Delta T_{CSH,max}$, the condensing superheated zone is considered not began yet and the refrigerant inside the cell is still totally superheated vapor. In this cases, as described in the chapter 2, the total heat transfer, hence the temperature in in both the inlet and outlet nodes, is calculated applying the energy balance for open systems (Eq. 2.3), in which the HTC is calculated with the correlation proposed by Gnielinski (1976).

When the ratio $\Delta T_{CSH,i}/\Delta T_{CSH,max}$ is between one and zero (case A-3 and case A-4), the cell is divided in two portions. In the first part, the refrigerant is still vapor; in the second, after the introduction of a new intermediate node, the refrigerant is considered inside the CSH zone.

The extension of the volume where the refrigerant is still superheated vapor is calculated with the Eq. 4.5, according which, the L_{vapor} is calculated as function of the $\Delta T_{CSH}/\Delta T_{CSH,max}$:

$$L_{vapor} = L_{cell} * \Delta T_{CSH} / \Delta T_{CSH,\max} \quad (4.5)$$

All the thermodynamic conditions at the intermediate node are calculated as function of the refrigerant temperature $T_{ref,CHS}$. This parameter is evaluated as follows. Defining $T_{ref,mean}$ as the average temperature between the inlet ($T_{ref,in}$) and outlet temperature ($T_{ref,out}$=$T_{ref,CSH}$), the temperature in correspondence of the intermediate node ($T_{ref,CHS}$) can be estimated by means of the resolution of the energy balance:

$$\alpha_{ref} \pi D_h L_{vapor} (T_{ref,mean} - T_{wall}) = \dot{m}_{ref} c_{p,ref} (T_{ref,in} - T_{ref,CSH}) \quad (4.6)$$

In this equation, the only unknown parameter is the $T_{ref,CSH}$ inasmuch, the parameters α_{ref} (see correlations in Table 4.2) and Cp_{ref} are calculated for the average temperature between the refrigerant inlet temperature ($T_{ref,in}$) and the T_{wall}.

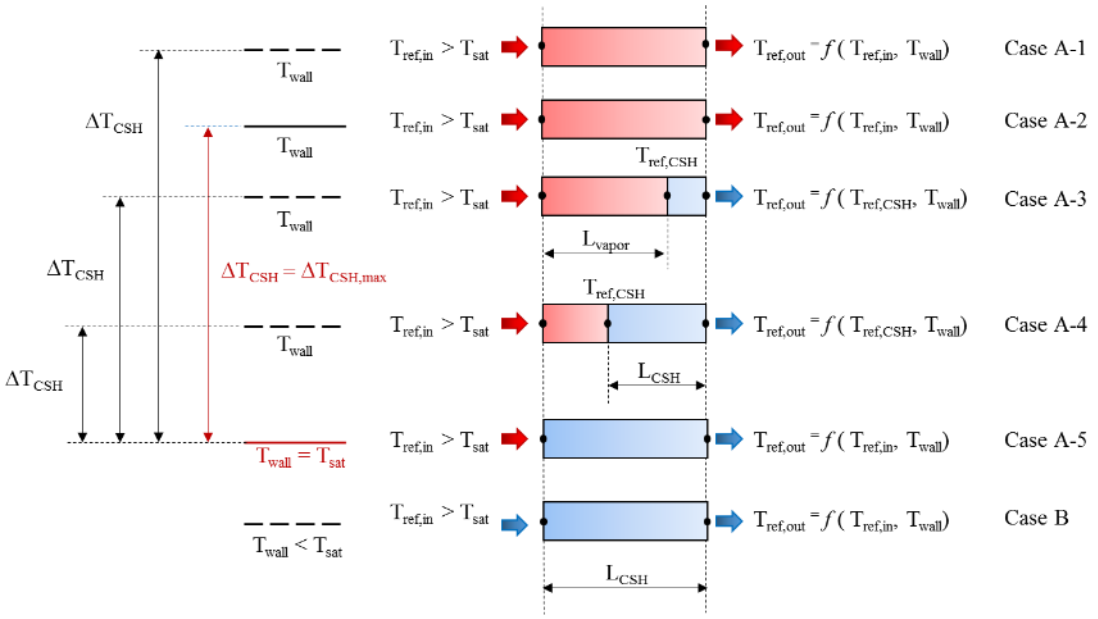

Figure 4.6: Temperature Approach Method

Once the thermodynamic characteristics at the intermediate node are calculated, they can be assumed as initial conditions for evaluating the heat transfer in the second part of the cell. Here, the refrigerant is completely in the CSH zone. The temperature at the outlet node is calculated again by means of the energy balance. However, being in the CSH zone, the Equation 4.3 is applied for the estimation of the HTCs in both the intermediate and the outlet nodes. According to the methodology proposed by Corberán *et al*. (2000), if the extension of the CSH zone (L_{CSH}) allows achieving the saturation conditions, then, the cell has to be furtherly divided. Otherwise, no more partitions are performed and the refrigerant at the outlet of the cell is still considered inside the CSH zone.

The conditions characterizing the case A-5 represent an exception of the cases A-3 and A-4. Indeed, in this case, ΔT_{CSH} is equal to zero and L_{vapor} is nullified according with the Equation 4.5. This

condition means that the CSH zone begins exactly at the cell inlet. As in the previous cases, if during the calculation the 2-phase flow conditions are not reached, the cell is completely in the CSH vapor zone and L_{CSH} is exactly equal to $L_{cell.}$ On the other hand, the cell has to be divided where the condensation starts ($T_{ref} = T_{sat}$; x=1). When in the cases A-3, A-4 and A-5 the saturated conditions are not reached, the CSH zone is shared between two adjacent cells. Evidently, in the case B of Figure 4.6, although the wall temperature is lower than the saturation temperature, the refrigerant is still not in the two-phase flow zone ($T_{ref,in} > T_{sat}$). In these conditions, the ΔT_{CSH} is lower than zero, hence, the heat transfer coefficient at the inlet node is calculated considering the Lee's *et al*. (1991), while at the outlet one, it is estimated with the Thome *et al.* (2003) correlation (for $T_{ref} = T_{sat}$ and x=1). As for the previous cases, the cell has not to be more divided, unless the saturation conditions are going to be reached. Finally, if $T_{ref,in} = T_{sat}$ or $T_{ref,in} < T_{sat}$, the $\Delta T_{CSH,i}$ is not calculated at all and the heat transfer is evaluated following in the traditional resolution strategy depending on the flow conditions.

4.2.4 Enthalpy approach method

As already anticipated earlier, the utilization of the Temperature approach method for the identification of the CSH transition section entails a higher number of iterations for satisfying the convergence criteria in all the control volumes. For this reason, in order to reduce the calculation time, the Enthalpy approach method was also developed. Although both the methods are aimed to identify the section where the condensation of the superheated vapor begins, they present some fundamental differences. On one hand, with the Temperature Approach Method, the thermodynamic conditions at the CSH zone inlet are estimated considering the correlation between of the bulk refrigerant temperature, saturation temperature and wall tube temperature (Paragraph 4.2.3), on the other, with the Enthalpy approach method, only the parameter h_{CSH} (enthalpy of the refrigerant at the inlet of the CSH zone) plays a fundamental role. Actually, unlike the Temperature approach method, the h_{CSH} is not explicitly calculated starting from thermodynamic the characteristics of the refrigerant in each cell, but, on the contrary, it is the result of a simpler numerical procedure. In practice, as it will be discussed later, the procedure is aimed to identify the particular value of the $h_{ref}=h_{CSH}$ such as, in one of the wall cells *i*, the difference $T_{wall,i} - T_{sat}$ is minimized. This method has a big advantage to avoid any deep change in the original structure of the calculation procedure described in the Chapter 2 of the present thesis, hence, it allows maintaining very low the calculation time.

From a practical point of view, as for any numerical procedure, the first iteration is performed considering an initial value of the h_{CSH}. It is estimated by means of the Equation 4.6:

$$h_{CSH} = a * \left(h_{liquid,sat} + \Delta h_{cond}\right) \tag{4.6}$$

Where, in order to guarantee that the convective condensation of the superheated vapor always starts in the superheated vapor zone, the parameter "*a*" is forced to be bigger than 1.

As already mentioned, with the Enthalpy approach method, the traditional calculation procedure has been completely maintained unchanged. It means that the refrigerant path is discretized in a certain number of control volumes, where the thermodynamic characteristic at the inlet and outlet can be estimated solving the energy balance (Corberàn *et al.*, 2001). In addition to the traditional calculation strategy, if in one cells the refrigerant reach the CSH zone ($h_{ref}=h_{csh}$), the cell is being split and the total heat transfer is calculated as the sum of the heat transfer in each portion. As in the traditional condenser model, after every iteration, a new T_{wall} distribution along the heat exchanger is calculated. Hence, the procedure is repeated as far as the heat transfer in the refrigerant side is equal to air side.

Nevertheless, in order to identify the section of the condenser where the CHS zone starts, besides the T_{wall} distribution, also a new value of the h_{CSH} is estimated every time. On one hand, it is continually changed as far as in a certain cell the convergence criteria is respected, on the other, it is also modified in order to force the wall temperature in one of the cells as close as possible to the value of the condensation temperature.

To do that, during every iteration, the coefficient "*a"* is estimated as function of the $\Delta T_{CSH,i}$ when that refrigerant gets in the cell *i* where it is assumed that the CSH zone begins. Here, the coefficient is calculated as:

$$a = a' - b * \Delta T_{CSH,i} = a' - b * \left(T_{wall,i} - T_{sat}\right) \tag{4.7}$$

If during the calculation of the cell *i*, the $\Delta T_{CSH,i}$ is positive, hence $T_{wall,i}$ is higher than the saturation temperature, the condensation of the superheated vapor cannot really take place. Evidently, the position of the h_{CSH} has been overestimated, so the coefficient "*a"* has to be necessarily decreased in comparison with in the previous iteration (*a'*). On the contrary, when $\Delta T_{CSH,i}$ is negative, the coefficient "*a"* was underestimated in the previous iteration, so, it has to be increased. Depending on the initial value of the of h_{CSH}, especially in the first iterations, the $\Delta T_{CSH,i}$ can assume too high values. Hence, the convergence criteria in all the cells might be achieved with a very high number of iterations. In order to minimize the calculation time, hence for reducing the fluctuations of the parameter "*a"* around its final value, the constant parameter *b* (<<1) was also introduced. Effectively, as verified during the model validation, this expedient allows calculating of the parameter "*a"* only in few iterations. In other words, in few iterations, the parameter "a", for which the $\Delta T_{CSH,i}$ variations can be considered negligible, is univocally identified.

Beside this, in order to reduce the possibility to have any convergence problems, the Enthalpy approach also takes into account another simplification. In practice, the HTC in CSH vapor zone is calculated with the Eq. 4.8 instead of using that proposed by Lee *et al.* (1997).

$$\alpha_{CSH} = \left(\frac{\alpha_{2-phase} - \alpha_{1-phase}}{h_{ref,sat} - h_{CSH}} \right) * \left(h_{ref} - h_{CSH} \right) + \alpha_{1-phase} \tag{4.8}$$

Where, in every iteration, the $\alpha_{2-phase}$ is evaluated as function of the saturation conditions (x=1), while the $\alpha_{1-phase}$ is calculated for the thermodynamic conditions of the refrigerant associated the h_{CSH}.

As will be discussed in the next paragraph, the utilization of the equation 4.8 instead of the 4.3 does not affect negatively the results of the model. On the contrary, against the lower calculation time, the Enthalpy approach provides very similar result to those achieved with the utilization of the Temperature approach method.

4.2.5 Model validation

4.2.5.1 Tube-and-fins heat exchanger

In the Figures 4.7-4.11 the experimental temperature profiles along the condenser are compared with those calculated by means of the utilization of IMST-ART 3.7 (standard version) and its modified version, distinguishing the results obtained by means of the application of the Temperature approach method and the Enthalpy approach method. In every figure, the diagrams are referred to the frontal circuit (identified with the letter A) and the rear one (identified with the letter B). As described in at the beginning of his chapter, the experimental refrigerant temperature (T_{ref}) was estimated by means of the application of the thermocouples along the two circuits (Figure 4.1), while the wall temperature (T_{wall}) of the frontal circuit was obtained with an infrared camera (Figure 3.2).

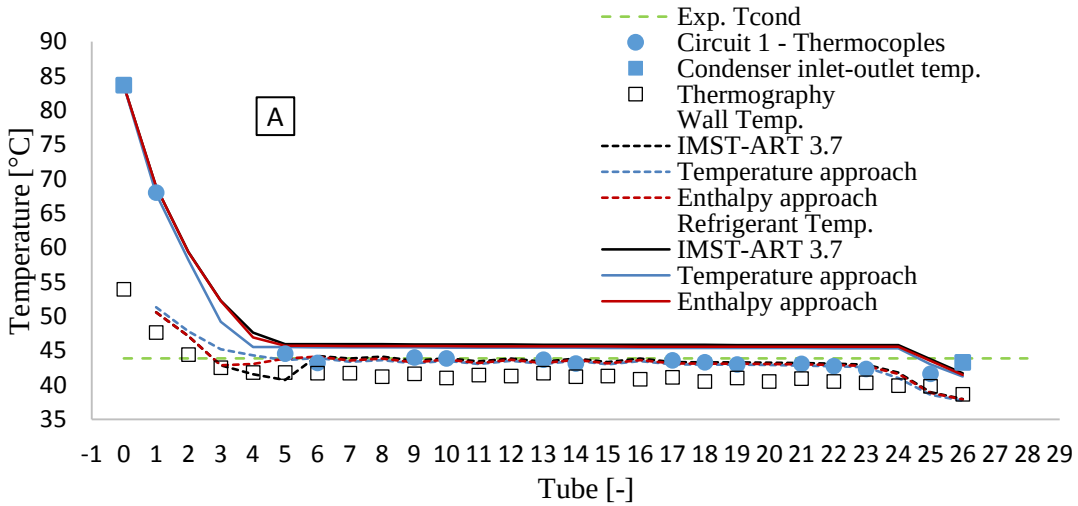

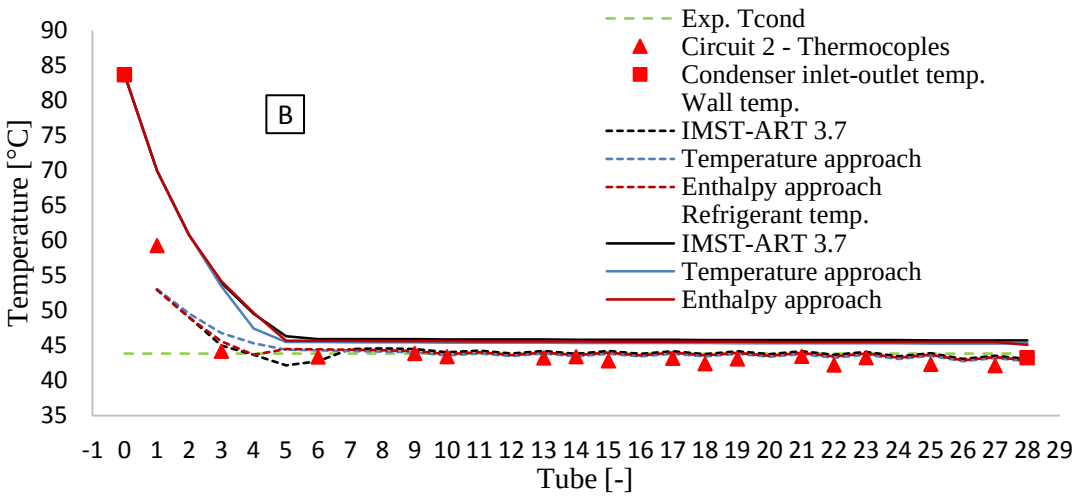

Figure 4.7: Reference test (SC=0°C; Tair,in=35°C; vair,in=2.5 m/s; mref=0.014 kg/s)

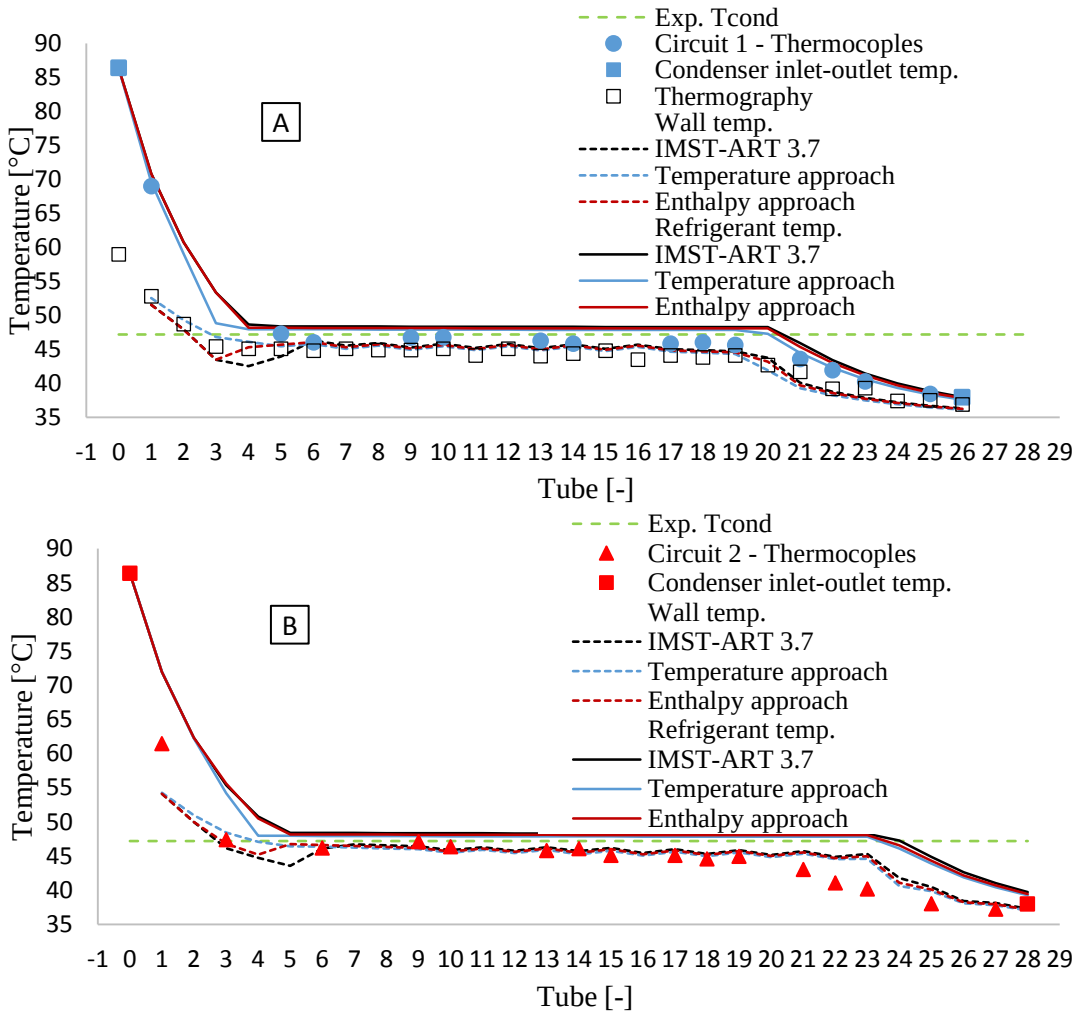

Figure 4.8: Test 2 (SC=10°C; Tair,in=35°C; vair,in=2.5 m/s; mref=0.014 kg/s)

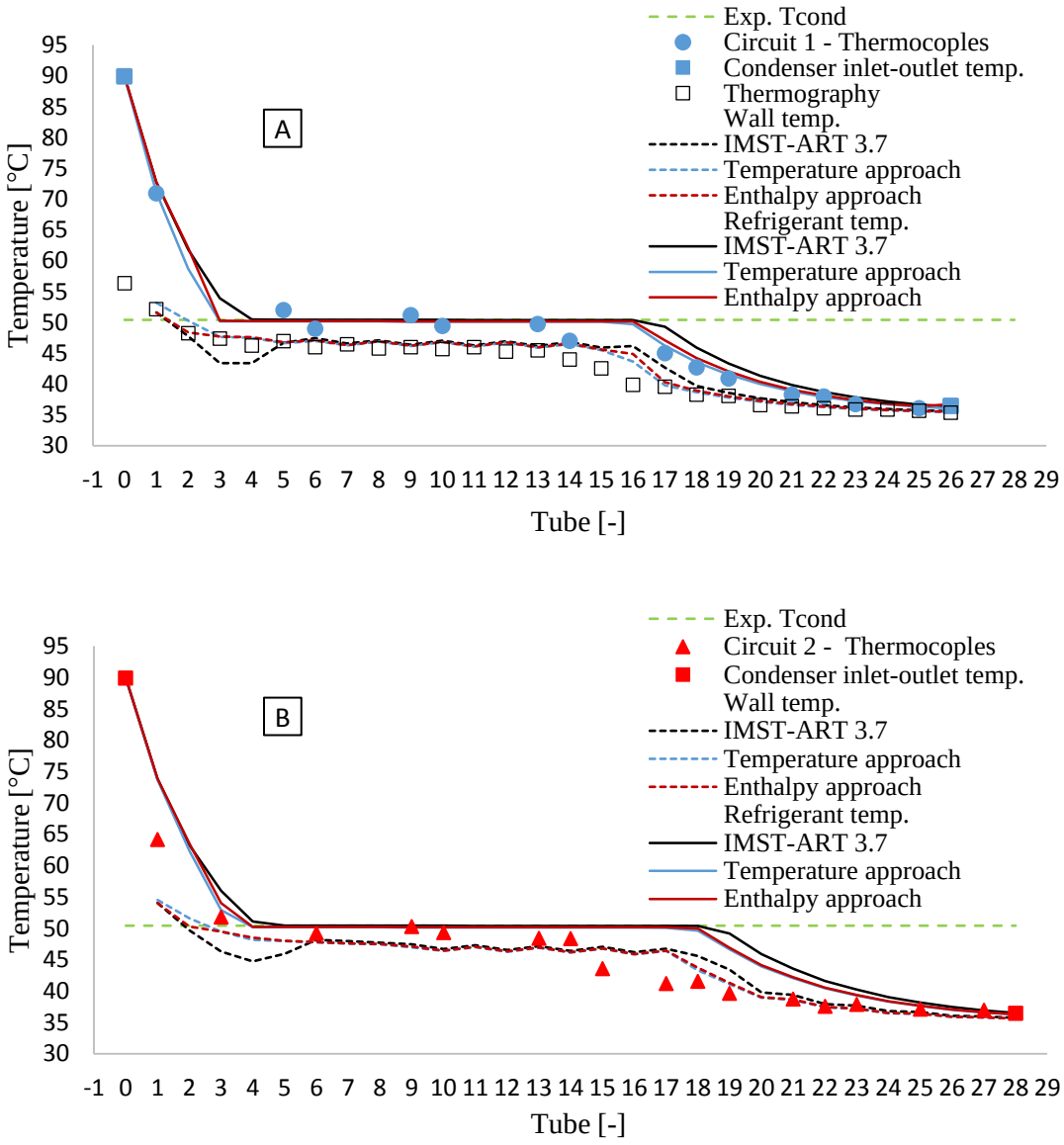

Figure 4.9: Test 3 (SC=14°C; Tair,in=35°C; vair,in=2.5 m/s; mref=0.014 kg/s)

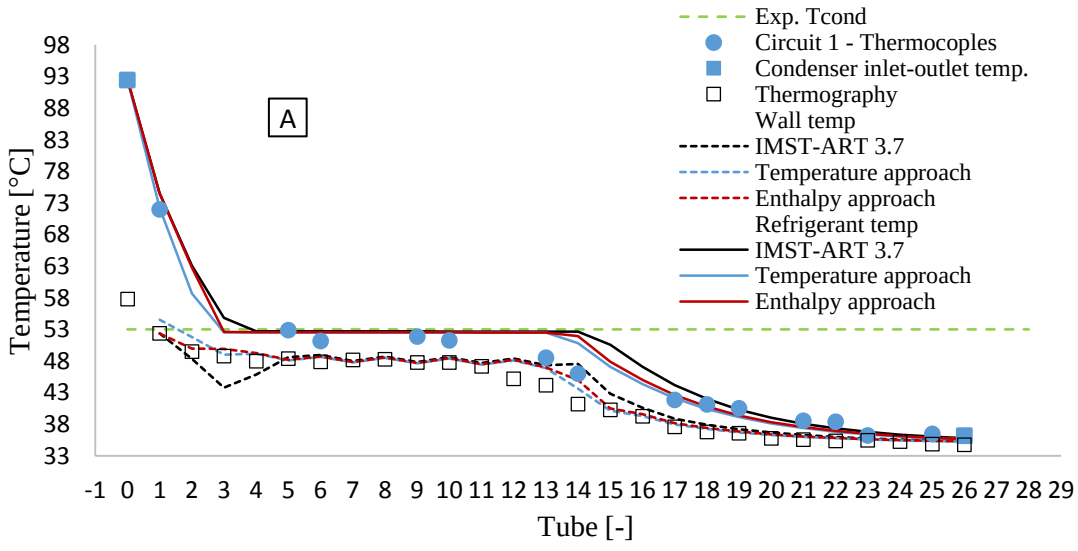

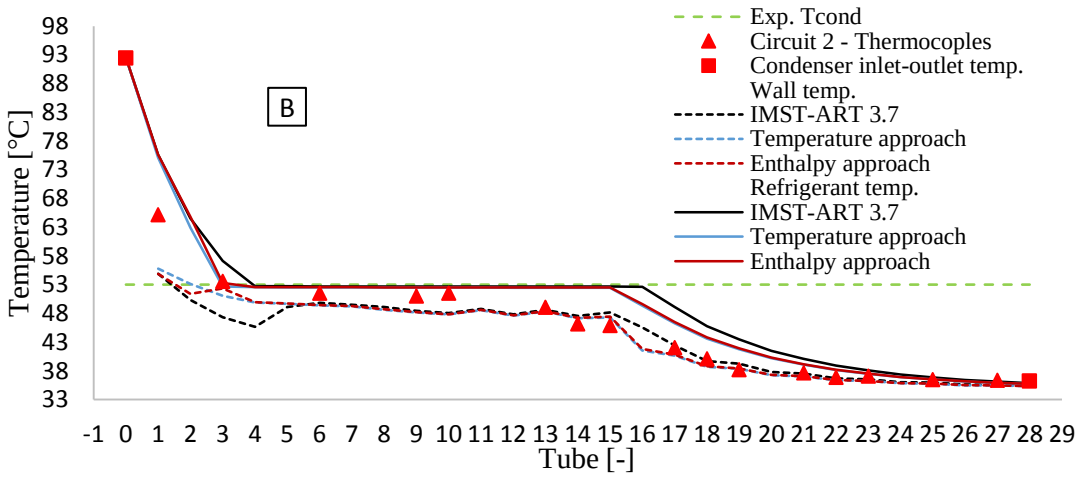

Figure 4.10: Test 4 (SC=17°C; Tair,in=35°C; vair,in=2.5 m/s; mref=0.014 kg/s)

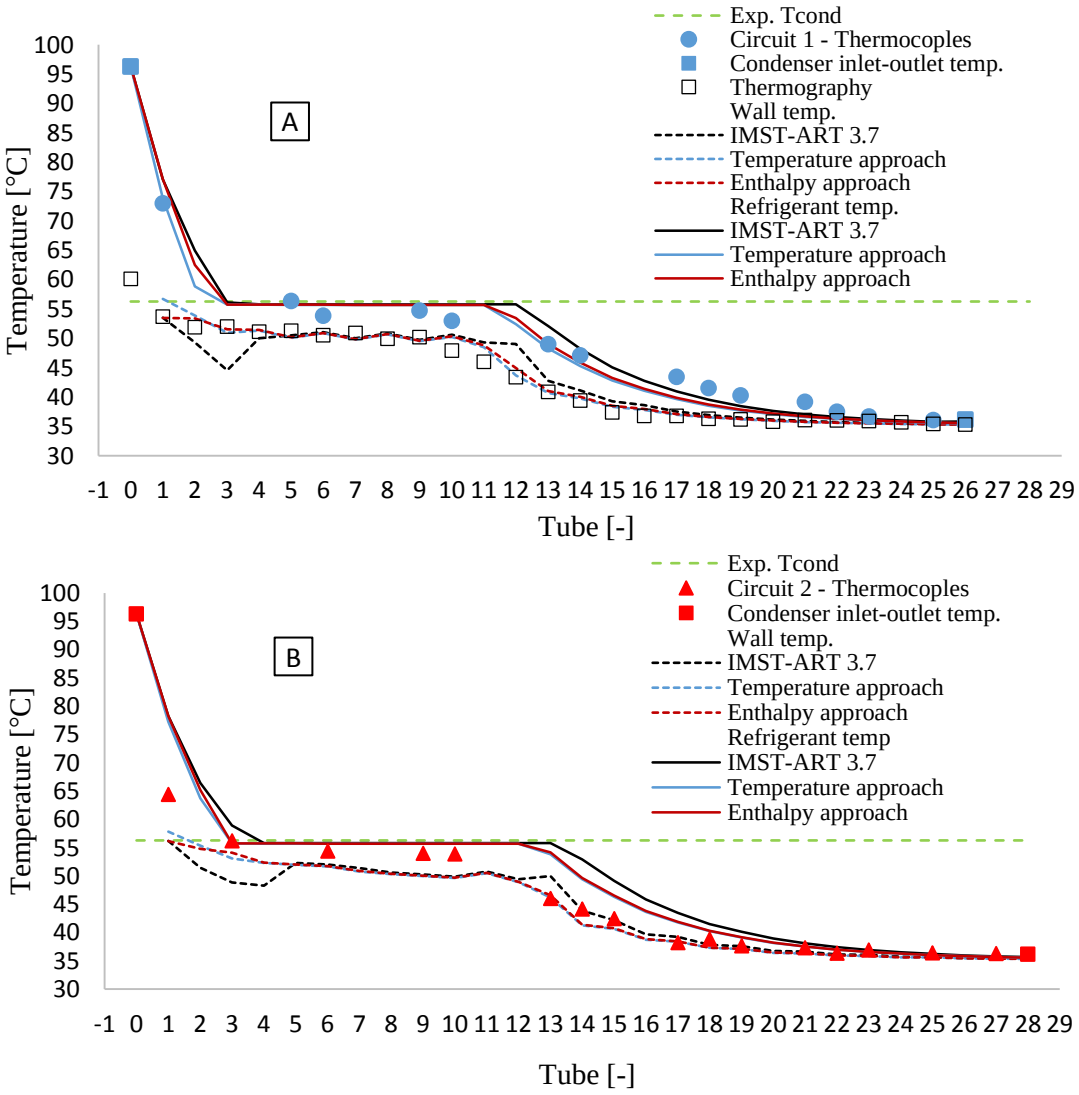

Figure 4.11: Test 5 (SC=20°C; Tair,int=35°C; vair,in=2.5 m/s; mref=0.014 kg/s)

The trend of the results is rather clear. Just considering the phenomena of the convective condensation of the superheated vapor and the consequent variation of the heat transfer coefficient at the end of the 1-phase flow zone, the temperature profiles calculated by the model becomes significantly more similar to the experimental ones. Indeed, as can be notice in the Figure 4.7-4.11, for all the operating points described in the paragraph 4.1.1, the application of both the Temperature and the Enthalpy approach methods generates the displacement towards the condenser inlet of the beginning of the two-phase zone (~1 tube). In addition to this, also the wall temperature estimation undergoes evident improvements. Effectively, the unusual dip at the beginning of the condensation process characterizing the results provided by IMST-ART 3.7 (traditional model) has been automatically levelled thanks the introduction of the CSH vapor zone and the consequent better evaluation of the local heat transfer coefficient.

Moreover, it is also important highlighting that the differences in the results due to the application of the two alternative methods can be considered negligible. Therefore, in the author's opinion, the slightly better prediction due to the utilization of the temperature approach method does not justify the application of this method to the detriment of a short calculation time. In conclusion, without considering any other modification, such as the refrigerant maldistribution, it is possible to affirm that the accuracy of the model in the evaluation of the temperature profiles has been notably increased.

Beside these considerations, it is important to point out that with the introduction of the condensing superheated vapor zone in the traditional condenser model, also the prediction of the global performance is slightly changed. Such affirmation is confirmed by the analysis of Table 4.3 and Figure 4.12 where the results of the traditional model are compared again with those obtained using its two modified versions. To be consistent with the results obtained in Chapter 3 of the present Ph.D. thesis, the simulations have been carried out using the best sets of correlations and without the application of any enhancement factor.

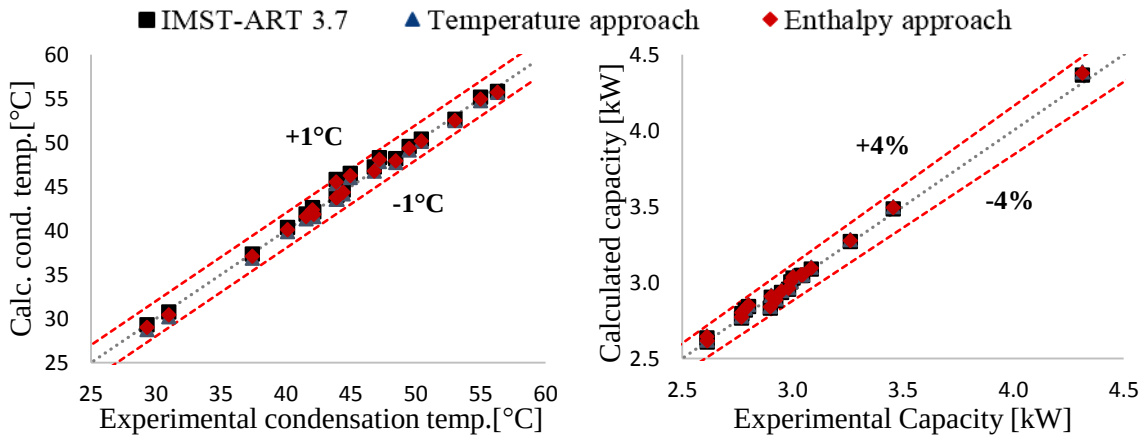

Figure 4.12: Traditional model vs. Temperature approach method Vs. Enthalpy approach method

Actually, from the analysis of the diagrams in Figure 4.12, it is possible to affirm that the results provided by IMST-ART 3.7 and by the modified models can be considered almost completely overlapped and very close to the experimental data. The detailed analysis of the figure leads to affirm that the condensation temperature is always calculated with an error lower ±1°C, that becomes even less than ±4% talking about the thermal capacity. Beside this, for appreciating the advantages due to the introduction of the convective condensation of the superheated vapor, the results of the simulations have to be also compared in terms of general metrics such as mean error (ME) and standard deviation (SD).

Table 4.3: comparison between IMST-ART 3.7, Temperature approach method and Enthalpy approach method in terms of global performance

	IMST-ART 3.7		**Temperature approach method**		**Enthalpy approach method**	
	Tcond [K]	Qcond [%]	Tcond [K]	Qcond [%]	Tcond [K]	Qcond [%]
ME	0.602	0.150	-0.174	0.545	-0.004	0.378
SD	0.614	0.941	0.591	0.949	0.603	0.943

Effectively, as already discussed in the third chapter of this thesis, the results provided by IMST-ART 3.7 already showed very good agreement with the experimental data. However, as shown in Table 4.3, both the mean error and the standard deviation in the evaluation of the condensation temperature have been furtherly reduced thanks the application of both the Temperature approach and Enthalpy approach methods. On the other hand, although the condensation temperature is better estimated, no big changes can be really appreciated in terms of capacity. Actually, the error in the estimation of the performance has been even negligibly increased with the introduction of the CSH zone in the model.

4.2.5.2 Microchannel heat exchanger

As described in Chapter 2, the main model for simulating the performance of microchannel and gas cooler was proposed by Martinez-Ballester (2013). The main differences in the MCHX and the RTFFs modelling approaches can be identified in the different interpretation of the phenomena occurring in the airside and in an alternative discretization of the heat exchanger. Otherwise, in the refrigerant side, the discretization in cells, the governing equation and the methodology adopted for their integration are practically the same. In other words, it means that all the modification implemented in the refrigerant side of RFPFs model can be moved to the MCHX model with a relatively negligible extra-effort. Starting form this consideration, the Enthalpy approach method, which is turned out to be reasonably accurate and less time consuming compared with Temperature approach method, has been implemented also in the MCHX model.

Differently from the RTPFs condenser, due to its geometric characteristics, the attempt to evaluate experimentally the temperature profiles along the heat exchanger has provided highly unreliable

results. Therefore, in this case, the model validation has been carried out only comparing the global performance, hence analyzing the results only in terms of condensation temperature and thermal capacity.

In Figure 4.13 is depicted the results of the validation using IMST-ART in version 3.7 and the MCHX model including the convective condensation of the superheated vapor (Enthalpy Approach method). As for the RTPFs condenser, the simulations have been performed using the best HTC correlations (listed in Chapter 3) and no enhancement factors.

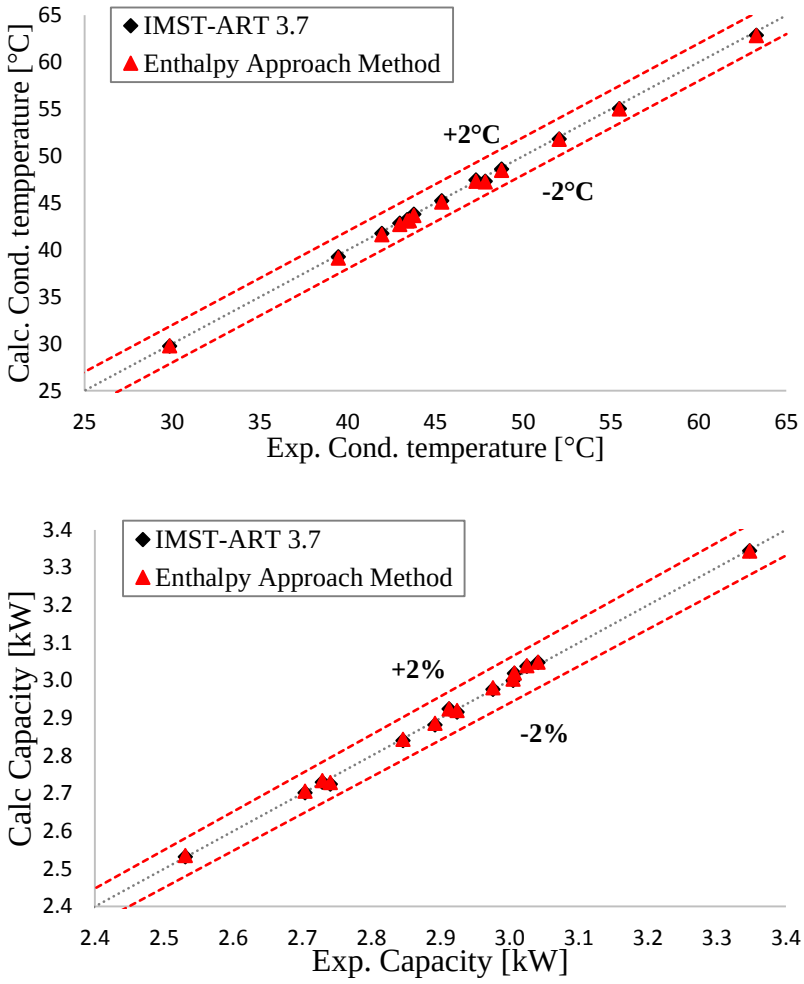

Figure 4.13: Microchannel condenser model - Imst-ART 3.7 vs. modified model (Enthalpy approach method)

The results show that the inclusion of the superheated vapor zone only affects marginally the model prediction. Indeed, both the traditional model and the modified one are able to evaluate the condenser performance (Condensation temperature and thermal performance) with extremely low mean error and standard deviation (Table 4.4).

Table 4.4: MCHX - IMST-ART 3.7 vs. Enthalpy approach method

	Condensation Temperature		**Thermal Capacity**	
	IMST-ART 3.7	Enthalpy app. method	IMST-ART 3.7	Enthalpy app. method
ME	-0.202 K	-0.302 K	-0.008 %	0.086 %
St. Deviation	0.181 K	0.155 K	0.296 %	0.260 %

4.3 Conclusions

The discussion regarding the validation of a condenser model considering different correlations for the evaluation of the HTCs led to identify a possible "weak point" of the current methodology for the simulation of the condensation process. Indeed, by the comparison of the temperature profiles (wall tube and refrigerant) calculated by the IMST-ART 3.7 and those measured experimentally along the circuits of the tested round tube heat exchanger, it was possible to noticed that the heat transfer coefficient at the end of the one-phase flow zone was incorrectly estimated. Effectively, in the condenser model built-in IMST-ART 3.7, the convective condensation of the superheated vapor was not taken into account. On the other hand, since this phenomena was the objective of many experimental studies (See the introductive chapter), which demonstrated an evident variation of the local heat transfer just before the beginning of the condensation process, in the present chapter, two methodologies for upgrading the original model have been presented and implemented.

The methodologies have been respectively referred as "Temperature Approach method" and "Enthalpy approach method". The first methodology allows evaluating with high accuracy the performance of the condenser, but its application entails a significant increasing of the calculation time. On the contrary, being based on some simplification hypothesis, the Enthalpy approach keeps very low the calculation efforts, maintaining adequate the agreement with the experimental results.

The results of the model validations can be summarized as follows:

- The modification of the original condenser model with the possibility to consider the convective condensation of the superheated vapor guaranties a better interpretation of the entire heat rejection process characterizing both coils and microchannel heat exchangers.
- The temperature profiles along the RTPFs condenser are calculated with higher accuracy. In other words, it means that the correct evaluation of the local value of the HTC in the superheated vapor zone affects notably the estimation of the temperature profiles.
- Nevetheless, the impact on the prediction of the global performance is not so significant. Indeed, for both the heat exchangers, in comparison with original model, just negligible changes can be appreciated after the application of both the Temperature approach and Enthalpy approach methods.

In addition to the just listed results, the validation process has also highlighted that the condenser model can be furtherly improved considering:

- The different distribution of the refrigerant in the two circuits of the coil.
- The presence of the subcooled liquid zone as already experimentally investigated by Kondou and Hrnjak (2012).

Chapter 5

5. Effect of the air maldistribution on the performance of a condenser

Once the convective condensation of the superheated vapor was implemented in the condenser model, the research work was oriented exclusively towards the experimental analysis of the effects of the air maldistribution on the performance of condensers.

As pointed out in the introduction, the air and refrigerant maldistribution seem to affect significantly the performance of parallel flow evaporators much more than that of condensers.

It is first necessary to point out the high number of parameters that affect both the air and refrigerant distribution. Indeed, on one side, the air distribution is strongly depending on the specific geometry of the heat exchanger, its position in the unit frame, as well as on the performance and the position of the fan. On the other, the performance degradation due to the refrigerant maldistribution strongly depends on the configuration of the circuits in the coils, shape of the headers and distributors in the MCHX, and to some extent also to the air maldistribution. Due to such a big number of variables and to the difficulties on experimentally characterizing those two maldistributions, air and refrigerant, a full analysis of their influence on the performance of a condenser lies outside the scope of the present PhD, which had to be focused only on the air maldistribution effect.

The study presented in this chapter consists mainly of three parts. First, the development of an experimental methodology for generating in a "controlled" way whatever air velocity profile at the inlet of a heat exchanger; hence, second, the application of the developed methodology to the experimental analysis of the effects of air maldistribution on the performance of the two condenser samples described in Chapter 3. Finally, the validation of the developed model for situations with air maldistribution. For this purpose, the kernel code of both the RTPFs and MCXH condenser models was deeply modified in order to consider any air velocity profile as input parameter.

5.1 Experimental method to generate a non-uniform air flow distribution

For the identification of a reliable experimental method for analyzing the effect of the air maldistribution on the performance of a heat exchanger, two main issues have to be first dealt with:

- The identification of the best technology for measuring the local value of air velocity.
- The development of a simple methodology for generating a "controlled" air maldistribution.

Regarding the first point, during the first part of the doctoral work, some different solutions were considered and compared. In most of the applications in which it is necessary to measure the velocity inside an airflow, the Pitot tube is the instrument most widely used. However, although this measuring device is simple and reliable, its use requires the knowledge of the exact flow direction and, furthermore, its accuracy is not very high. As an alternative, where the orientation of the streamlines is not well defined, or where the installation of the Pitot tube is rather difficult, other technologies are generally preferred. For instance the hot-wire anemometry or, if very accurate measurement and high resolution is required, the PIV (Particle Image Velocimetry) are widely used. In comparison to the PIV, the hot-wire anemometry presents the following important advantages: i) the instrument is very easy to handle and set-up; ii) the sensor is relatively cheap; iii) it provides reasonable accuracy; iv) the anemometer can be quickly and easily placed in different positions of an air duct for measuring the air flow distribution. Due to such characteristics, in this work of thesis, the hot-wire anemometry was selected as the most convenient instrument for measuring the air velocity distribution at the inlet of the studied heat exchangers.

Once identified the technology for the air velocity measurement, as previously commented, the second issue to sort out is connected to the identification of a simple method for generating a "controlled" uneven air velocity profile at the inlet of a heat exchanger. The word "controlled" has been especially used for highlighting the intention to provide a general method through which whatever air velocity profile can be firstly defined by the designer and then easily generated. For instance, Figure 5.1A shows a linear air velocity profile at the inlet of a generic the heat exchanger (HX).

Generating any continuous air velocity profile, as the linear case shown in Figure 5.1A is probably not feasible and for sure very difficult. Instead, any theoretical velocity profile can be approximated using a *step function*. Undoubtedly, the higher is the number of steps (air layers) used, the better will be the approximation to the original profile. From a practical point of view, every step can be obtained positioning different obstructions in front of the heat exchanger as it is schematically depicted in Figure 5.1B and 5.1C. The methodology represented in Figure 5.1 B, consists of inserting pieces of different filtering material, so producing different pressure drop across them, in order to generate a controllable velocity profile in front of the HX. Alternatively, the methodology represented in Figure 5.1C consists of employing different thickness of the same filtering material in order to provide the required velocity profile. B methodology is not easy to employ since it requires to find the required filter porosity for each layer. C methodology is much easier to implement since it only consists on evaluating which is the thickness of filtering material one must insert in order to generate a given velocity downstream the filter layer. Of course, these two options (B and C) can be combined if required. Along this doctoral work, both techniques were tried and C methodology was found to be much more flexible and easier to handle.

Porous materials are available in a huge number of porosities and therefore it is easy to select the most appropriate material for the application. For the present work, thick air conditioning filters (polymer foams) were considered the easiest material to handle and turned out to be a good solution for the developed methodology. This kind of material provide many features extremely suitable for our particular application:

- Air conditioning filters are in general provided as big sheets in different thicknesses. This allows selecting the most suitable "size" according to the heat exchanger geometry.
- The commercial filters for air conditioning systems have an adequate porosity and rigidity. In principle, they can keep stuck to the frontal surface of the heat exchanger without the utilization of any other supporting structure due to the air drag.

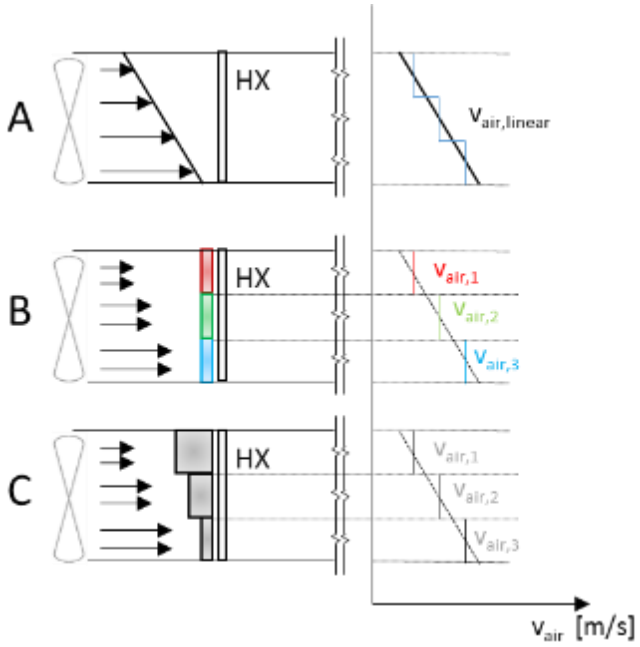

Figure 5.1: comparison between different methods for generating an uneven velocity profile at the inlet of a heat exchanger

- Thick foams (sponges) are in general very easy to handle. They can be cut and modelled with a very small effort.
- Different porosity characterizes the material used for the filters. The different velocities are obtained by increasing the length of the air path through the porous materials (filter length). The difference in pressure drop through the different layers being the origin for the differences in velocity. High pressure drop will require a higher fan power and could maybe increase the generation of undesired or uncontrolled turbulence, vortex or wakes. Therefore, the foam with the minimum pressure drop per length will be used provided that the necessary filter lengths are feasible for the experimental rig.

A specific wind tunnel rig was built in the lab in order to identify the connection between the physical characteristics of the filters, their position in front of the heat exchanger and the measured air velocity profile. The test section is described in the next section.

5.1.1 The wind tunnel: design and technical characteristics

The developed test rig is basically a simple wind tunnel, and it is depicted schematically in Figure 5.2. The installation was designed in order to reproduce partially the experimental air-to-refrigerant heat pump described in the paragraph 3.1. One of the components of the installation was a plane tube radiator. The unit was characterized by the header-to-header length equal to 471 mm, the core height of 330 mm and a core depth equal to 19 mm. The fins were louvered and the tube thickness was 1.9 mm. As indicated, the radiator and filters were positioned at the inlet of the wind tunnel which was 4.5 m long.

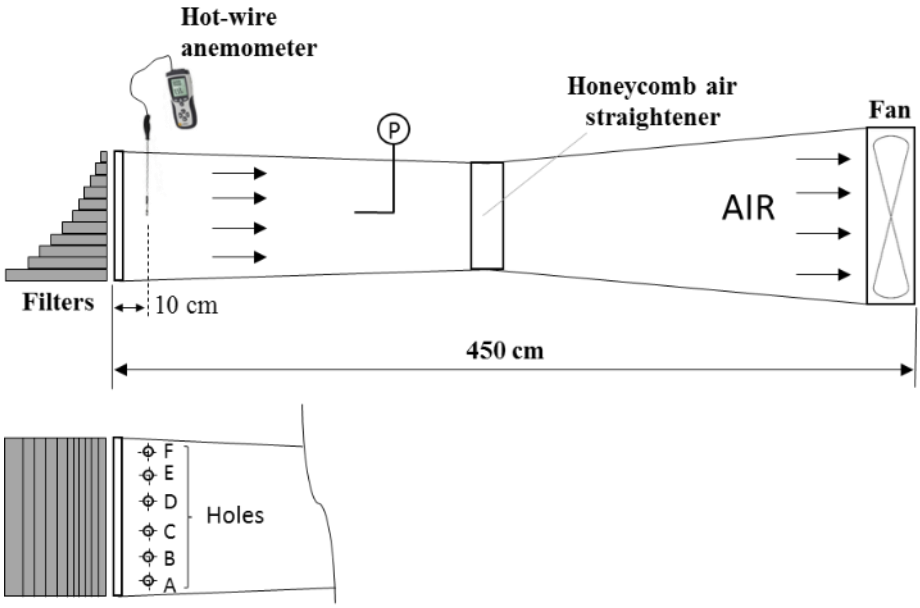

Figure 5.2: The wind tunnel

At the other end, a variable speed axial fan moved the air that went through the duct crossing firstly the filters, then the radiator and finally a honeycomb straightener. The straightener was installed to eliminate the swirl that could be generated by the fan motion. In the shown scheme, the anemometer was positioned close to the filters and the radiator, in particular, 10 cm downstream in the air flow direction. The probe was inserted in the duct through a perforated transparent window placed on the top of the tunnel. The window had six holes (A-F in Figure 5.2), having the same diameter of the probe, and disposed perpendicularly to the stream direction and distributed as suggested by log-Tchebycheff rule (ISO 3966- ASHRAE, 2009). The distance between the measurement points and the outlet section of the radiator was found empirically. Indeed, due to the turbulence induced by the tubes and fins, if the measurement were made too close to the outlet section, the air velocity

measurement was very variable. On the other hand, at longer distances (>> 10cm), we observed a high mixing and the velocity profile became more and more uniform. This aspect of the methodology was significantly improved as it will be described later on. Finally, the wind tunnel was also equipped with a pressure transducer, which measured the total pressure drop across the heat exchanger and filters.

5.1.2 Testing procedure and first results

As previously commented, for simulating the operating conditions of the air-to-water heat pump described in the paragraph 3.1, the variable speed axial fan regulated the air flowrate through the filters and the heat exchanger as depicted in the Figure 5.2. The first attempts to generate the air maldistribution were done considering two different strategies. As discussed in the previous subsection, the same air velocity profile can be can be generated by placing in front of the heat exchanger some filters with different densities and porosity (Figure 5.3A) or, instead by using several layers of the same filter with different thickness (Figure 5.3B).

The first measurements were performed according with the first strategy, by positioning the filter with the lowest permeability (blue one) in the lower part of the frontal section of the heat exchanger, while a higher permeability filter (yellow one) was placed on the top, as it can be seen in Figure 5.3A. The corresponding measured velocity profile is presented below the corresponding picture.

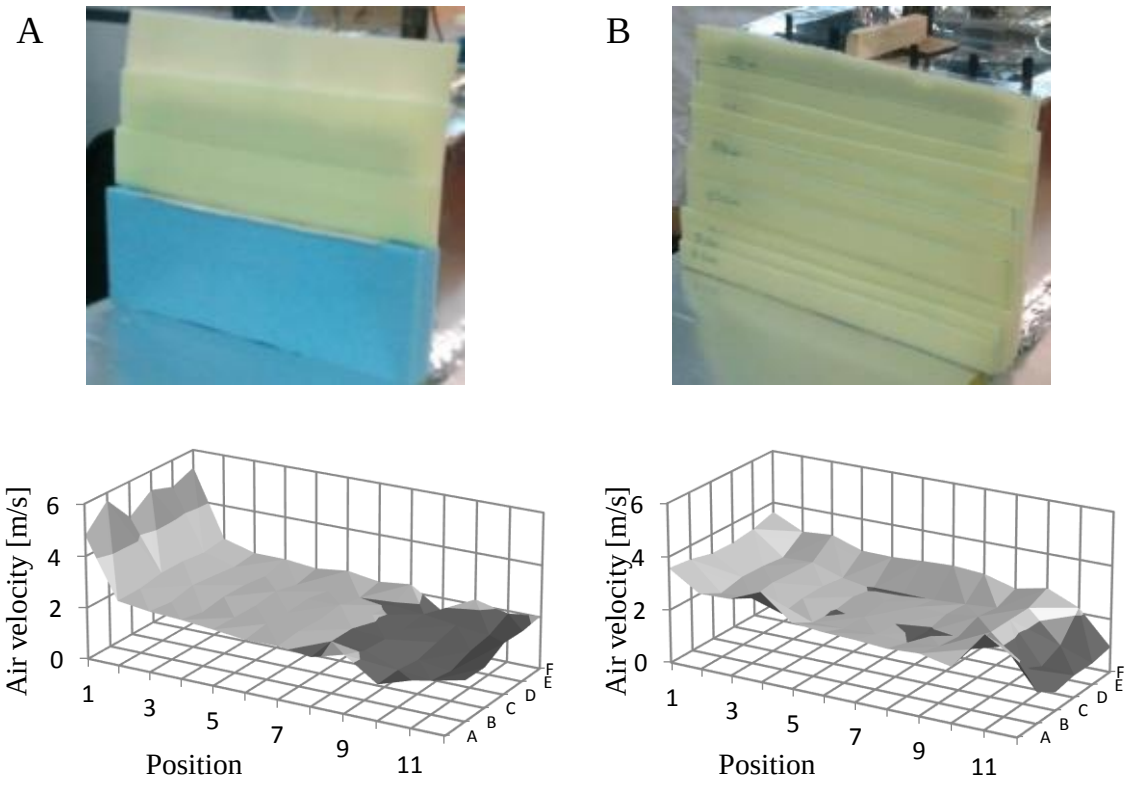

Figure 5.3: Air velocity measurement with the Log-T method

In order to get a better detail in the velocity profile, the tests were performed measuring the velocity in a 6x11 grid in this occasion, instead of the standard 6x6 grid of the log-Tchebycheff rule. The anemometer was inserted in the duct thought the six holes characterizing the measuring section (A-F in Figure 5.2), thus, for each of them, the air was measured in 11 positions along the heat exchanger height. In the diagrams, position No. 1 corresponds to the top of the radiator, while position 11 corresponds to the bottom.

The results of option A show clearly the presence of three sections:

- Most of the air was crossing the layer of high permeability filter in the upper part of the HX (measuring point No.1). Here, the measured air velocity achieved the highest value (~5 m/s).
- From point 2 to 8, the air velocity profile can be considered linear. The slope is very small and the air velocity decreases less than 1 m/s. This result was due to the presence of three overlapped sheets of yellow filter (Figure 5.3 A) blocking progressively the frontal face starting from the top of the heat exchanger until the height occupied by the blue filter.
- Starting from to the measuring point No.9, the air velocity gets a very low value of around 0.5 m/s but with a non-uniform profile.

In conclusion, most of the air was crossing the filter and the heat exchanger though the upper part, while at the very bottom the airflow rate was almost zero. In other words, the blue filter was almost totally blocking the frontal face area. In addition to this consideration, this filter configuration presented another disadvantage: the identification of the relation between the filters characteristics and air velocity profile was even more complex due to combination of materials with different porosity/permeability.

For this reason, in order to reduce the design parameters, instead of using different filters, the research team decided to try to reproduce the air velocity profile by using the same filter material and just varying the thickness of the filter layer in the flow direction. Figure 5.2 B shows a picture of this configuration and the results of the corresponding velocity field at the bottom. With this configuration we were able to reach an approximately linear velocity profile from top to bottom of the heat exchanger, starting with a value of around 4 m/s until a minimum velocity of ~1.8 m/s. However, as it can be seen, the velocity map was rather uneven and the air measurement was characterized with very high uncertainty especially in the lower part of the heat exchanger (characterized by the strong fluctuation of the measured velocity value with the anemometer).

5.1.3 The filters box

The explanation to the difficulties in building and measuring the velocity profile shown in figure 5.3 is mainly connected to the variation of flow regime due to the presence of the filters with different thickness, inducing vertical motion besides the horizontal component, and to the fact that the

measurements were taken downstream the heat exchanger in a zone where large eddy motion and turbulence is very high. Figure 5.4A illustrates the different phenomena that could be appearing when the above described methodology is employed. First, as it is illustrated in the figure, due to the long length of the filter path at the bottom layers, the air tends to flow upwards looking for a lower pressure drop path, so that a completely two dimensional profile with important vertical velocity component is produced. Therefore, the flow is accelerated towards the upper layers of the channel. At the same time, a strong redistribution of the flow downstream the heat exchanger is produced leading to vortex and high turbulence. This motion makes really difficult the measurement of the velocity profile downstream the heat exchanger. On the other hand, if one tries to move the measuring point towards the heat exchanger, then one finds the strong perturbation produced by the fins and the tubes. Therefore, this methodology is clearly not adequate for the purpose of generating a given velocity profile.

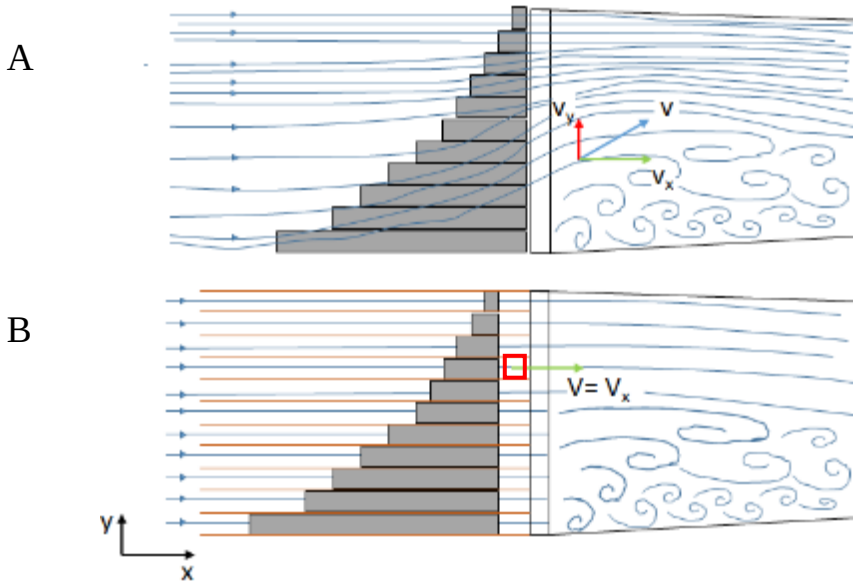

Figure 5.4: Qualitative representation of the streamlines through the filters

Two are the causes of the encountered problems with the configuration shown in figure 5.4A, the first one is the appearance of vertical components of the velocity due to a certain cross flow in between the different layers of filter. This issue can be easily solved by just installing a thin sheet of any impermeable material (paper, plastic…) in a way that the flow through a given layer is only allowed to flow quasi-one dimensionally along the filter layer, as it is shown in figure 5.4B. The second problem comes from the measurement of the velocity profile downstream the heat exchanger where strong flow perturbations occur. However, the installation of the horizontal division sheets allows the creation of an empty space (gap) in between each filter layer and the heat exchanger, where the velocity can be accurately measured since flow in the gap is very stable and almost one-dimensional.

As it is illustrated in figure 5.4B, a restructuration of the flow pattern also takes place downstream the heat exchanger. Flow perturbations occurring there will certainly affect the pressure distribution downstream the filter layers and produce certain flow instability upstream at the air velocity measurement section. However, experience have proven that stability is quite high and only small oscillations of the measured velocity with the hot wire anemometer are observed in this configuration. As a matter of fact, local value of the air velocity could be measured with high accuracy (uncertainty of ±3%) with this configuration. This is probably also helped by the pressure drop produced by the heat exchanger. Concerning the probable non-uniformity of the pressure field induced by the downstream air restructuration, it certainly exists, but we have not observed to produce a big influence in the evaluation of the filter length layers. This is probably due to the fact that where the differences in pressure are the highest is where the length of the filter layer is the longest, so unevenness of the pressure field having less influence on the total pressure drop across the bottom layers.

Therefore, the methodology represented in figure 5.4B is the one which was selected for the study of the air flow maldistribution across condensers, which has been part of the present doctoral work. As explained, the methodology for imposing a given air velocity profile to the studied condenser basically consists of constructing a channel box, with several parallel, well separated horizontal channels, containing each a different length of filter material. Furthermore, the box can be placed upstream (as it is shown in figure 5.4B) or downstream (as it will be commented later on) the heat exchanger. The filter layers do not reach the heat exchanger but leave an empty gap that it is employed to insert the anemometer and measuring the air velocity along that channel layer. This is the reason why we called this section “the filters box”.

5.1.4 The filter material characterization

Once identified the experimental methodology for evaluating with sufficient accuracy the local value of the air velocity, the following step for “controlling” the air maldistribution at the inlet of the heat exchanger was represented by the characterization of the filter. Whit this denomination, we mean the evaluation of a univocal correspondence between the filter thickness and the air velocity in each channel formed between two consecutive slabs. The procedure was carried out in the installation described in paragraph 5.1.1 and consists of the following consecutive operations.

The first step of the process is the evaluation of the airside pressure drop only due to the heat exchanger. This operation was performed changing the rotational speed of the fan (six different volumetric airflow rates) and evaluating experimentally the pressure drop across the heat exchanger (Δp_{HX}) by means of the pressure transducer placed inside the duct (Figure 5.2).

After that, only a single even layer of filter, having a determined thickness (L_{filter}), was positioned in front of the heat exchanger blocking completely the entire frontal surface as depicted in Figure 5.5 and six operating points were measured again. From previous experiments, an adequate density filter material was selected. This material comes in 2cm panels so, for the characterization a single 2 cm thick layer was employed. During this second step, the rotational speed of the fan was regulated in order to maintain the same airflow rate of the first measurements with the heat exchanger without filter. This is not necessary, but it helps the direct comparison of results. This time the pressure transducer measured the total pressure drop due to the filter and the heat exchanger ($\Delta p_{total} = \Delta p_{filter} + \Delta p_{HX}$). Then, the pressure drop across the filter can be estimated as the difference between the pressure drop measured at each of the experiments. The results of the pressure drop evaluated as described are depicted in figure 5.5. After analyzing the results, the measured pressure drop seems to correlate well with turbulent flow patterns. Therefore, the following expression was employed for its characterization.

$$\Delta p_{filter} = \Delta p_{total} - \Delta p_{HX} = f \cdot \frac{L_{filter}}{D} \cdot \rho \frac{u^2}{2} = K_{filter} \cdot L_{filter} \cdot u_{air}^2 \qquad (5.1)$$

In Eq. 5.1, the only unknown parameter is K_{filter}, which will be called "characterization parameter". Figure 5.5 shows the result of the plot of the measured pressure drop vs. the product L_{filter} times u^2. As it can be observed the correlation is quite linear supporting the assumption of turbulent flow characteristics.

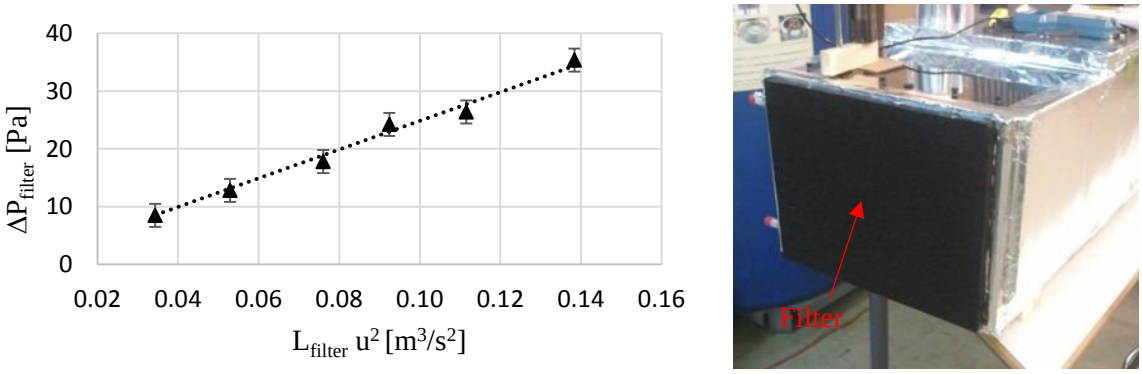

Figure 5.5: Filter characterization process

The characterization parameter (K_{filter}) can be easily evaluated from the obtained results as:

$$K_{filter} = \Delta p_{filter} \Big/ \left(L_{filter} \cdot u_{air}^2\right) \qquad (5.2)$$

Once, the parameter K_{filter} has been experimentally evaluated any air velocity profile can be generated by evaluating the necessary length of the filter material which must be employed for each channel layer.

Taking into account that the maximum velocity of the air velocity profile will be the one circulating across the path with the minimum filter length, this gives the condition for the evaluation of the design pressure drop ΔP_{design}:

$$\Delta p_{design} = K_{filter} L_{filter,min} u_{air,max}^2 \tag{5.3}$$

Where, $L_{filter,min}$ is the minimum thickness of the available filter material we would like to employ. The length of every filter layer (i) inside the filter box can then be simply evaluated by using the following formula:

$$L_{filter,i} = {\Delta p_{design}}\Big/{\left(K_{filter} \cdot u_{air,i}^2\right)} \tag{5.4}$$

Where $u_{air,i}$ represents the local air velocity desired at layer (i).

Of course, the developed methodology does not allow to generate a continuous velocity profile *u=f(y)* but a discretized approximation of it; the number of layers in the box giving the maximum possible discretization. In any case, in our experience this is enough to reproduce the effect of possible air maldistribution at the inlet of any heat exchanger. On this regard, it is important to highlight that the presence of the tubes or minichannels naturally impose a certain discretization of the air flow through the heat exchanger. Actually, it is recommendable that the number of employed parallel layers were coincident with the number of spaces in between the minichannels. To do that, the thin slabs separating the different filter layers can be constructed with a thickness very similar to the minichannels. In this way, providing an exact matching with the frontal opening and one dimensional different air velocity at the inlet of each of the individual passages in between the minichannels, a very good approximation of what can be the actual velocity profile through this kind of heat exchangers can be reproduced. For the round tube heat exchanger it is enough to employ one channel per frontal finned tube with the slab just in front of it, and also a very good approximation of the air velocity profile can be obtained.

Notice that the developed experimental methodology could also generate non even profiles in the other dimension of the heat exchanger (fin tube length) if necessary. It will be sufficient to subdivide the horizontal layers in the box with vertical separators generating further individual sub-channels.

5.1.5 Validation: Linear velocity profile generation

The method described in the previous section for defining the filters thickness was applied for generating a linear profile at the inlet of the radiator installed in the wind tunnel (Figure 5.2). As previously mentioned, what it has to be initially defined is the wished velocity profile as function of the heat exchanger height (y). In this case, a linear profile was defined in order to get the maximum

velocity equal to 2.5 m/s and the minimum equal to 0.5 m/s. According with the radiator geometry, the velocity profile is defined as follows:

$$u = f(y) = 0{,}0632 \cdot y + 0{,}4853 \tag{5.5}$$

Where *y* is expressed in centimeter.

For the low density filter used in this application, the characterization parameter was evaluated experimentally (Eq. 5.2) and turned to be equal to 255.2. Considering the $L_{filter,min}$ equal to 2.2 cm and the required maximum velocity of 2.5 m/s, the Δp_{design} was calculated by means of Eq. 5.3, resulting 35 Pa.

Taking into account that the radiator had 16 intervals in between the flat tubes we employed the same number of channels. In Figure 5.6, the thickness of the sixteen filter layers placed in front of the heat exchanger is depicted, and at the bottom, the measured velocity profile is shown.

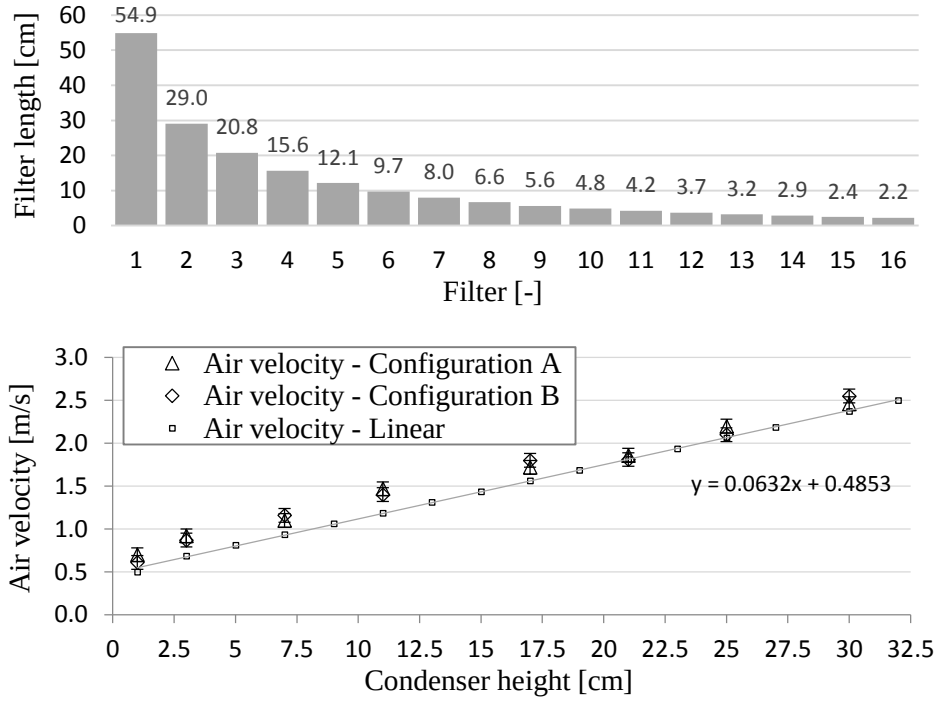

Figure 5.6: Experimental generation of a linear profile

As it can be observed, the obtained velocity profile was not exactly the expected one (shown also in the graph as a straight line). There is a slight deviation in the average velocity, which is not a problem at all since it can be adjusted just by modifying the fan velocity. It is also apparent a slight deviation from the linear profile at the points with lowest velocity values (except at the lowest one). This is due to the approximate nature of the developed calculation method for the filter layer length which assumes one dimensional flow and even distribution of the total pressure drop across the filters box and heat exchanger set. If a better accuracy in the velocity profile is required, a readjustment of the

filter length per channel can be easily evaluated. In any case, it should be pointed out that the objective of the developed methodology is to generate an uneven but controlled velocity profiles in order to be able to study the influence of possible air flow maldistribution on the performance; therefore, the objective is the ability to generate uneven distributions rather than generating an exact velocity profile. This objective is easily fulfilled with the developed methodology.

The filters box could in principle be placed either upstream the studied heat exchanger, as in the previous figures, or downstream. No big differences could be expected in the results. We tested it and no real difference was found.

For the practical testing of the studied condensers, a special testing setup was designed in order to reproduce the actual operation of the condenser on the air-to-water heat pump described in Chapter 3. Initially, in order to modify rapidly the filters configuration for studying the effect of different uneven air velocity profiles on the performance of the condensers (round tube and minichannel) the filter box had to be placed in front of the heat exchanger as depicted in Figure 5.7 A. In this configuration, the air first flows through the filters box and then through the condenser, exactly in the same position as the filters box was tested in the wind tunnel with the radiator. If, on one hand this configuration allows modifying very quickly the filter configuration, on the other, it presents a big disadvantage: the filter box would be situated upstream the condenser avoiding any vision of its frontal area. Consequently, all the information related to the refrigerant distribution through the condenser, that we could generate thanks to the infrared thermography would be missed.

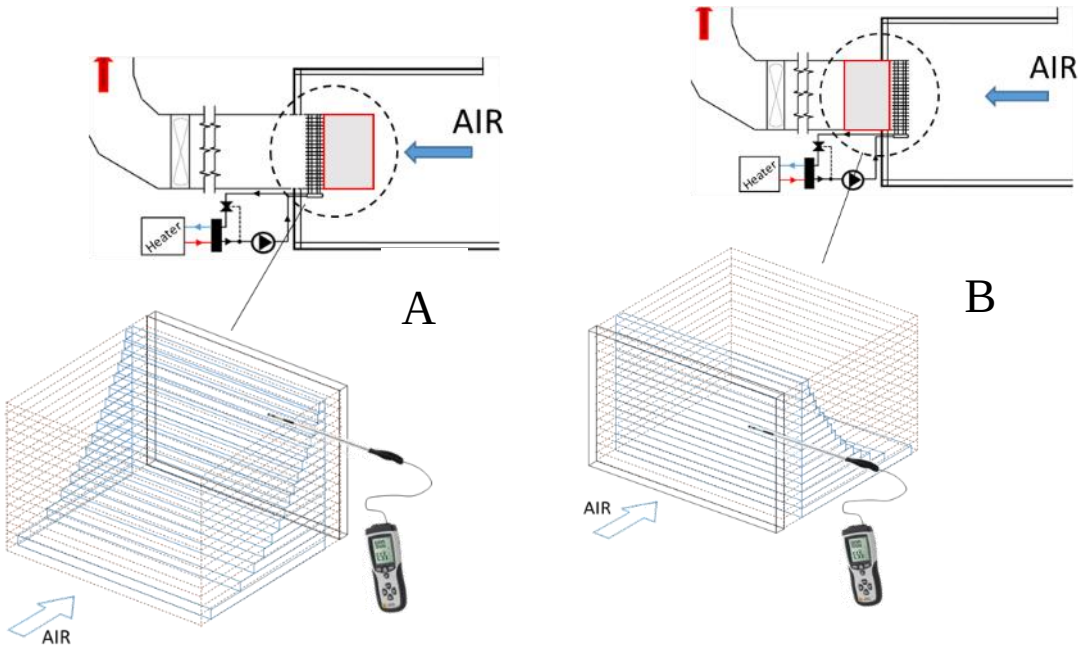

Figure 5.7: Optimal position of filter box in the air-to-refrigerant heat pump

The solution to this problem was given by the possibility of installing the filters box downstream the condenser inside the air handling tunnel duct (Figure 5.7 B). In this case the air goes first through the condenser and then through the filters. Although much more uncomfortable for filters box changes, this configuration had important advantages. The main one is that the frontal face is kept completely uncover. It allows the use of the infrared thermography to investigate the frontal temperature field. Additionally, the filters box added to the dumping of any disturbance in the flow generated downstream in the air handling duct and system so producing a better controlled air velocity profile.

In principle, the position of the filters box in respect to the heat exchanger should not influence the local value of the air velocity. In order to prove that the position of the filter box does not influence the air velocity measurement, the linear velocity profile at the inlet of the radiator was measured in the wind tunnel considering both positions. This corresponds to configurations A and B shown in figure 5.6, which as can be easily observed led to almost identical results.

5.2 Experimental study of the effect of the air maldistribution on the performance of a condenser

5.2.1 Air velocity profile

The methodology discussed in the first part of the chapter can be used for reproducing any air velocity profile at the inlet of a heat exchanger. Indeed, after performing the process called filter characterization, any air velocity profile can be reproduced positioning some filters, with different length and with a certain order, upstream or downstream the heat exchanger, in what we have synthetically called “filters-box”.

As showed in section 5.1.4, the application of an adequate filters-box allowed the generation of a quasi linear profile at the inlet of a flat tube radiator. However, a linear profile is clearly more an academic idealization than a real situation; in a real installation, a linear velocity profile is seldom to occur. The velocity profile characterizing the heat exchanger inlet is, in general, strongly irregular, basically influenced by the fan characteristics, and the shape of the condenser and fan box. For this reason, for testing the effects of the air maldistribution on the performance of the studied condensers it was necessary to previously define which is the characteristic velocity profile in a usual condenser-fan configuration.

The A-Shape (or V-shape) condensation units represent one of the most typical configurations for evaporators and condensers in which there is the suspicion that a strong air maldistribution could occur. These units are widely used for their modularity and relative compactness. Indeed, many heat exchangers can be combined in this way for rejecting high heat fluxes. The analysis of the airflow distribution in one of this multi-coil A-shape units was performed a few years back by Lee *et al*.

(2010). The main objective of their work was the optimization of the angle ϑ included between the condensers of the A-shape unit represented in Figure 5.8A.

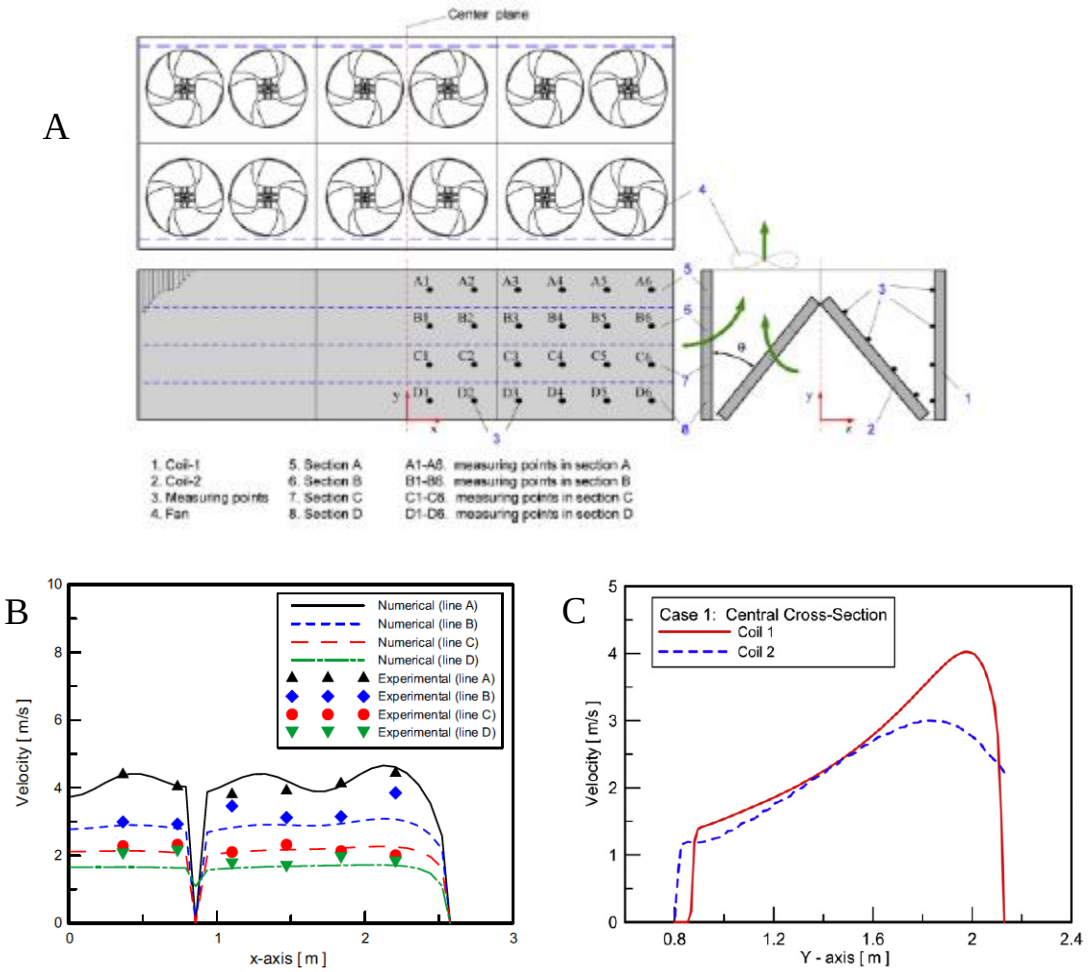

Figure 5.8: Air velocity profiles at the inlet of a A-Shape condensation unit (Lee et al., 2010)

With such purpose, Lee *et al.* (2010) studied numerically and experimentally the air distribution at the inlet of the condensers 1 and 2. In Figure 5.8B, the validation of their CFD model is shown. The experimental velocity field was measured by means of a hot-wire anemometer positioned in positions A1-A6, B1-B6, C1-C6. D1-D6 (see Figure 5.8A) along the vertical heat exchanger (coil 1). The agreement found between the model and the experimental data was very good. The results of the air velocity distribution in the central cross section plane (Figure 5.8A) are represented in Figure 5.8C. As pointed out by the authors of the work," *the outer condenser (coil 1) has more air volume passing through and the air velocity is in general higher in the upper ends of the coil. The reduced flow velocity at the lower part of the coil makes it the lees efficient part of the coil. Finally, the velocity almost drop down to zero on both the top and bottom part of the coil".*

The air maldistribution of this air velocity profile can be considered rather high, therefore this air velocity profile was selected as the reference case to be generated and tested in the installation

described in chapter 3. As will be dealt in the following section, one special filters-box was designed for the finned tube HX and another one for the MCHX.

5.2.2 Design of the Filters-boxes

The design of the filters boxes for the two tested condensers was performed using the software CATIA V5 (Dassault). The filter boxes were designed for fitting perfectly the geometry of each of the heat exchangers. Indeed, the main dimensions of frontal cross section area, the position of the slabs and their thickness were defined according with the disposition of the tubes in the heat exchangers and the characteristics of the air duct used in the experimental air-to-water heat pump (chapter 3). The 2-D drawings of the filters-box are reported in Appendix A. The materials used for the boxes were wood fiber board (MDF) for the main structure, aluminum for the slabs and transparent plastic panel for the windows. All the components of the filters-boxes were manufactured in a specific laboratory where the wood fiber board (MDF), the aluminum and the plastic were cut and assembled with high accuracy.

For reproducing the air velocity profile depicted in Figure 5.8, the thickness of each filter in the flow direction and their position along the heat exchanger height were identified according with the methodology described in section 5.1.1.

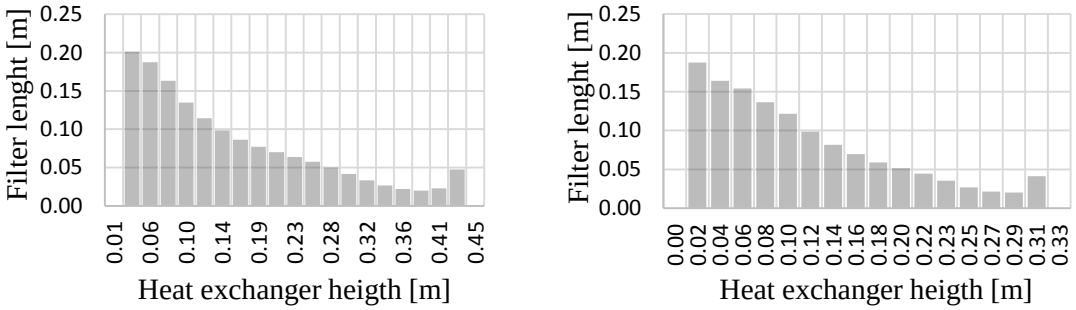

Figure 5.9: Design of the filter for the finned tube condenser and for the microchannel condenser

First, the air velocity profile (Lee *et al.*, 2010) was converted in a function of the heat exchanger height and then the thickness in the flow direction of each filter was the result of the filter characterization process. First, the characterization parameter of the filter material was determined by means of Eq. 5.2. Afterwards, considering a minimum filter length of 2 cm thick (L_{min}) and the maximum velocity equal to 4.4 m/s (Figure 5.8) the length of the different filter layers were calculated adopting equations 5.3 and 5.4. As depicted in Figure 5.9, the boxes were designed in order to place twenty-one filter layers for the tube and fins condenser, and eighteen filter layers for the microchannel heat exchanger. In fact, the total number of filter layers were respectively nineteen and sixteen but the first and last channels in between the slabs were totally blocked for generating a null air velocity, as it turns out to happen in the actual case (Figure 5.8).

5.2.3 Filters-boxes: installation and air velocity measurement

As previously commented in section 5.1.4, the filters-boxes for both condensers were positioned in the experimental installation as shown in Figure 5.7B. That is to say, the filters-boxes were installed in the air duct just behind the condenser in the airflow direction. Although the initial installation of the filters-box was rather uncomfortable, mainly due to the partial modification of the original installation described in chapter 3, the configuration B of Figure 5.7 presents many advantages:

- The first one is related to the air temperature measurement at the inlet of the heat exchanger. Indeed, the grid of thermo-resistances placed in the climatic chamber to measure the inlet temperature in different positions could stay in the same position as it was used with uniform air velocity profile.
- The second advantage is connected to the air velocity measurement. Placing the filters-boxes in the duct behind the heat exchanger, the air velocity could be measured directly form the outer side of the climatic chamber.
- Finally, as discussed above, configuration B of Figure 5.7 allows keeping the frontal section of the heat exchanger totally uncovered. In this way, the infrared thermography could provide interesting information regarding the refrigerant distribution inside the heat exchanger.

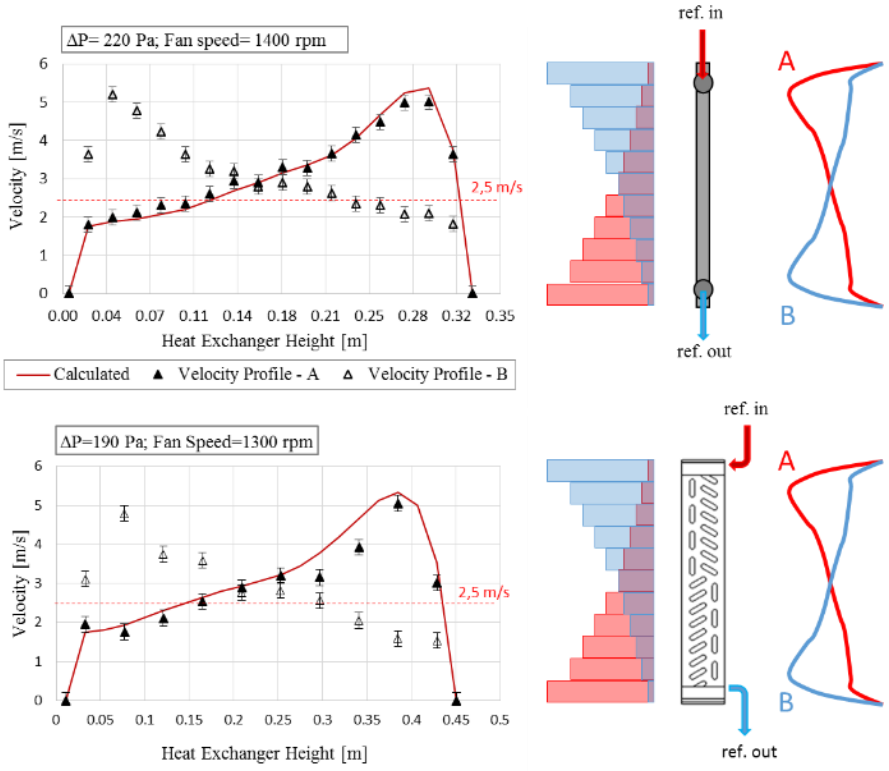

Figure 5.10: Experimental air velocity profiles

The first step of this part of the work was the evaluation of the "calculated" air velocity profile; "calculated" is used for pointing out that the velocity profile is not directly measured but the result of the application of Eq. 5.6. The value of $u_{air,i}$ across the filter layer "*i*" was estimated as:

$$u_{air,i} = \sqrt{\Delta p_{\exp} / \left(K_{filter} \cdot L_{filter,i}\right)} \tag{5.6}$$

As can be observed, once the filter length for each layer has been defined, the resulting velocity profile and flow rate will be proportional to the square root of the applied pressured drop. This makes possible to produce a velocity profile with the same shape but with different mean flow rate, which can be set by simply regulating the fan speed of the air handling duct. In order to compare the results with the uneven velocity profile with results with uniform velocity and with other tests performed with the same condensers a nominal mean value of 2.5 m/s was selected for the average air velocity.

$$\frac{\sum_j u_j}{i} = 2.5 \text{ m/s}; \quad i = \text{number of filters} \tag{5.7}$$

The fan speed was therefore regulated in order to produce this same average velocity for all tested cases.

Figure 5.10 shows the obtained velocity profiles for the two studied condensers: tube and fins and microchannel, for both vertical possible positions. It is important to point out that, although, just reversing the position from top to bottom and viceversa would generate the same velocity profile, just reversed, the effect on the condenser performance will be different given that each position leads to a very different air flow distribution in respect to the circulation of the refrigerant flow, which goes from top to bottom.

Figure 5.10 also shows the comparison of the measured velocity with the 'calculated' one. Again, it can be seen that the actually obtained velocity profile is quite close to the one we wanted to generate, and very similar in shape to the one taken as a reference.

The comparison has been performed only considering profile A (the highest velocity is at the top, in correspondence with the refrigerant inlet), but in the same figure is also reported the air velocity measurement when the filters-box is reversed (profile B). In this case, the velocity profile presents the peak in correspondence of the lower part of the heat exchanger, closer to the refrigerant outlet. The identification of profiles A (velocity peak at the top) and B (viceversa) is important since it will allow the analysis of the effect of the air maldistribution on the actual performance of the tested RTPFs and MCHX condensers.

5.2.4 Analysis of the results

For studying the effects of the air maldistribution on the performance of the round tube and MCHX condensers, the wide experimental campaign described in Chapter 3 was extended. New tests were carried out in order to measure the performance of both condensers under the effect of the uneven air velocity profiles A and B discussed in section 5.2.3. With this purpose, some of the operating points reported in Table 3.2 and Table 3.4 (Chapter 3) were measured again with special attention for the tests with different subcooling. As already commented in the first part of the present chapter, during the new tests, in addition to all the other parameters, the volumetric airflow rate was maintained constant. To do that, as described in the previous section, the speed of the fan was adjusted in order to have an average speed equal to 2,5m/s for all cases, with and without the filters-box. Thanks to this procedure, the performance degradation of the condenser can be considered exclusively attributed to the air maldistribution. For both studied condensers, first the analysis of the thermography results will be presented and commented; then, the global performance defined in terms of condenser thermal capacity and condensation temperature will be presented and discussed.

5.2.4.1 Tube-and-fins

First, in order to see the effects of irregular air velocity profiles on the refrigerant evolution during the entire heat rejection process, the results of the thermography were analyzed. In Table 5.1, for the finned tube condenser, six thermographic images are compared considering two different values of the subcooling at the condenser outlet.

Each photo represents the temperature distribution of the frontal face of the heat exchanger; being the camera placed inside the climatic chamber just in front of the heat exchanger, only the temperature distribution of the frontal circuit can be effectively analyzed.

Three columns and two rows characterize the table. In the central column, the images obtained with the uniform velocity profile are placed, while in the lateral ones, the images generated considering the velocity profile A and B are reported. In the first row, the images related to the operating points having subcooling equal to 0°C are compared; below, the temperature profile of the frontal circuit can be analyzed when the subcooling was maintained equal to 10°C.

Table 5.1: Thermography for the finned tube condenser under different airflow distributions

	Velocity profile			
	Profile A	**Uniform profile (reference)**	**Profile B**	**Scale**
	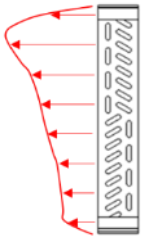	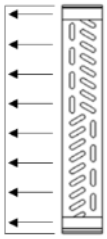	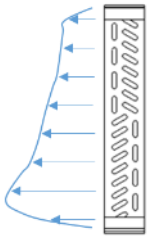	
SC = 0°C	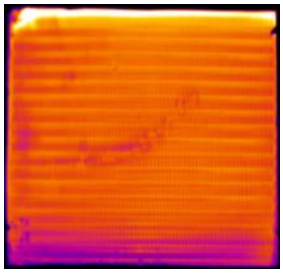	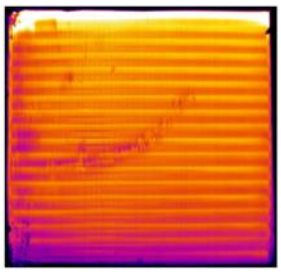	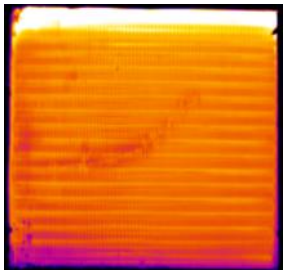	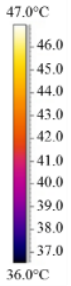
SC = 10°C	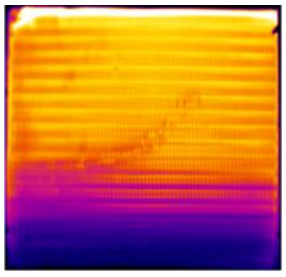	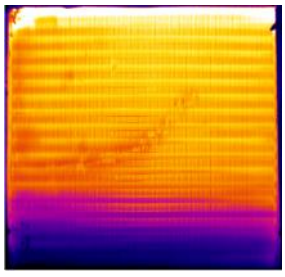	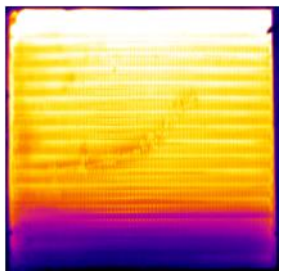	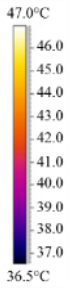

The analysis of the thermographic images leads to one general conclusion: the volume occupied by the vapor is inversely proportional to the air velocity at the upper part of the condenser. The same for the liquid and the lower part of the condenser. For instance, when the profile A is tested, the refrigerant is quickly cooled down in the first part of the circuit, hence the vapor occupies a reduced volume. At the same time, due to the reduction of the heat transfer coefficient at the lower part of the condenser, at least in the frontal circuit, the subcooled liquid region seems to increase. This conclusion is not completely supported by the results of analysis of the refrigerant temperature profiles depicted in Figure 5.11, generated using the results provided by the thermocouples placed on the return bends of the condenser (Figure 4.1).

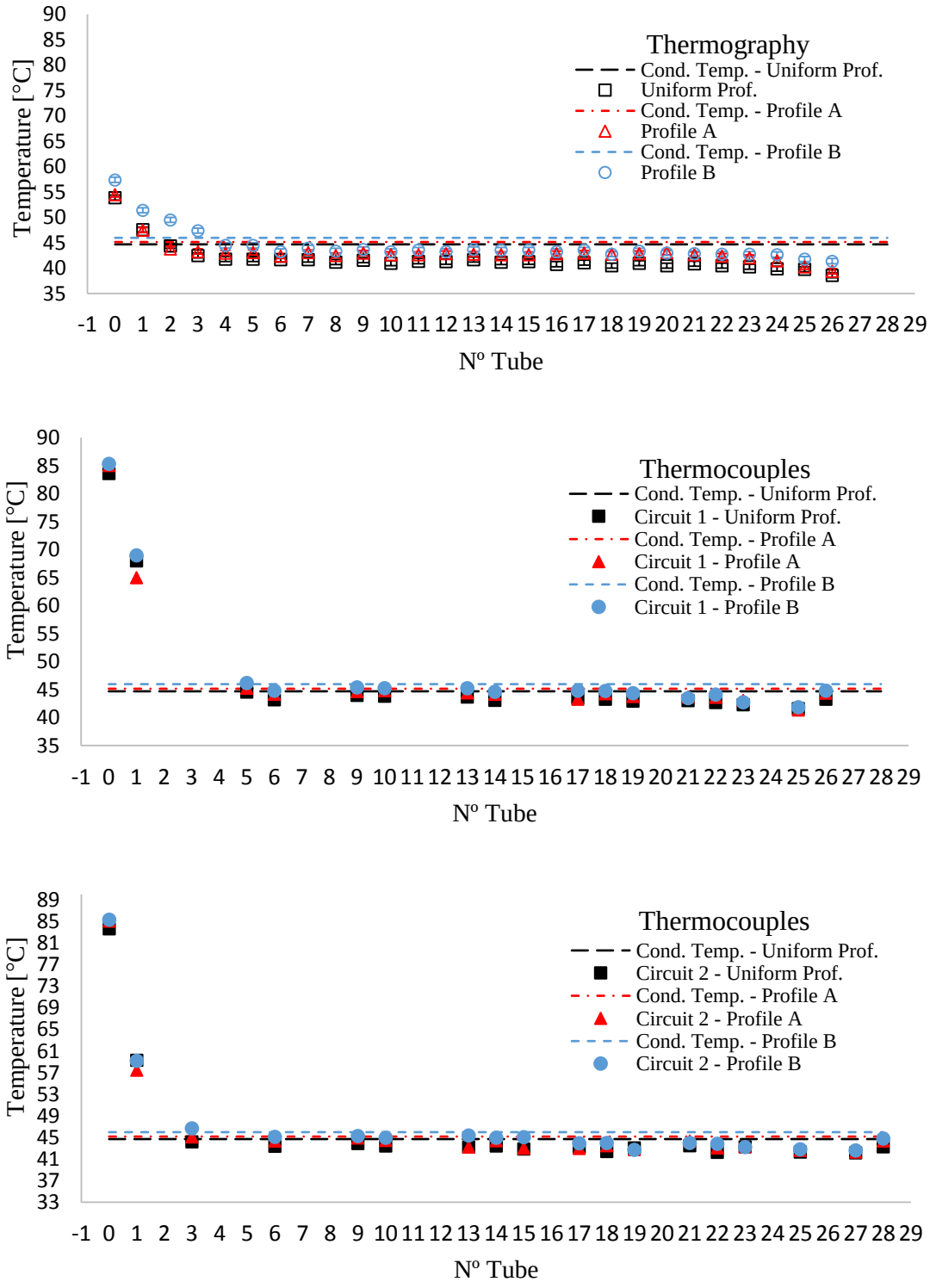

Figure 5.11: Variation of the temperature profiles in the refrigerant and in the tube wall due to the uneven velocity profiles A and B (SC=0°C)

As it can be observed, the analysis of the temperature profiles is very complex, especially because of many unknown factors, such as the refrigerant distribution. From this point of view, as already commented in the third chapter of the present PhD work, the temperature profile of the second circuit shows that the refrigerant is cooled down more quickly compared with the first circuit. This leads to

hypothesize that in this circuit the refrigerant mass flow rate is lower. Also under the effect of the air maldistribution, such consideration can still be considered valid.

Nevertheless, the analysis of the refrigerant temperature profiles when the subcooling is 0°C does not point out significant differences strictly connected to the irregularity of the air velocity profile. Despite of the great difference between velocity profiles A and B, only some minor differences appear at the superheated vapor area. In particular, only in the frontal circuit the temperature in correspondence of the first tube seems to be affected by the inhomogeneity of the air velocity. Due to the characteristics of Profile A the refrigerant temperature seems to be slightly lower than its temperature when the other velocity profiles are tested. Such behavior is confirmed also by the trend of the wall temperature.

In Figure 5.12, the temperature profiles are compared when the SC is maintained equal to 10°C.

Also in this case, only minor changes can be observed when the different air velocity profiles are tested. However, although just appreciable, the temperature profile variation are this time consistent with the shape of the velocity profile A and B.

Due to the application of the air velocity profile B, the temperature seems to be always higher in comparison with the reference test, the subcooled liquid region is shorter and, in general, the condensation temperature looks higher. Vice versa, the application of the profile A reduces the volume occupied by the vapor, increasing, at the same time, the portion of heat exchanger occupied by the subcooled liquid. In this case, the condensation temperature is between the reference test and the results of the application of profile B.

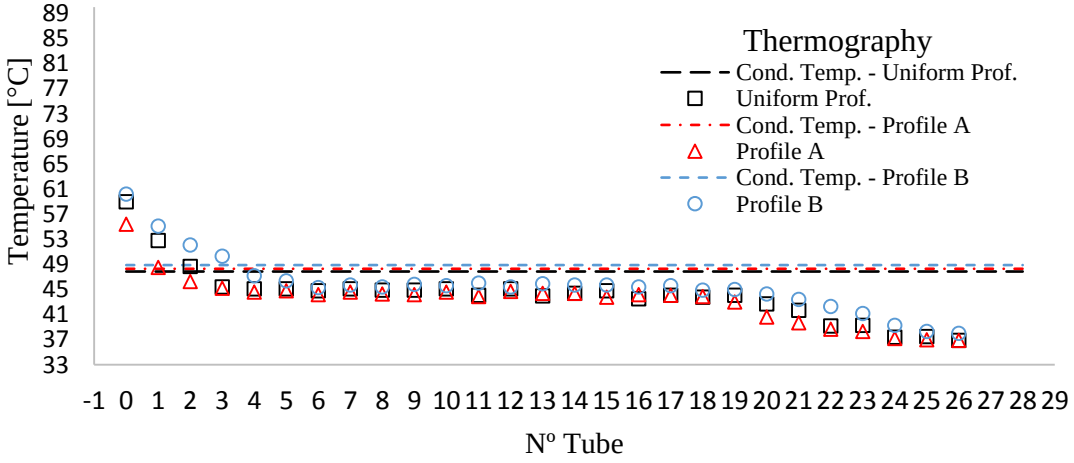

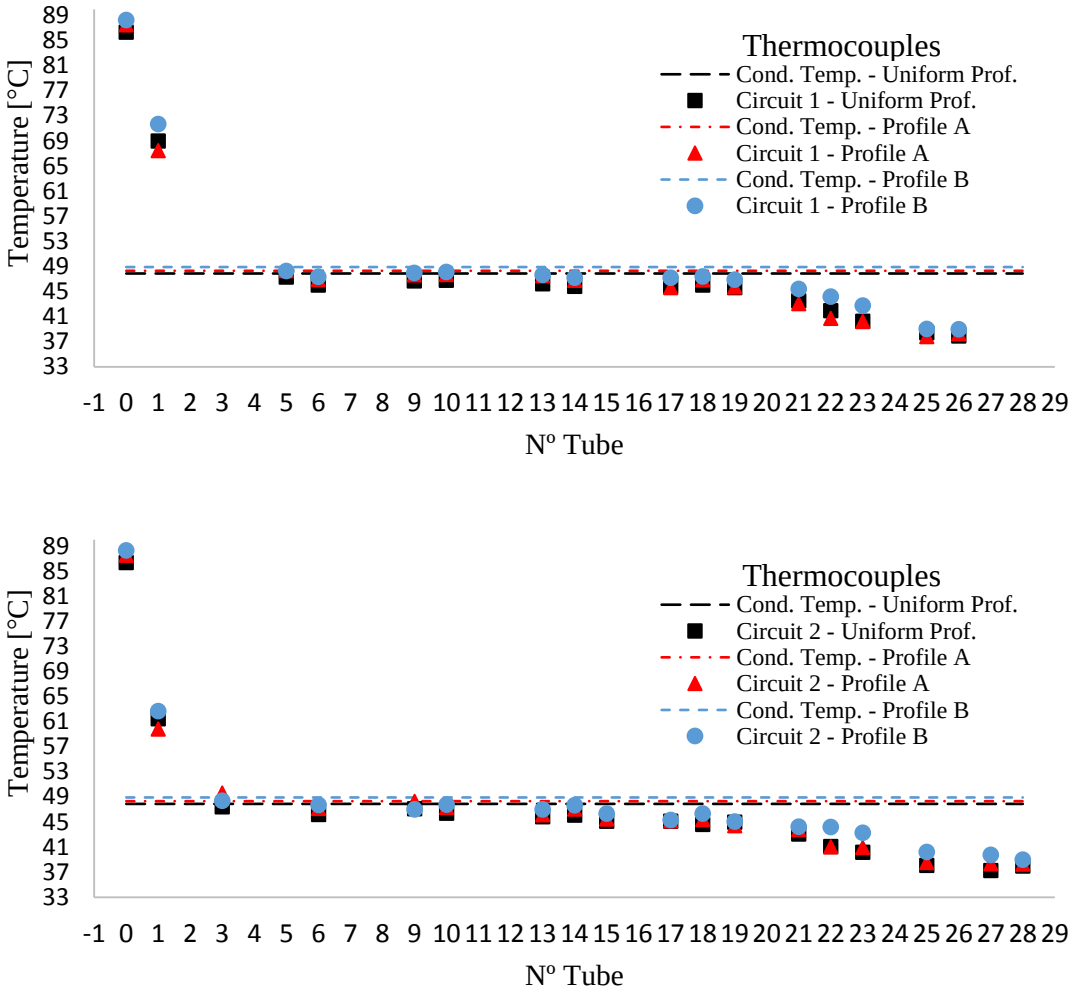

Figure 5.12: Variation of the temperature profiles in the refrigerant and in the tube wall due to the uneven velocity profiles A and B (SC=10°C)

These conclusions drawn from the analysis of the temperature profiles could be combined with the results showed in Figure 5.13, where the global performance of the condenser are analyzed.

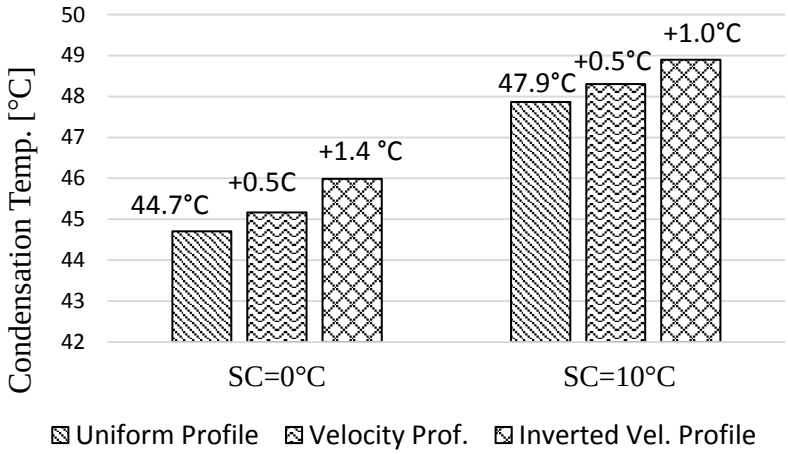

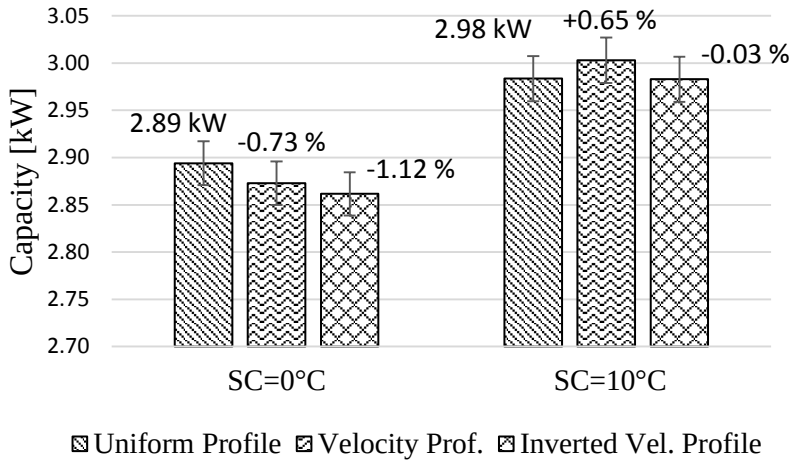

Figure 5.13: Performance degradation of the RTPFs condenser due to the air maldistribution

In the above figures, the experimental value obtained with the uniform profile is reported as the reference value. The label for the tests corresponding to air velocity profiles with maldistribution indicates the deviation on the capacity (%) or the temperature difference (ºC) in respect to the reference case.

Compared with the reference test (uniform velocity), when the velocity profile A is tested and the subcooling is 0°C, the thermal capacity undergoes a reduction of about 0.7% while the condensation temperature increases by 0.5°C. When the subcooling is maintained equal to 10°C, while the thermal capacity increases about 0.65%, the condensation temperature increases of 0.5% as well. In general, if the condensation temperature increases, the thermal capacity should decrease. However, this is not what we are able to see in the reported results. The most probable cause for this is simply that the uncertainty in the evaluation of the condenser capacity is higher than the differences observed, apart from the fact that the capacity is affected by all operating conditions and it is very difficult to test at the very same conditions. The variation of the condensing temperature is much more sensitive, and much directly related to the heat transfer occurring at the condenser, so those variations are much more significant for drawing conclusions about heat transfer process at the condenser.

Similar conclusions can be drawn for the inverted velocity profile B. Indeed, compared with the uniform profile, when the subcooling is 0°C, the thermal capacity decreases of about 1.1% while the condensation temperature increases 1.4°C. For the highest subcooling, the capacity decreases of about 0.03% while the condensation temperature increases of 1.0°C.

5.2.4.2 Microchannel condenser

Also for the MCHX, the results of the thermography has been used for analyzing the effects of the air maldistribution on the refrigerant distribution. Indeed, even though the temperature profiles cannot be analyzed in as much detail as for the coil since the refrigerant does not go in MCHX

through separated circuits, the qualitative analysis of the thermographic images gives us important information regarding the refrigerant distribution and the condensation process. Actually, the analysis of the thermographic images not only provide a detailed information about the evolution of the condensation process inside the condenser, but additionally allows the identification of the interaction in between the air maldistribution and the performance.

In general, when the thermographic images of a parallel tubes heat exchanger are analyzed, what it is observed in the pictures is the temperature distribution along the external (frontal) surface of the heat exchanger. The more uniform is the temperature distribution along the refrigerant path; the better is the refrigerant distribution.

If in one hand, in single-phase heat exchangers such temperature homogeneity can be easily obtained with a suitable design of the headers, in two-phase heat exchangers, especially with vertical headers, the refrigerant maldistribution is very difficult to avoid mainly due to the simultaneous presence of liquid, vapor and phase changing.

In this latter case, a temperature profile cannot be plotted as for the coils, but the volumes occupied by each phase can potentially be identified by analyzing the thermographic images. This means that for the MCHX, the thermography provides only a sort of temperature distribution maps. For the parallel flow condenser employed for this PhD (Chapter 3), all temperature maps are reported in the Table 5.2 including different operating conditions at different air velocity profiles. In the central column of the table, the images obtained for given subcooling and uniform velocity profile are presented. It is interesting to notice that, even though the measured subcooling at the condenser outlet is equal to zero, part of the tubes, starting from the end of the second pass, seem to be occupied by saturated (or slightly subcooled) liquid. The presence of more and more liquid characterizes the third and fourth passes.

This observation points out that different mass flow rates are characterizing every tube of the microchannel heat exchanger and consequently, a different heat transfer is taking place. For the case of null subcooling, the mixture of liquid and vapor in the header and at the condenser outlet can be considered exactly at saturated conditions as imposed by the presence of the liquid receiver. For higher subcoolings, the liquid is clearly occupying an increasing part of the bottom channels, and consequently of the heat exchanger volume: for SC=10°C the third pass is almost full of liquid; for subcooling equal to 20°C the second, the third and the fourth pass are totally filled up with liquid. In those cases, it is very difficult to identify the section of the heat exchanger where the condensation starts and finishes.

Table 5.2: Thermography for the microchannel condenser under different airflow distributions

	Velocity profile			
	Profile A	**Uniform profile (reference)**	**Profile B**	**Scale**
	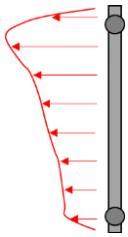	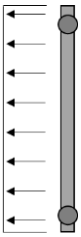	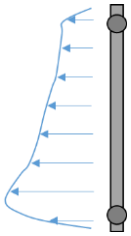	
SC = 0°C	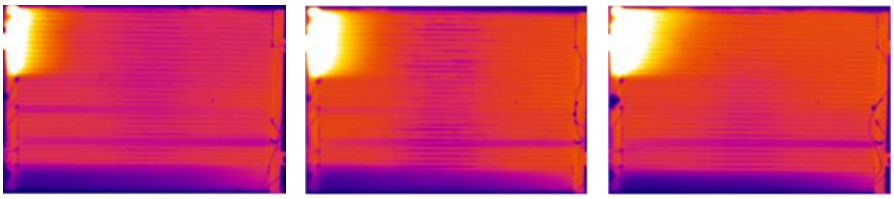			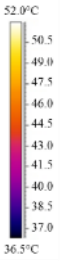
SC = 10°C	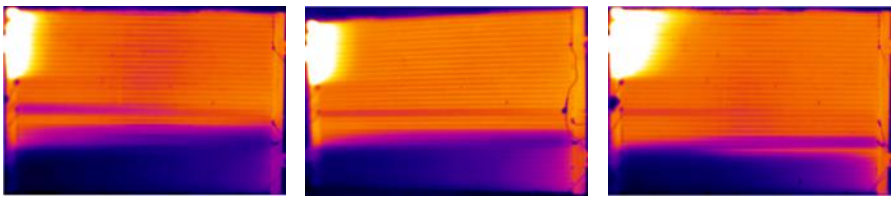			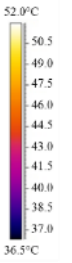
SC = 20°C	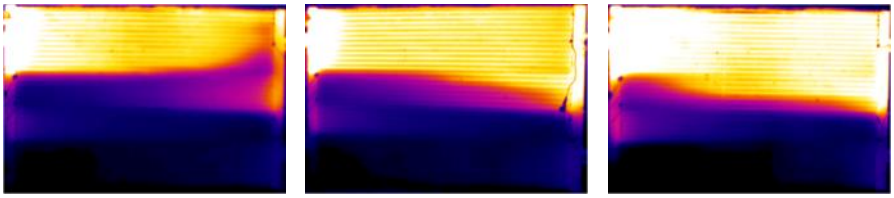			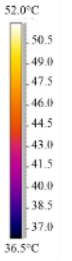

The analysis of the temperature maps is even more complex when the uneven air velocity profile A and B are considered. For all the operating conditions, the effects of the application of the velocity profile A can be summarized as follows:

- The highest air velocity at the refrigerant inlet reduces the volume occupied by the superheated vapor compared to the reference case.
- Where the air velocity gets lower than the uniform value, due to the reduction of the airside heat transfer coefficient, the volume of the heat exchanger occupied by liquid tends to increase.

When profile B is tested (symmetrical to profile A) exactly the opposite behavior can be described: the superheat area increases, while the subcooled area decreases compared with the reference test.

However, as shown in Figure 5.14, only slight variations of the global performance are produced by the air maldistribution.

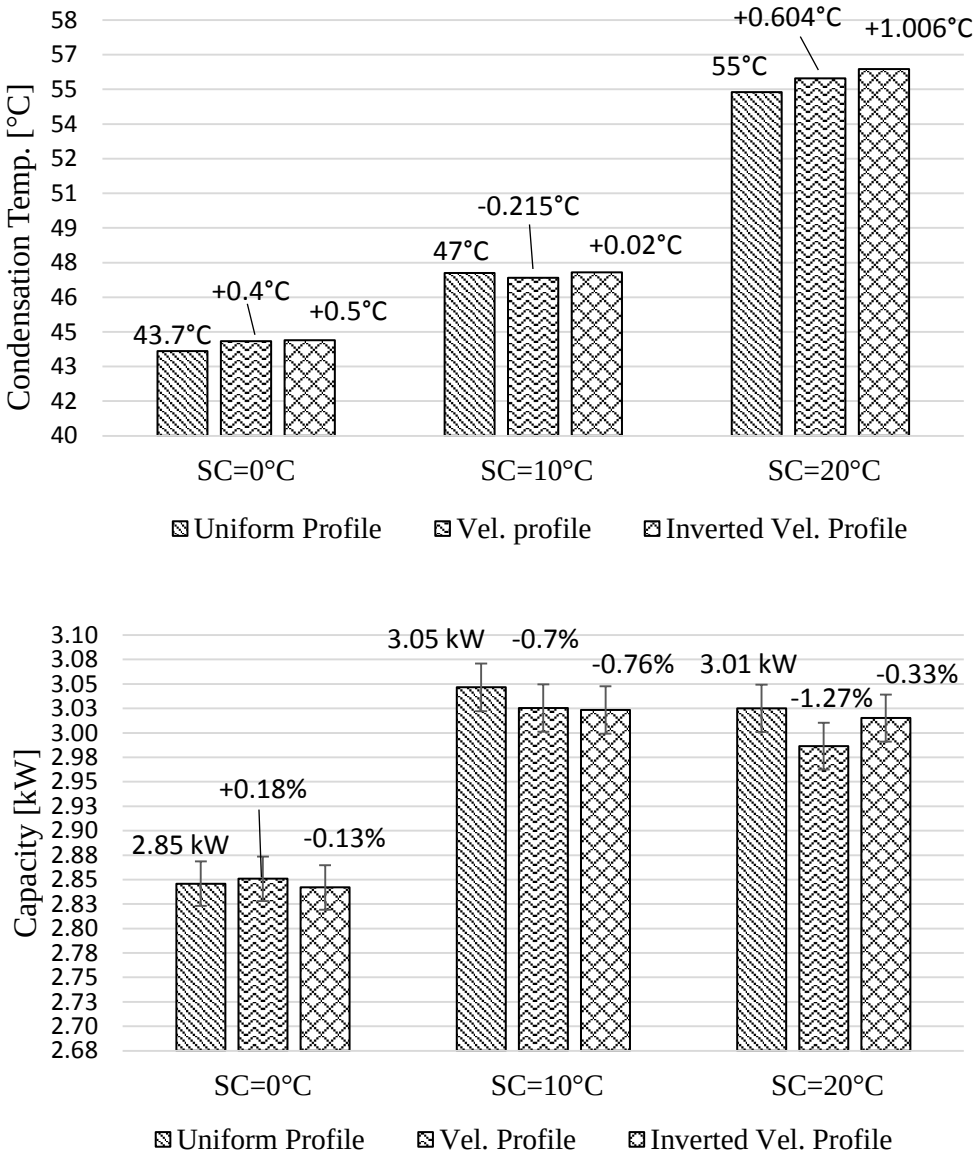

Figure 5.14: Performance degradation of the microchannel condenser due to the air maldistribution

Actually, the main changes in thermal capacity are just due to the subcooling variations not to the air maldistribution. Again, it must be pointed out that the uncertainty on the evaluation of the condenser capacity (~0.8%) is of the same order of magnitude than the registered variations.

Also in terms of condensation temperature, the variations can be considered almost negligible. As depicted in Figure 5.14, the condensation temperature undergoes very slight changes with airflow maldistribution. The variation of the condensation temperature is much lower than 0.5ºC when the subcooling is equal to 0°C and 10°C. Slightly higher variation can be appreciated when the profile B is tested with the subcooling equal to 20°C. Only in this case, the condensation temperature increases up to 1ºC.

Such results leads to conclude that, for every value of the subcooling, the performance of the microchannel condenser is much less sensible to the air maldistribution than the RTPFs condenser. However, this conclusion cannot be generalized based on the test of just two samples. In the next future, more tests should be performed in order to confirm some of the conclusions extracted from the presented experimental campaign.

5.3 Numerical studies: Model Validation

In the current version of IMST-ART 3.7 (IMST-ART, 2010), the option of considering an uneven air velocity profile at the inlet of the heat exchangers is not yet allowed to the normal user. Actually, as well as all the other input parameters (Chapter 2), the users can only define the uniform air volumetric flow rate or, alternatively, the homogenous air inlet velocity. From a mathematical point of view, as described in the second chapter of the present thesis, such parameters represent one of the boundary conditions used during the standard calculation procedure. However, as mentioned in the first part of the current chapter, uniform air distribution is not found in the real applications. In most of the cases, a considerable air maldistribution is always present at the heat exchanger inlet.

Although the results of the experimental campaign highlighted that the effect of an uneven air distribution on the performance of the studied condensers can be considered almost negligible in terms of performance degradation, it is not excluded that for other heat exchangers types (e.g. different geometries, number of circuits or number of passes, and especially at evaporators) the influence might be much stronger. Starting from this consideration, and in order to have a more complete simulation tool, the original IMST-ART condenser models (both RTPFs and MCHX) were modified in order to include the option to select an uneven air velocity profile as input parameter.

In general, excluding some specific applications, what is measured in a real installation is only the volumetric airflow rate, and the actual air distribution is practically unknown. In most of the cases the hypothesis of uniform distribution is considered. However, during the design phase, it may be also interesting investigating how a generic uneven air velocity profile at the heat exchanger inlet could affect its performance. Starting from this consideration, with this objective in mind, the strategy used for the model development was based on the definition of the following input parameters:

- The total air mass flow rate (m_{air}) or the total volumetric flow rate.
- The air velocity profile as a function of the heat exchanger height:

$$\frac{u_{air}}{\overline{u_{air}}} = f(y)$$

Where $\overline{u_{air}}$ is the average frontal air velocity. In this way, during the simulations, the airflow rate can be maintained constant (for example equal to the experimentally measured value) and the

performance variation can be evaluated only as function of different velocity profiles. The designer has to have the possibility to define any f(y) with the unique restriction imposed by the total mass flow rate:

$$\frac{1}{N_{cell}(y)}\int f(y) = \frac{1}{N_{Cell}(y)} \sum_{i}^{N_{cell}(y)} u_{air,i}\,(y) = \overline{u_{air}} = \frac{m_{air}}{A_{frontal,tot} \cdot \rho_{air}} \tag{5.8}$$

In the above, the hypothesis that the velocity profile only changes with the height and not with the condenser length is implicitly assumed. The computer software is of course able to employ two dimensional velocity profiles. However, as commented previously it is difficult to have that kind of empirical information, and this part of the doctoral thesis has been devoted to the analysis of the influence of air flow maldistribution on the condenser performance, so taking into account only the vertical variation of the velocity profile is enough for that purpose.

In the next subsections, both the round tube and the MCHX models have been initialized following the criteria described by Eq. 5.8.

5.3.1 Tube-and-fins condenser

In addition to the air velocity profile, the RTPFs condenser model was initialized considering the set of boundary conditions including the refrigerant mass flow rate, the subcooling and the inlet temperature. Therefore, as already discussed in chapter three, the validation process has been performed comparing the results of the model with the experimental obtained condensation temperatures and thermal capacities.

The results of the validation process have been depicted as bar charts in Figure 5.15. The experimental data are depicted as black bars (three bars at the left), while the results provided by the model are colored in red (three bars at the right). On the top of the black bars the corresponding experimental value is indicated, while on the top of the red bars the deviation between the model results and the experimental data is reported. The deviations are shown in absolute value (ºC) for the condensation temperature; while for the thermal capacity are shown in relative value (%).

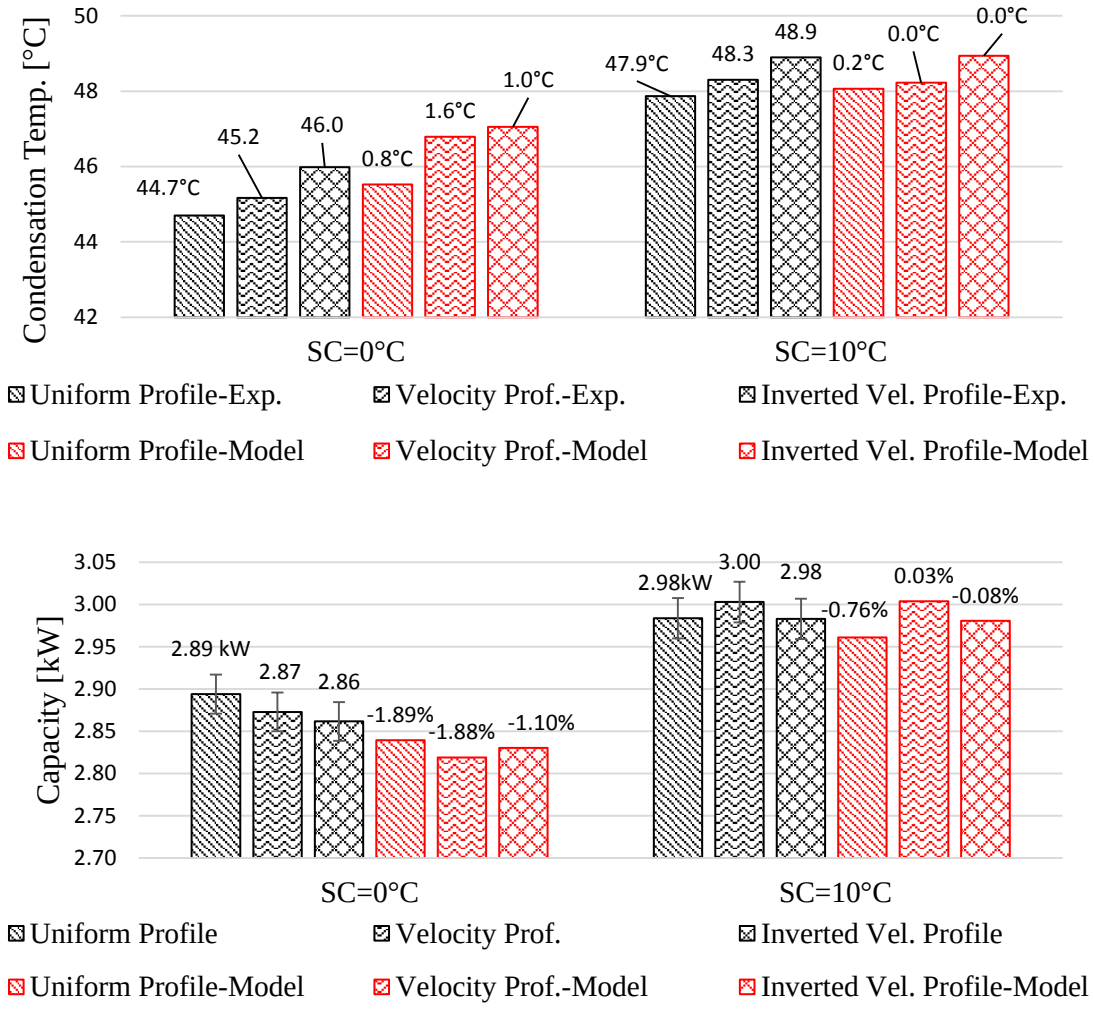

Figure 5.15: Model validation - Round tube plate fins condenser

As already commented, the performance variation due to the air maldistribution is very small, independently of the subcooling. As it can be observed, the model is able to reproduce with high accuracy the general trends of both performance and condensation temperature. Indeed, according to the model prediction, the application of the velocity profiles A and B generates only a maximum variation of about 1ºC of the condensation temperature. Consequently, only a slight performance degradation (which as indicated previously is lower than the measurement uncertainty) can be appreciated.

For the RTPFs condenser, the validation process includes also the analysis of the temperature profile along the heat exchanger. In Table 5.3 and Table 5.4, the experimental temperature profiles are compared with those calculated for all the measured operating points. Analyzing the diagrams in the tables, when the air distribution is set-up as input parameter, the model has even more difficulties to reproduce properly the experimental temperature profiles. In practice, when the profile A and B are imposed, the error due to considering the same mass flow rate in both circuits seems to be even more

amplified in comparison with those obtained with the uniform profile. For the case of subcooling equal to 10°C, the temperature profiles can be still considered similar to the experimental ones. Otherwise, when the subcooling is maintained equal to 0°C, the differences seem to be even more accentuated. In general, for any velocity profile, the model always predicts some degrees of subcooling at the outlet of the frontal circuit. If on one side, some liquid might really occupy part of the frontal circuit when the profile A is tested, on the other, this circumstance cannot be directly observed in the experiments when the uniform profile or the profile B are tested. As already commented in the previous chapter, such differences may be widely reduced if there is a different refrigerant mass flow rate per circuit.

The differences in the evolution of the refrigerant between the frontal and rear circuits is not only actually due to the air flow maldistribution but probably also to the refrigerant flow maldistribution. Although the studied condenser has only two circuits and the distribution in condensers is usually quite even because it is mainly done under vapor phase conditions, geometrical differences and the fact that the heat transfer are clearly different between frontal and rear positions, indicates that it probably exists a non-negligible refrigerant maldistribution.

From a modelling point of view, a general method for predicting the refrigerant distribution is possible but requires a big development effort. Hence, given the very good results of the model in terms of global parameters, the effect of the correct distribution of the refrigerant in the circuits has not be considered in this PhD work and has remained as the objective of future research activity.

Table 5.3: Simulated temperature profiles considering the air flow maldistribution – Subcooling = 0°C

Frontal circuit	Rear circuit	Velocity profile
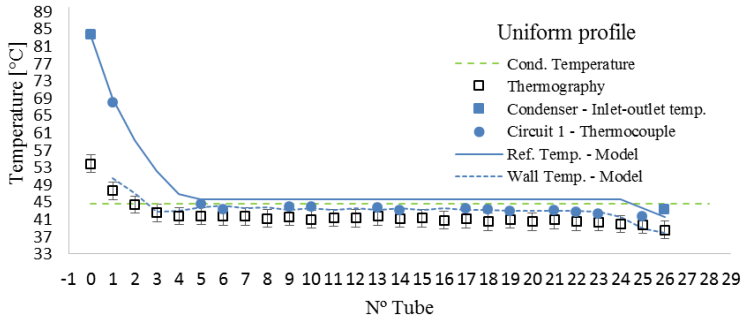	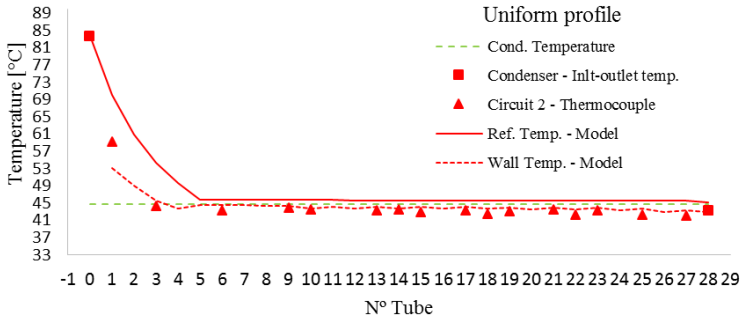	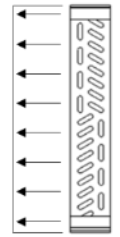
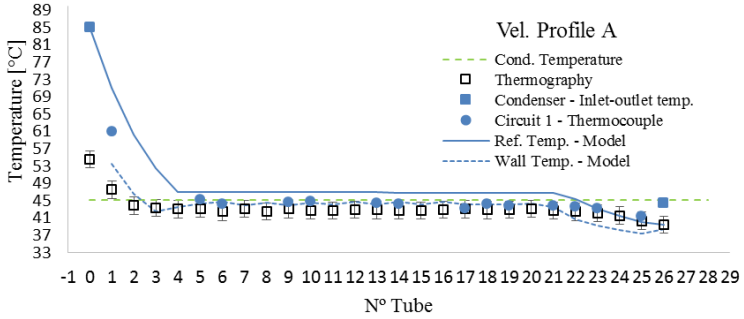	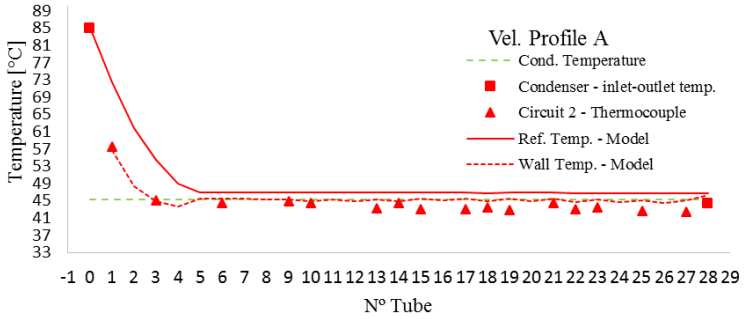	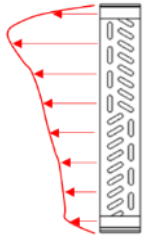
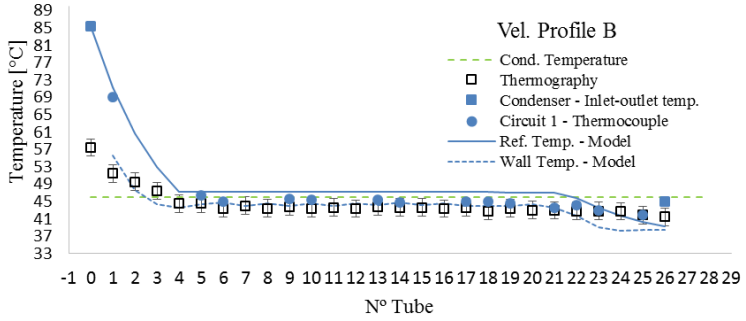	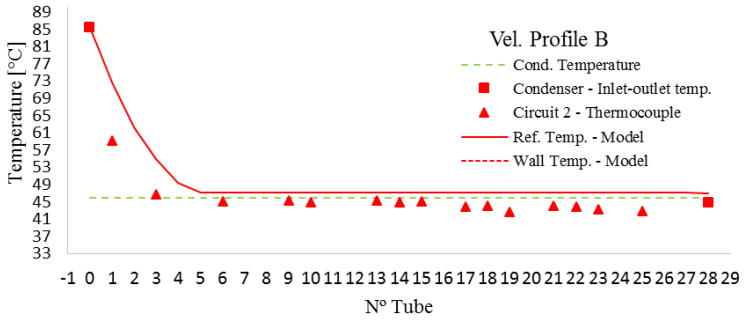	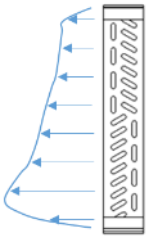

Table 5.4: Simulated temperature profiles considering the air flow maldistribution – Subcooling = 10°C

Frontal circuit	Rear circuit	Velocity profile
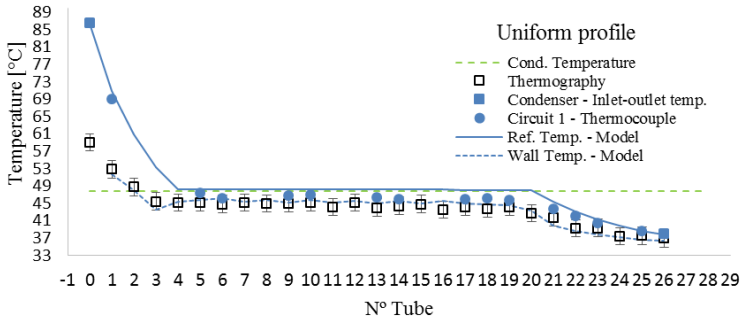	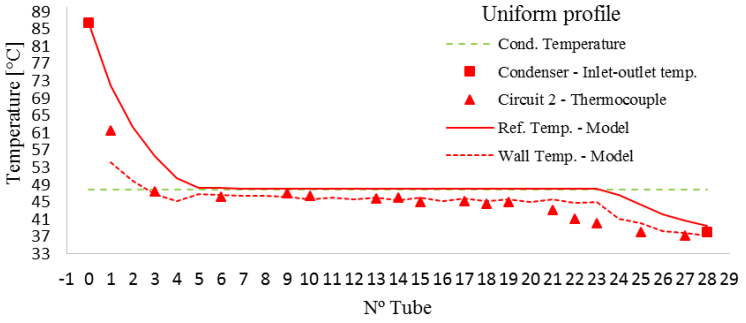	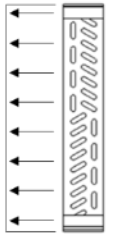
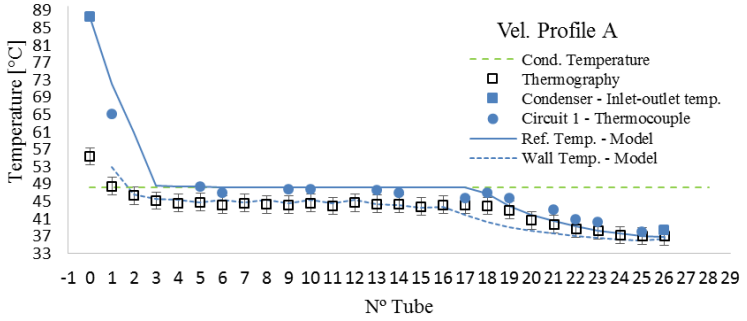	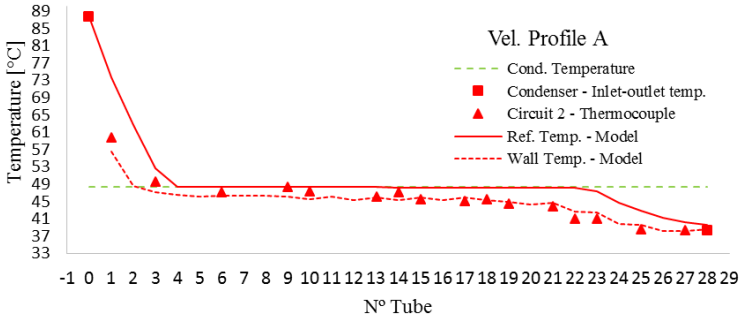	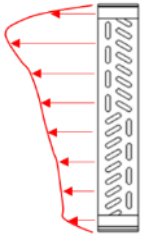
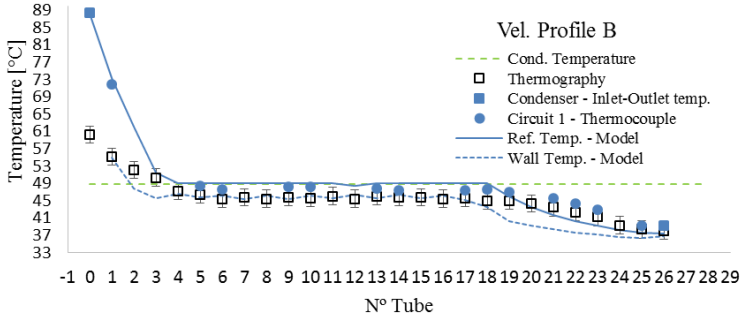	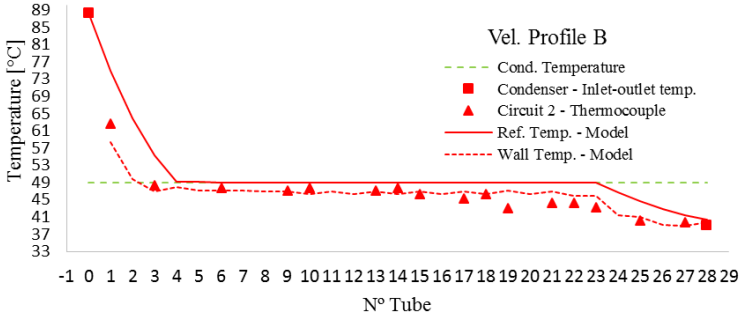	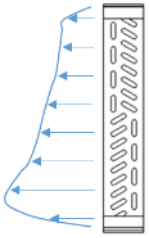

5.3.2 Microchannel condenser

As the RTPFs model, also in the microchannel condenser model has been added the possibility to set-up any air velocity profile as input parameter. According to equation 5.8, the simulations have been ran considering the velocity profiles depicted in Figure 5.10, hence maintaining equal to the reference test (uniform velocity profile) the air volumetric flow rate.

As in the previous subsection, the results of the simulations have been compared with the experimental data in terms of condensation temperature and thermal capacity. The comparison is represented as bar charts in Figure 5.16.

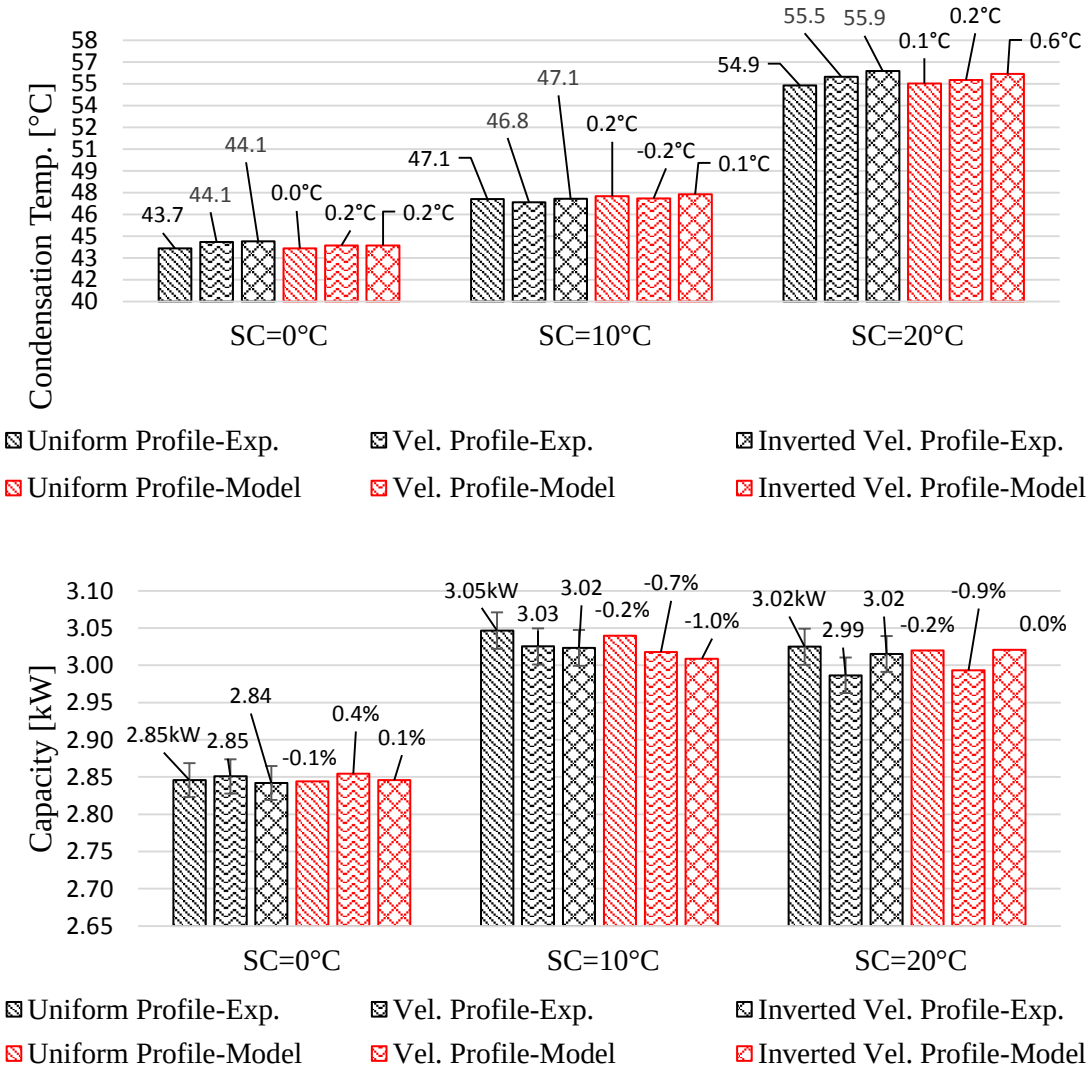

Figure 5.16: Model validation - Microchannel condenser

As commented in paragraph 5.2.4.2, from an experimental point of view, the effect of the air maldistribution on the performance of the parallel flow condenser is very small. Considering the velocity profile A and B, the condensation temperature undergoes only very small changes with the

maximum increase of about 1°C. Consequently, so small variations are combined with almost negligible performance degradation. As for the RTPFs, the general trend of the performance is characterized by a performance reduction of less than 1% in the worse cases. Even though very small, these performance changes are very well simulated by the microchannel condenser model, which is able to evaluate both condensation temperature and thermal capacity with very good approximation, for all operating conditions. Such result is also confirmed by analyzing the deviation between simulation and experimental data. As reported in Figure 5.16, the mean deviation is equal to 0.15°C in condensation temperature and only -0.3% in capacity. In conclusion also the model confirms that the microchannel is less sensible to the air maldistribution than the RTPFs condenser.

5.4 Conclusions

In the present chapter, a long discussion about the effect of the air maldistribution on the performance of a condenser has been performed. The research work has been divided in three consecutive steps: the development of a new experimental methodology for generating any air velocity profile at the inlet of a heat exchanger; the application of the developed methodology in a real installation; and finally the development of the condenser models in the commercial software IMST-ART for considering the air velocity profile as input parameter.

From an experimental point of view, any uneven air velocity profile can be easily generated placing in front of the heat exchanger inlet the adequate type of obstruction. Depending on the characteristics of the obstruction and its position with respect to the heat exchanger inlet, it is possible to affirm that the relationship obstruction-air maldistribution can be considered univocally defined. Starting from this assumption, the first part of the research work was mainly focused on the identification of such relationship. The experimental work was initially carried out in a dedicated wind tunnel where, considering different types of obstructions, the air velocity profile at the inlet of a plate tube radiator was varied and measured by means of a hot-wire anemometer. After many initial attempts, an adequate and feasible methodology for generating a "controlled" air velocity profile was identified. It mainly consists in placing a stack of filter layers having different path length, in front of the heat exchanger. In order to eliminate the effect of transversal flow on the air velocity profile, the stack of filters was placed in a special structure where thin slabs separate the filters. In this way, the air velocity is generated and measured with high accuracy in the narrow channels formed between the slabs. The relationship between the length of each filter layer and the air velocity was defined by means of what was called "characterization process".

The just summarized method is highly flexible and can be used for different types of heat exchanger and in different experimental facilities. In this thesis, a specific filter configuration was designed for the generation of the air velocity profile characterizing the inlet of an A-Shape condensation unit.

The filters box was placed in front of two different heat exchangers: a round tube heat exchanger and a parallel flow microchannel condenser. Both samples were tested in the dedicated wind tunnel described in the chapter three.

The experimental campaign was organized in order to study the effect of two symmetrical air velocity profiles on the performance of the condensers. The main results of the experiments can be summarized as follows:

- Analyzing the refrigerant and wall temperature profiles it is possible to conclude that the extension of the internal volume occupied by vapor, two-phase flow and liquid inside the heat exchanger is strongly depending on the air characteristics of the air maldistribution.
- Nevertheless, for both tested condensers, the effect of the air maldistribution on the condenser performance can be considered almost negligible. Indeed, in comparison with the reference test (uniform profile), the performance degradation is in the order of magnitude of the measurement uncertainty.
- Although the variations are very small, the results of the experiments lead to affirm that the air maldistribution always affects negatively the performance of the condensers. Furthermore, a velocity profile that facilitates the heat transfer in the area of the heat exchanger occupied by subcooled liquid seems to generate the highest performance degradation.
- For the RTPFs condenser the maximum increase of the condensation temperature (about 1.4ºC) is combined with the maximum performance degradation of 1.12%.
- The MCHX condenser is even less sensible to the air maldistribution. In this case, the maximum condensation temperature increase has been about 1°C, corresponding to a performance reduction of 0.33%.

The last part of the chapter is dedicated to the final model validation. Indeed, both condenser models (RTPF and MCHX) in IMST-ART were modified in order to allow the definition of any uneven air velocity profile as input parameter. Simulating all the tested points, the following results were obtained:

- Both heat exchanger models are able to simulate with good accuracy the variation of the condensation temperature and thermal capacity due to the air maldistribution.

- Due to the impossibility to consider the refrigerant distribution in the two circuits, the RTPFs model is not able to reproduce with high accuracy the temperature profiles along the condenser. For this reason, especially for the case with subcooling equal to 0°C, the global performance are obtained with the slightly lowest accuracy Nevertheless, the agreement between experimental and calculated results can be considered as very good.

Chapter 6

6. Conclusions

In this final chapter, the main conclusions of the studies presented in this thesis will be gathered and summarized. I addition, also the starting point for the next research activities will be listed and commented.

6.1 Global conclusions

As pointed out in the introduction, in many industrial sectors, the utilization of simulation tools during the phases of design and optimization of new products is nowadays fully integrated. This trend is getting more and more popular also in the HVAC&R sector. Indeed, in the last two decades, many researchers have focused their efforts on the development of simulation tools for simulating with growing accuracy the behavior of heat pumps and air conditioning systems. The objective of the thesis was not the design of a completely new model, but the further development and optimization of an already existing model for the simulation of the heat exchangers. In particular, all the numerical studies and experimental activities have been mainly focused on the analysis of the phenomena linked to the heat transfer in the round-tube and microchannel condensers for heat pumps or refrigeration equipment.

Specifically, the research project has been targeted to the improvement of the condenser models built in the commercial software IMST-ART. As discussed in the second chapter, in this calculation platform, the traditional round-tube and microchannel condenser models share the same modelling philosophy. However, depending on the characteristics of each kind of heat exchanger, the models present some common characteristics and some differences: the segment-by-segment approach, combined with the application of the SEWTLE method for the integration of the governing equations in the refrigerant side, is the common denominator; specific correlations for the estimation of the heat transfer coefficients and friction factors, as well as a different volume discretization for the integration of the governing equations in the air side, represent the main differences.

In this context, the word “optimization” assumes a double meaning. On one hand, optimization means the identification of the best correlations for calculating the HTCs and friction factors in the internal and external sides of the heat exchangers. On the other, optimization means the inclusion in

the models of more and more complex phenomena connected to the two-phase heat transfer, mass transfer and flow distribution.

The identification of the best set of correlations for calculating the HTCs and friction factors in both the internal and external sides of a condenser was the goal of the first part of the thesis. With this target, in the third chapter, the most suitable validation methodology for comparing the behavior of the condenser model with different correlations was analyzed and discussed. Initially, the discussion was focused on the analysis of the boundary conditions used for the simulation of a condenser. The following conclusions came out:

- In order to compare properly the results of a condenser model with different correlations for the evaluation of the HTCs and friction factors, instead of using the inlet pressure as one of the boundary condition, the utilization of the condenser subcooling is proposed.
- The utilization of the condenser subcooling makes possible to compare all the correlations for the estimation of the two-phase HTC and friction factor without missing any information. Indeed, by using the subcooling as an input, the comparison can be performed over the entire range of variation of the vapor quality, condition that might not be respected using the inlet pressure.
- The use of the subcooling as an input presents another important advantage. Traditionally, the validation process has been always performed comparing the calculated capacities with the experimental values. However, if the condenser subcooling is used as an input, the main validation result turns out to be the condensation temperature. From an experimental point of view, the condensation temperature has a much lower uncertainty than the condenser capacity. Therefore, it represents the best parameter to compare with the results of the simulation and identifying the best set of correlations for the estimation of HTCs and friction factors.

As already widely known, the estimation of the global thermo-hydraulic performance of a condenser is strongly connected to the combination of the correlations used for the evaluation of the HTCs and friction factors in both the refrigerant and air sides. In order to isolate the effect of one correlation for analyzing in detail its influence on the results provided by the condenser model, a new validation process was proposed. It mainly consists on splitting the model validation in some consecutive steps. During each of them, when a certain correlation is studied, the model validation is performed maintaining the rest of heat transfer and the pressure drop coefficients constant. With this method, the best correlations for each factor can be identified independently of each other, analyzing the results of each validation step in terms of metrics such as Mean Error, Mean Square Error and Standard Deviation. The analysis of the obtained results led to an interesting conclusion: instead of the mean deviation, the standard deviation represents the most important statistic parameter for the

evaluation of the correlations. Indeed, when one correlation is analyzed, the mean deviation strongly depends on the constant values used for the other HTCs and friction factors.

The correlations that allow getting the best agreement between the results of the simulations and the set of experimental data employed in this thesis are summarized in Table 6.1.

Table 6.1: Summary of the best correlations for calculating the two-phase HTC and friction factor in both the Round-tube and microchannel condenser models

	Correlations	
	Tube-and-fins condenser	**Microchannel condenser**
Two-phase HTC	Thome *et al.* (2003)	Lopez *et al.* (2014)
Air side HTC	Granryd *et al.* (2003)	Kim and Bullard (2002)
Two-phase friction factor	Friedel (1979)	Friedel (1979)
Air side friction factor	Wang *et al.* (2000) for $v_{air} > 2.5$ m/s Granryd *et al.* (2003) for $v_{air} \leq 2.5$ m/s	Chang *at al*. (2006) or Kim and Bullard (2002)

Once identified the best correlations for the evaluation of the HTCs and friction factors, although the model calculates the global performance of the round-tube condenser with very good accuracy, the validation process pointed out to some possible "weak point" of the current approach for the simulation of the condensation process. Indeed, some evident discrepancies between the results of the simulations and the experiments came out comparing the temperature profiles (wall tube and refrigerant) along the circuits of the round tube and fins condenser. Neglecting some secondary heat transfer phenomena, such as the convective condensation of the superheated vapor, or the refrigerant flow distribution, would lead to some inaccurate evaluation of the local value of the refrigerant heat transfer coefficient and would negatively affect the calculation of the temperature profiles along the condenser. In this thesis, two different methodologies for implementing in the current condenser models the convective condensation of the superheated vapor have been proposed, discussed, and finally implemented in the simulation model.

The first methodology, called "Temperature approach method", was aimed to:

- Identifying with high accuracy the section of the heat exchanger in which the convective condensation of the superheated vapor begins.
- Simulating with high accuracy the variation of the HTC in the condensing superheated vapor zone by means of the application of specific correlations.

Nevertheless, even though this method provided evident improvements in the evaluation of the local heat transfer coefficient at the beginning of the condensation process, its application entailed a significant increase in the calculation time. This issue was solved with the application of the second method, named "Enthalpy approach method", which was designed to identify the value of enthalpy at which the condensing superheated vapor zone began by means of a simpler iteration procedure.

The main conclusions of the model validation in regard to these two developed methodologies for the evaluation of the convective condensation of the superheated vapor are:

- The results of the application of the Temperature approach method can be considered only slightly different to those obtained by using the Enthalpy approach method.
- The modification of the original condenser model with the possibility to consider the convective condensation of the superheated vapor guaranties a better interpretation of the entire heat rejection process occurring at both coil and microchannel studied condensers.
- The temperature profiles along the RTPFs condenser are calculated with a clearly higher accuracy than the original model. The improvement in the evaluation of the local HTC in the condensing superheated vapor zone affects very positively to the estimation of the temperature profile all along the condenser.
- Nevertheless, the impact of the implementation of the convective condensation of the superheated vapor on the prediction of the global performance of a condenser is not so significant.

Apart from the inclusion of the condensing superheated vapor zone in the condenser model, in order to have even better agreement between the experimental data and the results of the simulation software, the research work might have been oriented exclusively towards the analysis of the effects of the refrigerant maldistribution. However, dealing with this topic would have required a huge experimental effort, lying out of the scope of the present doctoral work. Therefore, it was decided to orient it into a different direction: the evaluation of the effect of the air maldistribution on the condenser performance. This has constituted the last part of the present PhD work and it has been developed following the steps presented below:

- Identification and development of a new experimental methodology for generating any air velocity profile at the inlet of a heat exchanger.
- Application of the developed methodology in a real installation equipped with both round tube and microchannel condensers, and evaluation of the effect of the air flow maldistribution on the condenser performance.
- Improvement of the condenser models built-in in the commercial software IMST-ART for considering the air velocity profile as input parameter.
- Final model validation.

The new experimental methodology designed for generating any air velocity profile at the inlet of a heat exchanger mainly consists in placing a certain number of filter layers in front of the heat exchanger. Playing with the length of each filter in the air flow direction, due to a different local pressure drop, any value of the air velocity can be obtained. The development of this experimental methodology led to the following conclusions:

- In order to eliminate the effect of transversal flows and measuring with high accuracy the local value of the air velocity, the filter layers must be separated by thin slabs defining parallel air channels. The filters, the slabs and the frame of the structure were synthetically called “filters-box”.
- The relationship between the required length of the filter layer and the air velocity can be identified by means of the “characterization process”. It consists of a series of steps aimed at identifying experimentally the pressure drop characteristics of the filter material, hence the ratio (local Δp)/ (local air velocity).

In order to study experimentally the effects of the air maldistribution on the performance of a round-tube or a microchannel condenser, specific filters-boxes were designed for generating the uneven air velocity profile characterizing the inlet of an A-Shape condensation unit.

During the experimental campaign, the desired velocity profile was tested in two different arrangements:

- In the first arrangement, the highest air velocity was in correspondence with the upper part of the condensers where the refrigerant inlet takes place, so that the heat transfer was enhanced in the zone occupied by the superheated vapor and penalized where the refrigerant is subcooled liquid.
- The second arrangement was the reversed one with the highest velocities facing the bottom part of the condenser. In this case, the highest air flow rate enhances the heat transfer in the subcooled region of the heat exchanger, meanwhile, the heat transfer is penalized at the condenser inlet, where the refrigerant is superheated vapor.

The main results from the experimental campaign for both condenser technologies can be summarized as follows:

- Analyzing the refrigerant and wall temperature profiles, it is possible to conclude that the volume occupied by the vapor, two-phase flow and liquid inside the heat exchanger is strongly dependent on the air velocity profile.
- Nevertheless, the effect of the air maldistribution on the condenser performance appears to be almost negligible with a very small performance degradation, for both studied condensers: round-tube and microchannel.
- The highest performance degradation has been obtained when the highest velocities are placed at the bottom of the condenser so maybe facilitating the heat transfer in the area occupied by subcooled liquid but worsening the heat transfer at the inlet of the superheated vapor. Comparing the results with the reference test (uniform air velocity profile):

- For the RTPFs condenser the maximum increase of the condensation temperature is about 1.4°C is combined with the maximum registered capacity degradation of about 1.12%.
- The MCHX condenser is even less sensible to the air maldistribution. In this case, the maximum condensation temperature increase is only about 1°C leading to a capacity reduction of about 0.33%.

The last part of the thesis was dedicated to the final model validation. Both RTPF and MCHX condenser models built-in in IMST-ART, were modified in order to allow the input of any uneven air velocity profile. After simulating all the experimentally tested points for both condenser technologies, the following conclusions can be drawn:

- Both heat exchanger models are able to simulate with good accuracy the small variation of the condensation temperature and thermal capacity due to the air maldistribution. The condensation temperature is always evaluated with deviations lower than 1°C, while the deviation in the estimation of the thermal capacity is always smaller than the uncertainty characterizing the experimental value.
- Due to the impossibility to consider the refrigerant maldistribution, the RTPFs model is not able to reproduce with high accuracy the temperature profiles along the two circuits of the condenser. The discrepancies between calculated and experimental profiles are more accentuated for the tests with subcooling equal to 0°C. This points out some difficulties in calculating correctly the local value of the HTC along the refrigerant path. This issue also slightly affects the correct estimation of the global performance.
- All in all, the accuracy in the prediction of both performance and temperature evolution is high and proves that the developed models can be employed with great confidence to assist the design and optimization of condensers of any of the studied technologies.

6.2 Recommendations for further works

The recommendations for the further works are divided in two groups: model improvement (next IMST-ART versions) and further activities.

6.2.1 Model improvements (next IMST-ART versions)

In this paragraph will be briefly comment the modifications that might be added to the current condenser model in order to simulate with even better accuracy the experimental data. Some words will also be spent about the improvement of next version of the commercial software IMST-ART.

1. Most of the validation procedure for identifying the best correlations for the calculation of the HTCs and friction factors has been performed manually. In order to be useful for most of IMST-ART users, the commercial software may be improved with a sort of "automatic optimization tool". The geometry of the heat exchanger and the set of experimental data should be considered as input parameters. Hence, the entire validation procedure could be ran in background and only the best correlations could be shown as a result.
2. Currently, the condenser models (tube-and-fins and microchannel heat exchangers) are able to calculate the experimental data with good accuracy. Nevertheless, some other phenomena and details might be included. In particular, the next research works might be focused on:
   - ✓ The inclusion of the phenomena having place in the condensing subcooled liquid zone.
   - ✓ The implementation of specific correlations for calculating the two-phase friction factor in the microchannel heat exchanger.
   - ✓ The implementation of a suitable model for calculating the pressure drop in the headers of the microchannel heat exchangers.
   - ✓ The identification and implementation in the models of a simple strategy for considering the refrigerant maldistribution.

Currently, only the source code of IMST-ART has been modified for considering the air side maldistribution as input parameter. The user interface should be partially modified and modernized. In other words, the users should be able to define any uneven air velocity profile at the inlet of the heat exchanger in the easiest and most flexible possible way.

6.2.2 Further activities

Besides the further research activities aimed to improve the condenser models, other experimental studies may be interesting to be carried out:

1. For the RTPFs condenser, the validation process has been performed taking into account only one geometry. An extension of the experimental campaign with substantially different geometries and sizes would be very useful for confirming the results obtained.
2. More experimental studies related to the analysis of the effect of the air and refrigerant maldistribution should be performed. This is essential to support future software developments targeting the consideration of these complex situations.

   As discussed in the introduction, previous work pointed out that the performance of the evaporators is very sensitive to air maldistribution. The experimental methodology presented in this thesis for the generation of uneven air velocity profiles might be used for testing both round-tube and microchannel evaporators.

7. Appendices

7.1 Appendix A: drawings

7.1.1 Filter box for the tube-and-fins heat exchanger

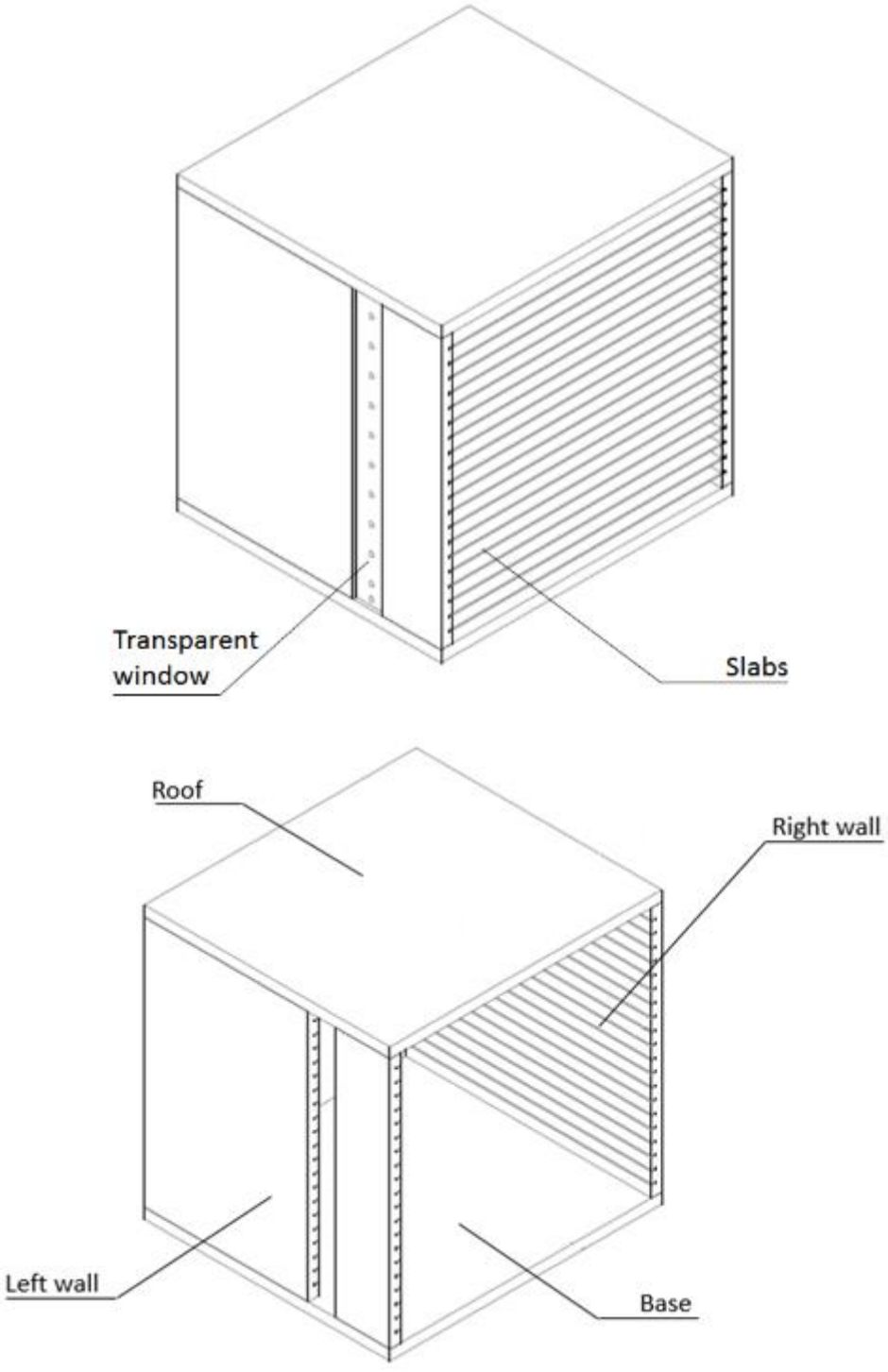

Figure 7.1: Isometric view of the filer box

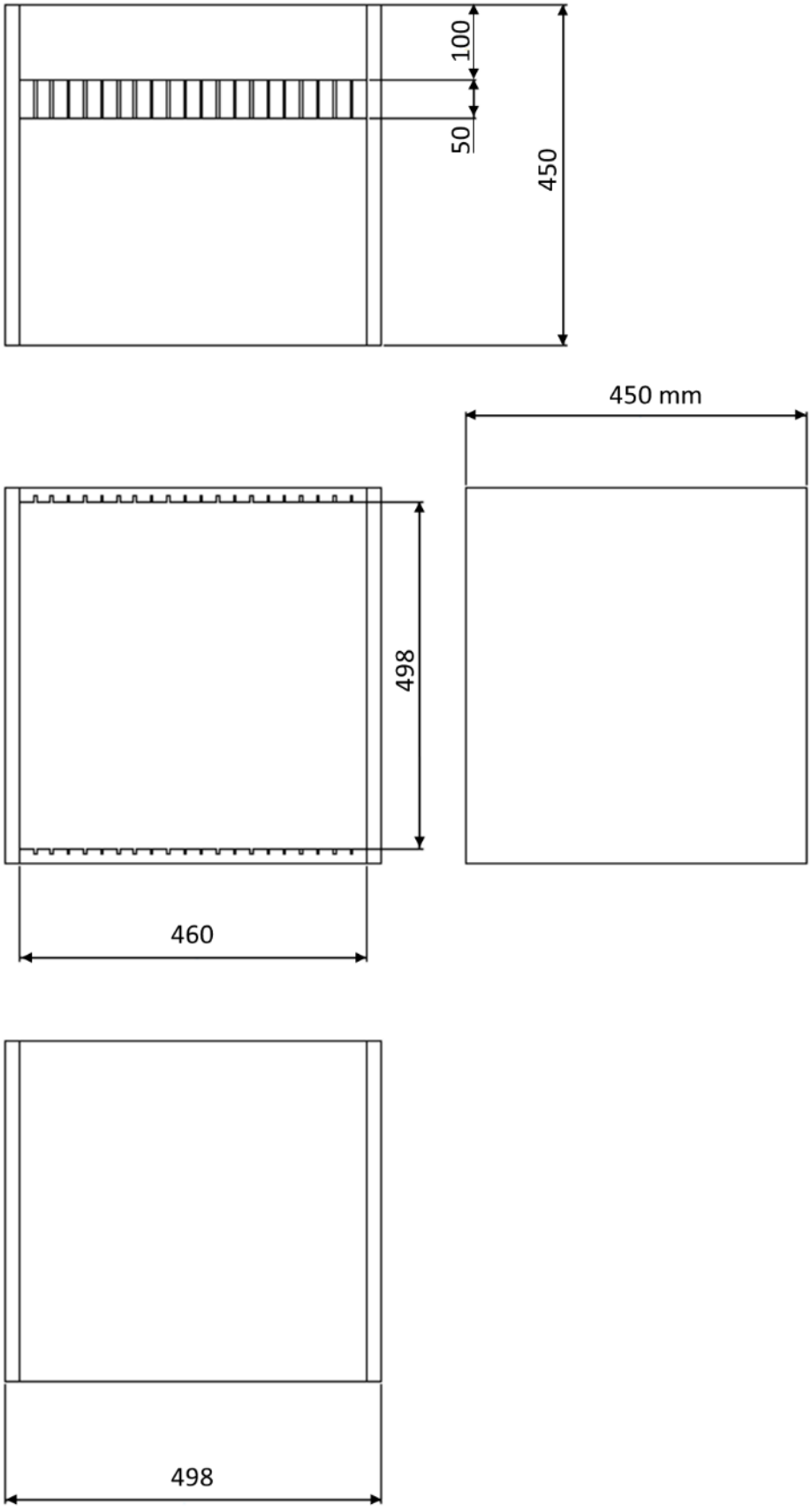

Figure 7.2: Main dimensions of the frame

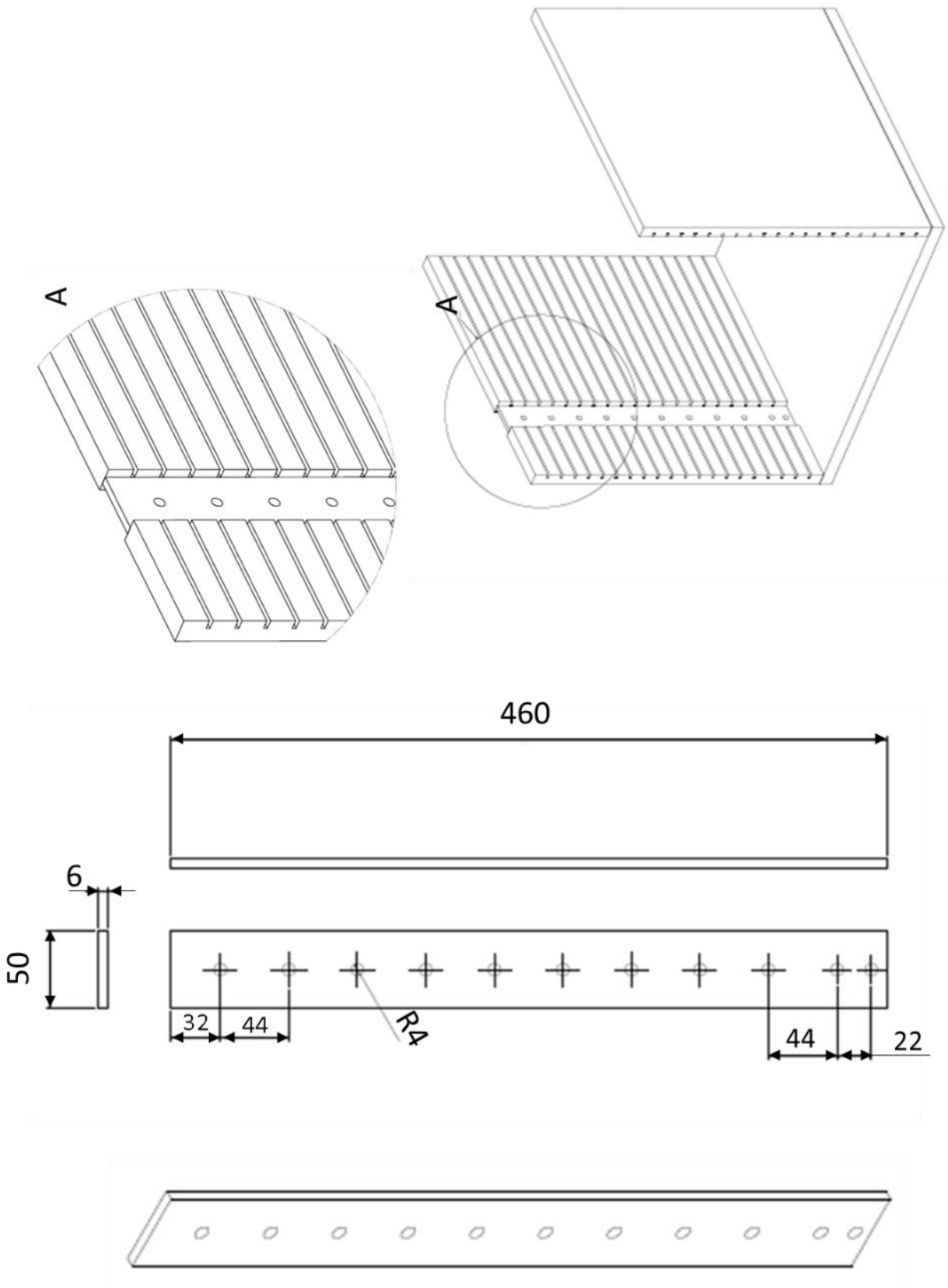

Figure 7.3: Transparent window

7.1.2 Filter box for the microchannel heat exchanger

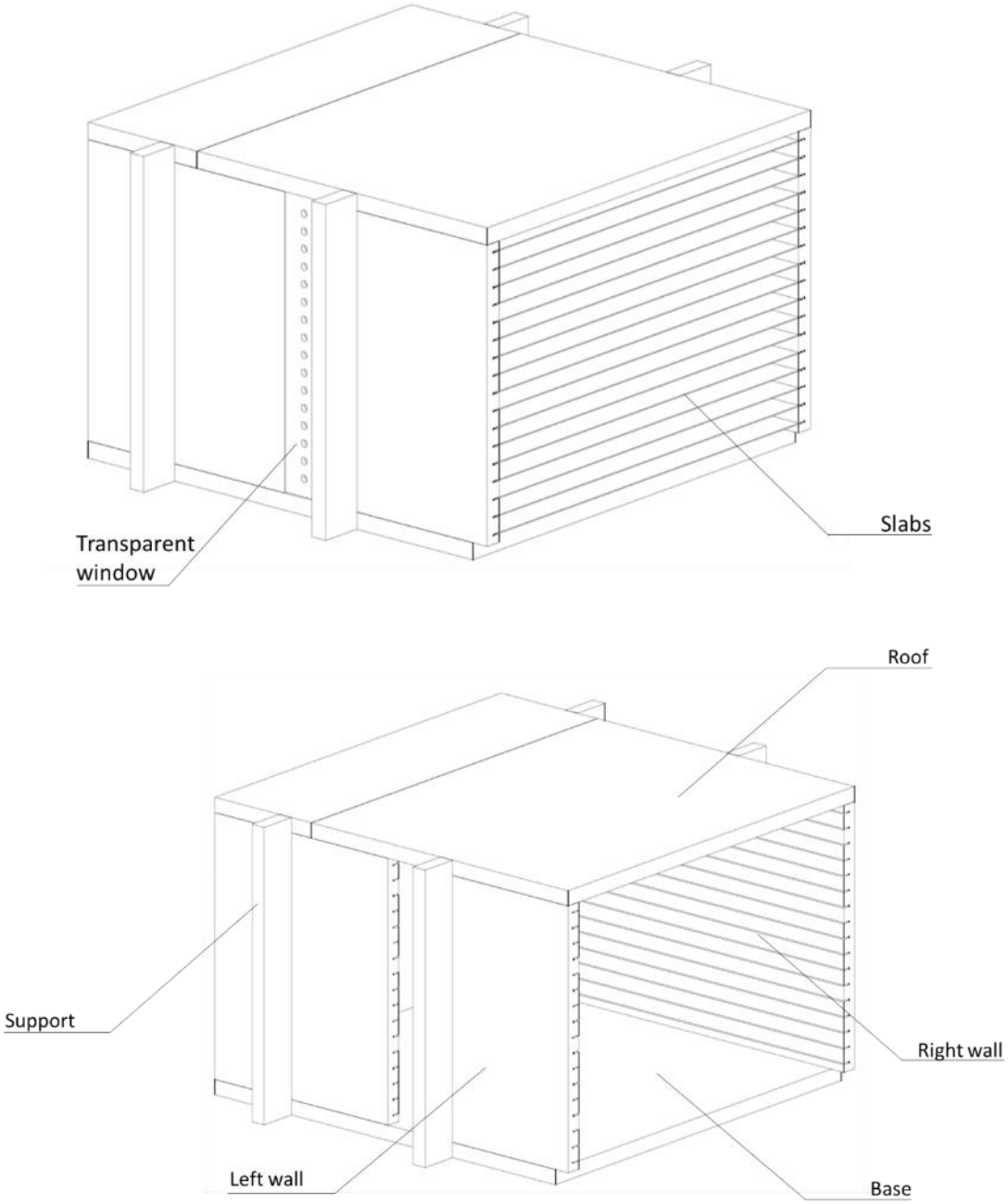

Figure 7.4: Isometric view of the filter box for the microchannel heat exchanger

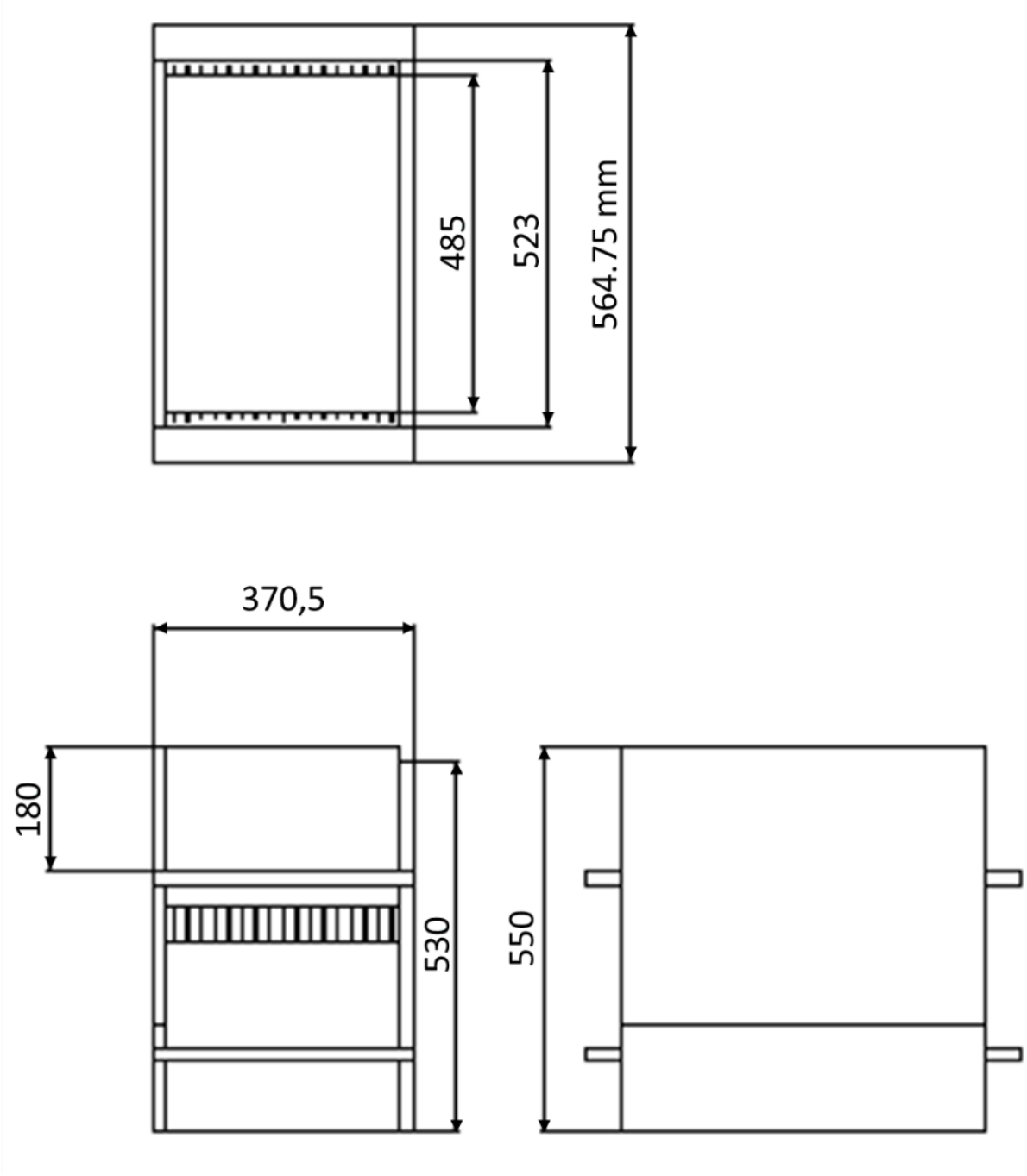

Figure 7.5: Main dimensions of the filter box for the microchannel heat exchanger

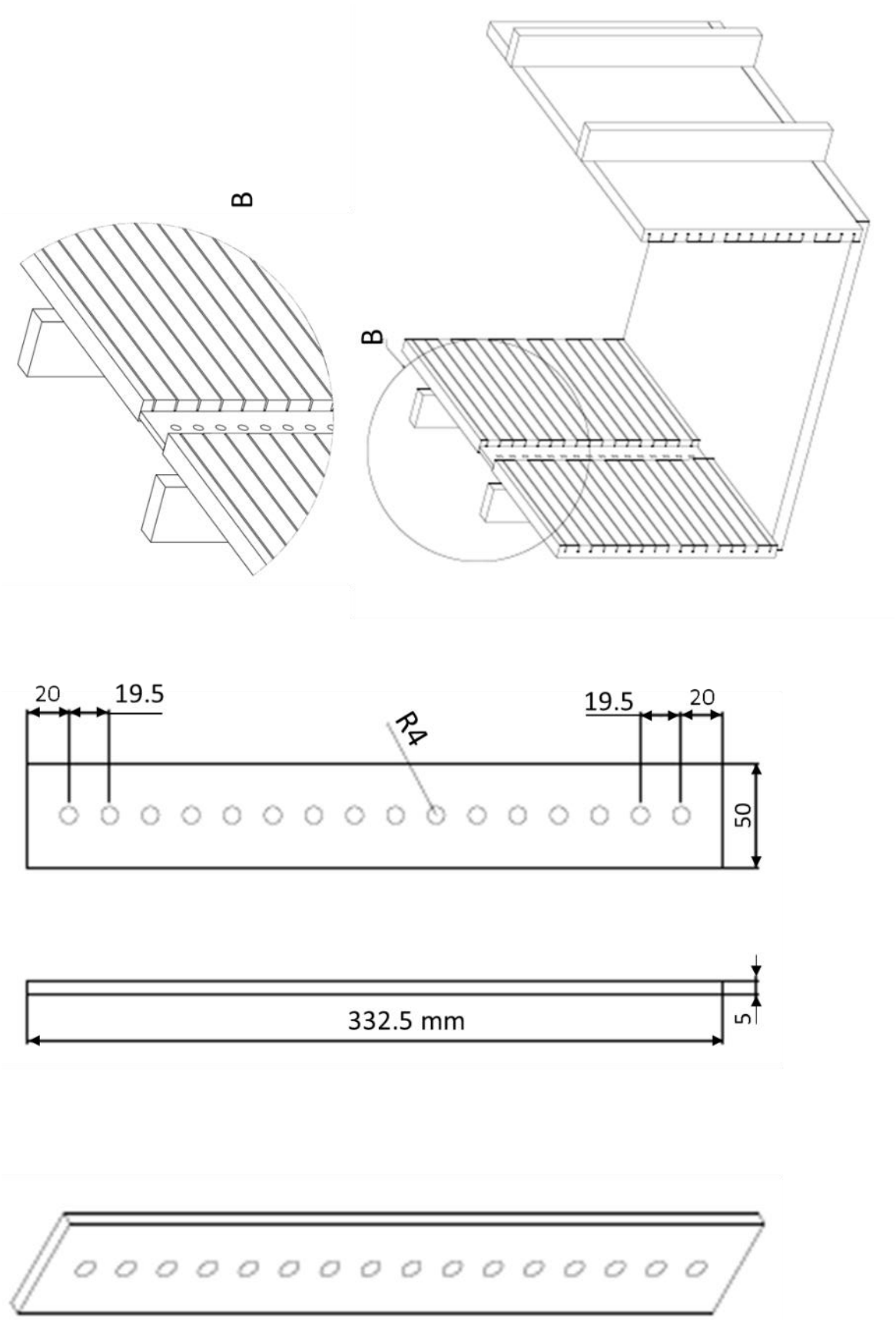

Figure 7.6: Transparent windows for the filter box – Microchannel heat exchanger

References

Aganda, A., Coney, J. and Sheppard, C., 2000. Airflow maldistribution and the performance of a packaged air conditioning unit evaporator. *Applied Thermal Engineering*, Volume 20, pp. 515-528.

Agarwal, A., Bahndauer, T. and Garimella, S., 2010. Measurement and modeling of condensation heat transfer in non-circular microchannels. *Int. J. Refrigeration*, pp. 33(6), 1169–1179.

Agarwal, R. and Hrnjak, P., 2013. Condensation in two-phase and desupeheating zone for 1234ze (E), R134a and R32 in horizontal smooth tubes. *International Journal of Refrigeration*, in print.

Agarwal, R. and Hrnjak, P., 2014. Effect of sensible heat, condensation in superheated and subcooled region incorporated in unified model for heat rejection in condenser in horizontal round smooth tubes. *International Journal of Refrigeration*, Volume 71, pp. 378-388.

Akers, W., Deans, H. and Crosser, O., 1959. Condensation Heat transfer within horizontal tubes. *Chem. Eng. Prog. Symp*. Ser., pp. Vol. 55, p. 171-176.

Altman, M., Staub, F. and Norris, R., 1960. Local Heat Transfer and Pressure Drop for Refrigerant R22 Condensing Horizontal Tubes. *Chem. Eng. Progress Symp*. Ser., 56(30), pp. 151-159.

ASHRAE, 2009. ASHRAE Handbook – Fundamentals (I-P edition) - American Society of Heating, Refrigerating and Air-Conditioning Engineers, Inc.

Asinari, P., 2004. Finite volume and finite element hybrid technique for the calculation of complex heat exchangers and Semiexplicit method for wall temperature linked equations (SEWETLE). *Numerical heat transfer Part B - Fundamentals*, Volume 45, pp. 221-247.

Ayad, F., Benelmir, R. and Souayed, A., 2012. CO2 evaporators design for vehicle HVAC operation. *Applied Thermal Engineering*, pp. 36, 330–344.

Bach, C., Groll, E., Braun, J. and Horton, W., 2014. Mitigation of air flow maldistribution in evaporators. *Applied Thermal Engineering*, Volume 73, pp. 879-887.

Bahndauer, T., Agarwal, A. and Garimella, S., 2006. Measurement and modelling of condensation heat transfer coefficient in circular minichannles. *Journal of Heat Transfer*, Volume 128, pp. 1050-1059.

Belakjian, G. and Katz, D., 1958. Heat transfer from superheated vapors to a horizontal tube. *AlChe Journal*, Vol. 1, 43-48.

Bell, I., 2012. Air conditioning and Heat Pump Model (ACHP), s.l.: Sourceforge SCM Repository.

Bell, K., 1972. Temperature profile in condensers. *Chem. Eng. Prog.*, Vol. 68 (7), 81-82.

Bertsch, S., Groll, A. and Garimella, E., 2008. Refrigerant flow boiling heat transfer in parallel microchannels as a function of local vapor quality. *International Journal of Heat and Mass Transfer*, pp. 51 (19–20), 4775–4787.

Bhuiyan, A., Amin, M. and Islam, A., 2013. Three dimensional performance analysis of plain fin tube heat exchanger in traditional regime, *App. Thermal Eng.*, pp. 50, 445-454.

Boissieux, X., Heikal, M. and Johns, R., 1999. Two-Phase heat transfer coefficients of three HFC refrigerants inside a horizontal smooth tube, part II: condensation. *International Journal of Refrigeration*, pp. Vol. 23, p. 345-352.

Briggs, A. and Rose, J., 1994. Effect of fin efficiency on a model for condensation heat transfer in a horizontal tube. *Int. J. of Heat and Mass Transfer*, pp. Vol. 37, p. 457-463.

Cavallini, A. and Zecchin, R., 1974. A dimensionless correlation for heat transfer in forced convention condensation. Tokyo, Proceedings sixth *International Heat Transfer Conference*, Vol. 3, pp. 309-313.

Cavallini, A., Censi, G., Del Col, D., Doretti, L., Longo, G.A. and Rossetto, L., 2001. Experimental investigation on condensation heat transfer and pressure drop of new HFC refrigerants in a horizontal tube. *International Journal of Refrigeration*, pp. Vol. 24, p. 73-87.

Cavallini, A., Censi, G., Del Col, D., Doretti, L., Longo, G.A. and Rosetto, L., 2002. In-tube condensation of halogenated refrigerants. *ASHRAE Trans*, pp. 108 (1), pp. 146–161.

Cavallini, A., Del Col, D., Doretti, L., Matkovic, M., Rossetto, L. and Zilio, C., 2005. A model for condensation inside minichannels. San Francisco, Proceedings of HT2005, *ASME Heat Transfer Conference*.

Cavallini, A., Del Col, D., Doretti, L., Matkovic, M., Rossetto, L. and Zilio, C., 2005. Two-phase frictional pressure gradient of R236ea, R134a and R410A inside multiport mini-channels, port mini-channels. *Experimental Thermal and Fluid Science*, pp. 29, 861-870.

Cavalini, A., Del Col, D., Doretti, L., Longo, G.A. and Rossetto, L., 2009. Frictional pressure drop during vapor–liquid flow in minichannels: Modelling and experimental evaluation. *International Journal of Heat and Fluid Flow*, pp. 30(1), 131–139.

Chang, Y-J., Chang, W-J., Li, M-C. and Wang, C-C., 2006. An adamant of the generalized friction correlation for louver fin geometry. *International Journal of Heat and Mass transfer* pp. 4250-4253.

Chang, Y., Hsu, K., Lin, Y. and Wang, A., 2000. A generalized friction correlation for louver fin geometry. *International Journal of Heat and Mass Transfer*, pp. 43, 2237-43.

Chang, Y. and Wang, C., 1996. Air side performance of brazed aluminum heat exchangers. *ASHRAE Trans.*, 100(2), pp. 643-652.

Chen, Y., Yang, K. and Wang, C-C., 2001. Two-phase pressure drop of Air-Water in Small Horizontal Tubes. *Journal of Thermophysics and Heat Transfer*, pp. Vol. 15, No. 4 (2001), pp. 409-415.

Chisholm, D., 1983. Two-phase flow in pipelines and heat exchangers, s.l.: G. Godwin in association with Institution of Chemical Engineers, page 304.

Chisholm, D., 1973. Pressure gradients due to friction during the flow of evaporating two-phase mixtures in smooth tubes and channels. Int. J. Heat Mass Transfer, pp. Vol. 16, p. 347.

Chisolm, D., 1972. A theoretical basis for the Lockhart-Martinelli correlation for two-Phase flow. *Int. Journal of Heat and Mass Transfer*, pp. Vol. 10, pp. 1767-78.

Choi, J. M., Paane, W. P. and Domanski, P., 2003. Effects of non-uniform refrigerant and air Flow distributions on finned-tube evaporator performance. Washington, D.C., *International Congress of Refrigeration*.

Choi, C., Yu, D. and Kim, M., 2011. Adiabatic two-phase flow in rectangular microchannels with different aspect ratios: Part I - Flow pattern, pressure drop and void fraction. *International Journal of Heat and Mass Transfer*, pp. 54, 616-624. .

Churchill, S., 1977. Friction-Factor Equation Spans All Fluid-Flow Regimes. *Chemical Engineering*, pp. 91-92.

CoilDesigner, 2010.Tool to Aid in the Design, Simulation and Optimization of Air-Cooled Heat Exchangers.

Colburn, A., 1933. A method of correlating forces convection heat transfer data and comparison with fluid friction. *AlChe Journal*, vol. 29, pp. 174-210.

Corbeàn, J. and Melòn, M., 1998. Modelling of plate finned tube evaporators and condensers working with R134a. *International Journal of Refrigeration*, Vol. 21, pp 273-284.

Corberàn, J., Fernàndez de Cordoba, P., Gonzàlvez, J. and Alias, F., 2001. Semiexplicit method for wall temperature linked equations (SEWTLE): a general finite-volume method technique for the calculation of complex heat exchanger. *Numerical Heat Transfer*, Part B: Fundamentals, pp. 37-59.

Corberàn, J. and Montagut C. Project NextHPG: Next generation of heat pumps working with natural fluids. Institute for Energy Engineering. University Polytechnic of Valencia.

Corberán, J. M., Fernandez de Cordoba, P., Ortuno, S., Ferri, V., Gonzalvez, J., Setaro, T., Boccardi, G., 2000. Modelling of Compact Evaporators and Condensers. WIT *Transactions on Engineering Sciences*, Volume 27, pp. 1-10.

Datta, S., Das, P. and Mukhopadhyay, S., 2014. Obstructed airflow through the condenser of an automotive air conditioner – Effects on the condenser and the overall performance of the system. *Applied Thermal Engineering*, Volume 70, pp. 925-934.

De Souza, A. and Pimenta, M., 1995. Prediction of pressure drop during horizontal two-phase flow of pure and MIXED refrigerants. *Cavitation and Multiphase Flow*, pp. ASME, 210.

Dobson, M. and Chato, J., 1998. Condensation in smooth horizontal tubes. *J. Heat Transfer*, pp. 120, p.p. 193-213.

Domanski, P., Yashar, D. and Lee, S., 2010. Evaporator optimization for non-uniform air distribution. Stockholm, Proceedings of *Sustainable Refrigeration and Heat Pump Technology*.

EVAP-COND, 2010. Simulation Models for Finned Tube Heat Exchangers with Circuitry Optimization.

Fernando, P., Palm, B., Ameel, T., Lundqvist, P. and Granryd, E., 2008. A minichannel aluminum tube heat exchanger – Part II: Evaporator performance with propane. *Int. J. Refrigeration*, pp. 31(4), 681–695.

Fernando, P., Palm, B., Lundqvist, P. and Granryd, E., 2004. Propane heat pump with low refrigerant charge: design and laboratory tests. *Int. J. Refrigeration*, pp. 27(7), 761–773.

Friedel, L., 1979. New friction pressure drop correlations for upward, horizontal and downward two-phase pipe flow. Oxford, HTFS Symposium, p. Hoechst AG Reference 372217/24698.

Fronk, B. and Garimella, S., 2011. Water-Coupled carbon dioxide microchannel gas cooler for heat pump water heaters: Part II - Model development and validation. *International Journal of Refrigeration*, Volume 34, pp. 17-28.

Fuji, T., Honda, H., Nozu, S. and Nakarai, S., 1978. Condensation of Superheated Vapor inside Horizontal Tube. *Heat Transfer - Japanese Research*, 4(3), pp. 1-48.

García-Cascales, J.R., Vera-García, F., Gonzálvez-Macía, J., Corberán, J.M., Johnson, M.W., Kohloer, G.T., 2010. Compact heat exchanger modeling: Condensation. *International Journal of Refrigeration*, Volume 33, pp. 135-147.

Garimella, S., Agarwal, A. and Killion, J., 2005. Condensation Pressure Drop in Circular Microchannels. *Heat Transfer Engineering*, pp. 26(3), 28–35.

Garimella, S., Killion, J. and Coleman, J., 2001. An Experimentally Validated Model for Two-Phase Pressure Drop in the Intermittent Flow Regime for Circular Microchannels. *Journal of Fluids Engineering*, pp. 124, 205-214.

Gnielinski, V., 1976. New Equations for Heat and Mass Transfer in Turbulent Pipe and Channel Flow. *Int. Chem. Eng*., pp. 16 (2), 359-368.

Granryd, E., Ekroth, I., Lundquvist, P., Ake, M., Palm, B. and Rohlin, P., 2003. Refrigerating Engineering. Stockholm: Department of Energy Technology, Royal Institute of technology, KTH.

Gray, D. and Webb, R., 1986. Heat transfer and friction correlations for plate finned-tube heat exchangers having plain fins, Proc. *8th. Heat transfer Conference*, pp. pp. 2745-2750.

Gronnerud, R., 1972. Investigation of liquid hold-up, flow resistance and heat transfer in circulation type evaporator Part IV. Two-phase flow resistance in boiling refrigerants, I.I.R. meeting Freudenstadt comm. B1, B2 and E1.

Haraguchi, H., Koyama, S. and Fujii, T., 1994. Condensation of refrigerants HCFC22, HFC134a and HCFC123 in a horizontal smooth tube (2nd report, proposal of empirical expressions for local heat transfer coefficient). Trans. JSME, Vol. 60 (574), 245–252.

Hrnjak, P., 2010. Developments in Charge Reduction and Microchannel Technology. Stockholm, Sustainable Refrigeration and Heat Pump Technology Conference.

Hwang, Y. and Kim, M., 2006. The pressure drop in microtubes and the correlation development. *International Journal of Heat and Mass Transfer*, Volume 49, Issues 11–12, 1804–1812.

IMST-ART, 2010. Simulation tool to assist the selection, design and optimization of refrigerator. Available at: http://www.imst-art.com.

Jiang, H., Aute, V. and Radermacher, R., 2006. CoilDesigner: A general purpose simulation and design tool for air-to refrigerant heat exchangers. *International Journal of Refrigeration*, Volume 29, pp. 601-610.

Jordan, A. and Jacobi, A., 2005. Impact of leading edge delta-wing vortex generators on the thermal performance of a flat tube, louvered-fin compact heat exchanger. *International Journal of Heat and Mass Transfer*, p. 1480–1493.

Kaern, M., Brix, W., Elmergard, B. and Larsen, L., 2011. Performance of residential air-conditioning systems with flow maldistribution in fin-and-tube evaporators. *International Journal of refrigeration*, Volume 34, pp. 696-706.

Kandlikar, S. and Grande, W., 2002. Evolution of Microchannel Flow Passages-Thermohydraulic Performance and Fabrication Technology. *Heat Transfer Eng.*, pp. 3-17.

Kew, P. and Reay, D., 2011. Compact/micro-heat exchangers – Their role in heat pumping equipment. *Applied Thermal Engineering*, Vol. 31(5), 594–601.

Kim, M. and Bullard, C., 2002. Air side thermal hydraulic performance of multi-louvered fin aluminum heat exchangers. *International Journal of Refrigeration*, Volume 25, pp. 390-400.

Kim, M. and Bullard, C., 2001. Development of a microchannel evaporator model for a CO2 air-conditioning system. *Energy*, Vol. 26(10), 931–948.

Kim, S. and Mudawar, I., 2012. Consolidated method to predicting pressure drop and heat transfer coefficient for both subcooled and saturated flow boiling in micro-channel heat sinks. *International Journal of Heat and Mass Transfer*, Vol. 55, 3720-3731.

Kondou, C. and Hrnjak, P., 2012. Condensation from superheated vapor flow of R744 and R410 at subcritical pressure in a horizontal smooth tube. International journal of refrigeration, Volume 55, pp. 2779-2791.

Koyama, S., Kugawhara, K. and Nakashita, K., 2003. Condensation of refrigerant in a multi-port microchannel. New York, Proceedings of the first *International conference on Microchannels and Minichannels*.

Kumar, A., Joshi, J., Nayak, A. and Vijayan, K., 2016. 3D CFD simulations of air-cooled condenser-III: Thermal–hydraulic characteristics and design optimization under forced convection conditions. *International Journal of Heat and Mass* Transfer, Volume 93, Pages 1227–1247.

Lee, C., Teng, Y. and Lu, D., 1991. An Investigation of Condensation Heat Transfer of Superheated R22 Vapor in a Horizontal Tube. Dubrovnik, Proc. *World Conf. on Experimental Heat Transfer, Fluids Mechanics and Thermodynamics*.

Lee, J. and Domanski, P., 1997. Impact of air and refrigerant maldistributions on the performance of finned-Tube evaporators with R-22 and R-407C, The air-Conditioning and Refrigeration Technology Institute.

Lee, T., Wu, W., Chuang, Y. and Wang, S., 2010. An improvement of airflow and heat transfer performance of multi-coil condensers by different coil configurations. *International Journal of Refrigeration*, Volume 33, pp. 1370-1376.

Lia, B., Peuker, S., Hrnjak, P. and Alleyne, A., 2011. Refrigerant mass migration modeling and simulation for air conditioning systems. *Applied Thermal Engineering*, Vol. 31(10), 1770–1779.

Lockhart, R. and Martinelli, R., 1949. Proposed Correlation of Data for Isothermal Two Phase Flow, Two-Component Flow in Pipes. *Chem. Eng. Prog.*, Vol. 45, pp. 39–48..

Lopez-Belchì, A., 2014. Characterization of heat transfer and pressure drop in condensation processes within mini-channel tubes with last generation of refrigerant fluids. Cartagena: PhD. Thesis, Universidad Politécnica de Cartagena.

Lopez-Belchi, A., Illán, F., García-Cascales, J. and Vera-García, F., 2015. Heat transfer coefficient during condensation inside a mini-channels multiport tube with R32 and R410A as working fluids. *Science and Technology for Built Environment*, Vol. 21(5), pp. 535-544.

Mao, J.N., Chen, H.X., Jia, H., Wang, Y.Z. and H.M. Hu, 2013. Effect of air side flow maldistribution on thermal–hydraulic performance of the multi-louvered fin and tube heat exchanger. *International Journal of Thermal Sciences*, Volume 73, pp. 46-57.

Martínez-Ballester, S., Corberán, J. and Gonzálves-Maciá, J., 2013. Numerical model for microchannel condensers and gas coolers: Part I - Model description and validation. *International Journal of refrigeration*, Volume 36, pp. 173-190.

Martinez-Ballester, S., Corberán, J., Gonzálvez-Macia, J. and Domanski, P., 2011. Impact of Classical Assumptions in Modelling a Microchannel Gas Cooler. *Int. J. Refrigeration*, Vol. 34 (8), pp. 1898-1910.

Mc Williams, J., 2002. Review of Airflow Measurement Techniques, Berkeley: Energy Performance of Buildings Group.

McQuiston, F., 1978. Correlation of heat, mass and momentum transport coefficients for plate-fin-tube heat transfer surface. *ASHRAE Transactions*, vol. 84 (1), 294-308.

Meng, J., Liu, M., Zhang, W., Cao, R., Li, Y., Zhang, H., Du, X. and Geng, Y., 2015. Experimental investigation on cooling performance of multi-split variable refrigerant flow system with microchannel condenser under part load conditions. *Applied Thermal Engineering*, pp. 232-241.

Meyer, M. and Hrnjack, P., 2014. Pressure Drop in Condensing Superheated Zone. Purdue-USA, Proc. *15th International Refrigeration and Air Conditioning Conference*.

Miropolky, Z., Shneersva, R. and Teernakova, L., 1974. Heat Transfer at Superheated Steam Condensation inside Tubes. Tokyo, Proc. *5th. Int. Heat transfer Conference* - Vol. 3 - pp. 246-249.

MPower, 2010. Modine's Custom Vapor Compression System Design.

Muller-Steinhegen , H. and Heck, K., 1986. A Simple Friction Pressure Drop Correlation for Two-Phase Flow in Pipes. *Chem. Eng. Process*, vol. 20, 291-308.

Oliet, C., Oliva, A., Castro, J. and Pérez-Segarra, C., 2007a. Parametric studies on automotive radiators. *Applied Thermal Engineering*, vol. 27 (11–12), 2033–2043.

Oliet, C., Pérez-Segarra, C., Castro, J. and Oliva, A., 2010. Modelling of fin-and-tube evaporators considering non-uniform in-tube heat transfer. *International Journal of Thermal Sciences*, vol. 49(4), 692–701.

Oliet, C., Pérez-Segarra, C., Danov, S. and Oliva, A., 2007. Numerical simulation of dehumidifying fin-and-tube heat exchangers: Semi-analytical modelling and experimental comparison. *International Journal of Refrigeration*, vol. 30(7), 1266–1277.

Oliver, J. and Liebenberg, L., 2004. Pressure drop during refrigerant condensation inside horizontal smooth, helical microfin, and herringbone microfin tubes. *Heat Transfer*, vol. 126, pp. 687-696.

Padilla, Y., 2012. Experimentally validated models of refrigerant distribution in microchannel heat exchangers used to evaluate charge reduction of various working fluids. Urabana-Illinois: Master Thesis - University of Illinois.

Park, C. and Hrnjak, P., 2007. Effect of Heat Conduction through the Fins of a Microchannel Serpentine Gas Cooler of Transcritical CO2 System. *Int. J. Refrigeration*, vol. 30 (3), 389-397.

Park, J., Vakil-Farahani, F., Cosolini, L. and Thome, J., 2011. Experimental Study on condensation heat transfer in vertical minichannels for new refrigerant R1234ze (e), versus R134a and R236fa. *Experimental Thermal and fluid Science*, vol. 35, 442-454.

Park, Y. and Jacobi, A., 2009. Air Side heat transfer and friction factor for Flat-tube louver-fin heat exchanger. *Journal of Heat transfer*, Volume 31, pp. 1-10.

Palm, B., 2007. Refrigeration systems with minimum charge of refrigerant. *Applied Thermal Engineering*, Vol. 27(10), 1693–1701.

Quiben, J. and Thome, J., 2007. Flow pattern based two-phase frictional pressure drop model for horizontal tubes Part II: New phenomenological model. *International Journal of Heat and Fluid Flow*, pp. vol. 28, issue 5, pp. 1060-1072.

Qu, X., Chen, J. and Radermacher, R., 2009. Investigating performance of new mini-channel evaporators, *Applied Thermal Engineering*, Vol. 29(17–18), 3561–3567.

Revellin, R., Mishima, k. and Thome, J., 2009. Status of prediction methods for critical heat fluxes in mini and microchannels. *International Journal of Heat and Fluid Flow*, Vol. 30(5), 983–992.

Revellin, R. and Thome, J., 2007. Adiabatic two-phase frictional pressure drops in microchannels. *Experimental Thermal and Fluid Science*, Vol. 31(7), 673–685. .

Revellin, R. and Thome, J., 2007. Experimental investigation of R-134a and R-245fa two-phase flow in microchannels for different flow conditions. *International Journal of Heat and Fluid Flow*, Vol. 28, 63-71.

Rossetti, A., Minetto, S. and Marinetti, S., 2015. A simplified thermal CFD approach to fins and tube heat exchanger: Application to maldistributed airflow on an open display cabinet. *International Journal of Refrigeration*, pp. Volume 57, Pages 208–215.

Shah, M., 1979. A general correlation for heat transfer during film condensation inside pipes. *Int. J. Heat and Mass Transfer*, Vol. 22, pp. 547-556.

Shao, L., Yang, L. and Zhang, C., 2010. Comparison of heat pump performance using fin-and-tube and microchannel heat exchangers under frost conditions. *Applied Energy*, Vol. 87(4), 1187–1197.

Shao, L., Yang, L., Zhang, C. and Gu, B., 2009. Numerical modelling of serpentine microchannel condenser. *International Journal of Refrigeration*, Volume 32, pp. 1162-1172.

Singh, V., Abdelaziz, O., Aute, V. and Radermacher, R., 2011. Simulation of air-to-refrigerant fin-and-tube heat exchanger with CFD-based air propagation. *International Journal of Refrigeration*, pp. Volume 34, Issue 8, Pages 1883–1897.

Singh, V., Aute, V. and Radermacher, R., 2008. Numerical Approach for Modeling Air-To-Refrigerant Fin-And-Tube Heat Exchanger with Tube-To-Tube Heat Transfer. *Int. J. of Refrigeration*, pp. 1414-1425.

Soliman, M., Schuster, J. and Berenson, P., 1968. A General heat transfer correlation for Annular Flow Condensation. *J. Heat Transfer*, Vol. 90 (2), 267-274.

Stern, F. and Votta, F., 1968. Condensation from superheated gas-vapor mixtures. *AlChe Journal*, Vol. 14 (6), 928-933.

Tammaro, M., Montagud, C., Corberán, J.M., Mauro, W. and Mastrullo, R., 2015. A propane water-to-water heat pump booster for sanitary hot water production: Seasonal performance analysis of a new solution optimizing COP. *International Journal of Refrigeration*, pp. 59-69.

Thome, J.R., El Hajal, J. and Cavallini, A., 2003. Condensation in horizontal tubes, part 2: new heat transfer model based on flow regimes. *International Journal of Refrigeration*, Volume 46, pp. 3365-3387.

Thome, J. Chapter 13: Two-Phase pressure drop. *Wolverine Engineering Data Book III*, Wolverine tube, INC.

Threlkeld, K., 1974. Thermal Environmental Engineering. Englewood Cliff, NJ: Prentice Hall.

Timoney, D. and Foley, P., 1993. Some effects of air flow maldistribution on the air performance of a compact evaporator with R134a. Edinburgh, *Eurotherm* Seminar No.26.

Tondon, T., Varma, H. and Gupta, C., 1995. Heat transfer during forced convection condensation inside horizontal tube. *International Journal of Refrigeration*, Volume 18, Issue 3, 210–214.

Travis, D., Baron, A. and Rohsenow. , W., 1971. Forced convection condensation inside tube: a heat transfer equation for condenser design. American Society of Heating, Report No. DSR 72591-74.

Triplett, K.A., Ghiaasiaan, S.I., Abdel-Khalik, S.M., LeMouel, A. and McCord, B.N., 1999. Gas-liquid two-phase flow in microchannels: Part II: void fraction and pressure drop. *International Journal of Multiphase Flow*, pp. 25, 395-410.

Wambsganss, M. and Jendrzejczyk, J., 1992. Two-Phase Flow and Pressure Drop in Flow Passages of Compact Heat Exchangers. SAE Technical Paper 920550.

Wang, C-C., Chi, K-Y. and Chang, C-J., 2000. Heat transfer and friction characteristics of plain fin-and-tube heat exchangers, part I-II. *International Journal of Heat and Mass Transfer*, Vol 43, pp. 2681-2691/2693-2700.

Wang, C., Hsieh, Y., Chang, Y. and Lin, Y., 1996. Sensible heat and friction characteristics of plate fins-and-tube heat exchangers having plane fins. *International Journal of Refrigeration*, Vol. 19, 223-230.

Wang, W., Radcliff, T. and Christensen, R., 2002. A condensation heat transfer correlation for millimeter scale tubing with flow regime transaction. *Experimental Thermal and Fluid Science*, Volume 26, pp. 473-485.

Webb, R., 1998. Convective Condensation of Superheated Vapor. *Transactions of the ASME*, Volume 120, pp. 418-421.

Webb, R., Zhang, M. and Narayanamurthy, R., 1998. Condensation heat transfer in small diameter tubes. Kyogju, proceeding of the *11th IHTC*, vol.6.

Xia, Y., Zhong, Y., Hrnjak, P. and Jacobi, A., 2006. Frost, defrost, and refrost and its impact on the air-side thermal-hydraulic performance of louvered-fin, flat-tube heat exchangers. *Int. J. Refrigeration*, Vol. 29 (7), 1066–1079.

Yaïci, W., Ghorab, M. and Entchev, E., 2014. 3D CFD analysis of the effect of inlet air flow maldistribution on the fluid flow and heat transfer performances of plate-fin-and-tube laminar heat exchangers. *International Journal of Heat and Mass Transfer*, Volume 74, p. 490–500.

Yang, C. and Webb, R., 1996. Condensation of R-12 in small hydraulic diameter extruded aluminum tubes with and without micro-fins. *International Journal of Heat and Mass Transfer*, Vol. 39, 791-800.

Yashar, D. and Cho, H., 2007. Air-Side velocity Distribution in Finned-tube Heat Exchangers, Gaithersburg - Maryland (USA): National Institute of Standard and Technology.

Yashar, D., Cho, H. and Domanski, P., 2008. Measurement of Air-Velocity Profiles for Finned-tube heat Exchangers Using Particle Image Velocimetry. West Lafayette, Proceedings of *International Refrigeration and Air Conditioning Conference*.

Yin, J., Bullard, C. and Hrnjak, P., 2001. R-744 Gas Cooler Model Development and Validation. *Int. J. Refrigeration*, Vol. 24 (7), 692-701.

Zhang, M. and Webb, R., 2001. Correlation of two-phase friction for refrigerants in small-diameter tubes. *Experimental Thermal and Fluid Science*, Vol. 25, 131-139.

Zhao, C., Jiang, P. and Zhang, Y., 2011. Flow and convection heat transfer characteristics of CO2 mixed with lubricating oil at super-critical pressures in small tube during cooling. *International Journal of Refrigeration*, pp. 34, 29-39.

Zheng, W., Chen, Y., Hua, N., Zhong, T. and Gong, Y., 2014. Comparative Performance of Automotive Air Conditioning System Using Micro-channel Condensers with and Without Liquid-vapor Separation. Taipei, *Energy Procedia*, pp. 1646–1649.

Zhong, Y., Joardar, A., Gu, Z., Park, Y.G. and Jacobi, A.M., 2005. Dynamic dip testing as a method to assess the condensate drainage behavior from the air-side surface of compact heat exchangers. *Experimental Thermal and Fluid Science*, Vol. 29 (8), 957-970.

Zilio, C., Brown, J., Schiocheta, G. and Cavallini, A., 2011. The refrigerant R1234yf in air conditioning systems. Energy, Vol. 36 (10), 6110–6120.